TECHNICAL NOTE N° IDB-TN-03139

Review of Methods and Software Tools for Disaster Risk Assessment

María Carolina Rogelis
María Alejandra Escovar
Andrés Abarca
Kenneth Otálora
Walter Cortes
Ginés Suarez

Inter-American Development Bank
Disaster Risk Management Unit

September 2025

Review of Methods and Software Tools for Disaster Risk Assessment

María Carolina Rogelis
María Alejandra Escovar
Andrés Abarca
Kenneth Otálora
Walter Cortes
Ginés Suarez

Inter-American Development Bank
Disaster Risk Management Unit

September 2025

REVIEW OF METHODS AND SOFTWARE TOOLS FOR DISASTER RISK ASSESSMENT

Authors:

María Carolina Rogelis
María Alejandra Escovar
Andrés Abarca
Kenneth Otálora
Walter Cortes
Ginés Suarez
(CSD/DRM)

REVIEW OF METHODS AND SOFTWARE TOOLS FOR DISASTER RISK ASSESSMENT

Authors:
María Carolina Rogelis, María Alejandra Escovar, Andrés Abarca, Kenneth Otálora, Walter Cortes, Ginés Suarez (CSD/DRM).

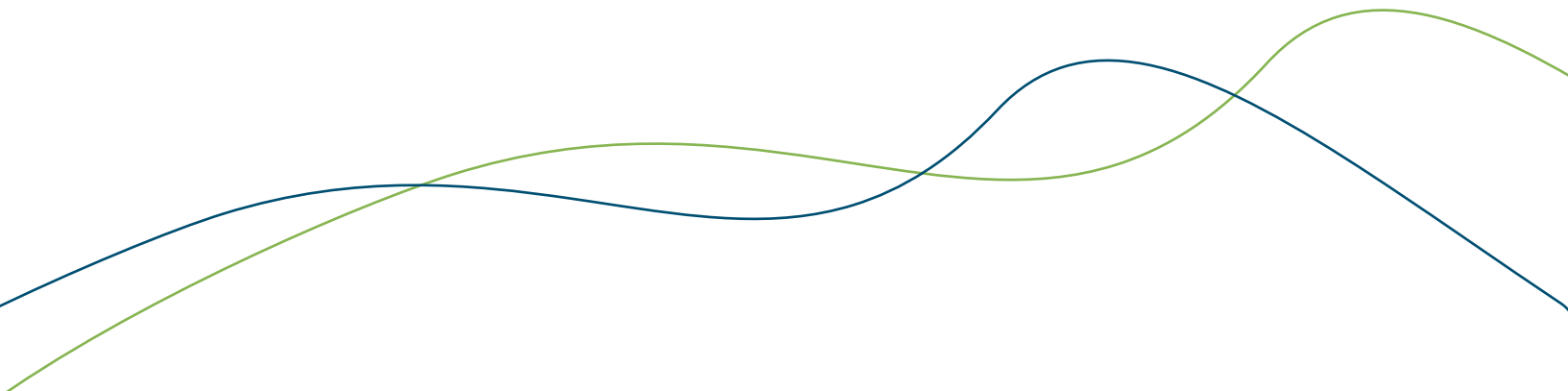

Image: Adobe Stock

INTRODUCTION

Disaster risk assessment is a fundamental component of risk management and planning for risk reduction[1] and adaptation measures. In recent years, the development of specialized tools has enhanced analytical capabilities through the use of advanced methodologies incorporating analysis for various types of hazards, mathematical modeling, artificial intelligence, governance approaches and climate change considerations. This document provides a detailed review of the main platforms and methods used in risk calculation, highlighting their capabilities, limitations and areas of application.

The document is organized into eight sections. Section 2 presents existing risk calculation tools, distinguishing between multi-hazard[2] platforms and those focused on specific risks like floods and earthquakes. Section 3 explores the use of artificial intelligence in disaster risk management, including applications in mitigation, preparedness, and response. Section 4 describes the mathematical models used for risk estimation, from approaches based on probabilistic events to specific methods for quantification of uncertainty implemented in various tools. Section 5 analyzes methodologies that incorporate social vulnerability and governance into risk analyses. Section 6 is devoted to risk assessment in the context of climate change, with a particular emphasis on CLIMADA (CLIMate ADAptation), the only reviewed platform with specific methods for this purpose. Subsequently, Section 7 describes the freely available global precipitation products that can be used in hydrometeorological hazard analysis. Finally, Section 8 discusses the global information available for exposure and vulnerability assessment, key aspects in disaster risk estimation.

This document provides a comprehensive overview of available tools and methodologies to help users select and apply them in risk studies across various scales and contexts.

[1] The conceptualization of the classification of risk reduction measures may vary depending on the country and its regulations. For example, in Colombia (Law 1523 of 2012), risk reduction is composed of corrective intervention for existing risk, prospective intervention for new risks and financial protection.

[2] The term multi-hazard, according to the United Nations Office for Disaster Risk Reduction (UNDRR), means: (1) the selection of multiple major hazards that the country faces, and (2) the specific contexts where hazardous events may occur simultaneously, cascadingly or cumulatively over time, and taking into account the potential interrelated effects.

SECTION 1

REVIEW OF EXISTING RISK CALCULATION TOOLS

Existing tools for risk calculation are presented, distinguishing those that allow multi-hazard assessment from those specialized in specific risks such as floods and earthquakes.

SECTION 2

ARTIFICIAL INTELLIGENCE METHODS IN RISK CALCULATION

It explores the use of artificial intelligence in disaster risk management, including applications in mitigation, preparedness, and response.

SECTION 3

MATHEMATICAL MODELS IN THE CALCULATION OF DISASTER RISK IN THE AVAILABLE RISK CALCULATION PLATFORMS

It analyzes methodologies that incorporate social vulnerability and governance into risk analyses.

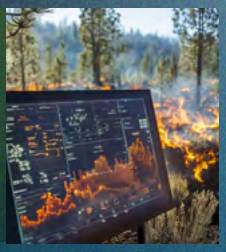

SECTION 4

METHODS INCORPORATING SOCIAL VULNERABILITY AND/OR GOVERNANCE IN RISK ANALYSIS

It analyzes methodologies that incorporate social vulnerability and governance into risk analyses, with a focus on specific risks such as floods and earthquakes.

SECTION 5

CLIMATE CHANGE AND RISK CALCULATIONS

It is dedicated to risk assessment considering climate change, with a particular emphasis on CLIMADA, the only platform reviewed that includes specific methods for this purpose.

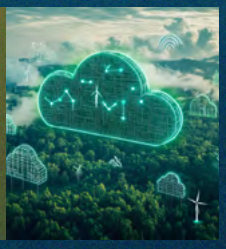

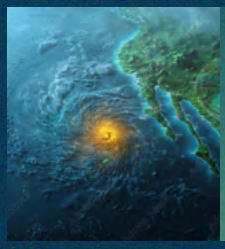

SECTION 6

GLOBAL PRECIPITATION PRODUCTS WITH FREE ACCESS

It describes open-access global precipitation products that can be used in hydrometeorological hazard analyses.

SECTION 7

OPEN ACCESS GLOBAL INFORMATION FOR EXPOSURE AND VULNERABILITY ANALYSIS

It addresses the available global information for assessing exposure and vulnerability, which are key aspects in disaster risk estimation.

CONTENTS

Image: Flickr - IDB Sustainable Cities // Panamá

SECTION 1

Image: Adobe Stock

REVIEW OF EXISTING RISK CALCULATION TOOLS

1.1. INTRODUCTION

Image: Adobe Stock

The ability to assess and manage risk is a priority for national, regional and local governments, organizations and financial institutions. Risk calculation platforms are fundamental tools for analyzing, modeling and projecting the impacts of various scenarios, facilitating informed decision making. In recent years, these platforms have rapidly evolved, incorporating advanced statistical analysis, probabilistic modeling, simulation, and artificial intelligence. These enhancements enable more sophisticated risk calculations using the latest knowledge and computational resources.

The development of risk calculation platforms and tools marks a significant advance in risk assessment. Today, a wide range of platforms is available, each with unique features that make them particularly useful for different contexts, such as seismic risk assessment or climate impact modeling. Its implementation not only allows for the quantification of potential economic and social damages but also promotes better preparedness and resilience in the face of disasters.

This chapter provides an analysis of various risk calculation platforms, highlighting their features, functionalities and specific applications. This chapter summarizes the literature review of available tools for multi-hazard, flood, and seismic risk calculation. It evaluates each tool based on criteria such as accessibility, developer and user support, software availability, graphical interface, and conceptual framework for risk estimation. Annex A includes additional details on each of the platforms, as well as examples of use that expand on the content presented in the chapter. This analysis aims to help the Inter-American Development Bank identify the most suitable solutions for the types of risk analysis it offers to countries in Latin America and the Caribbean.

1.2. MULTI-HAZARD PLATFORMS

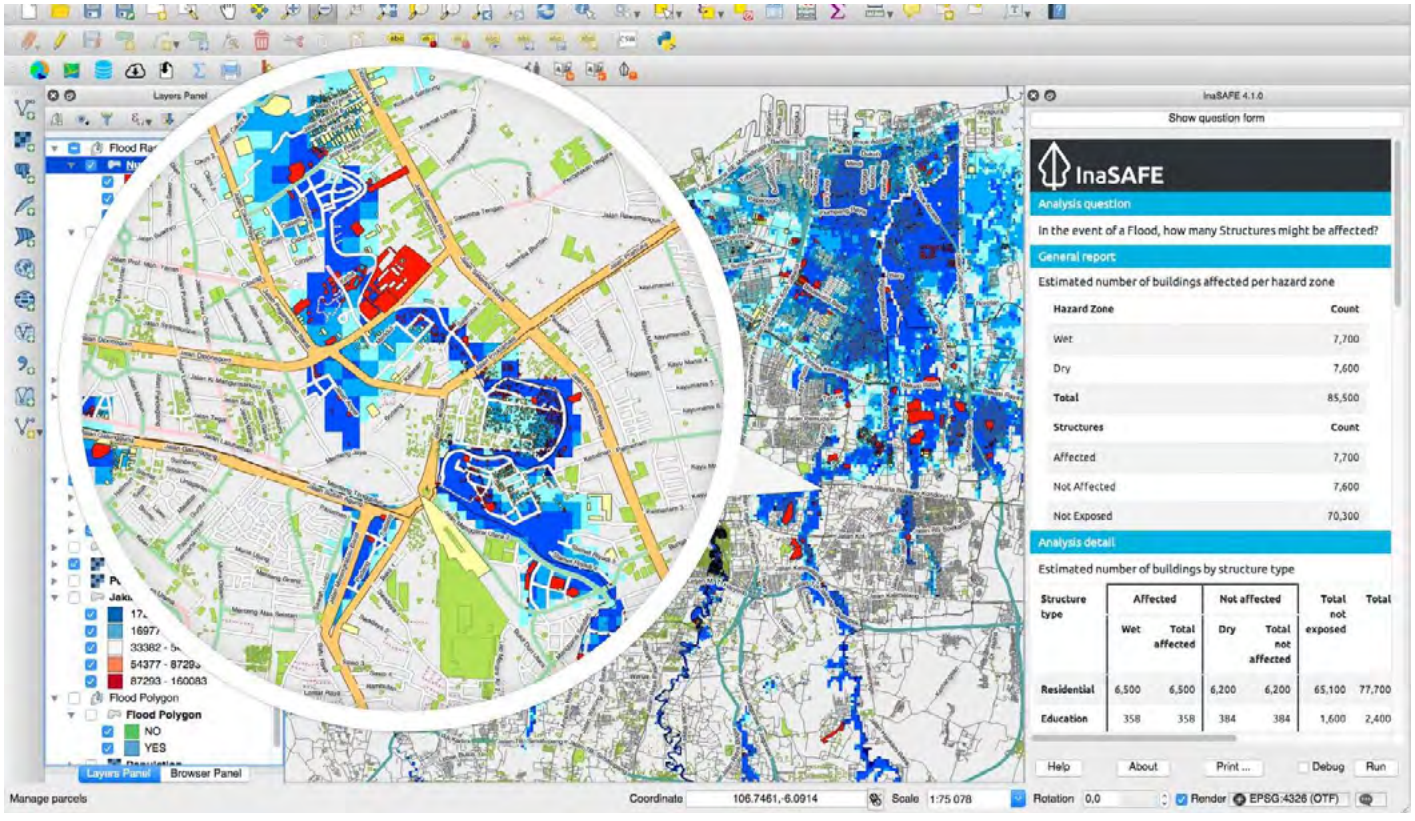

Source: https://inasafe.org/

1.2.1. Description

These platforms are designed to analyze various types of hazards and although some of them may be designed for specific hazards, due to their flexibility, they could be used with other hazards. Below is a brief description of the evaluated platforms. For more details, see **Annex A**.

CAPRA (Probabilistic Risk Assessment Platform) (https://ecapra.org/) is a platform that uses a probabilistic approach to disaster risk assessment. It allows for the quantification and analysis of risk associated with earthquakes, tsunamis, volcanoes, mass movements, hurricanes, floods, precipitation and drought (Universidad de Los Andes 2024a). It generates metrics such as risk curves, spatial distribution of damage and expected annual loss (World Bank et al. 2009).

HAZUS (https://www.fema.gov/flood-maps/products-tools/hazus) is a software developed by the Federal Emergency Management Agency (FEMA) that focuses on disaster risk assessment using a standardized methodology. It is used to estimate the impacts of earthquakes, hurricanes, floods and tsunamis. Its results include estimates of physical damage to structures, economic and social losses (FEMA 2023).

RiskScape (https://riskscape.org.nz/) is an application that processes spatial data to perform multi-hazard risk analysis. It combines spatial layers to assess the exposure of buildings and other infrastructure, providing an analysis of potential risks (National Institute of Water and Atmospheric Research Ltd and Institute of Geological and Nuclear Sciences Ltd 2024c).

InaSAFE (https://inasafe.org/), a free software tool, also specializes in assessing the impacts of disasters, particularly earthquakes, tsunamis and floods. Its focus is on generating impact scenarios and creating map layers to show the effects of different hazards. It does not perform an economic analysis of risk, but rather focuses on element exposure and response planning (InaSAFE 2019a).

OASIS (https://oasislmf.org/) focuses on catastrophe modeling, providing standardized tools for risk assessment and financial loss quantification. Users can assess potential losses and high-risk areas through models that integrate exposure data and catastrophic scenario analysis (OASIS 2024a).

IN-CORE (Integrated Computational Resilience) (https://in-core.org/) is a platform developed by Colorado State University to analyze the resilience of infrastructure and communities to disasters. It integrates simulation models to assess both the physical and socioeconomic impacts of disasters, analyzing community recovery and providing tools to optimize resilience planning and disaster response (IN-CORE 2024).

CLIMATE ADAptation (https://climada.ethz.ch/) is a probabilistic modeling tool that assesses the socioeconomic risk of climate events, but can be used for the analysis of other hazards, considering both the present and future projections. It allows for the study of individual and joint events, and evaluates how adaptation measures can reduce the impacts of climate change (Aznar-Siguan and Bresch 2019).

CATSIM (Catastrophe Simulation Tool) (https://iiasa.ac.at/models-tools-data/catsim), developed by the International Institute for Applied Systems Analysis (IIASA), focuses on helping policymakers identify the best financial strategies to address disaster risks. CATSIM includes a module for assessing risk and another for showing the costs and benefits of different financial strategies, allowing users to adjust parameters and simulate various economic and risk conditions (IIASA 2024a).

RiskChanges (https://riskchanges.org/) was developed by the University of Twente and the Asian Institute of Technology, Geoinformatics Center. It is an open source tool designed to analyze dynamic multi-hazard risks. It allows for the assessment and management of risks associated with different natural and anthropogenic hazards, considering their interactions and cumulative effects (PreventionWeb 2023).

Besides these nine platforms, other tools were identified online. However, they were excluded from the comparative analysis and Annex A because their continued development could not be confirmed. One example is PRAISys (Probabilistic Resilience Assessment for Interdependent Systems), which has a website (Lehigh University and Florida Atlantic University 2020) that allows the software to be downloaded upon request, providing a Google Drive link for downloading. However, no detailed documentation was found, and the latest version of the software dates back to 2020, with no clear evidence that the initiative has continued.

1.2.2. Accessibility

The reviewed multi-hazard platforms have varying licenses and source code accessibility, which affects how easily they can be used or modified. CAPRA does not publicly specify its license, and although it was originally envisioned as open source, it is not currently available for public access. The software is designed for use on Windows systems with enhanced support for 64-bit operating systems, and was developed in VB.NET 2005. It does not have a public repository for its code, which limits the possibility for users to customize or extend the platform (Universidad de Los Andes 2024a). HAZUS is free, but requires the use of ArcGIS, which is a paid software. Although some of the HAZUS add-on tools are open source, and there is a FEMA project to create an open-source Python distribution (FEMA 2020), the full code is not accessible for free modification.

As for RiskScape, this software is available under the AGPLv3 license[3] and is open source. It can be run on Windows, Linux and macOS, as long as Java version 17 or higher is installed. The platform is developed in Java and Python, and its source code is available on the software's official website, allowing users to research, modify and contribute to the project. InaSAFE is a fully open source tool under the GPLv3 license, compatible with Windows, macOS and Linux. Developed in Python, InaSAFE is available in its GitHub repository, making it easy to customize and adapt to specific needs.

On the other hand, OASIS is open source with a Berkeley Software Distribution (BSD) 3 license[4], but the use of the models it employs is not free. It is available on Windows via Docker containers or the Linux subsystem for Windows, and was developed in Python 3 and C++ 11. Its source code is available on GitHub. IN-CORE also distributes its source code under an open source license, specifically the Mozilla Public License 2.0[5]. It is compatible with Windows, macOS and Linux, and is developed in Python and Java. Its repository on GitHub allows users to access the code and contribute to the development of the platform.

[3] The Affero General Public License version 3 (AGPLv3) is a free and open source software license. The AGPLv3 requires that any modification of the software, even if it runs on a server and is not distributed directly to users, must also be released under the same license (https://www.gnu.org/licenses/agpl-3.0.html).

[4] The BSD 3-Clause License is a free and open source software license that allows the use, modification and distribution of the software with minimal restrictions. It is a more permissive version of the original BSD license, eliminating the advertising clause but maintaining three main conditions: (1) the copyright notice and list of conditions must be preserved in all copies or distributions of the software; (2) the name of the authors or contributors may not be used to endorse derivative products without permission; and (3) the original developers are exempt from liability (https://opensource.org/licenses/BSD-3-Clause).

[5] The Mozilla Public License 2.0 (MPL-2.0) is a free and open source software license that combines features of both permissive and copyleft licenses. It allows for code licensed under MPL-2.0 to be used, modified and distributed, even in proprietary projects, as long as files modified under MPL remain under the same license and are shared with the community (https://opensource.org/licenses/MPL-2.0).

CLIMADA, another open source tool is licensed under the GNU GPL3 (General Public Licenses)[6] and is compatible with Windows, macOS and Linux. Developed in Python, MATLAB and Octave, it also has its code available on GitHub, facilitating access and collaboration. RiskChanges is distributed under an open source MIT (Massachusetts Institute of Technology) license[7]. This tool is compatible with Windows, Linux and macOS operating systems, and has been developed using the Python programming language.

Finally, CATSIM has a custom license, which means that it is not open source, although access to the software can be requested under certain conditions. Its repository is not publicly available.

Table 1 summarizes the accessibility criteria selected for comparing platforms, where it has been considered highly important that the tool is open source and also makes the code available to the public through GitHub.

Table 1. Accessibility criteria

Criteria	CAPRA	HAZUS	RiskScape	InaSAFE	OASIS	IN-CORE	CLIMADA	CATSIM	RiskChanges
Open Source	✗	✗ [1]	✓	✓	✓	✓	✓	✗	✓
GitHub	✗	✗ [2]	✗ [3]	✓	✓	✓	✓	✗	✓

Notes:
1.2. There is a FEMA project to create an open-source distribution of HAZUS as a Python package. The progress of this project is unknown, although the package is available for download and installation under GNU General Public License v3 (GPLv3+). https://fema-ftp-snapshot.s3.amazonaws.com/Hazus/hazpy/build/html/index.html https://github.com/nhrap-hazus Last updated 5 years ago.
3. The RiskScape code is not on GitHub but can be downloaded from the official website.

[6] The GNU General Public License, version 3 (GPL-3.0), is a free software license with a strong copyleft approach, which means that any derivative or distributed software that includes code under this license must also remain under GPL-3.0. It guarantees users the freedom to run, study, modify and distribute the software, but imposes restrictions to prevent the code from being converted into proprietary software (https://www.gnu.org/licenses/gpl-3.0.html).

[7] The MIT License is a permissive open source software license, which means that it allows developers to use, modify and distribute the software with few restrictions. Its only condition is that the original copyright notice and disclaimer be included on all copies or modified versions (https://opensource.org/license/mit/).

1.2.3. Development and support community

In the case of CAPRA


No direct contact channel with the developers is specified.


It includes built-in help tools within its graphical interface to guide users.


The available manuals date back to 2009, and no updates have been recorded since then, which could limit up-to-date support.

In the case of HAZUS


It provides technical assistance through a specific contact email: FEMA-Hazus-Support@fema.dhs.gov.


It offers user and technical manuals.


It includes an integrated help menu within the tool, improving accessibility.

In the case of RiskScape


It offers a manual and help tools.


It provides online documentation and tutorials.


No direct contact channel with the developers is specified.

In the case of InaSAFE


It offers a manual and help resources.

In the case of OASIS


It has extensive documentation available in its repository.

In the case of IN-CORE


It provides usage examples and detailed documentation on its website.

In the case of CLIMADA

It stands out for its extensive documentation and available usage examples, which facilitate understanding of the platform.

In the case of CATSIM

It does not have a public repository.

It provides direct contact with the project lead for support.

It includes a user manual and practical guidelines for using the software.

In the case of RiskChanges

The website provides contact information for the developers.

It includes help tools.

The documentation is very basic and focused on operational use, without details on calculation procedures.

Table 2 presents the criteria for comparing the tools in relation to the development and support community. The availability of some form of contact with the developers was considered essential, alongside the existence of manuals and support tools. However, the quality of the latter was not included as an evaluation criteria.

Table 2. Development and support community criteria

Criteria	CAPRA	HAZUS	RiskScape	InaSAFE	OASIS	IN-CORE	CLIMADA	CATSIM	RiskChanges
Contact with developers	X	✓	✓	✓	✓	✓	✓	✓	✓
Manuals and support	✓	✓	✓	✓	✓	✓	✓	✓	✓

1.2.4. Software updates and continuous improvement

The frequency with which software updates are made available to the public was considered a key criterion for evaluation, as it reflects the developers' commitment to maintenance, incorporation of improvements, bug fixes and adaptation to new needs or methods.

CAPRA GIS (CAPRA risk calculation engine)

- Development began in 2008.
- The latest update was released in 2018 with version 2.4.
- The fact that its last update was seven years ago may indicate a possible pause in its evolution (Universidad de Los Andes, 2024a).

HAZUS

- It was initiated in 1997.
- It has maintained a more active update cycle.
- The latest version (7.0) was released in November 2024 (FEMA, 2024a).

RiskScape

- It began in the early 2000s.
- The most recent stable version, v1.6.0, was released in April 2024.
- It maintains a relatively consistent update cycle.

InaSAFE

- It began in October 2012.
- The latest update was released in November 2018 with version 5.0.0.
- It shows a lower frequency of updates compared to other platforms.

OASIS

- It began in 2012.
- It is currently under active development, with version 2.4.0 released in February 2025.

IN-CORE

- It began in 2015.
- It is actively updated.
- Version 5.5.1 was released in November 2024.

CLIMADA

- It began in 2018.
- It is updated on a regular basis.
- The latest version (v5.0.0) was released in July 2024.

CATSIM

- No specific start date is available.
- It is in the process of expanding toward an interactive web-based version.
- The last update to the user manual was in August 2021, indicating that active development is ongoing.

RiskChanges

- The development start date could not be identified.
- The last modification to the code on GitHub was in June 2022.
- There is no information on subsequent updates.

Table 3 presents the criteria selected to evaluate software updates and continuous improvement, which establishes that at least one update must have been performed in the last two years.

Table 3. Software upgrades and continuous improvement criteria

Criteria	CAPRA	HAZUS	RiskScape	InaSAFE	OASIS	IN-CORE	CLIMADA	CATSIM	RiskChanges
Update in the last two years	✗	✓	✓	✗	✓	✓	✓	✗	✗

1.2.5. Graphical user interface (GUI)

Multi-hazard platforms vary in terms of their user interface and integration with other software. CAPRA has a graphical interface in Spanish, and is presented as standalone software, which means that it can be used independently without depending on other applications. In contrast, HAZUS, which has a graphical interface in English, requires ArcGIS for its operation, which makes it a non-standalone software and requires the user to purchase the ArcGIS license.

RiskScape and OASIS are both platforms with graphical interfaces in English that operate as stand-alone software and do not depend on other applications such as QGIS or ArcGIS, although RiskScape does not have a graphical interface and user interaction is performed via the command line. InaSAFE, on the other hand, is integrated as a QGIS plugin and has a graphical interface in English and Indonesian, allowing it to be an easy-to-use tool within the QGIS environment.

The IN-CORE and CLIMADA platforms do not have their own graphical interfaces. IN-CORE is used in the Python/Jupyter environment, which means that users interact through code instead of visual interfaces. Similarly, CLIMADA is also a Python package that is used through Python/Jupyter, without a dedicated GUI. CLIMADA also has a MATLAB version that dates back to 2016 but is no longer supported.[8]

In the case of RiskChanges, this tool has a user interface that functions as a web tool and, in addition, it can be used as a Python library, allowing user interaction through code (RiskChanages 2021).

[8] https://github.com/davidnbresch/climada

Finally, CATSIM has a graphical interface in English and is a standalone application, although an interactive web version is in the process of being launched.

Table 4 shows the selected criteria, which consist of the software not depending on other software that requires a paid license and verifying whether or not it has its own user interface.

Table 4. Graphical user interface criteria

Criteria	CAPRA	HAZUS	RiskScape	InaSAFE	OASIS	IN-CORE	CLIMADA	CATSIM	RiskChanges
No dependence on other paid software	✓	x [1]	✓	✓ [2]	✓	✓	✓	✓	✓
Proprietary user interface	✓	✓	x [3]	✓	✓	x [4]	x [4]	✓	✓

Notes:
1. The use of HAZUS requires ArcGis but the functions that have been developed in Python do not require this software.
2. InaSAFE is a license-free QGIS plugin
3. RiskScape operates from the command line
4. Both IN-CORE and CLIMADA run in the Python/Jupyter environment so they have no interface of their own and the functions and visualization are done through user-generated Python code.

1.2.6. Conceptual framework for risk estimation

Multi-hazard platforms are structured in modules that address different aspects of risk analysis. CAPRA, for example, includes modules to assess specific hazards such as floods, mass movements, hurricanes and earthquakes, as well as a vulnerability module and CAPRA-GIS, a specialized tool for probabilistic risk calculation. In the case of HAZUS, the modules correspond to the following hazards: earthquakes, hurricanes, floods and tsunamis.

On the other hand, tools such as RiskScape and OASIS are designed with modules that integrate hazard, exposure and vulnerability analysis. OASIS adds a financial module to assess the economic impact of disasters. IN-CORE extends this functionality by including modules focused on social impacts, recovery and optimization, while CATSIM focuses exclusively on macroeconomic risk assessment and financial strategy analysis. Although CLIMADA does not present modules in the traditional sense, it organizes its functionalities in packages covering entities[9], hazards and specific utilities. Finally, RiskChanges divides

[9] The entity class is a container class that stores the exposures and impact functions (vulnerability curves) needed for a risk calculation, as well as the discount rates and adaptation measures for a cost-benefit analysis of adaptation. Like hazard objects, entities can be read from files or created using code.

its tools between exposure modeling (section of the web tool where the layers of exposed elements and hazards are selected for exposure analysis), loss (section of the web tool where the type of loss to be calculated is chosen between population, quantification of objects, costs or geometry, which can be area, length or number and an event characterized by a return period) and risk (section of the web tool where you can configure a complete risk analysis by scenario, for a hazard or multi-hazard). Riskchanges also contains a vulnerability curve database that allows users to share curves.

Regarding the results and metrics calculated, the platforms can generate risk curves, which allow for the calculation of the expected annual loss (EAL) for both physical and human losses, depending on how the exposed elements and vulnerability are entered. InaSAFE is an exception, as it only performs exposure calculations and does not generate risk estimates.

In the case of OASIS and CATSIM, no documentation was identified indicating that these tools calculate social metrics. CATSIM, in particular, is restricted to an exclusively macroeconomic approach.

Tools such as CAPRA, OASIS, RiskScape, IN-CORE and CLIMADA stand out for their flexible and robust design

- **CAPRA and OASIS,** in particular, were designed primarily to perform probabilistic analyses spanning hundreds or thousands of events.
- **RiskScape, IN-CORE and CLIMADA** have an approach that covers both the analysis of a limited number of events and the execution of calculations with an unlimited number, thanks to their integration in Python environments.
- **HAZUS and RiskChanges** are designed for the analysis of limited groups of events, particularly floods and earthquakes in the case of HAZUS, and all hazards in RiskChanges

- The initial versions of HAZUS even restricted the number of events analyzed (5 for floods and 8 for earthquakes), although in version 7 this limitation seems to have been overcome, requiring manual configuration in ArcGIS.
- In the case of RiskChanges, in its web-based version, it also requires manual configuration of the analyses, although its integration with Python could allow the flexibility to run analyses with a high number of events through code developed by the user.

The quantification of uncertainty in the tools evaluated focuses on hazards, with three notable exceptions: CAPRA, which includes uncertainty in vulnerability curves; IN-CORE, which employs advanced methods in vulnerability uncertainty quantification such as Monte Carlo Limit State Probability; and CLIMADA, which uses its Unsequa module to perform global uncertainty analysis, including hazard, exposure, and impact function (Kropf et al. 2022).

In general, the tools do not impose restrictions on the use of files for analysis. Typically, hazards are modeled using standard format raster files, exposure using shapefiles, and vulnerability curves are entered using text files or directly into the interface. The only exception is CAPRA, which requires hazard descriptions in a specific *.ame file format.

All platforms allow for spatial visualization of results, except CATSIM, whose focus is limited to macroeconomic analysis.

Table 5. Conceptual framework criteria

Criteria	CAPRA	HAZUS	RiskScape	InaSAFE	OASIS	IN-CORE	CLIMADA	CATSIM	RiskChanges
Risk curve and expected annual loss (EAL)	✓	✓	✓	X	✓	✓	✓	✓	✓
Some type of social risk metric	✓	✓	✓	✓ [3]	X	✓	✓	X	✓
Designed for probabilistic analysis[4]	✓	X [1]	✓	X	✓	✓	✓	X	X
No restrictions on the use of some file formats	X	✓	✓	✓	✓	✓	✓	✓	✓
Methods for analyzing uncertainty in the vulnerability component	✓	X [1]	X [2]	X	✓	✓	✓	X	X
Spatial visualization of results	✓	✓	✓	✓	✓	✓	✓	X	✓

Notes:

1. Although the tools have not been designed to perform fully probabilistic analyses in the case of floods, earthquakes and tsunamis, the exception is hurricanes, where Hazus does consider events generated over a long period and takes into account the uncertainty in the impact.
2. Although the methods are not available in the tool they could be developed using Python and integrated into the RiskScape workflow.
3. InaSAFE can produce population exposure values, although not strictly risk values. However, this will be considered sufficient from a human risk analysis point of view.
4. In this document, probabilistic analysis implies that it is necessary to analyze hundreds or thousands of scenarios.

1.2.7. Comparison of tools

The consolidation of the evaluated aspects is shown in **Table 6**. The three tools that meet the highest number of criteria are CLIMADA, IN-CORE and OASIS with 12 criteria met.

Table 6. Summary of criteria met by each tool evaluated

Criteria	CAPRA	HAZUS	RiskScape	InaSAFE	OASIS	IN-CORE	CLIMADA	CATSIM	RiskChanges
Open Source	✗	✗	✓	✓	✓	✓	✓	✗	✓
GitHub	✗	✗	✗	✓	✓	✓	✓	✗	✓
Contact with developers	✗	✓	✓	✓	✓	✓	✓	✓	✓
Manuals and support	✓	✓	✓	✓	✓	✓	✓	✓	✓
Update in the last two years	✗	✓	✓	✗	✓	✓	✓	✗	✗
No dependence on other paid software	✓	✗	✓	✓	✓	✓	✓	✓	✓
Proprietary user interface	✓	✓	✗	✓	✓	✗	✗	✓	✓
Risk curve and expected annual loss	✓	✓	✓	✗	✓	✓	✓	✓	✓
Some type of social risk metric	✓	✓	✓	✓	✗	✓	✓	✗	✓
Designed for probabilistic analysis	✓	✗	✓	✗	✓	✓	✓	✗	✗
No restrictions on the use of some file formats	✗	✓	✓	✓	✓	✓	✓	✓	✓
Methods for analyzing uncertainty in the vulnerability component	✓	✗	✗	✗	✓	✓	✓	✗	✗
Spatial visualization of results	✓	✓	✓	✓	✓	✓	✓	✗	✓
Total criteria met	**8**	**8**	**10**	**9**	**12**	**12**	**12**	**6**	**10**

Although all the tools evaluated have valuable aspects that can contribute to risk calculation, IN-CORE and CLIMADA stand out for their significant progress compared to the others. In addition to the criteria evaluated and consolidated in **Table 6**, a more in-depth exploration of these two tools, which included the review of manuals and the development of tutorials, made it possible to identify the advantages presented in the **Table 7**.

Table 7. Advantages of IN-CORE and CLIMADA

IN-CORE	CLIMADA
Contains specific functions for risk analysis in infrastructure such as roads, electrical and drinking water systems.	Provides functions for direct access to climate change models and has an API (Application Programming Interface) that allows access to exposure and hazard data.
Contains functions to estimate population impacts, for example, population displacement after a disaster.	Provides methods for generating exposure layers from global information.
Contains functions for analysis of socio-economic impacts of disasters.	Allows use of Google Earth Engine.
Contains functions for analyzing recovery.	CLIMADA can be run on the Euler cluster at ETH Zurich University, although the documentation does not clearly specify whether people outside the university can use the cluster or under what conditions.
Has web tools, and through the In-CORE lab, it is possible to develop and execute code on the NCSA (National Center for Supercomputing Applications) cloud system.	Has a particular focus on the cost-benefit assessment of adaptation measures.
	The Unsequa module allows uncertainty and sensitivity analysis for hazard, exposure, vulnerability function, and adaptation measures parameters.

- Free, open source.
- Flexible and adaptable to the user's needs.
- It works in the Python environment, so it can be combined with any other library.
- The methods developed are supported by peer-reviewed publications.

Both IN-CORE and CLIMADA have been developed for probabilistic risk analysis, implementing various uncertainty quantification methods that have been developed and published by the Center of Excellence for Community Risk-Based Resilience Planning located at Colorado State University in the case of IN-CORE and by ETH Zurich in the case of CLIMADA. The advantages presented in **Table 7** are not shared by the other tools evaluated, which makes them stand out. However, both have disadvantages. Both tools have their documentation developed in English, which could limit their access in Latin America, requiring the development of material in Spanish. In addition, both require user experience in Python, which makes the user profile specific; in addition to being an expert in hazard analysis and risk calculation, the ability to develop code in Python is required. In the case of IN-CORE, some of the functions are based on information available in the United States, so adaptations would be necessary for other contexts.

1.3. PLATFORMS FOR FLOOD RISK CALCULATION

Image: Adobe Stock

The literature review identified platforms developed primarily to analyze flood risk. These platforms do not show the degree of development and sophistication of methods found in the IN-CORE and CLIMADA platforms analyzed in section 1.2 and therefore will not be compared in detail in this section, although all their characteristics along with the other platforms can be consulted in Annex A.

The tools reviewed were:

- **FloodRisk:** a free and open source plugin for QGIS that provides an assessment of the consequences of flooding, including loss of life and direct economic damage. The plugin allows users to perform a simple risk assessment considering fixed events where the probability of each event is estimated separately and the consequences are calculated deterministically.

- **FloodRISE (Flood Resilience, Insurance, and Spatial Equity)** is a project led by the University of California, Irvine, that focuses on improving flood resilience through the development of high-resolution flood hazard simulations. The project aims to provide flood risk visualizations that are useful for local decision making by involving communities in the process of co-developing flood hazard maps. FloodRISE uses metric-scale flood hazard simulations to

assess risks in different types of floods (coastal, fluvial, pluvial). The approach includes iterative stakeholder engagement through meetings, surveys, and training sessions to develop customized flood hazard maps for each community.

- **Delft-FIAT (Flood Impact Assessment Tool)** is a tool developed by the Deltares research institute that is used to quickly assess the direct economic impacts caused by floods on infrastructure, buildings, and roads. This open source, Python-based tool is particularly useful in climate adaptation planning, as it allows for rapid modeling of the impacts of different flood scenarios and corresponding mitigation measures. Delft-FIAT stands out for its automation capacity and flexibility, making it a solution that can be adapted to different analysis needs.

- **HEC-FDA (Hydrologic Engineering Center - Flood Damage Reduction Analysis)** is a tool developed by the U.S. Army Corps of Engineers (USACE). Its main objective is to assess and quantify the economic damages associated with flood events, assisting decision making in flood risk reduction projects. HEC-FDA employs probabilistic methods to analyze the relationship between flood frequency and potential damages, allowing the estimation of benefits and costs associated with different risk mitigation measures.

Of these four tools evaluated, Delft-FIAT and HEC-FDA stand out. The former stands out because it is a script that can be used simply and effectively to calculate damage in scenarios ranging from a few to hundreds. Moreover, being a Python script, it can be integrated into more complex codes according to the needs of the analysis. In the case of HEC-FDA, one of its major contributions is that it integrates the evaluation of the performance of protection measures, such as a dam, into the risk analysis, assessing the capacity of the protection systems and the probability of their failure. The tool uses Monte Carlo simulations to evaluate the uncertainty of the functions that describe the frequency of flow, water level, flood damage, etc., and the performance of the protection system, generating a probabilistic risk assessment. No advantage was identified for Delft-FIAT over IN-CORE or CLIMADA, apart from its greater simplicity, particularly the possibility of using this tool through Excel. In the case of HEC-FDA, the method implemented to integrate protection systems into the risk assessment is an advantage over IN-CORE or CLIMADA. However, in Latin America, few risk analyses consider these systems, so this tool would be especially useful only in situations where it is necessary to evaluate the uncertainty associated with the functioning of protection systems or to implement a methodology for quantifying curve sampling uncertainty (for more details on the method, see **Annex A**).

1.4. PLATFORMS FOR SEISMIC RISK CALCULATION


Image: Adobe Stock

In terms of platforms that are exclusively for seismic risk calculation, the only tool that stood out from the literature review was the OpenQuake Engine (https://www.globalquakemodel.org/product/openquake-engine), developed by the Global Earthquake Model (GEM) Foundation. Other popular tools used in the field of seismic analysis, such as R-CRISIS (http://www.r-crisis.com/) are excluded from this review because they focus on the hazard component and do not incorporate exposure and vulnerability to perform seismic risk estimates.

The review of OpenQuake was carried out considering the same criteria with which multi-hazard risk platforms were evaluated.

1.4.1. Accessibility

OpenQuake is an open source development that is available in a public repository on GitHub (https://github.com/gem/oq-engine) under an open AGPL v3.0 license. Its development is almost entirely carried out in the Python language. In addition, for each release of new versions, compiled executables are available to run the platform on Windows, Mac, and Linux systems.

1.4.2. Development and support community

In the case of OpenQuake

The initial version of OpenQuake was released in 2013, demonstrating stability in development and sustainability over an extended period of time.

The platform receives ongoing maintenance provided by the GEM Foundation, which has been operating since 2009. GEM receives funding from multiple sponsors, which ensures the project's continued support.

OpenQuake has successfully built a strong and active community of users and developers.

The community that interacts through an online public forum (https://groups.google.com/g/openquake-users), where users can ask questions about its operation and these are answered directly by GEM's team of developers, as well as by the general public.

1.4.3. Upgrades and continuous improvement

OpenQuake

OpenQuake is continuously updated, ensuring ongoing improvements and the introduction of new functionalities. The platform follows a structured development cycle that includes Long-Term Support (LTS) versions. These LTS releases remain stable for several years, facilitating their use in long-term projects without the need for frequent updates.

In parallel, experimental versions are developed that incorporate the latest technical innovations. This approach allows users to choose between stability and access to advanced features, depending on their specific needs.

The latest stable version available at the time of writing this report is version 3.23 ("Bellamy"), released in February 2025. This release reflects the development team's continued commitment to the evolution and maintenance of OpenQuake.

1.4.4. Graphical user interface (GUI)

The OpenQuake Engine does not have a separate graphical user interface, however, there is the possibility of installing a QGIS plugin (https://plugins.qgis.org/plugins/svir/) that allows you to run the platform's analyses when both are installed on the same system. The plugin does not have the full functionality of the OpenQuake Engine, but focuses on the most recurrent functions for beginner to intermediate users. At the same time, the plugin development scheme is different from that of the platform and does not have the same update cycle. However, the plugin is a great advantage as it allows users to familiarize themselves with the platform in a visual way, using QGIS which is itself a very popular and freely available system.

1.4.5. Conceptual framework for risk estimation

The OpenQuake Engine has a set of calculation modules to perform probabilistic analyses, which can consider only hazard estimates or incorporate exposure and vulnerability information to calculate seismic risk metrics. For hazards, the platform can perform individual event assessments or seismic hazard potential estimation considering multiple sources (seismic faults and magnitude-recurrence functions), either through the integration of the sources (identified as the classical method in the documentation), or through the simulation of a set of events. The platform uses its own input file definition for hazard definition (XML files to represent faults and logical trees), exposure (CSV files) and vulnerability (XML files). The documentation provides examples for generating these files in the correct format, and the GEM Foundation makes compatible files available under open licenses, representing its interpretations of each component for most parts of the world. Finally, the platform has commands to easily obtain products and risk metrics, such as economic loss exceedance curves, estimates of average annual fatality, displaced populations and other humanitarian metrics.

Image: Adobe Stock

1.5. CONCLUSIONS


Image: Adobe Stock

The multi-hazard platforms IN-CORE and CLIMADA stood out in the evaluation conducted, as they meet a number of key criteria, such as accessibility, support from the development community, software availability, graphical user interface and a sound conceptual framework for risk estimation. They outperform the other platforms evaluated in these aspects and have advantages that place them at the forefront of risk calculation for multi-hazard platforms.

Regarding flood risk assessment, two tools with notable advantages were identified: Delft-FIAT, for its simplicity and flexibility, although without exceeding the capabilities of IN-CORE or CLIMADA, and HEC-FDA, which is particularly useful in cases where the operation of protection systems is to be included in the risk analysis.

Regarding the calculation of seismic risk, the OpenQuake platform is the only one found in the literature that meets the open source requirements required for this review. However, the platform stood out for meeting a number of key criteria and represents an excellent option for use in estimating seismic risk metrics.

SECTION 2

Image: Adobe Stock

ARTIFICIAL INTELLIGENCE METHODS IN RISK CALCULATION

2.1. INTRODUCTION


Image: Adobe Stock

Artificial intelligence (AI) encompasses computer science-related activities that seek to develop intelligent machines capable of performing tasks that, traditionally, require human intervention (Abid et al. 2021). According to McCarthy (2007), AI is “the science and engineering of making intelligent machines, especially intelligent computer programs”.

There are several classifications of artificial intelligence (AI), and one of which is shown in Figure 1, proposed by Ivić, (2019). In this figure, the branches of AI include machine learning (ML), deep learning (DL), natural language processing (NLP), expert systems (ES), as well as robotics, computer vision and speech recognition.

Figure 1. Artificial intelligence branches

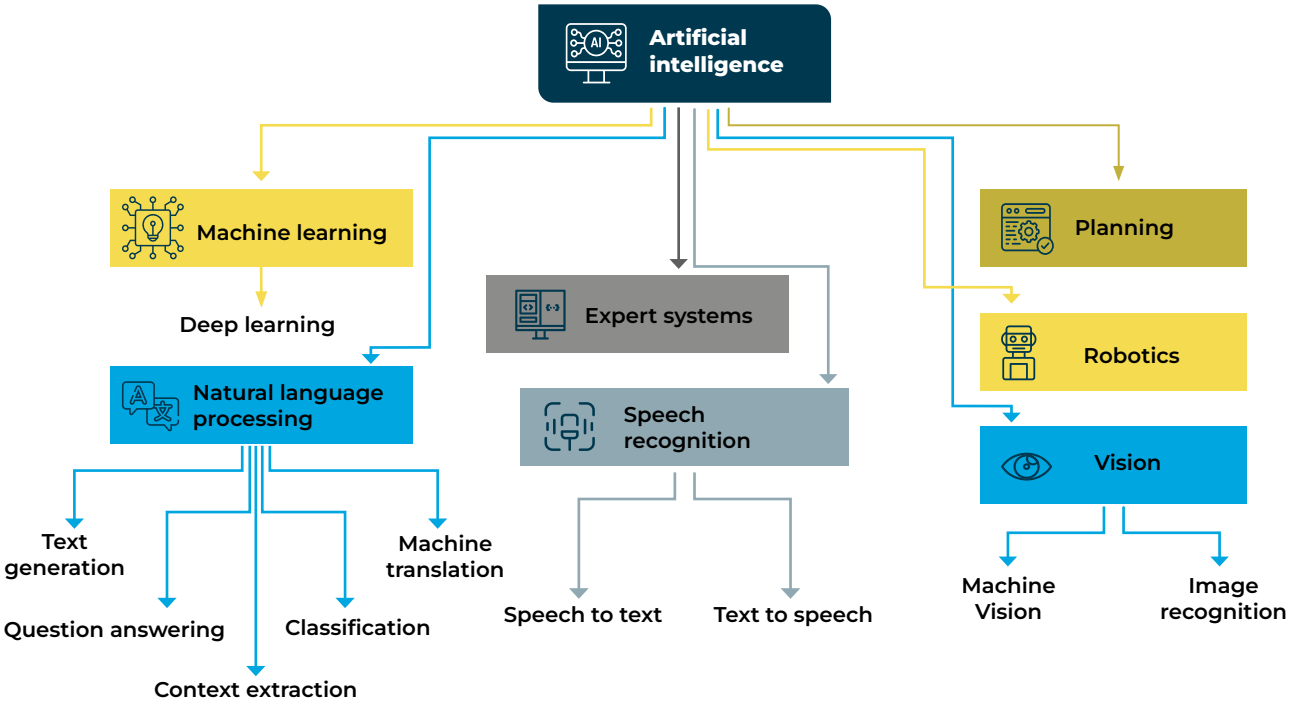

Source: Ivić (2019).

ML is present in most AI applications. It is a branch of AI that allows systems to learn and improve from experience without being explicitly programmed (expert.ai 2024). There are three main types of ML: supervised, unsupervised and deep learning (DL). Machine learning algorithms that are trained by humans based on pre-existing data are called supervised, while those that learn solely from data without human intervention are known as unsupervised (Global Facility for Disaster Reduction and Recovery (GFDRR) 2018). Deep learning uses artificial neural networks inspired by the human brain to process data at multiple layers of abstraction (GFDRR 2018; Ivić 2019).

Supervised learning is divided into classification and regression problems. In classification, the expected result is a semantic label or class. Regression problems, on the other hand, seek to predict a continuous variable. There are different types of supervised learning algorithms, sometimes with fundamentally different architectures. The most common algorithm for classification is logistic regression, while the most commonly used algorithm for regression is linear regression. Among the most well-known classification algorithms are random forests, gradient boosting, support vector machines (SVMs), naive Bayesian models, and gradient boosting Bayesian networks (GFDRR 2018).

One of the most common applications of unsupervised ML is clustering, where samples are grouped according to their similarity. Other applications include dimensionality reduction and anomaly

detection to reduce variance in a dataset and filter outliers. Unsupervised methods rely solely on data patterns, which depend on the statistical characteristics of the input samples. Frequently, the results of unsupervised learning algorithms are fed into supervised learning algorithms, where human intervention can help to achieve higher accuracy on the data set more quickly. There are three types of unsupervised machine learning: k-means clustering, principal component analysis (PCA) and t-SNE (t-distributed Stochastic Neighbor Embedding) (GFDRR 2018).

Table 8 shows the classification of AI methods proposed by Sun et al. (2020) including not only supervised, unsupervised and DL models but also reinforcement learning, deep reinforcement learning and optimization. Reinforcement learning is a type of machine learning inspired by behavioral psychology. In simple terms, the training dataset and rules in a machine learning algorithm are not binary decisions (yes or no), but seek to strike a balance between data exploration and accuracy. In other words, the model is allowed to make errors and explore the data within certain parameters (GFDRR 2018).

Table 8. Classification of AI methods

Name of method	Description	Uses
Supervised Models	Algorithms trained with labeled data, where both inputs and outputs are known. They use regression and classification methods to predict results.	Object recognition in computer vision, information extraction, pattern and speech recognition.
Unsupervised Models	They use statistical methods to find hidden structures in unlabeled data based on the inherent characteristics of the data.	Data clustering, dimensionality reduction, anomaly detection, data detection, data aggregation.
Deep Learning	Algorithms that use multiple layers to progressively extract data features. Suitable for complex problems requiring high processing capacity.	Motion detection, natural language processing (NLP), facial recognition, transportation prediction, etc.
Reinforcement Learning	Algorithms that learn through reinforcement (punishments and rewards) to make decisions in a sequence of actions. They are based on Markov decision processes.	Robotics, traffic control, resource management in complex and changing environments.
Deep Learning by Reinforcement	It combines reinforcement learning with deep neural networks to solve complex sequential tasks, optimizing long-term decisions.	Computer vision, robotics, finance, smart grid management.
Optimization	Techniques used in most AI methods to improve the performance of models by evaluating their performance using an objective function.	Optimization of models for disaster management, improvement of AI algorithms in various domains such as planning and logistics.

Source: Sun et al. (2020).

Machine learning (ML) methodologies are increasingly being applied in all fields, including disaster risk management (DRM). These applications aim to improve risk modeling and resource prioritization during response and reconstruction. Satellite imagery analysis and computer vision approaches have been used to better understand physical and socioeconomic exposure, as well as to identify vulnerabilities. In addition, artificial intelligence is enhancing hazard modeling through the use of physical and remote sensor data, and has advanced damage prediction. Applications have also been developed to prioritize resources during the response and recovery phases, including inspection prioritization, social media mining, and computer monitoring reconstruction using computer vision (GFDRR 2018).

Jones et al. (2023) grouped AI methods into three categories in relation to their application to flood risk assessment as shown in **Table 9**, highlighting that they can improve the computational efficiency of models, allowing the quantification of uncertainty by taking advantage of new geospatial datasets. This not only optimizes model performance, but also increases the accuracy of predictions and analysis, providing better tools for decision making and planning in various contexts

Table 9. Artificial intelligence method groups

Name of method	Description	Advantages	Disadvantages
Data-driven modeling	Refers to the use of machine learning (ML) techniques to create empirical models based solely on observed data. These models can address the lack of scientific knowledge or complexity of the system. They are useful for predicting specific events at the local level by adjusting existing physical models. Examples include fire hazard prediction and flooding patterns.	It reduces computational costs and is ideal for adapting to local conditions.	Difficulty in interpreting the results ("black box") and the need for accurate local data.
Surrogate modeling	It consists of training an ML model using simulated data, in order to replace the original simulations with versions that are more efficient and faster to run. This approach is efficient for performing calibration tests and sensitivity analysis, especially in situations where simulations are expensive.	Reduces simulation time and computational cost. It can be applied in climate model calibrations and impact predictions.	Accuracy may decrease if the surrogate model does not capture all the complexities of the original.
Exploitation of geospatial big data	It uses AI and ML techniques to analyze large amounts of geospatial data such as satellite imagery or sensor data. These methods are particularly useful in the automatic detection of extreme weather events such as floods or forest fires.	Accelerates the analysis of large volumes of data and improves the accuracy of climate risk mapping.	It requires advanced computing infrastructure to handle large volumes of data, and the complexity of the data can be a major challenge.

Source: Jones et al., (2023).

The following sections present a literature review of the main applications of AI in risk management processes.

2.2. AI APPLICATIONS IN DISASTER RISK MANAGEMENT

Image: Adobe Stock

To illustrate how various AI methods have been applied in disaster management, Sun et al. (2020) identified a total of 26 artificial intelligence methods and 17 representative areas of application. To perform this analysis, the names of the methods and areas of application were used as keywords in searches on academic websites such as Google Scholar and Web of Science. The results are presented in **Figure 2**, which show the applications of AI methods in the four phases of disaster management and their sub-areas. Each solid line in the figure indicates the presence of applications in a given area. The mitigation and response phases stand out as having more solid lines connecting to the areas of application, suggesting a greater number of studies applying AI methods in these phases.

Artificial intelligence methods, such as regression (linear, nonlinear and logistic), are used to assess hazards and risks, as well as to evaluate the potential impact of disasters. Support vector machines also provide forecasts and risk assessments. Neural networks, hierarchical clustering, k-means, fuzzy clustering and principal component analysis have been used to develop and compare mitigation strategies, training systems and disaster evacuation procedures. However, deep learning (DL) techniques, such as convolutional neural networks, deep neural networks and multilayer perceptron, are mainly used for risk mapping. In addition, more recent techniques, such as Deep Q networks and genetic algorithms, have been employed to assess loss and repair costs (Abid et al. 2021).

Another field in which AI has begun to play a key role in disaster risk modeling, especially in the hydrological and hydraulic field, is assisted coding. Tools such as ChatGPT and AI-assisted coding environments are revolutionizing the way engineers and data scientists approach risk model simulation and analysis. These tools enable efficient manipulation of model files, extraction of relevant data, and automation of complex tasks, resulting in a more streamlined and efficient workflow (Australian Water School 2024).

Image: Adobe Stock

Figure 2. Artificial intelligence methods and areas of application in disaster risk management

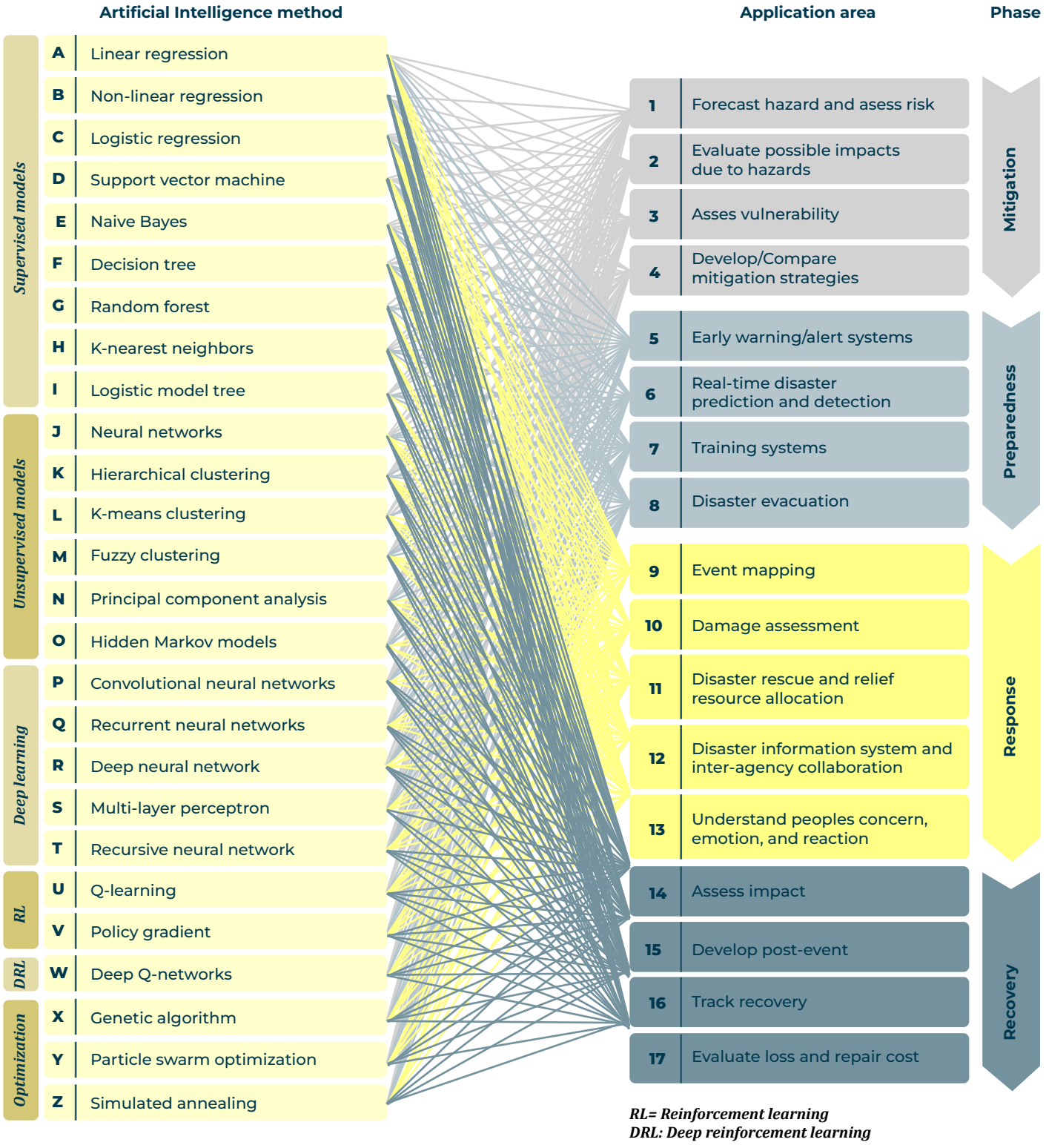

Source: Sun et al. (2020).

2.2.1. Disaster mitigation and preparedness

AI methods have been widely used in hazard and risk assessment. Among them, supervised and unsupervised models are the most common, while reinforcement learning and DL are more recent and emerging methods. Traditional risk identification techniques can be laborious and have high false-positive rates, making AI techniques particularly useful for analyzing large volumes of data more quickly and efficiently (Sun et al. 2020). Hazard assessment is the stage most studied by academics, employing methods such as evolutionary systems (ES), artificial neural networks (ANN), fuzzy logic (FL), support vector machines (SVM) and adaptive neuro-fuzzy inference systems (ANFIS). Research focuses on disaster risk assessment, monitoring and early warning, covering floods, earthquakes, mass movements and other hazards (Tan et al. 2020).

Several studies have shown that AI can assess hazards through data analysis. For example, decision tree, computer vision, deep learning, and machine learning methods have been used to analyze floods, mass movements, and forest fires. These techniques have proven to be effective in hazard mapping and event forecasting.

AI techniques are also applied to estimate potential impacts, assess vulnerability and predict structural damage through fragility curves. Although there are fewer applications of AI in impact estimation and vulnerability assessment compared to hazard assessment, these tools hold promise for developing more effective mitigation strategies. In addition, AI techniques can help identify management priorities and optimize response plans. On the other hand, research on the use of AI to compare mitigation strategies is still limited (Sun et al. 2020).

Image: Adobe Stock

One of the main benefits of AI is its ability to analyze large volumes of data quickly and accurately. This makes it an invaluable tool for identifying the areas most vulnerable to the effects of climate change, such as areas prone to floods, mass movements or droughts. By analyzing data such as climate models, satellite imagery and weather patterns, governments and communities can develop risk-specific adaptation plans. AI facilitates access to information, which makes it possible to design adaptation strategies in the face of climate change (Jain et al. 2023).

From a **flood** management perspective, studies focus on four main aspects: flood risk assessment, level and flow forecasting, rainfall-runoff modeling, and flood frequency analysis (Tan et al. 2020). For level and flow forecasting, both single and hybrid methods have been used, with hybrids being those that combine different approaches to improve the accuracy and scope of the assessments. In addition, in the modeling of the rainfall-runoff process, several methodologies have been used to simulate flows in basins, highlighting studies that integrate optimization algorithms. Although flood frequency analysis is still in its infancy, some research has begun to address this issue by using neural networks and support vector regressions to estimate flood quantiles in specific areas (Tan et al. 2020).

In the literature review conducted by Bentivoglio et al. (2022), they found that multilayer perceptron (MLP) methods and convolutional neural networks (CNNs) were the most common types of deep learning models in flood mapping, while recurrent neural networks (RNNs) were used less frequently. To overcome their lack of inductive biases and to achieve good accuracy, MLPs are often combined with other statistical techniques. On the other hand, thanks to their spatial and temporal inductive biases, CNNs and RNNs were found to regularly outperform other models. Regardless of the application, the results show that deep learning solutions outperform traditional approaches and other machine learning techniques. Deep learning models used for surrogate modeling offer significant acceleration (up to three orders of magnitude) while maintaining sufficient accuracy (Bentivoglio et al. 2022). An example of the application of deep learning models in flood hazard assessment is the work of McSpadden et al. (2023) which compared surrogate rainfall flood models showing the advantages of deep learning (DL) for quantification of uncertainty while maintaining high levels of accuracy and showing its high potential in disaster risk management.

AI-supported **climate modeling and projections** refer to the use of techniques to improve the accuracy and reliability of these models. Climate modeling uses simulations to understand how factors such as greenhouse gas emissions affect the Earth's climate over time. From these models, projections are made to predict future climate changes. AI can analyze large volumes of data from a variety of sources, such as satellite imagery and weather patterns, to identify trends and patterns not evident through traditional methods, helping to reduce uncertainties in climate simulations and predictions. There are several AI techniques that can be applied, such as machine learning algorithms and neural networks. The benefits of AI-supported climate modeling include increased accuracy, faster and more efficient analysis of climate data, and a better understanding of the potential impacts of climate change in different regions

and ecosystems. This information is crucial for informing policy decisions and guiding climate change adaptation and mitigation efforts. Examples of AI-supported climate modeling and projection systems include Google Earth Engine, Climate.ai, IBM Watson, and Microsoft Azure as shown in Table 10 (Jain et al. 2023).

Table 10. AI-supported climate modeling and projection systems

AI System	Function	Reference
Climate.ai	Uses AI to analyze climate data and generate probabilistic climate change scenarios for future modeling and projections.	Dewitte et al. (2021).
DeepMind	Uses AI to improve climate modeling accuracy by reducing uncertainties in climate simulations and predictions.	Subramaniam et al. (2022).
Google Earth	Uses AI to analyze satellite data and generate high-resolution climate models and projections.	Yang et al. (2022).
Engine IBM Watson	Uses AI to generate climate projections and assess risks of climate impacts on infrastructure and supply chains.	Yigitcanlar et al. (2020).
Microsoft Azure	Uses AI to create high-resolution climate models and projections using satellite data and machine learning algorithms.	Khan et al. (2023).

Source: H. Jain et al. (2023).

In addition, AI-based climate models allow policymakers to anticipate impacts and design strategies. For example, AI-powered sensors and drones enable real-time monitoring and analysis of the impacts of extreme weather events, improving response and management of their effects. Similarly, machine learning algorithms help create predictive models of climate change, allowing decision makers to plan and take proactive measures to protect communities and businesses (Jain et al. 2023).

Table 11 presents several projects and models that use AI techniques to address different aspects related to **flood analysis and the impact of climate change** on coastal infrastructure. Each project is characterized by the technology it uses, its main objective and the types of data it analyzes. For example, CoastalDEM (Kulp and Strauss 2018), focuses on the creation of digital elevation models to identify areas exposed to coastal flooding. In addition, projects such as CoastalAI and Deltares (Jain et al. 2023) use AI to simulate the impact of sea level rise on infrastructure, enabling the development of adaptation strategies that protect at risk communities and infrastructure. Overall, these initiatives show how AI can be a powerful tool for improving resilience to climate-related challenges.

Table 11. Examples of projects using AI in flood and climate change analysis

Project/Model	Technology used	Objective	Data analyzed	Expected results
CoastalDEM	Neural networks.	Create high-resolution elevation maps.	Satellite images, elevation data.	identify at risk areas.
DeepSD	Deep learning.	Predicting changes in weather patterns.	Climate model data.	Regional temperature and precipitation forecasts.
Climate Informatics Toolbox	Automatic learning.	Provide tools to analyze climate data.	Climate model data.	Identification of patterns and trends in climate data.
CoastalAI	Automatic learning.	Simulating the impact of sea level rise on infrastructure.	Climate and infrastructure data.	Adaptation strategies to protect vulnerable communities.
Deltares	Automatic learning.	Simulating the impact of sea level rise on infrastructure.	Climate and infrastructure data.	Adaptation strategies to protect vulnerable communities.

Source: H. Jain et al. (2023).

AI can be used to develop **early warning systems for weather events** such as hurricanes and floods, allowing communities to prepare and evacuate before disaster occurs. Machine learning, in particular, makes it possible to predict floods by analyzing historical data and detecting patterns that indicate the possibility of flooding (see Table 13 and Box 1 for examples of its application in early warning systems). By analyzing variables such as weather patterns, water levels, and other relevant variables, algorithms can estimate the likelihood of flooding and issue early warnings to people at risk, facilitating a rapid and effective response (Jain et al. 2023). In particular, AI has proven to be essential for improving the accuracy and coverage of flood forecasts. For example, neural network-based models such as LSTM (Long Short-

Term Memory) are being used to predict floods in real time, even in uncalibrated basins, where the lack of data typically makes forecasts less accurate. These models can integrate multiple data sources and generate reliable simulations of extreme events, which is crucial for disaster risk management (Nevo et al. 2022; Gegenleithner et al. 2024; Zhu et al. 2023).

An example of the use of AI in operational-level flood early warning systems is Google's system, which has demonstrated its effectiveness in helping vulnerable communities prepare for and respond to flooding. Google's system was developed to provide real-time alerts on river flooding in large monitored rivers (see Box 1 for more information on this system). Operational since 2018, it has expanded its geographic coverage and currently consists of four subsystems: data validation, level forecasting, flood modeling, and alert dissemination. Artificial intelligence is used in level forecasting and flood modeling, using LSTM networks and linear models to predict levels and to calculate flood extent and depth. During the 2021 monsoon, the system operated in India and Bangladesh, covering a region of 470,000 km² and sending more than 100 million alerts to the affected population and relevant authorities (Nevo et al. 2022).

In the field of **mass movements** , AI is being used in three key areas: detection, susceptibility and hazard assessment, and mass movement displacement prediction with very promising results. For example, Akosah et al., (2024) concluded that machine learning and deep learning algorithms and remote sensing technologies reasonably assess the mapping of susceptibility to mass movements, with prediction accuracy ranging from 56% to nearly 100%. He et al. (2024) condensed their findings on the most commonly used AI techniques in the above development areas into the diagram shown in Figure 3.

Mass movement detection consists of identifying and mapping events that have already occurred in a region, providing key information such as location, type, volume and date. Traditionally, this was done through visual interpretation of remote sensing imagery and aerial photographs, which was costly, time consuming and subject to interpretation bias. AI has facilitated the automation of this process,


Image: Adobe Stock

using image recognition technology that can identify mass movements more accurately and efficiently, reducing reliance on human interpretation and improving objectivity and reproducibility (He et al. 2024).

In the assessment of susceptibility and In the assessment of mass movement susceptibility and hazard of mass movements, IA helps to determine the probability of occurrence in a specific region. This evaluation is based on factors such as altitude, slope, soil type, distance to rivers and roads, among others. Traditionally, statistical methods and expert knowledge that depended on practical experience were used. With AI, machine learning (ML) models are used to map susceptibility more objectively and efficiently, eliminating highly correlated influencing factors and retaining those that are less correlated (He et al. 2024). In the case of single methods, trigger analyses, statistical classifiers (logistic regression and generalized additive model) together with machine learning techniques such as random forest (RF) and support vector machines (SVM) (Tan et al. 2020). On the other hand, hybrid methods integrate different approaches to provide a more complete assessment. Within these approaches, neuro-fuzzy networks and machine learning models, such as maximum entropy, SVM and artificial neural networks (ANN), have been used to perform spatial simulations (Tan et al. 2020).

An example of the application of computer vision in mass movement risk assessment is the Landslide Reporter project (NASA 2024), which uses data collection through public participation and machine learning to identify areas at risk of mass movement from satellite imagery. This project has been successful in identifying mass movement events and could help communities to take proactive measures to mitigate potential impacts (Prakash et al. 2021; Shameem Ansar et al. 2022; Jain et al. 2023).


Image: Adobe Stock

Figure 3. Current practices and future prospects for the application of AI in the assessment of susceptibility and hazard from mass movements

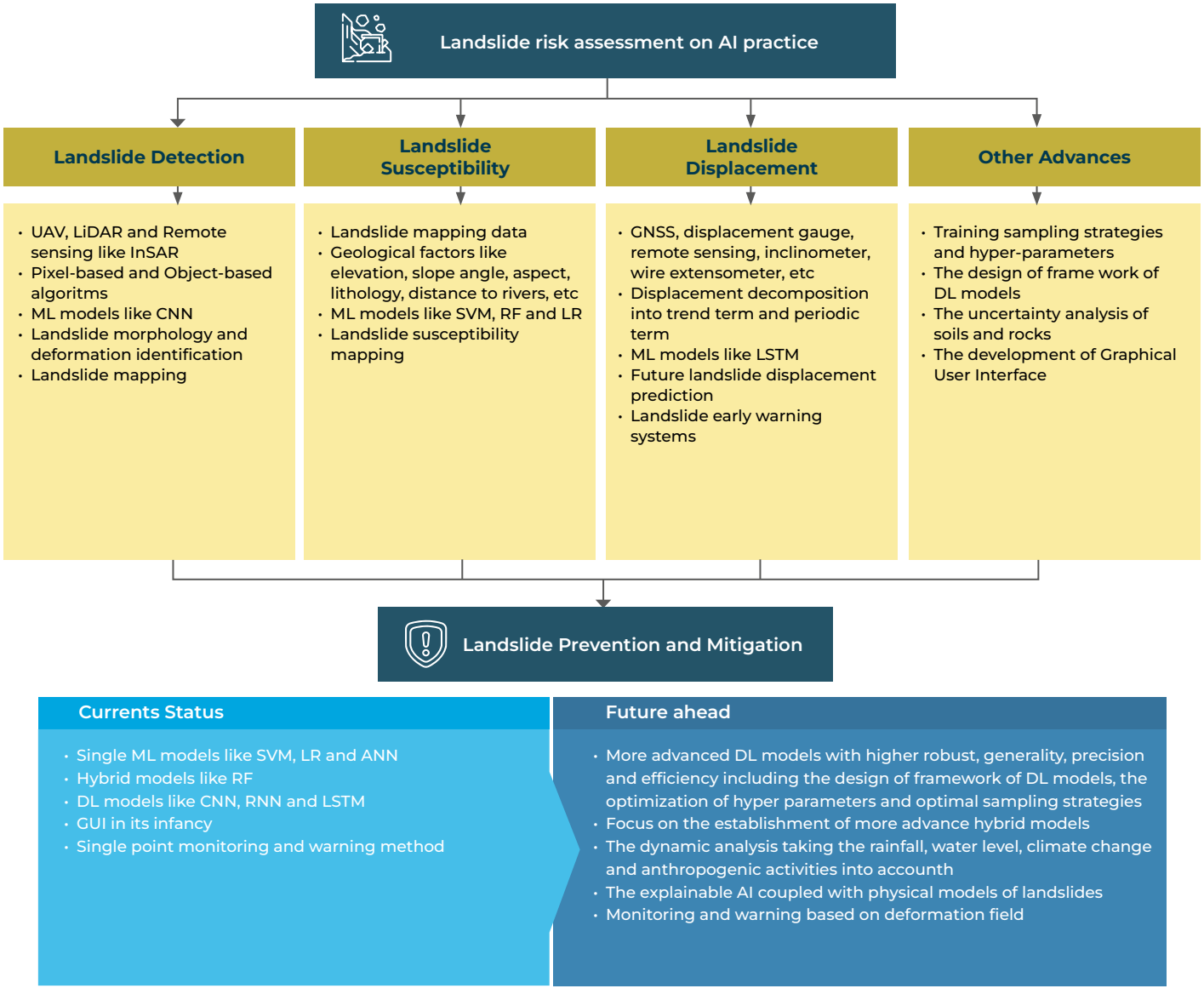

Source: He et al. (2024).

In terms of mass movement displacement prediction, AI, in particular deep learning (DL), is being used to predict the future movement of existing mass movements. Neural network models, such as convolutional networks (CNNs) and recurrent neural networks (RNNs), have proven to be useful in this regard. Although deep learning is still under development in this area, it has already been shown to provide higher accuracy results than conventional machine learning methods (He et al. 2024).

Table 12 summarizes the methods identified by He et al. (2024) as the best performers in the field of mass movements.

Table 12. Models with the best performance for each application in mass movements

Field	Best performing models
Detection of mass movements	Support vector machine, convolutional neural network, recurrent neural network and related hybrid models.
Mapping susceptibility and hazard to mass movements	Support vector machine, logistic regression, random forest, convolutional neural network, recurrent neural network and related hybrid models.
Prediction of mass movement displacement	Short- and long-term memory, transformer and hybrid models.

Source: He et al. (2024).

In the area of **seismic risk management**, AI is revolutionizing risk mapping by enabling more accurate and dynamic analyses. By processing large volumes of data and recognizing patterns, AI can refine hazard models, providing maps that are updated in real time as new data emerges (Plevris 2024). Both stand-alone and hybrid methods have been used. In the case of stand-alone methods, evolutionary systems have been used to predict the potential risk level of buildings due to seismic hazard, neural networks and deep learning technologies. Hybrid methods, on the other hand, combine different approaches to provide more robust assessments. For example, evolutionary SVM-based inference systems have been generated to integrate AI models (Tan et al. 2020). Figure 4 (a) shows an illustration of the interrelationship between AI techniques and data science in seismology. Machine learning algorithms, such as artificial neural networks (ANN), genetic programming (GP), self-organizing maps (SOM), support vector machines (SVM) and decision trees (DT), are used to train and find implicit determinations for seismic events. Deep learning, one of the most advanced algorithms in the field of machine learning, employs the concept of artificial neural networks (ANNs) to learn generalized representations of data sets in different domains and define complex nonlinear relationships between variables. The outstanding capabilities of machine learning on sequential datasets make it an optimal choice for the problem of phase association in seismology, suitable for real-time analysis of seismic networks (Jiao and Alavi 2020). Figure 4 (b) summarizes AI-based studies published in seismology between 1999 and 2019, showing that ANNs are the most widely used machine learning methods in this field, with increasing interest in the use of deep learning techniques (Jiao and Alavi, 2020).

Figure 4. Existing studies of AI and data science in seismology. (a) Illustration of the interrelationship between AI techniques and data science in seismology. (b) Summary of AI-based studies published in seismology during 1999-2019

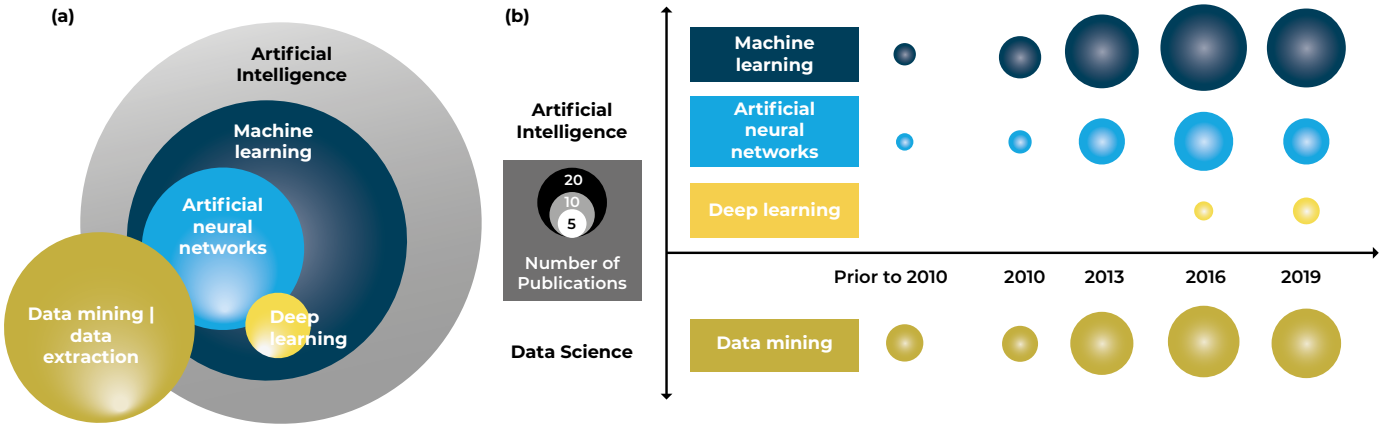

Source: Jiao and Alavi (2020)

Supervised and unsupervised learning approaches have attracted considerable attention in research on AI algorithms applied to seismology. Although machine learning (ML)-based seismic research has primarily focused on the use of supervised learning methods, unsupervised learning methods are likely to play a crucial role in seismology in the near future (Jiao and Alavi 2020). **Figure 5** shows the outlook for AI-based seismic analysis and highlights deep learning (DL) as one of the future trends for seismic prediction models. According to Jiao and Alavi (2020) although seismic systems developed with DL methods are still in their infancy, the biggest breakthrough in AI-enhanced seismology is likely to be achieved by combining DL with complex reasoning.

Figure 5. Future outlook and trends in AI-enhanced seismology, from machine learning (ML) to deep learning (DL).

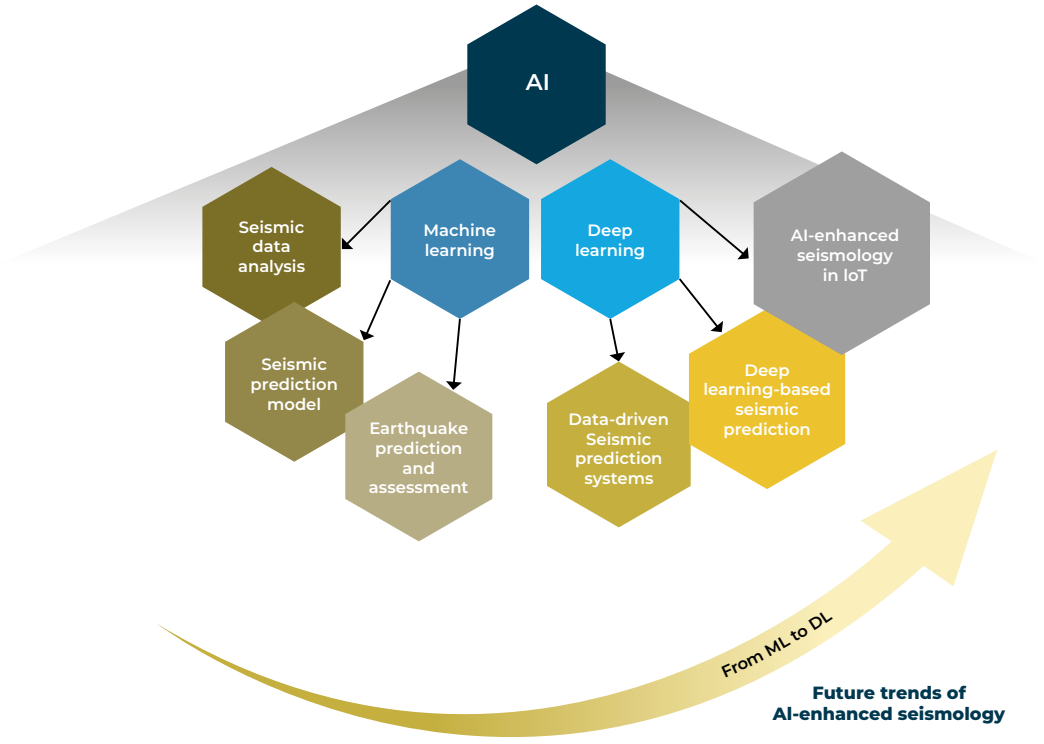

Source: Jiao and Alavi (2020)

In the field of earthquake early warning systems, the integration of AI promises to revolutionize these systems with the potential to improve their accuracy and speed. One example, of an AI-based earthquake early warning system is DeepShake, developed by researchers at Stanford University (Datta et al. 2022). This system uses deep spatiotemporal neural networks to improve earthquake detection. During the magnitude 7.1 earthquake that struck Ridgecrest on July 5, 2019, DeepShake issued specific alerts to all stations within its network 5 seconds prior to the arrival of seismic waves with an intensity greater than MMI IV (Modified Mercalli intensity scale - Light) (Plevris 2024). Another example is the EarthX system, in which researchers used AI technology to develop a real-time earthquake monitoring system capable of simultaneously processing data from more than 100 seismic stations in the Sichuan and Yunnan regions at the China Seismic Experimental Site (CSES). This system features automatic detection and collection of seismic phases (Zhang et al. 2020).

Seismic-resistant design faces limitations due to the increasing complexity of modern structures and the variability of seismic conditions. This is where AI plays a crucial role, offering advanced tools to process large volumes of data and optimize complex systems more efficiently. This results in innovative design solutions that balance safety, cost and sustainability. AI is revolutionizing this field through simulations that improve energy dissipation in different seismic scenarios, and optimize materials and structural

forms, achieving cost reductions of 18-26% through the use of large data sets (Plevris 2024). In addition, AI facilitates the development of generative designs, which offer multiple options for engineers to explore innovative alternatives that optimize seismic performance while reducing material usage and construction costs. Going forward, the integration of AI into earthquake-resistant design promises to transform the construction and maintenance of structures in seismically active regions by providing customized solutions that consider local and contextual factors (Datta et al. 2022).

In the case of **fires**, P. Jain et al. (2020) propose the classification of machine learning (ML) methods shown in **Figure 6**, finding that the application of ML methods in forest fire science and management has grown since the 1990s, mainly using traditional methods such as random forests (RF), support vector machines (SVM) and neural networks (ANNs). However, key areas such as predictive and prescriptive analytics have received less attention, opening up opportunities to apply ML in optimizing fire management. In addition, the increase in spatio-temporal data, such as remote sensing, favors the use of deep learning (DL) and agent-based learning to improve efficiency and accuracy in fire management. The use of DL has shown great capabilities as shown by Bjånes et al. (2021) in an application developed in two areas of Chile, finding that this method can generate fire susceptibility maps with very high performance metrics compared to other methods.


Image: Adobe Stock

Figure 6. Diagram showing the main machine learning (ML) types, data types and modeling tasks in relation to popular algorithms and possible applications in wildfire science and management. It should be noted that the algorithms shown in bold are fundamental ML methods, while algorithms that are not in bold are often not considered ML methods.

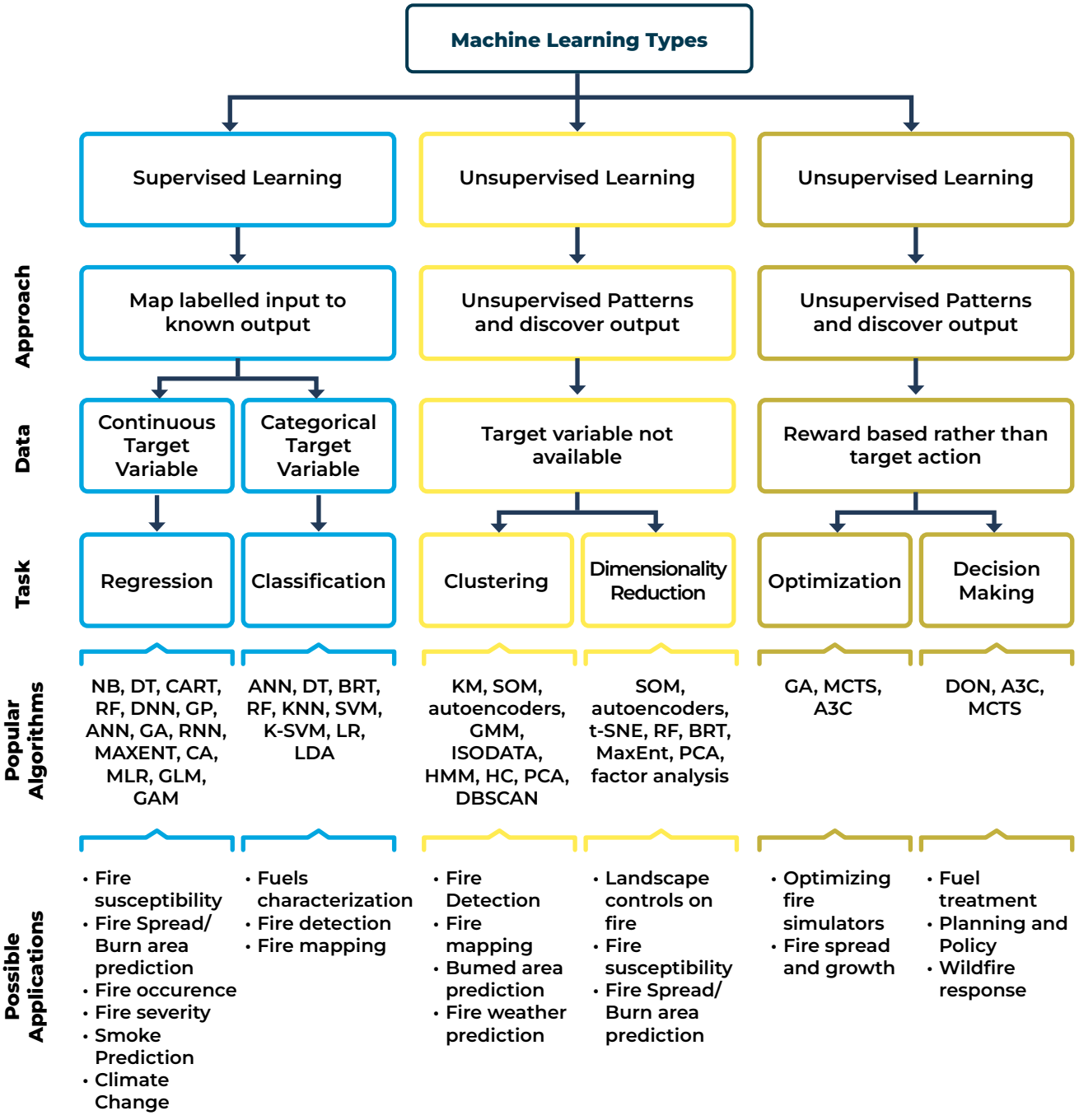

Source: P. Jain et al., (2020).

Table 13 presents a compilation of cases in which AI methods have been applied to assess hazard, vulnerability and risk in various contexts. Examples range from detecting seismic vulnerability in buildings using satellite imagery and deep learning algorithms to monitoring urban growth with convolutional neural networks. Each case includes details such as the project objective, input data, unit of analysis, algorithms used and a summary of the results obtained. This diversity of applications highlights the potential of AI in improving accuracy and efficiency in risk assessment, addressing complex issues such as floods, poverty, hurricanes, and mass movements, while providing critical information for disaster management and urban planning.

Table 13. Cases of application of AI methods in hazard, vulnerability and risk assessment

Project name and source	Description	Objective	Input data	Unit of analysis	Algorithm used	Summary of results
Guatemala City building earthquake vulnerability (GFDRR 2018)	Detection of the seismic vulnerability of buildings in urban areas of Guatemala City, using satellite images, drones and 360° street views to identify homes at high risk of collapse during an earthquake.	Quickly identify homes that are vulnerable to earthquakes.	Drone imagery (eBee, RGB, 4 cm), point cloud elevation data, street view imagery (Trimble MX, 30 megapixels), OpenStreetMap road layer.	Pixel/ object (building).	Deep learning.	This method made it possible to examine 5,000 houses and identify about 500 that require additional inspection and possible reinforcement. It captured 85% of the 'soft-story' buildings identified by engineers.
Saint Lucia building hurricane vulnerability (GFDRR 2018)	Vulnerability assessment of individual structures in St. Lucia facing a Category 5 hurricane, using the physical characteristics of the buildings, such as roof material, shape and size.	Estimate the vulnerability of roofs to hurricanes in small island states in the Caribbean.	Drone imagery (eBee, RGB, 4 cm), point cloud elevation data, street level imagery (Trimble MX, 30 megapixels), reference data: OpenStreetMap building lines downloaded from Charim geonode.	Building/ pixel.	Conditional random field model combined with MpGlue.	The destruction of each structure was estimated in St. Lucia using the variables that best predicted the damage in Dominica. The volume, shape and type of roof were influential variables: large roofs with steep slopes and PVF2-coated metal sheets showed the best results. The algorithm more easily predicted the roof shape (hipped vs. gabled) compared to the material, due to the three-band drone camera.

Project name and source	Description	Objective	Input data	Unit of analysis	Algorithm used	Summary of results
Monitoring urban growth through floor space index (GFDRR 2018)	Regular and cloud-free satellite imagery, combined with machine learning algorithms, is used to monitor horizontal and vertical urban growth. This study uses building footprints and height data obtained through community collaboration to train a machine learning model for urban monitoring in Dar es Salaam.	Monitor urban growth, focusing on built-up area and building height.	Satellite imagery (RGB, 3.7 m), digital surface model (DSM) extracted from stereoscopic satellite imagery (0.8 m).	Pixel.	Convolutional neural networks, deep learning.	OSM reference information was combined with machine learning methods. Building footprints were extracted with 77% accuracy; the correct number of floors was predicted for 23% of the buildings. Difficulties were encountered in densely built-up (informal) areas.
Poverty Mapping in Sri Lanka (GFDRR 2018)	Study investigating the suitability of characteristics derived from high-resolution satellite imagery for estimating poverty at the local level in Sri Lanka.	Estimating poverty levels.	Satellite imagery (RGB, < 0.5 m); object-based features: Number of buildings, number of vehicles, fraction of paved roads, shadow pixels (height of buildings), type/extent of crops, type of roof. Pixel-based features: Vegetation index; PanTex (density of settlements), Texture.	Pixel/object (administrative unit).	Deep learning (convolutional neural networks) - Support vector machines and visual identification.	• The analysis can explain 60-61% of the variation in a small area (compared to 15% when using night light analysis). • Building density, built-up area and shadows were some of the most influential characteristics describing variations in poverty. • Standardized error rates of 0.25-0.5 of poverty rates when applying the model to geographically adjacent areas.
Informal Settlement Mapping (GFDRR 2018)	This study, conducted by Graesser et al. in 2012, mapped informal settlements in four major cities using an automated ML algorithm to classify satellite imagery.	Identification of informal settlements.	Satellite imagery (RGB, < 0.5 m), pixel-based features (vegetation indices, GLCM (Gray-Level Co-Occurrence Matrix) PanTex, textures).	Pixel.	Decision Trees.	Textural characteristics in submetric satellite images are suitable for distinguishing formal from informal areas. The accuracy of the ML algorithm was 85-92% for the four cities studied.

Project name and source	Description	Objective	Input data	Unit of analysis	Algorithm used	Summary of results
Stanford Poverty Study (GFDRR 2018)	This study uses satellite imagery to predict the percentage of households above the poverty line in Uganda, since poverty mapping is costly and difficult to update.	Poverty mapping.	• Deep learning model trained on ImageNet • NOAA nighttime lights images • Images from Google Maps	Pixel (1 km x 1 km grid), object (districts).	Fully connected convolutional neural network and logistic regression classifier.	The proposed method can predict poverty levels with 72% accuracy, comparable to results from logistic regression using survey-based characteristics.
Catani, (2021) Jain et al. (2023)	Analyze satellite images to detect changes in land use and vegetation.		Satellite imagery, climate data, land use maps.		Deep Learning.	Identification of changes in land use and land cover patterns for deforestation monitoring and land use planning.

Risk

Project name and source	Description	Objective	Input data	Unit of analysis	Algorithm used	Summary of results
Flood Damage Prediction (GFDRR 2018)	This project investigates how the inclusion of additional variables can improve the transferability of flood damage prediction models.	Flood damage assessment.	Water depth, building type, building footprint area, floor area, building age, basement, household size, flow velocity, duration of flooding, return period, flood experience, precautionary measures	Tabulate (survey data).	Bayesian networks and random forests (regression).	Models trained with heterogeneous data (i.e., flood events with diverse characteristics) showed better performance. The importance of acquiring a heterogeneous training set for flood damage models is emphasized.
Machine Learning Powered Seismic Resilience for San Francisco (GFDRR 2018)	Models structural damage caused by earthquakes using a proprietary algorithm that predicts structural damage. This model uses multiple data sources to estimate the impact of earthquakes on the city of San Francisco.	Modeling earthquake structural damage.	Soil characteristics, seismic hazard parameters, building characteristics (material, number of floors, area, etc.)	Tabulate (survey data).	OneConcern proprietary algorithm.	Damage predictions were made at the census block level, providing real-time situational information before, during and after a seismic event. This allows detailed localized data to be visualized while maintaining anonymity of the block.

Project name and source	Description	Objective	Input data	Unit of analysis	Algorithm used	Summary of results
Cyclone Damage Assessment (GFDRR 2018)	The World Bank and UAViators collected Unmanned Aerial Vehicle (UAV) imagery after Cyclone Pam hit Vanuatu in 2015. UAV imaging was used instead of satellites. Volunteers from the Humanitarian OpenStreetMap Team (HOT) and the Digital Humanitarian Network annotated the damage in the images.	Damage assessment.	UAV optical images.	Pixel.	Deep learning.	A pipeline was developed combining crowdsourced damage annotation and deep learning with 63% accuracy.
Tounsi and Temimi, (2023) Jain et al. (2023)	Analyzing social media data to assess public perception of climate change.		Social media data (e.g., tweets, posts and messages related to climate change).		Natural Language Processing.	Analysis of public sentiment and opinion on climate change to engage the public in climate action and advocacy.
Oh et al. (2020) Jain et al. (2023)	Mapping and monitoring changes in land use and urban development.		Satellite imagery, land-use maps, urban planning data, etc.		Computer Vision.	Identification of changes in land use and urban development for land use planning and management, guiding urban development.

Hazard

Project name and source	Description	Objective	Input data	Unit of analysis	Algorithm used	Summary of results
Global mapping of mass movement hazards (GFDRR 2018)	An algorithm was trained that links mass movement susceptibility factors (slope, geology, road networks, fault zones and forest loss) to historical mass movement events. This model is applied to precipitation data from the Global Precipitation Measurement Mission (GPM) at three-hour intervals. If a region is classified as highly susceptible, a nowcast warning is issued.	Mapping of mass movement hazards.	Elevation, faults and geological regions, road networks, forest cover, rainfall.	0.1°.	Decision tree.	The model would have issued a nowcast for historical mass movement events with a false positive rate of less than 3% and a true positive rate of up to 60%.

Project name and source	Description	Objective	Input data	Unit of analysis	Algorithm used	Summary of results
Flood Extent Mapping (GFDRR 2018)	Project developed by Orbital Insight in 2017 that used synthetic-aperture radar (SAR) as input for an image classification algorithm.	Flood extent mapping.	Optical satellite imagery, SAR imagery (through clouds), digital elevation models (DEMs), geolocated imagery from crowdsourced data sources.	Pixel.	Deep learning.	The combination of various types of large-scale spatial data helped to estimate the extent of flooding. Geolocated crowdsourced imagery can help verify the accuracy of flood mapping.
Linardos et al. (2022) Jain et al. (2023)		Predicting future weather patterns and changes.	Climate models, historical climate data, satellite imagery.		Machine Learning.	Projections of temperature, precipitation, and other climate variables to inform climate policy, guide adaptation strategies.
Lawal et al. (2021) Jain et al. (2023)		Flood forecasting.	Sensor data (precipitation, river level).		Machine Learning.	Flood hazard maps and alerts for flood forecasting and warning systems.
Park et al. (2020) Jain et al. (2023)		Forest fire forecasting.	Satellite and meteorological data.		Deep Learning.	Fire hazard maps and alerts for forest fire prediction and warning systems.
Wang et al. (2021) Jain et al. (2023)		Identification of areas at risk of mass movements.	Satellite and meteorological data.		Computer Vision.	Mass movement hazard maps and alerts for mass movement prediction and warning systems.
Mosavi et al. (2018) Jain et al. (2023)		Flood forecasting.	Sensor data (precipitation, river level).		Machine Learning.	Flood hazard maps and alerts for flood forecasting and warning systems.
Tengtrairat et al. (2021) Jain et al. (2023)		Identification of areas at risk of mass movements.	Satellite and meteorological data.		Computer Vision.	Mass movement risk maps and alerts for mass movement prediction and warning systems.

2.2.2. Disaster response

In the disaster response phase, the main research approaches include analysis of the disaster environment, emergency rescue and evacuation of people. The methods applied include robotics, artificial neural networks (ANN), fuzzy logic (FL) and support vector machines (SVM), among others. This phase involves the management of various types of disasters, such as floods, earthquakes, mass movements and precipitation events. The research focuses on optimizing responses to crisis situations and improving the effectiveness of rescue and evacuation operations. For example, in the case of flooding, unmanned aerial vehicles have been used to obtain high-resolution data that enables the detection of flooded areas in complex urban landscapes using artificial intelligence algorithms (Tan et al. 2020).

Methods such as DL have been used to identify the areas most affected by a disaster and provide information for coordinating response actions (Ivić 2019). Algorithms such as multilayer feedforward neural networks, radial basis function neural networks (RBFNN) and random forests have been used to address complex prediction and classification problems in various areas based on damage detected from satellite image analysis, leveraging the capabilities of each algorithm to identify patterns and perform advanced analysis on large volumes of data (Ivić 2019).

Image: Adobe Stock

In terms of damage assessment, artificial intelligence models are mainly used to determine the severity of disasters and to produce damage maps. For example, Rodriguez et al. (2011) developed a decision support system based on fuzzy rules and compared it with other methods such as multiple linear regression and SVM to assess disaster severity. Kou et al. (2014) proposed a disaster assessment system that integrates fuzzy logic, surveys and multi-criteria decision making methods, showing high accuracy and adaptability (Tan et al. 2020).

Another innovative area in disaster response is the monitoring of social media through the use of natural language processing (NLP), a subfield of AI that enables interaction between computers and human language. NLP analyzes large volumes of unstructured data, such as social media posts (e.g. Twitter/X), to identify relevant information about ongoing disasters. This technology helps responders locate affected areas, monitor people's sentiments and understand their needs in real time, facilitating efficient resource allocation. For example, during Hurricane Harvey in 2017, the U.S. Coast Guard used NLP to locate people in need of help, improving their ability to respond. Overall, NLP plays a crucial role in providing real-time information and helping teams make more informed and effective decisions (Jain et al. 2023). Table 14 shows examples of the use of this technology during the response phase.

Table 14. Applications of natural language processing (NLP) in the response phase

NLP application	Description	Example
Sentiment analysis	Assesses the sentiment of disaster-related social media posts as positive or negative to inform response efforts.	Analysis of tweets during Hurricane Harvey to identify areas with the most negative sentiment and target response efforts accordingly (Tounsi and Temimi 2023).
Named-entity recognition	Identifies specific people, places and organizations mentioned in social media posts related to disasters.	Identification of names of shelters and evacuation centers mentioned in social media posts during a wildfire (Sufi 2022).
Topic modeling	Identify common themes or topics discussed in social media posts related to disasters.	Identification of frequently mentioned topics, such as "road closures" or "evacuation orders" during a hurricane (Anthopoulos and Kazantzi 2022).
Information extraction	Extracting specific pieces of information from disaster-related social media posts, such as requests for assistance or damage reports.	Identification of requests for assistance or reports of missing persons in social media posts during a flood (Sufi and Khalil 2024).

Source: H. Jain et al. (2023).

2.3. Challenges

Image: Adobe Stock

Although new AI-related concepts, technologies and applications have brought numerous benefits and are advancing rapidly with great potential in disaster risk management, they also face challenges. Some of these challenges, such as those mentioned by Xu and Xue (2024) and H. Jain et al. (2023) are presented below:

- The introduction of new technologies and applications requires that relevant **personnel** receive training to improve their skills and competencies. However, the training process may require time and resources, and the discrepancy between talent supply and demand must be resolved.

- Some of these new technologies require considerable data backup, but sharing data and **protecting privacy** remains a challenge. Ensuring the security and legality of data while facilitating its use and access requires cooperation between government and scientific research institutions. AI systems rely on large volumes of data, including personal and sensitive data. Ethical use of data is essential to protect privacy and prevent misuse of personal information.

- AI technology is increasingly crucial in disaster prediction and early warning. However, due to its “black box” nature, its **uncertainty** can lead to errors in judgment, which requires further research and solutions.

- Some new technologies and applications have high **costs** and require considerable investment. For regions with fewer resources or developing countries, these costs may be difficult to bear, leading to uneven application of the technology.

- It is important to ensure that new concepts, technologies and applications are **properly understood and used** by the public.

- The need for **high quality data, the potential for bias and error** in artificial intelligence models, and the importance of oversight. AI systems rely on large volumes of data to make predictions and recommendations. However, if the data used to train AI models are biased, this can lead to biased results. For example, if the data used to train an AI system only includes historical data from certain regions or populations, it may not reflect the experiences of other territories or groups. This could result in inaccurate predictions and recommendations that could disproportionately affect vulnerable populations.

- These models can be highly **complex**, making it difficult for policymakers and stakeholders to understand how they work and how to interpret their results.

- The **lack of transparency** in the algorithms used to develop and train AI models can also complicate the identification of potential sources of bias.

- AI-driven risk reduction strategies may have **unintended consequences** that could negatively affect communities or ecosystems. For example, if an AI system recommends the construction of a seawall to protect against sea level rise, this could have unintended consequences for marine ecosystems.

Box 1. Google Flood Early Warning System

Google Research has developed an advanced flood early warning system using artificial intelligence (AI) models that process public data from various sources. This system allows alerts to be issued up to seven days in advance, providing critical and accessible flood information through Google's Flood Hub. This platform is designed to meet the needs of governments, local aid organizations and people directly at risk by consolidating information and providing relevant local data in a free and publicly available manner. Alerts are also published on Google Search, Google Maps and Android notifications, making them easily accessible to a wider audience (Google 2024a).

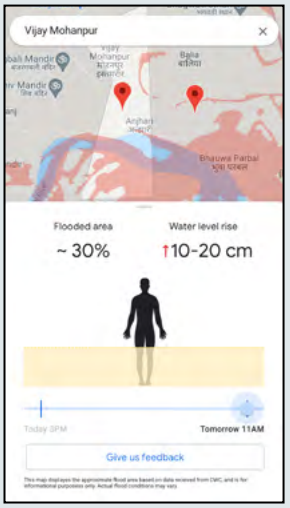

Source: https://blog.google/technology/ai/expanding-our-ml-based-flood-forecasting/

The forecasting system is based on two main components: the Hydrologic Model, which predicts possible river flooding by processing data such as rainfall and other meteorological and basin information; and the Flood Model, which simulates the behavior of water in flood plains. Both models are integrated through an AI approach that provides final forecasts (Google, 2024). The architecture of this system is based on an LSTM (Long Short-Term Memory) encoder-decoder model, where an LSTM encoder processes historical meteorological and geophysical data, and an LSTM decoder projects the forecast for the next seven days (Nearing et al. 2024).

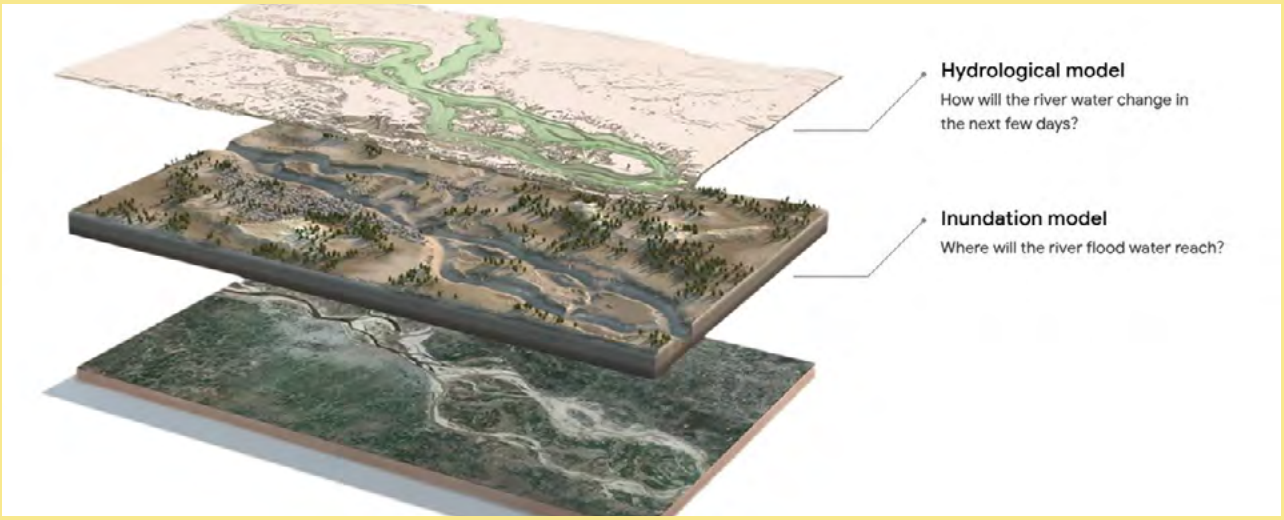

Image: Adobe Stock

The first pilot of the forecasting system was carried out in the Patna region of India, in the state of Bihar, one of the most flood-prone states in the country. Working with local officials and using real-time data, a flood forecasting system was developed and incorporated into Google Public Alerts in 2018, allowing local people to be warned of impending risks. In 2019, forecast coverage was expanded nationwide and extended to Bangladesh, covering a total of 360 million people. During that period, the system provided forecasts up to 48 hours in advance, but depended on the availability of local data, which limited its expansion to other countries (Google 2024b).

Faced with these limitations, Google shifted its focus to a global AI-based model to overcome reliance on local data. This new approach required global data sources to train the model using LSTM networks, with the objective of predicting floods in regions without local flow measurements. Thus, in 2022, Google launched the Flood Hub platform, which provided access to forecasts in 20 countries, including 15 in Africa, where forecasting capability had previously been restricted (Google 2024b).

In 2023, the Flood Hub platform expanded further, adding coverage in 60 new countries in Africa, the Asia-Pacific region, Europe, and South and Central America. This expansion made it possible to cover 460 million people worldwide, providing free, real-time forecasts for many vulnerable communities in developing countries. Thanks to advances in AI-based global modeling, equitable access to flood forecasting is now available, comparable in regions of Africa and Europe (Google 2024b).

SECTION 3

Image: Adobe Stock

MATHEMATICAL MODELS IN THE CALCULATION OF DISASTER RISK IN THE AVAILABLE RISK CALCULATION PLATFORMS

3.1. INTRODUCTION

Image: Flickr - IDB Sustainable Cities / Nassau Bahamas

Risk refers to the end result of combining the magnitude of a consequence with its frequency of occurrence, while impacts focus only on consequences, without considering frequency. The main objective of risk quantification is to estimate economic and/or human losses (Inter-American Development Bank (IDB) 2019). The following is the conceptual framework used in the Inter-American Development Bank (IDB 2019) methodology that will be used to analyze the calculation capabilities of the risk calculation platforms that have been evaluated in this document.

A risk model should include the following components, as shown in **Figure 7**:

1 Hazard assessment	2 Exposure assessment	3 Vulnerability assessment	4 Risk identification
Consists of analyzing the hazard(s) in terms of spatial extent, intensity, duration and frequency. Its objective is to pinpoint where and how each natural hazard could occur.	Involves the creation of a geo-referenced database of all physical (infrastructure, buildings, crops, etc.) and social (population) assets that may be affected by the natural hazard along with their characteristics.	Examines the susceptibility of exposed assets to damage from natural hazards. This requires studying the structural and social characteristics that determine their resilience or fragility to adverse events.	Integrates the three previous components (hazard, exposure and vulnerability) to calculate the resulting risk level.

Figure 7. Risk assessment components

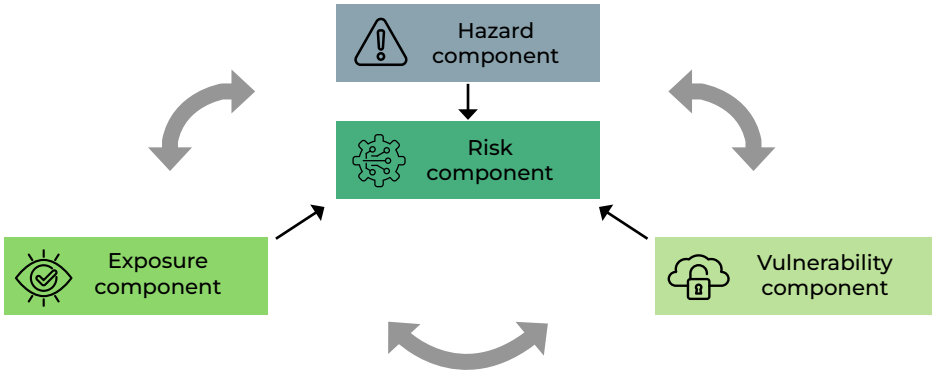

Source: IDB (2019).

Each of these modules operates individually, with specific methodologies and criteria. However, an effective risk model must guarantee the interconnection between modules, ensuring compatibility in data formats and consistency in the methods used.

For example, the exposure module should have a spatial representation that allows it to interact with the hazard module, identifying which assets or population are at risk. It should also include characteristics of the exposed assets that are relevant to the vulnerability module, allowing the potential damage to be assessed. Similarly, the vulnerability module should be expressed in terms of the intensity of the hazard and be consistent with the attributes represented in the exposure module.

The risk module acts as the integration center of the model, mathematically combining the three modules to calculate risk metrics. These metrics may include economic losses (in absolute or percentage values) and social losses (lives lost, people injured or affected). Depending on the methodological approach, these metrics may adopt different interpretations and extend to other indicators (IDB 2019). Uncertainty assessment plays a crucial role in risk analysis. In general terms, uncertainty is classified into two main types:

1. **Natural or random uncertainty:** Derived from the inherent variability in natural processes.
2. **Epistemic uncertainty:** Result of lack of knowledge or information about the system under study.

The most common approach in risk analysis addresses these types of uncertainty separately through probabilistic analysis, which allows for a probability distribution of risk outcomes based on variations in epistemic uncertainty. **Figure 8** presents the classification of risk assessment methods proposed by the IDB (2019). Deterministic methodologies are based on the analysis of a single event, either historical or critical, while probabilistic methodologies are divided into three subcategories according to the way they deal with uncertainty in the analysis. **Table 25** summarizes each methodology, and for a detailed description, the reader can consult the IDB's methodology document. IDB (2019). In this chapter, probabilistic and deterministic methodologies will be analyzed, excluding special approaches, since the objective of the document is to evaluate risk calculation platforms with quantitative, mainly probabilistic, approaches.

Figure 8. Risk assessment methods according to the IDB (2019)

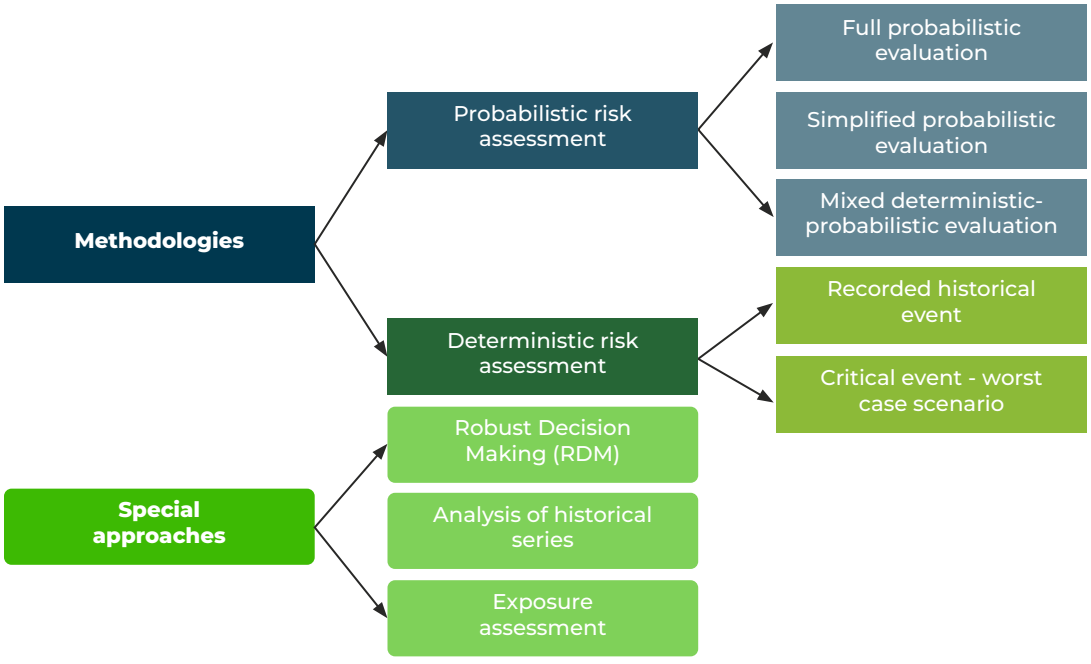

Source: IDB (2019).

The risk calculation platforms discussed in this document employ different mathematical approaches for risk estimation, which can be classified within the methods presented in **Figure 8**. Some of these platforms incorporate specific methods to quantify uncertainty, while others do not. In addition, some use vulnerability curves, while others use fragility curves.

This chapter examines the mathematical approaches used in the platforms for calculating probabilistic risk. The first section introduces the conceptual differences between vulnerability and fragility curves and discusses their application to the platforms studied. The following three sections present the main probabilistic approaches to risk assessment and describe the capabilities of the platforms evaluated against these methodologies. Finally, the fifth section summarizes in tables the probabilistic assessment methods available on each platform, as well as the uncertainty quantification techniques they offer. **Annex A** complements this section by detailing the methods used by each platform.

3.2. VULNERABILITY AND FRAGILITY CURVES

Image: Flickr - IDB Sustainable Cities / Tegucigalpa Honduras

To assess the physical damage that a structural element may suffer due to direct contact with a hazard, two main approaches are used (see **Figure 9**): **vulnerability curves** and **fragility curves** (Nirandjan et al. 2024). These curves allow for the modeling of the relationship between the intensity of a hazard and the potential damage to the exposed assets. There are also other methods, such as matrices and indices (Papathoma-Köhle et al. 2022); however, these will not be addressed in this document, as they are not commonly used in probabilistic risk calculation platforms.

Figure 9. Example of fragility curve (left panel). Example of vulnerability curve (right panel).

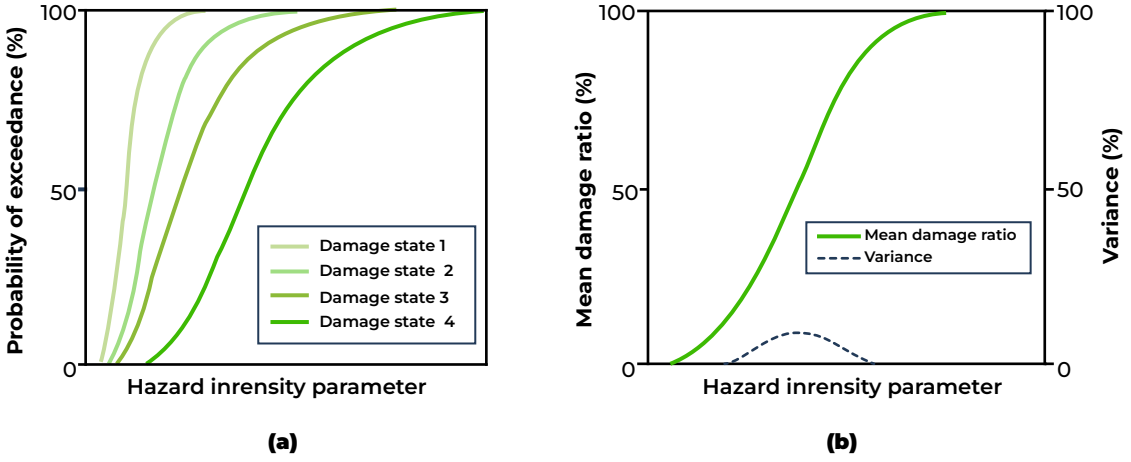

Source: The World Bank (2019).

Vulnerability curves link specific levels of intensity of a hazard (e.g., flood depth, wind speed) to the potential physical impact of an asset. Damage is expressed in absolute terms, as monetary repair costs, or in relative terms by the Mean Damage Ratio (MDR), defined as the ratio of the expected cost of repair to the total replacement cost of the structure (The World Bank 2019). In contrast, fragility curves describe the probability that an asset will reach or exceed a given state of damage given a level of hazard intensity. Damage states can be qualitative and descriptive, such as “slight”, “moderate” or “heavy”, and are most often used in seismic studies, while vulnerability curves are more commonly used in flood analysis (Papathoma-Köhle et al. 2022; Nirandjan et al. 2024).

A crucial aspect of risk modeling is the conversion of fragility curves to vulnerability curves, which allows for the quantification of economic damages. The transformation is based on the cumulative distribution of the expected cost given a damage state $E(C \mid dsi)$ and the probability that an asset will reach a given damage state $P(dsi \mid im)$ given a level of hazard intensity. The function that defines vulnerability is expressed in **Equation 1**.

Equation 1

$$E(C \setminus im) = \sum_{i=1}^{n} E(C \setminus dsi) \cdot P(dsi \setminus im)$$

Where n corresponds to the number of damage states and the damage state "none" is not considered in the sum of the damage states. If a range of values for $E(C \mid dsi)$ is available, it is used to define the upper and lower limits of the vulnerability curve; otherwise, the variance of the vulnerability is calculated using **Equation 2**.

Equation 2

$$\mathrm{var}(C\backslash im) = \sum_{i=1}^{n} (E(C\backslash dsi) - E(C\backslash im))^2 \cdot P(dsi\backslash im)$$

The probability of a building reaching a specific damage state is calculated using fragility curves, where each bar in the damage probability distribution is defined as the difference between two successive fragility curves for a given intensity level (The World Bank 2019). The repetition of this process for different intensity levels allows the creation of the corresponding vulnerability curve.

Figure 10. Calculation of damage probabilities from fragility curves for a specific level of intensity measurement (IM). a) Fragility curves corresponding to n = 4 damage limit states. b) Column of damage probabilities for different damage states given an intensity level (adapted from D'Ayala et al. 2015).

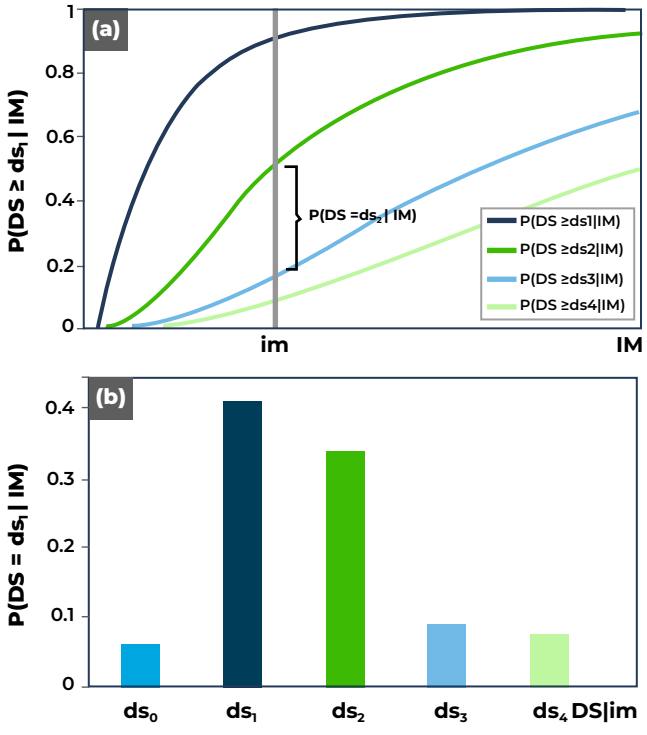

Source: The World Bank (2019).

Notes: Damage states (DS): DS0 = No damage, DS1 = Slight damage, DS2 = Moderate damage, DS3 = Extensive damage, DS4 = Complete.

Vulnerability and fragility functions are derived from statistical analysis of loss or damage values, which can be recorded, simulated or estimated for different levels of hazard severity. In practice, loss or damage statistics can be obtained from observation of past events (empirical approaches), analytical or numerical studies, expert judgments, or a combination of these methods (hybrid approach). Empirical approaches, based on post-event surveys to assess the performance of different asset classes, are generally considered the most reliable source of loss and damage data, as they are based on actual observations (Pregnolato et al. 2015).

Table 15 summarizes the types of vulnerability representation used by the risk calculation platforms analyzed in this document. Most of them use vulnerability curves, although some have the capacity to apply both approaches in the calculation.

Table 15. Type of vulnerability representation used by risk calculation platforms

Type of vulnerability representation used	CAPRA	HAZUS	RiskScape	OASIS LMF	IN-CORE	CLIMADA	CATSIM	RiskChanges	FloodRisk	Delft-FIAT	HEC-FDA	OpenQuake
Vulnerability curve	✓	✓ [1]	✓	✓	X	✓	✓	✓	✓	✓	✓	✓
Fragility curve	✓	✓ [2]	✓	X	✓	X	X	X	X	X	X	✓

Note:
1. Approach used by HAZUS for floods.
2. Approach used by HAZUS for tsunamis, earthquakes and hurricanes.

3.3. FULL PROBABILISTIC EVALUATION ON THE EVALUATED PLATFORMS

The full probabilistic risk assessment provides detailed information on potential losses and their probabilities of occurrence. In most cases fully probabilistic approaches model hazard and vulnerability probabilistically, but there are also advances in the quantification of uncertainty in the exposure component (Mistry and Lombardi 2023).

The phases of the analysis process are summarized below, for detailed information on the methodology refer to IDB (2019).

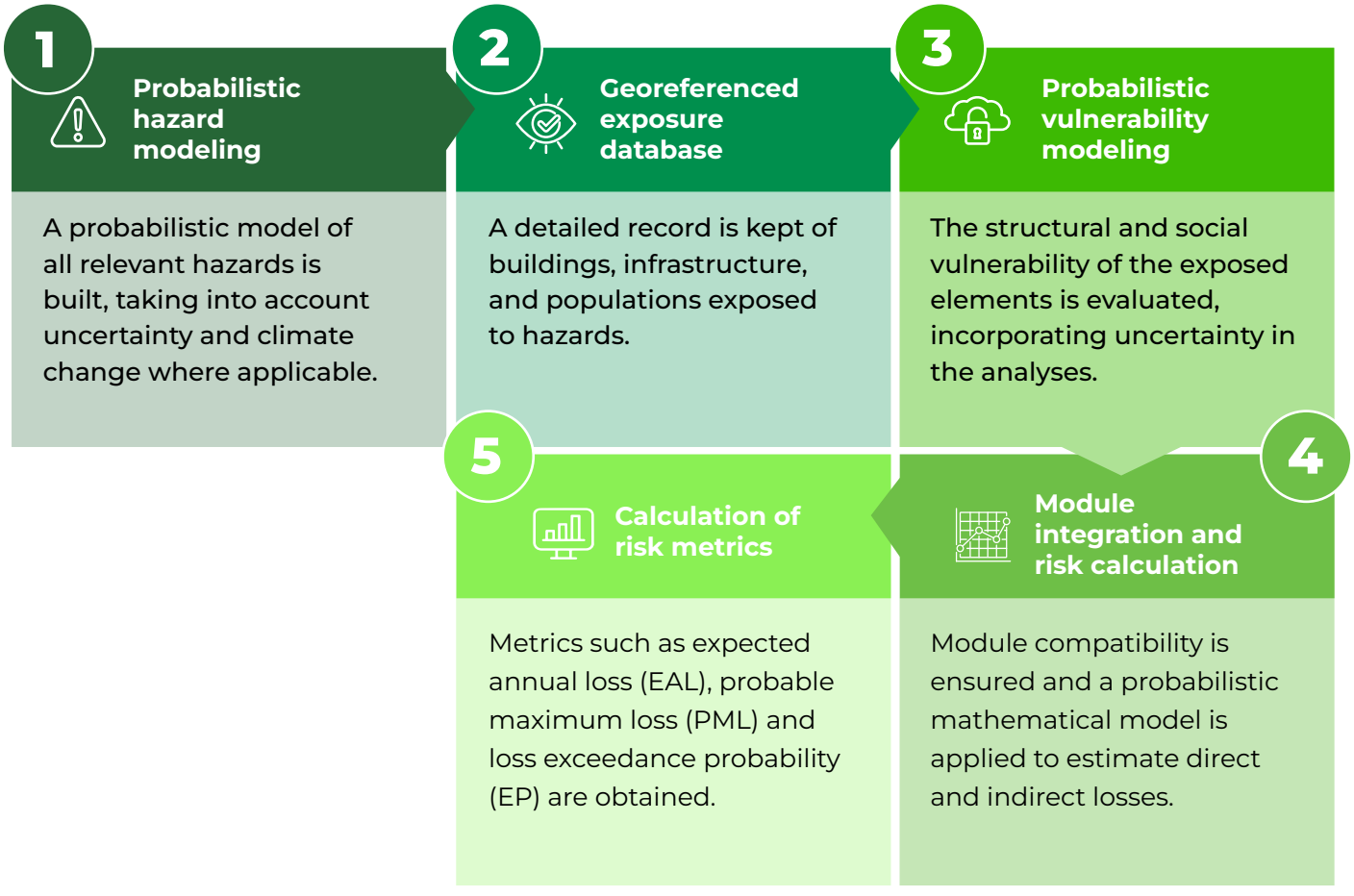

The method is based on probability theory and uses mathematical equations (such as the Total Probability Theorem) to calculate the probability of loss as a function of different hazard scenarios. This yields the loss exceedance curve, which allows the frequency of extreme losses to be estimated.

This type of approach is used by **Hazus Hurricanes** where the consequences of a hurricane in a city or region are estimated by means of a probabilistic set of events, the extent of which varies according to geography. The storm track simulation model begins by randomly sampling an initial position, date, time, direction and speed of movement of one of the tropical storms given in the HURDAT (Hurricane Databases) database[10]. The number of storms to be simulated in any year is obtained by sampling from a negative binomial distribution with a mean value of 8.4 storms per year and a standard deviation of 3.56 storms per year (FEMA 2022a). The loss model is a physical model that calculates direct economic losses using a combination of explicit and implicit cost techniques (FEMA 2022a).

The Hazus Hurricane wind model follows a probabilistic approach based on the hazard-load-resistance-damage-loss methodology, developed from an individual risk framework. The performance of buildings against extreme winds is formulated probabilistically by means of structural reliability concepts. The probability of failure of individual elements (such as windows or doors) is estimated by comparing the wind load with the resistance of the element. Through simulations on different types of buildings, damage probabilities are calculated and relationships between wind intensity and physical damage are established (FEMA). The average annual hurricane loss considers all future losses caused by the hurricane hazard resulting from potential hazard events with different magnitudes and return periods averaged by year (FEMA 2022a).

A fully probabilistic approach can be applied on platforms such as **CAPRA, RiskScape, OASIS FML, CLIMADA, IN-CORE, OpenQuake** and **Delft-FIAT**. In theory, it could also be implemented in RiskChanges and FloodRisk, as they are open source and can be adapted in Python. However, these tools will not be considered as fully probabilistic because they were not originally designed to perform this type of calculation with hundreds or thousands of simulations.

CAPRA, RiskScape, OASIS FML, CLIMADA, IN-CORE, OpenQuake and Delft-FIAT have the ability to perform impact or damage calculations using large numbers of hazard events with an assigned probability, allowing subsequent processing of the damage data to construct the loss exceedance curve. CAPRA, OASIS FML, CLIMADA, IN-CORE and OpenQuake have their own methods for uncertainty quantification which can be seen in Annex A. These methods involve repeated runs of the model with varying input parameters.

[10] https://www.aoml.noaa.gov/hrd/hurdat/Data_Storm.html

4.3. SIMPLIFIED PROBABILISTIC RISK ASSESSMENT ON THE EVALUATED PLATFORMS


Image: Adobe Stock

In a simplified probabilistic risk calculation, losses are calculated discretely for specific values of hazard intensity with an associated return period. These losses are reported individually and allow the direct determination of the expected annual loss (EAL). However, the loss exceedance curve can only be estimated by extrapolation, as opposed to a fully probabilistic calculation, which provides a complete loss distribution. In general, simplified approaches do not incorporate uncertainty in the vulnerability module and use average damage estimates. The calculation of the EAL is based on the hazard curve, which contains the exceedance rates (the inverse of the return period) for different hazard intensities, combined with the expected losses for each intensity (IDB 2019). For detailed information on the methodology, please consult the IDB (2019).

The tools described in section 2 can calculate damage using a simplified probabilistic approach for a given number of return periods and vulnerability or fragility curves (see **Table 15** for information on the type of vulnerability representation of each calculation platform), with the exception of **InaSAFE**[11] and **FloodRise** which do not perform economic risk calculations and therefore will not be considered in this chapter.

[11] Some simplified methods for calculating damage using available QGIS tools are described in the InaSAFE documentation (InaSAFE, 2023) but for the purposes of this document those methods will not be considered.

The equation used in this methodology corresponds to a discretization that converts the exceedance probabilities into occurrence probabilities and calculates the average losses between consecutive return periods. Finally, these losses are multiplied to obtain the EAL (IDB 2019). **FloodRisk** documentation gives a detailed explanation of the method (Albano et al., 2017). Relative damage functions are used that express damage as a proportion of total asset value (0 = no damage to 1 = total destruction). These damage functions can be represented as intensity-damage curves that combine the type of land use or exposed element and the intensity. The intensity parameter depends on the hazard analyzed, for example, FloodRisk uses flow depth (Albano et al. 2017c) .

Once the damage is calculated for events with various return periods by applying the vulnerability curve to the exposed elements, the EAL is determined as follows (Albano et al. 2017c):

Equation 3

$$PAE = \sum_{i=1}^{n} \Delta P_i D_i$$

where:

ΔP_i is the increase in the probability of exceedance.

D_i is the average damage from two events with exceedance probabilities P_i and P_{i+1}. For events with return periods i ranging from 1 to n return periods.

This method is used by **RiskChanges**[12] (Van Westen and Bakker 2015) **CATSIM** (IIASA 2024a) and **Delf-FIAT**, although in the case of the latter the documentation is not clear on whether the software calculates the EAL or only the impact for events, although the documentation clarifies that it can be used in conjunction with Excel and Python for post-processing of results and even be used in complex probabilistic analyses in a Python environment (Deltares 2024a). In the case of **OpenQuake** this approach can also be applied to event-based risk calculation with an associated return period, with the option of considering the uncertainty of parameters or not (see details in **Annex A**).

Although **CAPRA** and **CLIMADA** were designed for probabilistic risk analysis using uncertainty quantification methods and simulation of hundreds or thousands of events, they can make calculations by event or groups of events with an assigned probability. In the case of **RiskScape** the tool distinguishes between 3 approaches to risk calculation which are explained in detail in **Annex A**, one of them being based on events with an assigned exceedance probability. With regard to **OASIS LMF**, the tool has

[12] It should be noted that the documentation of the web tool on its website does not provide information on the algorithms used for the calculations. The documentation consulted to identify the method corresponds to a project progress report developed by Van Westen and Bakker (2015).

been designed for fully probabilistic risk calculation, so if an analysis using **Equation 3** is required for a limited set of scenarios, it may be preferable to use simpler tools, even though the tool can perform the calculation. Something similar occurs with **HEC-FDA** a tool designed for flood risk analysis that integrates the evaluation of protection systems and the associated uncertainty. Although it can analyze a given number of events with an associated probability, its main objective is not this, but rather the quantification of uncertainty in the hydrological, hydraulic and vulnerability components within the flood risk analysis, using Monte Carlo methods.

The application of the **Equation 3** is the approach used by **Hazus** for floods, which clarifies in its documentation that it does not address uncertainty, although it acknowledges its importance (FEMA 2022b) and warns that model results should not be considered exact figures and should be used accordingly. However, the FEMA Flood Committee believes that planning decisions made with the benefit of model results will be better than decisions made without any consideration of science (FEMA 2022b). For tsunami and earthquake Hazus uses fragility curves in the analysis. **IN-CORE** also uses fragility curves to perform damage calculations. First, a fragility score is obtained based on the type of hazard and the attributes of the building (or any other exposed element). Based on the fragility curve, the hazard intensity at the building location is calculated. With this information, the probability of exceeding each limit state is calculated, along with the probability of damage. In the case of seismic hazard, soil information can be used to modify damage probabilities to include damage due to liquefaction (IN-CORE 2024).

Image: Adobe Stock

3.5. MIXED DETERMINISTIC AND PROBABILISTIC EVALUATION

To implement this approach, it is necessary to define which components of the risk model will be treated probabilistically (either fully or in a simplified manner) and which will be treated deterministically.

There are two main cases:

1 Probabilistic hazard and deterministic vulnerability

It can obtain the loss exceedance curve (LEC), either directly if the analysis is fully probabilistic or by means of an approximation (proxy) if it is simplified probabilistic. Vulnerability is modeled without uncertainty and variability.

2 Deterministic hazard and probabilistic vulnerability

It does not obtain the LEC, only specific risk results. Loss estimation is based on detailed structural models, structural reliability theory, finite element and Monte Carlo simulations, among other methods.

Risk metrics depend on the approach adopted. If LEC is obtained, standard probabilistic analysis metrics are applied. In their absence, damage probabilities, probability of failure and other indicators specific to the sector and hazard assessed can be estimated. For detailed information on the methodology see IDB (2019).

Tools that have the capability to perform a full probabilistic assessment such as **Hazus Hurricanes, CAPRA, OASIS FML, CLIMADA, IN-CORE and OpenQuake** can be implemented to perform mixed deterministic and probabilistic and simplified probabilistic assessments. Tools such as **RiskScape** and **Delft-FIAT**, although their use cases and manuals refer primarily to simplified probabilistic applications, can be used for mixed analyses since, through additional code (Python), they could take into account the uncertainty of the vulnerability component.

In its online documentation CLIMADA presents an example of its use in a mixed deterministic and probabilistic implementation considering probabilistic hazard and deterministic vulnerability. It is worth mentioning that CLIMADA has the Unsequa module to consider the uncertainty of any component of the risk model, but it is a tool that can be used in different ways and complexity to quantify uncertainty. In the example, CLIMADA functions are used to analyze tropical cyclones using both historical data and synthetic simulations to assess the risk of these extreme events (ETH Zurich 2017a). Its TCTracks module has access to tropical cyclone data from the IBTrACS database, which compiles historical records since the 1950s (see **Figure 11**).

Figure 11. Example of historical storms downloaded by CLIMADA

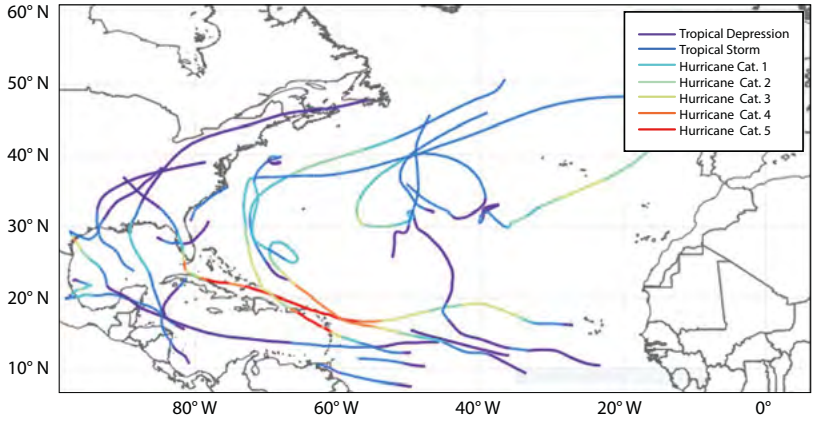

Source: ETH Zurich (2017a).

However, as historical records are limited and only a small fraction of cyclones make landfall each year, this information is insufficient to accurately assess the risk of rare events. To overcome this limitation, CLIMADA generates synthetic cyclones based on historical records using Wiener processes (a type of directed random walk). This allows large data sets to be created that help estimate the probability of rare extreme cyclones. With CLIMADA, users can:

1. Load historical cyclone data from IBTrACS using the from_ibtracs_netcdf() function, which downloads and stores the data for analysis.
2. Generate probabilistic data sets based on these historical records.
3. Simulate synthetic trajectories from existing ones, using the calc_perturbed_trajectories() method, which creates multiple versions of the same trajectory with small variations in its path.

The CLIMADA tutorial on tropical cyclone analysis in Puerto Rico (ETH Zurich 2017a) shows the use of this type of information in risk analysis (although with a small number of events for speed of calculation in the tutorial), which after being used with an exposure base created from LitPop[13] and vulnerability functions contained in CLIMADA, allows the impact exceedance curve and the EAL (expected annual loss) to be obtained, as shown in **Figure 12**.

Figure 12. Damage exceedance curve

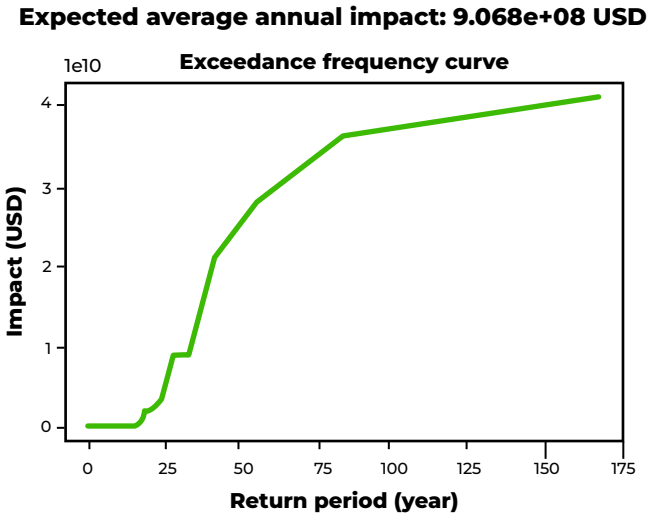

Source: ETH Zurich (2017a).

3.6. SUMMARY

Table 16 summarizes the probabilistic assessment methods that can be used by each tool and **Table 17** summarizes the uncertainty quantification methods available in tools that can be used for fully probabilistic assessment. For more information on the methods of each tool, please see **Annex A**.

[13] Litpop corresponds to the global exposure dataset for disaster risk assessment implemented in the CLIMADA software. https://www.research-collection.ethz.ch/handle/20.500.11850/331316

Table 16. Probabilistic evaluation methods that can be used by each tool

Probabilistic risk assessment methods																
Method	**Description**	**Tool**	CAPRA	HAZUS	RiskScape	OASIS LMF	IN-CORE	CLIMADA	CATSIM	RiskChanges	FloodRisk	Delft-FIAT	HEC-FDA	OpenQuake
Probabilistic risk assessment	A probabilistic risk assessment aims to address some of the uncertainties that are inherent in disaster risk. These uncertainties arise from (i) the limited availability of historical data, (ii) the fact that catastrophic events are very infrequent, (iii) the short observation window for disasters, and (iv) changing climate trends, among other factors (ERN-AL, n.d.a.). In a probabilistic risk assessment, the components that make up risk (primarily hazard and vulnerability) are modeled and then mathematically integrated in a probabilistic manner, formally recognizing and incorporating uncertainty throughout the entire model. In this way, the model can statistically represent the probability of all possible events, including those that have not yet occurred, which makes it a prospective model. This type of assessment can be applied both to individual projects and to large portfolios (e.g., cities, systems or networks, at the regional level and even at the national level), provided that the necessary adjustments are made to the model to address the different levels of detail required in each case. Although three types of probabilistic analyses are described, it should be noted that other types can be applied by combining several of their elements in different ways. For example, models can be developed in which some components are treated in a fully probabilistic manner, others in a simplified probabilistic manner, and others in a deterministic manner.	**Fully probabilistic assessment:** for the hazard module, tens, hundreds, or thousands of stochastic events are generated following probabilistic and statistical theory; likewise, all these events are used in the risk calculation. For the vulnerability module, structural behavior and response are treated in a fully probabilistic manner to integrate stochastic events and hazard intensity, exposure, and vulnerability values in order to calculate expected damages and their associated probabilities, propagating uncertainties through the model. A fully probabilistic treatment of risk calculations results in a probability distribution of losses. Based on this distribution, risk metrics are derived: the loss exceedance curve (LEC), the expected annual loss (EAL), and the probable maximum losses (PML).	✓	✓ [1]	✓ [3]	✓	✓	✓				✓ [4]	✓	✓
	Simplified probabilistic assessment: in this case, instead of using stochastic simulations, only selected hazard return periods are modeled. Return periods are defined using different methodologies. Some of the most common are: (i) statistical analysis of instrumental measurements of hazard-generating events (precipitation, earthquakes); (ii) geomorphological analysis of past events; and (iii) statistical analysis of historical records (surveys, newspaper articles). The return periods are selected to attempt to cover the full spectrum of possible events, from recurrent events to sporadic events. Losses for the hazard return periods considered are estimated by combining these hazard results with the vulnerability module (vulnerability or fragility curves used in a probabilistic manner). However, because the hazard module does not meet the requirements to calculate risk using a fully probabilistic method, the random uncertainties associated with the hazard are not propagated through the model. This still makes it possible to calculate the EAL if several return periods are used (generally five or more return periods are required for an adequate analysis). It is possible to obtain an approximation or proxy of the LEC and PML by extrapolating the results of the estimated return periods, but this introduces additional uncertainties into the model (see the United Kingdom manual as an example). This approach is more appropriate for individual infrastructure, since the calculation method allows greater detail in each component.	✓	✓ [2]	✓ [3]	✓	✓	✓	✓	✓	✓	✓ [4]	✓	✓
	Mixed probabilistic–deterministic assessment: in this method, some risk components are modeled probabilistically and others deterministically. For example, the following cases are common: (i) the hazard is modeled probabilistically using only selected return periods (simplified probabilistic), while vulnerability is evaluated deterministically; or (ii) the hazard is modeled deterministically and vulnerability probabilistically, a common approach for assessing landslide risk. Because some of the modules do not meet the requirements to calculate risk using a fully probabilistic method, random uncertainties are not propagated through the model. For the first case, and similarly to the simplified probabilistic case, the EAL and a proxy of the LEC and PML can be obtained by extrapolating the loss values corresponding to the hazard return periods. This method can be used to estimate the response of complex infrastructure where, for example, finite element models are required and it is impractical to model a large number of structural response scenarios. Likewise, in the modeling of complex risk models, it is more feasible to use a combination of probabilistic and deterministic methods.	✓	✓ [2]	✓ [3]	✓	✓	✓	✓	✓	✓	✓ [4]	✓	✓

Note:
1. Method used by Hazus for hurricanes.
2. Method used by Hazus for floods, earthquakes and tsunamis.
3. Code development by the user is required to implement the methods in RiskScape.
4. Code development by the user is required to implement the methods in Delft-FIAT.

REVIEW OF METHODS AND SOFTWARE TOOLS FOR DISASTER RISK ASSESSMENT

Table 17. Summary of uncertainty quantification methods available in tools for fully probabilistic assessment

Probabilistic risk assessment methods	
Tool	**Approach for quantifying uncertainty in fully probabilistic risk analysis**
Hazus Hurricaine	The consequences of a hurricane are estimated using a probabilistic set of events. The storm track simulation model is initiated by randomly sampling an initial position, date, time, direction and translation speed of one of the tropical storms given in the HURDAT database. The number of storms to be simulated in any year is obtained by sampling from a negative binomial distribution with a mean value of 8.4 storms per year and a standard deviation of 3.56 storms per year (FEMA 2022b). The loss model is a physical model that calculates direct economic losses using a combination of explicit and implicit cost techniques (FEMA 2022b). The Hazus Hurricane wind model follows a probabilistic approach based on the hazard-load-resistance-damage-loss methodology, developed from an individual risk framework. The performance of buildings against extreme winds is formulated probabilistically by means of structural reliability concepts. The probability of failure of individual elements (such as windows or doors) is estimated by comparing the wind load with the resistance of the element. Through simulations on different types of buildings, damage probabilities are calculated and relationships between wind intensity and physical damage are established (FEMA). The average annual hurricane loss considers all future losses caused by the hurricane threat resulting from potential hazard events with different magnitudes and return periods averaged per year (FEMA 2022b).
CAPRA	Total probability theorem to calculate the loss exceedance rate, considering the uncertainty in the intensity of the event and in the structural response. $$v(p) = \sum_{i=1}^{Events} \Pr(P > p \mid \text{Event } i) \cdot F_A(\text{Event } i)$$ The exceedance rate of the loss values v (p) is given as a function of $\Pr(P>p \mid \text{Event } i)$ the probability of loss exceedance given the occurrence of the event i, and $F_A(\text{Event } i)$ the annual frequency of occurrence of the event i. $$EAL = \sum_{i=1}^{Events} E(P \mid \text{Event } i)\, F_A(\text{Event } i)$$ The EAL is the expected annual loss where $E(P \mid Event\ i)$ is the expected loss of the event i, and $F_A(Event\ i)$ is its annual frequency of occurrence.
OASIS LMF	A set of events representative of all possible events that may occur, together with their intensity and probability over a period of time long enough to cover a complete distribution. $$p_{id} = p^f_i * p^v_d$$ Where: $\boldsymbol{p_{id}}$ is the probability that an intensity i will occur and cause damage $\boldsymbol{d}$. $\boldsymbol{p^f_i}$ is the probability mass for the intensity interval. $\boldsymbol{p^v_d}$ is the probability mass for the damage interval. This calculation of $\boldsymbol{p_{id}}$ is performed for each combination of event, hazard area (peril), and vulnerability function. Then, $\boldsymbol{p_{id}}$ is added up across the intensity intervals $$p_d = \sum_i p_{id}$$ This results in $\boldsymbol{p_d}$, which is the probability of a damage interval (d) for each event, hazard area and vulnerability function. **1. Deterministic Integration** $$x_{\varepsilon Y} = \text{tiv}_Y * d_{\varepsilon Y}$$

Probabilistic risk assessment methods	
Tool	**Approach for quantifying uncertainty in fully probabilistic risk analysis**
	Where: $\boldsymbol{x}_{\varepsilon\gamma}$ is the loss for event ε and coverage γ. tiv_{γ} is the total insured value. $\boldsymbol{d}_{\varepsilon\gamma}$ is the damage factor. **2. Random sampling (Monte Carlo)**
CLIMADA	Deterministic and probabilistic analysis and uncertainty and sensitivity analysis with Monte Carlo methods. $$x_{ij} = val_j f_{imp}(h_{ij} \mid y_j)$$ Where x_{ij} and h_{ij} are, respectively, the damage and intensity of the hazard due to event i at location j, val_j is the exposure value at location j, γ_j are the exposure parameters j that characterize its vulnerability, and f_imp is the damage function. $$EAI_j = \sum_{\bar{\imath}=1}^{N_{hist}} \sum_{\hat{\imath}} x_i F(E_i) = \sum_{i=1}^{Nev} x_{ij} F(E_i)$$ EAI_j is the expected annual damage of element j, where X is the random variable of damage, E its expectation, E_i is an event and F its frequency (annual). N_{hist} is the number of historical events, $\bar{\imath}$ represents a historical event, i $\hat{}$represents all members of the set of events $\bar{\imath}$, and Nev represents the total number of events.
HEC-FDA	Quantification of uncertainty in flood risk by Monte Carlo simulation for curve sampling including the performance of flood protection works. $$E[X] = \int_{-\infty}^{\infty} x f_x(x)\,dx = \int_{-\infty}^{\infty} (1 - F_x(x))dx \qquad F_x(x) = P(x \le x)\; y\; 1 - F_x(x) = P(X \ge x)$$ Where: X = consequences, such as flood damage, loss of life, or emergency care costs. $E[X]$ = expected value of the consequences x = value of the consequences $f_x(x)$ = probability density function of the probability of X $F_x(x)$ = cumulative distribution function of X
OpenQuake	Scenario-based calculation, probabilistic events, based on classic probabilistic seismic hazard analysis (PSHA) **1. Scenarios** $$LR = \frac{\sum_{n=1}^{m} LR_n \mid \mathrm{IML}}{m}$$ LR is the average loss rate for each asset across all possible simulations of the event, where m represents the number of simulated ground motion fields and IML represents intensity measurement levels. **2. Probabilistic events** $$\lambda(L_n) = \frac{NE_L}{TSES}$$ λ represents the exceedance rate of the respective loss ratio, NE_L represents the number of exceedances of the given loss, and $TSES$ represents the time period of all sets of stochastic events. $$PE(L_n) = 1 - exp - \lambda_n \times t$$ $PE(L_n)$ the probability that total losses will exceed a certain amount in a given period of time

SECTION

4

Image: Adobe Stock

METHODS INCORPORATING SOCIAL VULNERABILITY AND/OR GOVERNANCE IN RISK ANALYSIS

4.1. INTRODUCTION

Image: Adobe Stock

A holistic approach provides fundamental information that complements disaster risk assessments, helping decision makers understand the specific causes of significant losses among vulnerable groups (Nkwunonwo et al. 2015). The need to include social, economic, environmental, and physical factors in vulnerability assessments is embedded in the Hyogo Framework for Action and emphasized in the Sendai Framework for Disaster Risk Reduction 2015-2030, which establishes understanding disaster risks in all their dimensions as a priority (United Nations General Assembly 2015).

Quantification of the physical dimension of vulnerability can be done using empirical and analytical methods (Sterlacchini et al., 2014). However, when considering the multiple dimensions of vulnerability, challenges arise in measuring aspects that cannot be easily quantified. Birkmann (2006) suggests that indicators and indices can be used to measure vulnerability from a comprehensive and multidisciplinary perspective, capturing both direct physical impacts (exposure and susceptibility) and indirect impacts (socioeconomic fragility and lack of resilience). The importance of indicators lies in their potential use for risk management, as they are useful tools for (i) identifying and monitoring vulnerability over time and space, (ii) developing a better understanding of the processes underlying vulnerability, (iii) developing and prioritizing strategies to reduce vulnerability, and (iv) determining the effectiveness of these strategies (Rygel et al. 2006). However, developing, testing and implementing indicators that capture the complexity of vulnerability remains a challenge.

Although the extensive development of geoprocessing and statistical analysis tools provides a solid framework for indicator construction, the uneven availability of data in different geographic regions and the challenges associated with capturing the determinants of vulnerability in specific communities make the creation of vulnerability indicators and indices a complex and challenging task.

The process for the construction of indicators begins with the development of a theoretical framework that provides the necessary conceptual basis. The relevant variables that should represent the multiple dimensions of vulnerability are then selected. In the case of missing data, we proceed with the estimation of such data to complete the necessary information. Subsequently, a multivariate analysis is performed to explore the relationships between the variables. This process generally includes data normalization to ensure comparability between different sets. The variables are then weighted and aggregated to construct the final indicator. Finally, the robustness and sensitivity of the indicator are evaluated, and an uncertainty analysis can be performed (The Organisation for Economic Co-operation and Development (OECD) & Joint Research Centre (JRC), 2008). There are several methods for each of these steps. For example, multivariate analysis can use techniques such as principal component analysis, factor analysis, Cronbach's alpha coefficient and cluster analysis, among others. In terms of weighting, methods such as principal component analysis or hierarchical analysis, among others, can be used (OECD and JRC 2008).

Statistical methods are generally available in R or Python function packages, as well as in geographic information software (GIS) such as QGIS and ArcGIS. However, the greatest challenge lies in the construction of indicators that are consistent with the availability of information and that adequately capture the specific dimensions of vulnerability in each community.

This chapter presents a review of the free tools available for the construction of vulnerability indicators. However, it should be noted that there is no single, universally accepted framework for the construction of indicators.

4.2. METHODS INCORPORATED IN THE OPENQUAKE PLUGIN

Image: Adobe Stock

The OpenQuake Integrated Risk Modelling Toolkit (IRMT) plugin is a tool developed by GEM[14] that integrates with QGIS for a comprehensive assessment of seismic risks as well as any other type of risk. It facilitates the creation of indicators that allow the assessment of socioeconomic characteristics related to vulnerability and risk. The plugin also integrates the responsiveness of populations and combines measures of physical and social risk. It allows users to develop an integrated workflow for the construction of metrics that assess the social characteristics that affect seismic risk, providing a GIS-based platform for the creation of composite indicators and indices, which fosters comparative assessments (GEM, 2024c). The OpenQuake IRMT facilitates the integration of composite indicators of socioeconomic characteristics with measures of physical risk, such as human or economic loss estimates, from the OpenQuake Engine (OQ-engine) or other sources. The plugin can be used for any type of indicator development (GEM, 2024c).

[14] https://www.globalquakemodel.org/products

The OpenQuake IRMT plugin offers several capabilities for the creation and management of composite indicators in risk analysis. Users can define weighting and aggregation procedures for indicators, which can be simple (equal weighting) or more complex (specific weights, linear or geometric aggregation). In addition, it provides a dynamic graphical interface, which facilitates the creation and editing of composite models by means of a weighting and aggregation tree (see **Figure 13**). This interface allows users to develop models visually and easily.

The tree structure allows hierarchical integrated risk models to be developed. The starting point is a root node that corresponds to the development of a hierarchical model that can be: 1) an Integrated Risk Index (IRI) that is a function of the aggregation of a Social Vulnerability Index (SVI) and a Risk Index (RI); or 2) a Social Vulnerability Index (SVI) that is the result of the aggregation of several user-defined sub-indicators (e.g., Economy, Education and Environment, etc.). The tree can be modified dynamically by adding or deleting nodes, inverting variables, setting a weight for each variable or node and choosing the operators to be used to combine variables.

Figure 13. Tree structure for the development of composite indicators

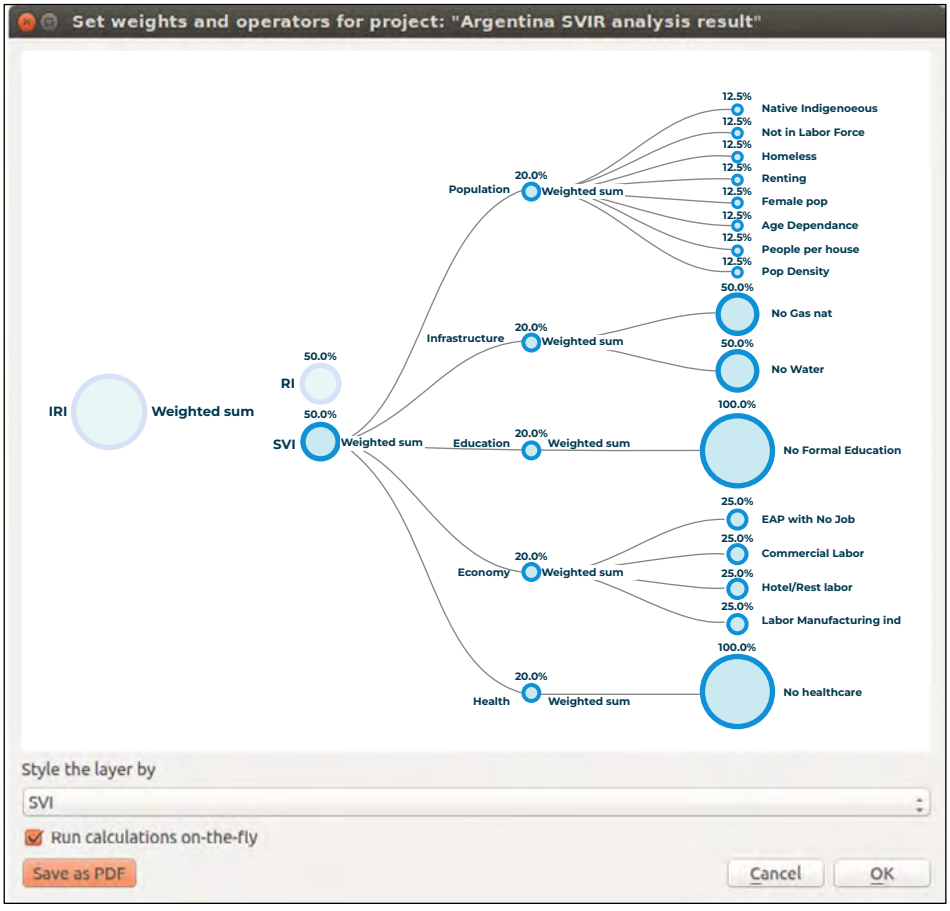

Source: GEM (2024c).

The plugin supports two main types of composite models for indicators:

1. **Deductive Models:**
   They generally use less than ten standardized and aggregated indicators.
2. **Hierarchical models**
   They use ten to twenty indicators, grouped into sub-indices (e.g., population, economy) that are aggregated to form a final composite index (e.g., social vulnerability index).

Users can modify the composite indicator tree by adding or deleting nodes, assigning weights, and choosing operators to combine variables. The changes are immediately reflected in the calculations and displays.

Physical risk calculations and composite indices can be run directly in QGIS, with the results displayed as vector layers.

The plugin provides basic operators for combining variables, and users can define custom formulas for calculating indicators. Weighting techniques can be based on statistical models or participatory approaches.

4.3. QGIS PLUGINS FOR MULTICRITERIA ANALYSIS

QGIS, a free software platform for Geographic Information Systems (GIS), is widely used to perform multi-criteria analysis (MCA), a methodology commonly employed in the creation of vulnerability and risk indicators. In QGIS, MCA can be performed directly using the calculation capabilities between vector or raster layers, or by using specialized plugins that facilitate the creation of indicators and the analysis of complex data. Among the most prominent are the Spatial Sustainability Assessment Model (SSAM) and the Weighted Multi-Criteria Analysis (WMCA).

4.3.1. Spatial Sustainability Assessment Model (SSAM)[15]

SSAM is a QGIS plugin designed for sustainability assessment in geographic settings, using environmental, economic and social criteria. It implements the TOPSIS (Technique for Order of Preference by Similarity to Ideal Solution) algorithm, which generates a ranking based on the distance to the worst point and the proximity to an ideal point for each criterion. Weights can be entered directly or using a pairwise comparison table, allowing the user to define a final vector of weights in a repeatable and verifiable manner. SSAM produces both geographic and graphical outputs, displaying maps of the multicriteria analysis results and numerical sustainability values using bars, bubbles and dots.

SSAM also implements the DOMLEM algorithm based on the "dominance based rough set" theory, allowing the user to know the decisional rules derived from the TOPSIS algorithm and to have a better view of the sustainability ranking displayed in maps and graphs. This approach significantly increases transparency and analytical capacity.

The plugin uses geographic vector files (shapefiles), where the graphical data represent the evaluation units and the alphanumeric data describes the environmental, economic and social indicators. The plugin's algorithms allow these indicators to be treated separately and calculate three different indices, whose linear combination gives an overall sustainability index for each geographic unit.

The user can use a wide variety of indicators or a self-prepared data set. The indicators to be used within an analysis correspond to the attributes assigned by the user in the shapefile of the analysis. Due to this flexibility, although the plugin was created for sustainability analysis, it could be adapted for the calculation of risk indicators considering multiple socioeconomic criteria.

4.3.2. Weighted Multi-Criteria Analysis (WMCA)[16]

The WMCA plugin is another key tool in QGIS to perform weighted multi-criteria analysis. This plugin allows users to assign specific weights to different criteria and calculate a combined evaluation based on those weights. The plugin displays the pixel values of a raster to the user, allowing weights to be assigned to each raster and ratings to each class within them. It was developed to perform weighted multi-criteria analysis, especially in environmental studies such as fragility or favorability analysis, environmental zoning and other types of zoning.

[15] http://maplab.alwaysdata.net/doc/html/index.html

[16] https://github.com/romariocarvalhoneto/Weighted-Multi-Criteria-Analysis---WMCA

SECTION 5

Image: Adobe Stock

CLIMATE CHANGE AND RISK CALCULATIONS

5.1. INTRODUCTION


Image: Adobe Stock

The incorporation of climate change into risk estimation requires robust methodologies to estimate potential future impacts on infrastructure and population. In this context, risk modeling under different climate scenarios becomes fundamental to inform adaptation and resilience strategies.

This section presents a review of the approaches taken by the platforms presented in section 1 to incorporate climate change into risk calculations, with a particular focus on the CLIMADA platform.

5.2. RISK ESTIMATION INCORPORATING CLIMATE CHANGE IN THE PLATFORMS

Image: Adobe Stock

Among all the platforms reviewed, CLIMADA is the only one with specific methods for climate change analysis in risk assessment. This makes it a particularly useful tool for decision making in contexts of climate uncertainty, as it makes it possible to assess not only current risks, but also their evolution under different emissions trajectories.

However, this does not mean that the other multi-hazard or flood platforms are incapable of incorporating climate change into their risk calculations. Provided that the hazard modeling includes projected climate scenarios, it is possible to assess risk by incorporating the impact of climate change in any of them. The assessment of future hazards will require projections or scenarios related to climate change, which should be generated from climate models that allow for the estimation of changes in key variables such as precipitation, temperature and sea level.

In the case of floods, for example, methods for analyzing precipitation projections and converting them into flows that can be used in hydrodynamic models to generate hazard layers under climate

change scenarios can be grouped into three main approaches, as shown in Table 18. These approaches include the use of projections based on climate models to which downscaling techniques are applied to refine global projections to local scales. Through these types of methodologies, it is possible to generate hazard scenarios that, when combined with economic, urban and population growth scenarios, allow for a risk assessment that considers future climate uncertainty and facilitates the formulation of adaptation and mitigation strategies.

It is important to mention that there is no agreed-upon methodology for estimating flooding under climate change (Wasko et al., 2021), but rather a large number of methods reported in the literature that vary widely depending on the scale, purpose of the analyses, and location of application. The selection of the appropriate method depends on factors such as data availability, the spatial and temporal resolution required, as well as the uncertainty inherent in climate projections.

Table 18. Sources of evidence that can be used to inform how climate change may affect future flooding

Method	Description	Advantages	Disadvantages
Heuristic approaches based on physical reasoning	They estimate changes in precipitation using physical principles, such as a global average increase of 2% °C-1 for average rainfall and 6-7% °C-1for extreme events due to the increased capacity of the atmosphere to retain moisture.	Simple to apply; based on understandable physical principles.	They do not capture the complexity of future changes; they may be too general for specific cases.
Projection of historical trends	They extrapolate trends observed in historical data, assuming that the causal relationships observed, such as non-stationarity in precipitation, will remain constant in the future.	They take advantage of observed data and may reflect changes already underway.	They assume that the observed relationships remain constant; they can be confused with other factors, such as urbanization.
Projections based on global climate models	They use climate models to simulate large-scale future changes, which are then scaled locally using statistical or dynamic methods to estimate design growths.	They represent complex physical processes on a global scale; they enable detailed analyses with multiple scenarios.	Do not capture key processes at the local scale; may introduce biases; require scaling and computational resources.

Source: Wasko et al. (2021).

Although CLIMADA can process a hazard layer generated through any method that considers climate change, its development is aligned with the Economics of Climate Adaptation (ECA) methodology (Souvignet et al. 2016), making it specially designed to assess the economic impact of climate change and possible adaptation strategies. In the following sections, this methodology will be presented along with CLIMADA's specific capabilities for climate risk assessment.

5.3. CLIMATE CHANGE APPROACH IN CLIMADA

Image: Adobe Stock

CLIMADA is the tool used for the Economics of Climate Adaptation (ECA) methodology developed by the The United Nations University Institute for Environment and Human Security (UNU-EHS) and the State Development Bank of the Federal Republic of Germany (KfW).

The ECA is an approach designed to flexibly and systematically identify the most cost-effective climate change adaptation (CCA) measures in different sectors and projects. Its main objective is to answer three key questions: what are the potential climate-related damages in the coming decades; how much of these damages can be avoided and through which adaptation measures; and what investments are required to implement such measures, ensuring that the benefits outweigh the costs? This approach allows climate risks to be assessed in a structured manner, promoting transparency and facilitating cross-sectoral discussions among the different stakeholders involved. Moreover, it can be applied at different levels, from national to local, and in various sectors and types of climate hazards (Souvignet et al. 2016).

The ECA provides a practical framework for national and local decision makers to comprehensively assess the climate risks facing their economies, minimizing adaptation costs through efficient strategies. Based on a robust and scientific approach, the methodology is composed of three main elements as shown in **Figure 14**: (1) identification of climate risk, analyzing hazards, vulnerable populations and sectors in a given region; (2) quantification of climate risk, assessing expected damages under different climate and economic scenarios; and (3) identification and prioritization of adaptation measures, using cost-benefit analysis to define optimal strategies. In addition, the ECA is divided into eight phases as shown in **Figure 15.** The first two phases establish the study area and manage key data acquisition. Subsequently, present and future climate and socioeconomic scenarios are defined (Phase 3), identified hazards are modeled (Phase 4), exposed assets are assessed (Phase 5) and damage functions are generated for risk analysis (Phase 6). In the final phases, adaptation measures are simulated (Phase 7) and the results are presented for decision making (Phase 8). Throughout the process, CLIMADA is used as the main tool particularly for phases 3 to 8 (Souvignet et al. 2016).

Figure 14. Elements of the ECA methodology

Source: Souvignet et al. (2016).

Figure 15. Phases of the ECA methodology

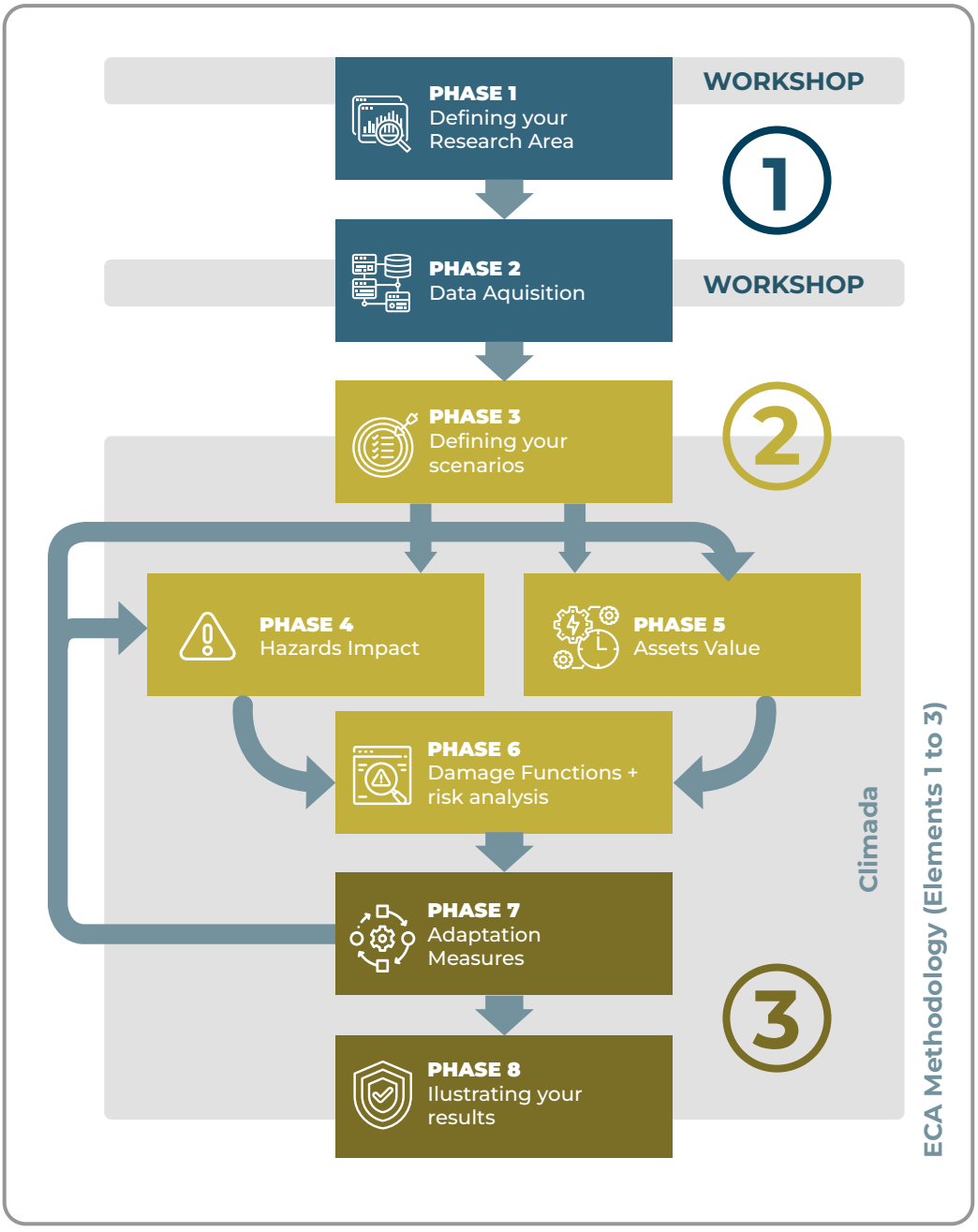

Source: Souvignet et al. (2016).

Phase 3, which involves scenario building, begins with the consistent description of possible futures, assessing the impact of climate variability and change on the population and assets at risk. To do so, three key steps are followed (Souvignet et al., 2016):

Step 1	Step 2	Step 3
Analyzing the current situation and identifies the key factors that will influence the magnitude and characteristics of climate impacts, such as economic growth, climate variability, population growth, and technological advances. It is important that these scenarios be consistent with existing development plans and that their number be limited to facilitate analysis.	A suitable time horizon is defined, balancing the need for realistic projections with the uncertainty inherent in long-term scenarios. ECA documentation recommends a minimum period of 20 to 30 years, considering different horizons (short, medium and long term) to assess the effects of climate change on assets and investments.	Climate scenarios are developed using projections based on climate models, scientific studies and historical data. These scenarios may include extreme events such as intense hurricanes, rising sea level or changes in precipitation.

Finally, the climate and socioeconomic scenarios are combined in an aggregated matrix (see **Figure 16**) that facilitates communication with stakeholders and allows their integration into CLIMADA for the assessment of adaptation measures.

Figure 16. Types of scenario aggregation

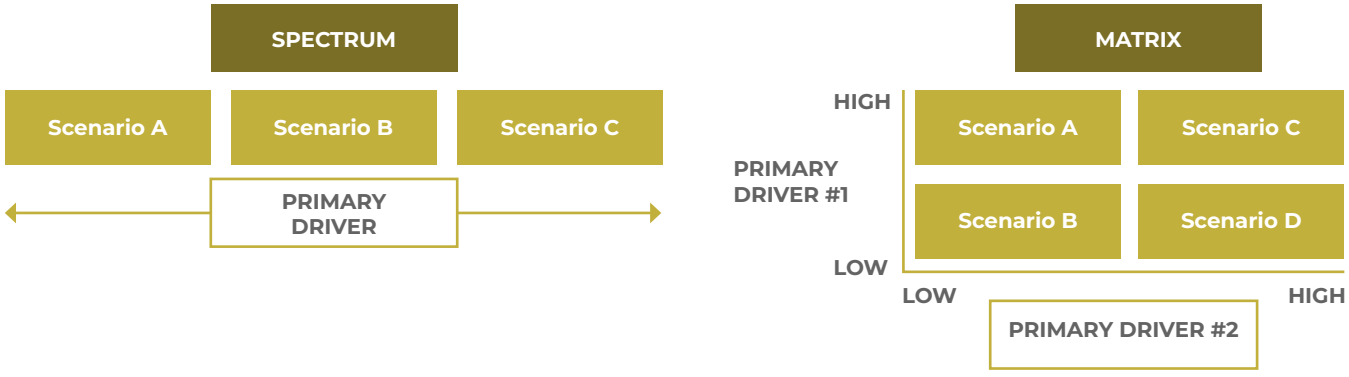

Source: Souvignet et al. (2016).

5.4. METHODS INCORPORATED INTO CLIMADA FOR CLIMATE CHANGE

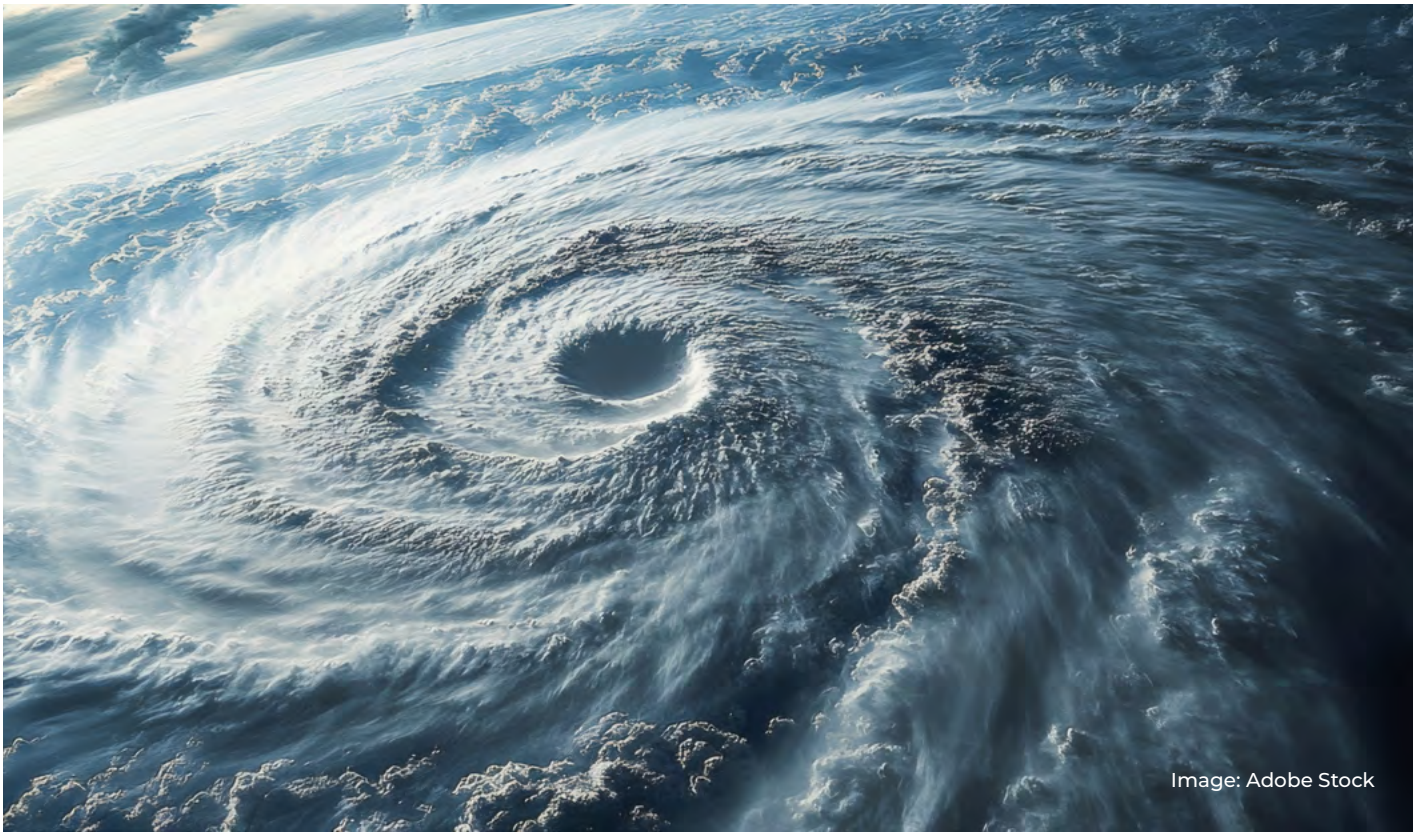

Image: Adobe Stock

CLIMADA enables the estimation of expected economic damage as a measure of current risk, as well as the increase derived from economic growth and the increase associated with climate change. The economics of climate adaptation methodology, implemented in CLIMADA, provides decision makers with an objective basis for understanding the impact of climate and weather events on their economies, including a cost-benefit analysis of specific risk reduction measures (ETH Zurich 2025).

CLIMADA incorporates climate change into the **tropical cyclone** analysis through the apply_climate_scenario_knu function, which implements changes in the intensity and frequency of these events based on the climate scenarios projected in the Knutson et al. (2015) study. This study uses dynamic downscaling of the CMIP5/RCP4.5 scenarios to estimate how tropical cyclone activity might evolve

towards the end of the 21st century. To represent other greenhouse gas concentration scenarios (RCPs - Representative Concentration Pathways), CLIMADA interpolates RCP4.5 values according to their relative radiative forcing, allowing a simplified approximation of the effects of climate change on tropical cyclones (ETH Zurich 2017b).

It is important to note that this method of implementing climate change focuses exclusively on changes in the frequency and intensity of tropical cyclones and does not capture all the factors that influence the damage caused by these events. Estimating economic losses associated with hurricanes remains a challenge due to the high variability in historical records, as the most destructive events are usually rare and depend on specific impact conditions at landfall (ETH Zurich 2017b).

The RiverFlood() module of CLIMADA enables the generation of **river flood** data from simulations of the ISIMIP (Inter-Sectoral Impact Model Intercomparison Project) (Sven Willner et al. 2024). Using the from_nc() method, data on the water depth (in meters) and the fraction of flooded area at each central point are extracted. These data come from global hydrological models using different climatic forcings.

The input data required for the RiverFlood module include spatially explicit information on flood depth and flooded fraction, available from ISIMIP. There are two rounds of simulation:

1 ISIMIP2a (1971-2010)

Uses 12 global hydrological models (GHMs) with four climate reanalysis datasets. The results include the maximum annual flood depth and fraction, with resolutions of 5 km and 10 km. Different protection standards are considered: no protection, protection against events with a return period of up to 100 years and the FLOPROS (FLOod PROtection Standards) layer (Scussolini et al. 2016) with global standards.

2 ISIMIP2b (2005-2100)

It employs six GHMs and four global circulation models (GCMs) to simulate climate change scenarios (RCP 2.6, 6.0 and 8.5). It also includes historical and pre-industrial runs, maintaining the same resolution and protection standards as ISIMIP2a.

The from_nc() method allows to define the centroids for different spatial levels (countries, regions or global).

An example of the application of the methods implemented in CLIMADA to consider climate change in risk analysis can be seen in the composite risk calculation presented by Stalhandske et al. (2024). This study analyzes 5000 years of multi-hazard impacts with composite spatial and spatiotemporal effects on physical assets and populations exposed to tropical cyclones (TC) and river floods (RF) from the ISIMIP

project. The hazard of tropical cyclones in CLIMADA is based on sets of TC trajectories, which are combined with a parametric wind model to simulate a two-dimensional wind field. In this study, TC trajectories from the ISIMIP archive are used, generated by a statistical-dynamic model of tropical cyclones, adjusted for four global climate models (HadGEM2-ES, MIROC5, IPSL-CM5A-LR, and GFDL-ESM2M) from the CMIP5 archive, under the RCP2.6 and RCP6.0 warming scenarios. As for fluvial flooding, spatially explicit global maps of flooded areas and flood depth are derived at a resolution of 150'' through the implementation of CLIMADA, using data derived from ISIMIP2 simulations. The applied dataset includes harmonized simulations from six global hydrological models (GHMs) participating in ISIMIP2b for the RCP2.6, RCP6.0 and RCP8.5 scenarios, although only RCP2.6 and RCP6.0 are considered in this study to maintain consistency with tropical cyclone modeling.

One of the most recent additions to CLIMADA is an API (Application Programming Interface) that allows access to exposure and hazard data on a uniform 4 km grid, facilitating consistent risk assessments. Currently, the API includes global hazard datasets for tropical cyclones, droughts, heat waves, wildfires, river flooding and agricultural yields. In addition, it provides region-specific data, such as winter storms in Europe (Stalhandske et al. 2022). Among the data available through the API are those shown in **Table 19** which correspond to the hazard datasets for which there is an attribute related to climate change scenarios.

Table 19. Hazard datasets available through the CLIMADA API with climate change attributes

Name	Description
Aqueduct_coastal_flood	Global probabilistic coastal flood maps for historical and future climates (~1 km resolution). Available for return periods of 2 to 1000 years in 2030, 2050 and 2080 under RCP 4.5 and 8.5 scenarios, considering three sea level rise projections and including or excluding subsidence.
Relative_cropyield	Global simulations of crop production in relative terms (4 km resolution), including corn, rice, soybeans and wheat. Based on crop models and bias-corrected climate models provided by ISIMIP.
River_flood	Global fluvial flood maps (water depth and fraction of flooded area) at 150-second resolution (~4 km at the equator). Based on CaMa Flood output and global circulation models. Available by country and IPCC future climate scenarios.
Storm_europe	Winter storm tracks in Europe (wind gusts in m/s). Data available from Copernicus Windstorm Information Service (WISC) projects (1940-2014) and CMIP6 (Coupled Model Intercomparison Project Phase Six) models (1980-2010 and 2070-2100). Coverage for European countries only.
Tropical_cyclone	Tropical cyclone wind tracks (m/s) with a resolution of 150 seconds (~4 km at the equator). Data available globally and by country, based on historical records and model-generated probabilistic events.
Wildfire	Global forest fire dataset with 4 km resolution, based on MODIS (Moderate Resolution Imaging Spectroradiometer) satellite data (2000-2021).

Source: ETH Zurich (2025a).

5.5. KEY POINTS FOR RISK ANALYSIS UNDER CLIMATE CHANGE

Image: Adobe Stock

In summary, the integration of climate change into risk calculations requires consideration of several methodological elements that directly affect the quality and usefulness of the results. The following is a summary of some key aspects to keep in mind when developing this type of analysis, especially in the context of adaptation planning and decision making.

Key points for risk analysis under climate change

Working with multiple climate scenarios

It is essential to avoid the use of a single scenario. Analysis with a set of future trajectories better captures the uncertainty inherent in climate projections.

Consider the scale of analysis

The spatial and temporal scale of the study should be consistent with the objective of the analysis. Resolution decisions directly affect the interpretation of results and the applicability of adaptation measures.

Carefully choose the downscaling method

There are multiple approaches (statistical, dynamic, hybrid) to bring global projections to local scales. Selection should be based on data availability, study region and technical resources.

Implement sensitivity analysis in risk models

It is advisable to assess how changes in key climatic variables (such as precipitation or temperature) affect the hazard and, consequently, the risk. This strengthens the robustness of the analysis and helps to prioritize interventions.

Leverage platforms that integrate climate projections with exposure and vulnerability data

Tools such as CLIMADA allow for an integrated assessment of potential climate change impacts and adaptation strategies, facilitating evidence-based decision making.

SECTION 6

Image: Adobe Stock

GLOBAL PRECIPITATION PRODUCTS WITH FREE ACCESS

6.1. INTRODUCTION

Image: Adobe Stock

Precipitation is one of the fundamental variables for flood, mass movement and drought risk assessment. Understanding their temporal and spatial variability is essential to address hazard modeling challenges. Atmospheric forcing in hydrological models, which includes precipitation, can come from reanalysis or satellite products in areas with a scarcity of data from hydrometeorological networks. With several decades of high-resolution records of near-global satellite precipitation data, these have become essential for analyzing flood frequency in regions with limited data (Dis et al. 2018).

In this chapter, various sources of precipitation data are explored, with emphasis on freely available global products. These products, generated from satellites and numerical models, provide valuable information for climate monitoring and assessment, especially in regions where in situ data are scarce or non-existent. A review of the main satellite and reanalysis products is made, highlighting their characteristics, applications and limitations.

6.2. SATELLITE PRECIPITATION PRODUCTS


Image: Adobe Stock

Satellites use reflected light to detect, collect, measure and record electromagnetic energy from the Earth's surface. Advances in satellite remote sensing have made it an excellent source of data, as it can provide meteorological information to support hydrological modeling. In addition, precipitation data obtained through remote sensing has the potential to complement traditional rain gauging systems (Masood et al. 2023). Recently, active remote sensing instruments have improved considerably, providing detailed information with high spatial and temporal resolution. As a result, both the number of available satellite precipitation products and the quality of the data they generate has increased (Tedla et al. 2024).

Some satellite-based precipitation products outperform ground-based measurement technologies in terms of higher spatial and temporal resolutions. However, they still present certain biases compared to the precipitation value measured with rain gauges (Q. Zhu et al. 2021).

Near real-time satellite precipitation products have demonstrated a high potential for flood monitoring in basins where there is no extensive network of rain gauges, which is fundamental for the implementation

of an early warning system (Llauca et al. 2021), producing good results in flood forecasting with errors in an acceptable range (Tedla et al. 2024).

The use of satellite precipitation to derive flood frequency distributions has also been explored, such as the work developed by Dis et al. (2018) in several sub-basins of the Connecticut River basin, concluding that satellite products can be valuable for deriving flood frequencies in regions with sparse ground-based measurement data.

Regarding the use of products with high temporal resolution, Q. Zhu et al. (2021) evaluated and statistically compared the accuracy of precipitation products compared to hourly in situ precipitation observations, finding that high temporality satellite precipitation products have great potential for flood prediction in areas with limited in situ data. Future developments should focus on reducing uncertainties and improving the accuracy of hydrological simulations to better forecast flood disasters.

However, satellite products have the following limitations:

- They may contain errors due to indirect estimations, sampling uncertainty and algorithms used. The characteristics of these errors vary considerably with climates, storms, seasons and altitudes (Masood et al. 2023). To reliably use satellite precipitation products in hydrological modeling, it is necessary to validate and improve their performance in advance.

- Multiple studies have found that the direct use of satellite data is not recommended and that bias correction is generally required (Tedla et al. 2024; Masood et al. 2023).

- Studies such as that developed by Sapountzis et al. (2021) analyzing the use of satellite products in flash flood assessment, found that it is not possible to use satellite products without prior calibration and validation. However, the study showed that combining satellite precipitation data with ground-based precipitation data can be very useful for flash flood analysis in unmonitored basins.

- Estimation methods are still under development and are continually undergoing considerable advances. Precipitation estimation by remote sensing is still a relatively young area of research, many of its products suffer from considerable inaccuracies (Nguyen et al. 2019). These drawbacks translate into major uncertainties that must be understood in order to take full advantage of the potential of satellite-based products.

- The northern and southern latitudes of approximately 60° limit most quasi-global products due to the increasing unreliability of satellite data readings as satellites in geostationary orbit (GEO) get closer to the poles (Nguyen et al. 2019).

Due to these limitations, it is essential to validate the accuracy of satellite precipitation products and their applicability in the area where they will be used. This validation process can be performed through statistical analyses based on ground-based rain gauge data and an appropriate hydrological modeling framework. Statistical analysis determines the accuracy and consistency of satellite precipitation data, while hydrological simulation clarifies its usefulness and application (Masood et al. 2023).

For example, Trinh and Molkenthin (2021) used satellite-derived precipitation products to evaluate their accuracy compared to rain gauge measurements before applying a temporal disaggregation technique, in order to select the most suitable product for the study area. Subsequently, they disaggregated the daily rain gauge data to sub-daily scales, dividing the daily precipitation measured at the monitoring stations by the accumulated sub-daily precipitation derived from satellite data, and then multiplying this result by the satellite sub-daily precipitation. Within the procedure, they also included a correction coefficient to adjust the satellite precipitation to a local scale. In this way, satellite precipitation at unmonitored locations can be corrected using the difference determined between monitored sites and satellite products from surrounding sites.

Table 20 summarizes the main characteristics of satellite precipitation products for potential use in hazard assessment.


Image: Adobe Stock

Table 20. Satellite precipitation products

Product	Finest spatial resolution	Temporal resolution	Spatial coverage	Temporal coverage	Latency	Descriptive information
PERSIANN-CCS (CHRS)	0.04°×0.04°.	Hourly.	Quasi-global (60°S–60°N; 180°W–180°E).	January 2003-present.	1 hour.	This product categorizes cloud patch characteristics based on cloud height, surface extent and texture variability estimated from satellite imagery (Tedla et al. 2024).
CMORPH (NOAA)	0.07°×0.07° (8 km at the equator).	30 minutes.	Quasi-global (60°S–60°N; 180°W–180°E).	January 1998-present.	18 hours.	The Climate Data Record (CDR) of Satellite Precipitation - CMORPH consists of satellite precipitation estimates that have been bias-corrected and reprocessed using the Climate Prediction Center (CPC) Morphology Technique to create a high-resolution global precipitation analysis.
IMERG (NASA)	0.1°×0.1°.	30 minutes.	90°S – 90°N; 180°W–180°E.	June 2000-present.	18 hours.	It is NASA's most advanced algorithm for estimating surface precipitation from satellite data. The Precipitation Processing System generates real-time IMERG (Early and Late IMERG, with latencies of 6 and 18 hours, respectively), which is complemented by the higher quality or research IMERG (Final IMERG, with a latency of 4 months)(Huffman et al. 2020; NASA 2020).
Hydro-Estimator (NOAA Star)	0.045°×0.045°.	15 minutes.	Global 65 S–65 N.	2002-present.	Real time (approx. 1 hour).	It uses infrared (IR) data from NOAA's Geostationary Operational Earth Observing and Meteorological Satellites (GOES - Geostationary Operational Environmental Satellites) to estimate precipitation rates. Hydro-Estimator products have been used in Central America for mass movement early warning and in the Central American Flash Flood Guidance (Scofield 1987;Scofield& Kuligowski 2003; Strauch 2009).

Product	Finest spatial resolution	Temporal resolution	Spatial coverage	Temporal coverage	Latency	Descriptive information
GSMaP (JAXA)	0.1°.	Daily.	60 N-60 S.	2014-present.	4 hours.	GSMaP consists of four types of products: two real-time (GSMaP-NRT and GSMaP-Gauge NRT) and two post real-time (GSMaP-Gauge and GSMaP-MVK). To calculate GSMaP-Gauge NRT precipitation with a four-hour latency period, the estimated error parameters for the GSMaP-Gauge real-time post product are used. GSMaP-Gauge also employs a combination of passive microwave (PMW) and infrared (IR) data, along with a unified rain gauge-based analysis of the Climate Prediction Center (CPC) global daily precipitation dataset (Masood et al. 2023).
CHIRPS (Climate Hazards Group Infrared Precipitation with Stations) (USGS and CHC)	0.05°.	Daily.	50 N-50 S.	1981-present.	48 hours.	CHIRPS is a quasi-global precipitation dataset consisting of three types of temporal data (daily, pentanary (every 5 days) and monthly) with two types of spatial resolution (0.05° and 0.25°). Daily data is considered real-time data with a latency period of 2 days, while pentanary and monthly data is considered post-real-time data sets with a latency period of 21 days. Their algorithm is based on cold cloud duration (CCD) and rain gauge observations to approximate precipitation (Masood et al. 2023).

6.3. REANALYSIS PRODUCTS

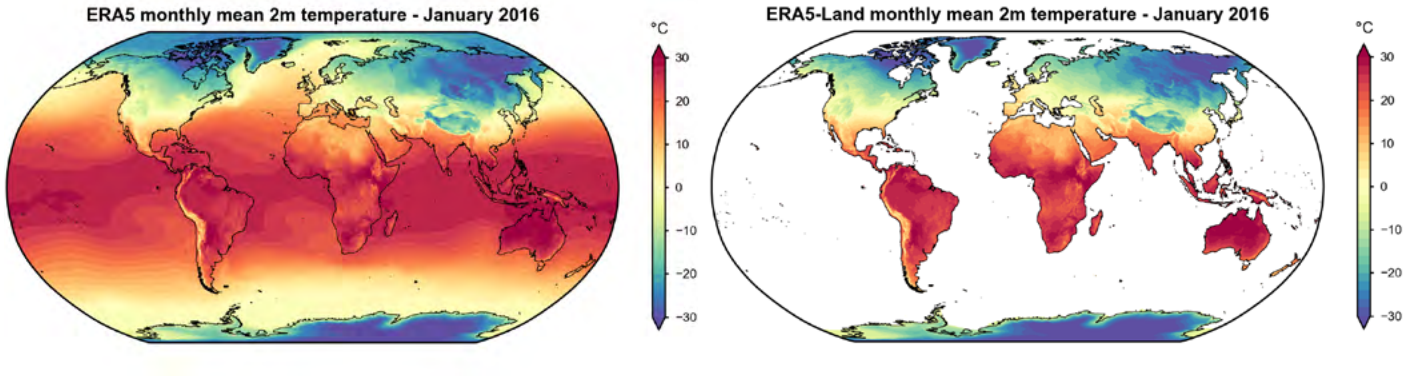

Source: European Commission, Copernicus, ECMWF, Climate Change Service.
https://climate.copernicus.eu/sites/default/files/inline-images/era5_t2m_201601.png

Reanalysis products are generated using numerical models driven by recorded meteorological observations, thus creating a historical series of various climate variables. These datasets typically have global coverage and span multiple decades (see **Table 21** for a summary of the most commonly used products and their attributes). Reanalysis precipitation data have been used extensively in flood risk modeling at continental and global scales. Its main advantages are its wide spatiotemporal coverage and ease of access. In areas where there are a limited number of rain gauges providing high quality observations, reanalysis products are often the best or only source of precipitation inputs for flood and other climate hazard simulations. However, they are not guaranteed to accurately represent extreme events nor adequately characterize flood risk (McClean et al. 2023).

There are several different reanalysis products, and their quality varies with recurring updates. As with satellite precipitation products, it is essential to evaluate them carefully before use. Therefore, field validation of reanalysis precipitation is very important, but also very challenging, especially in areas where rain gauge networks are sparse. Comparison of reanalysis data with precipitation measured by rain gauges has shown variable results depending on the approaches used, regions, and time scales, implying that site-specific performance evaluation may be necessary (Wanzala et al. 2022a).

Flood risk studies that have used reanalysis data have reported satisfactory results, indicating a potentially positive use. However, global or regional reanalysis data should not yet be considered as a replacement for high-resolution local observations. Uncertainties in flood risk assessment using reanalysis data must be adequately quantified and communicated to ensure that flood risk management decisions are not misinformed (McClean et al. 2023).

Although some studies have shown better performance of certain products compared to others, such as the study by (Wanzala et al. 2022b) which found that ERA5 performed better in Kenya, and in general ERA5 has been found to outperform other reanalysis products (Carr et al. 2024). In addition, the literature suggests that it is preferable to use multiple products, such as ERA5, CFSR and MERRA-2, to capture the full range of uncertainty in precipitation. This is because each of these products has demonstrated better performance in different areas or under different evaluation criteria (McClean et al. 2023).

The ERA5 product was used to generate the global dataset of precipitation intensity, duration, and frequency (IDF), known as Parametrized eXtreme Rain (PXR), produced by Courty et al. (2019). Within the evaluation of these global IDFs, Carr et al. (2024) found that it shows promise for assessing flood risk at the urban scale, for both low- and high-frequency events.

Table 21. Reanalysis products

Product	Resolution	Coverage	Period	Frequency	Information
ERA-5	~30 km	Global	1979–	Hourly	The European Centre for Medium-Range Weather Forecasts' (ECMWF) reanalysis product 5 (ERA-5) replaces and improves upon ERA-Interim, which ceased production in August 2019. ERA-5 offers higher spatial and temporal resolution, along with an updated modeling and data assimilation system, which has resulted in a better representation of convective precipitation. In addition, it has proven to outperform several other reanalysis products.
MERRA-2	~55 km	Global	1980–	Hourly	The Modern Era Retrospective Analysis for Research and Applications Version 2 (MERRA-2) builds on its predecessor, MERRA, and features reduced biases in aspects of the water cycle, among other improvements. MERRA-2 uses observed precipitation products to correct forecasts and provide better estimates.
CFSR	~35 km	Global	1979–2011	Hourly	The National Centers for Environmental Prediction (NCEP) Climate Forecast System Reanalysis (CFSR) replaces the previous NCEP/NCAR reanalysis and uses an analysis system very similar to MERRA-2.
JRA-55	~60 km	Global	1958–	3-hours	The Japan Meteorological Agency's reanalysis product, JRA-55, replaces JRA-25, incorporating higher resolution and better data assimilation, among other improvements.

Source: McClean et al. (2023).

SECTION 7

Image: Adobe Stock

OPEN ACCESS GLOBAL INFORMATION FOR EXPOSURE AND VULNERABILITY ANALYSIS

The following sections will explore open access global information sources that are essential for exposure and vulnerability analysis in the context of disaster risk management.

7.1. EXPOSURE

Image: Adobe Stock

The following highlights some of the global exposure models, which are international efforts to develop databases and methodologies that enable the assessment of globally exposed assets. The available information that can be used to generate exposure layers is also presented, providing an overview of the accessible tools and data that facilitate the creation of exposure maps at various geographic scales.

7.1.1. Global models

There are several international efforts to develop global exposure models. For example, (i) De Bono and Mora (2014) developed an open-access global exposure model with a spatial resolution of 5 km, which was initially presented in the Global Evaluation Report (GEG-2013) with a later update (de Bono and Chatenoux 2015) creating the GEG-2015 database; (ii) the Global Earthquake Model (GEM) foundation introduced the Global Exposure Database (GED4GEM) (Gamba 2014). The most recent exposure database produced by GEM is version v2023.1 (Yepes-Estrada et al. 2023), which provides a spatial distribution of residential buildings and population at three different spatial resolutions: national, level 1 and level 2 administrative boundaries (Mistry 2023). (Mistry and Lombardi 2023); and (iii) in the framework of the CLIMADA function library, LitPop and BlackMarble methods were generated to produce global exposure layers (Eberenz et al. 2019). These examples are described in detail below.

The main objective of **GEG-2013** is to generate a global assessment of exposed assets in urban areas. Its purpose is to provide specific exposure data that can be used in general and large-scale risk assessments. This model considers only direct physical damage to urban buildings, using national socioeconomic data, models of geographic distribution of population and Gross Domestic Product (GDP) as the main sources of information. One of the most important features of the top-down approach adopted by the GEG-2013 is that it ensures comparability between countries and territories around the world, facilitating consistent analysis on a global scale (De Bono and Mora, 2014).

The GEG-2013 focuses on exposed assets, defined mainly as the stock of buildings (both housing and commercial or industrial buildings) and the population living or working in them. For this purpose, an approach based on the capital produced in urban areas is used, where the economic value of assets is assessed without considering indirect or secondary effects, which are explicitly outside the scope of the GAR 2013 report. The model is supported by World Bank data and presents a subnational exposure database on a global 5 x 5 km^2 grid, suitable for probabilistic risk assessment in urban areas at the national level. This approach is implemented through the CAPRA platform(http://www.ecapra.org) (De Bono and Mora 2014).

The exposure in GEG-2013 is represented as the value of a group of buildings within each 5 x 5 km^2 cell. To estimate the characteristics of buildings at the subnational level, four socioeconomic sectors are considered, where the distribution of building types is related to the population living in each type, rather than to the total number of buildings by construction type. The value of the capital produced (assets) is distributed by sector and type of building in each cell of the grid, taking into account the occupancy density and the unit cost per sector. Its ultimate goal is to contribute to the probabilistic estimation of risk on a global scale, presenting the results in relative terms using risk classes. This approach makes it possible to compare potential economic losses between countries and to provide an order of magnitude of expected impacts. (De Bono and Mora 2014).

Image: Flickr -IDB Sustainable Cities / Natal, Brasil

GEG-2015 is the updated version of GEG-2013. GEG-2015 is composed of two exposure grids: a 5x5 km global grid suitable for large area risk assessment and a 1x1 km high resolution coastal global grid for finer scale risks, for tsunami and storm surge risk assessment. Each GEG-2015 record represents a specific structural building type, associated with an income level or sector, with a specific representation at the centroid of the corresponding cell. One of the most important features of GEG-2015 is the inclusion of the rural population, which was not considered in the 2013 edition, multiplying the total number of exposed assets by approximately 18 times. In addition, significant improvements were made, such as the use of an improved built-up area mask and corrections to the limitations of the MODIS 500 model in densely populated regions, such as Southeast Asia. The base layers were also updated, including the population distribution database and construction data. Another key improvement was the geographic distribution of the capital produced, weighted by a new indicator that considers the variation between GDP values at the national and subnational levels (de Bono and Chatenoux 2015). **Figure 17** presents an example of the database in a test area showing the total capital stock.

The **Global Exposure Model developed by GEM** (Yepes-Estrada et al. 2023) is a mosaic of local and regional models containing information on the inventory of residential, commercial and industrial buildings in the smallest available administrative division of each country. It includes details such as the number of buildings, occupants, vulnerability characteristics, average built area and average replacement cost. This model is developed and maintained by the GEM Foundation through a bottom-up approach

on a global scale, using national statistics, socio-economic data and local data sets. The inputs used come from national institutions, regional programs or bilateral collaborations, and are based on the best publicly available data and models. This model makes it possible to identify the most common types of construction worldwide, regions with high proportions of informal construction and areas with a high concentration of population and building inventory. The underlying data used to create the maps are available for all regions of the world, aggregated at administrative level 1 under a CC BY-NC-SA[17] license , or disaggregated to a higher level of detail upon request, for which specific licenses are issued depending on the required use (GEM 2024b).

Figure 17. Example of the GEG-2015 database

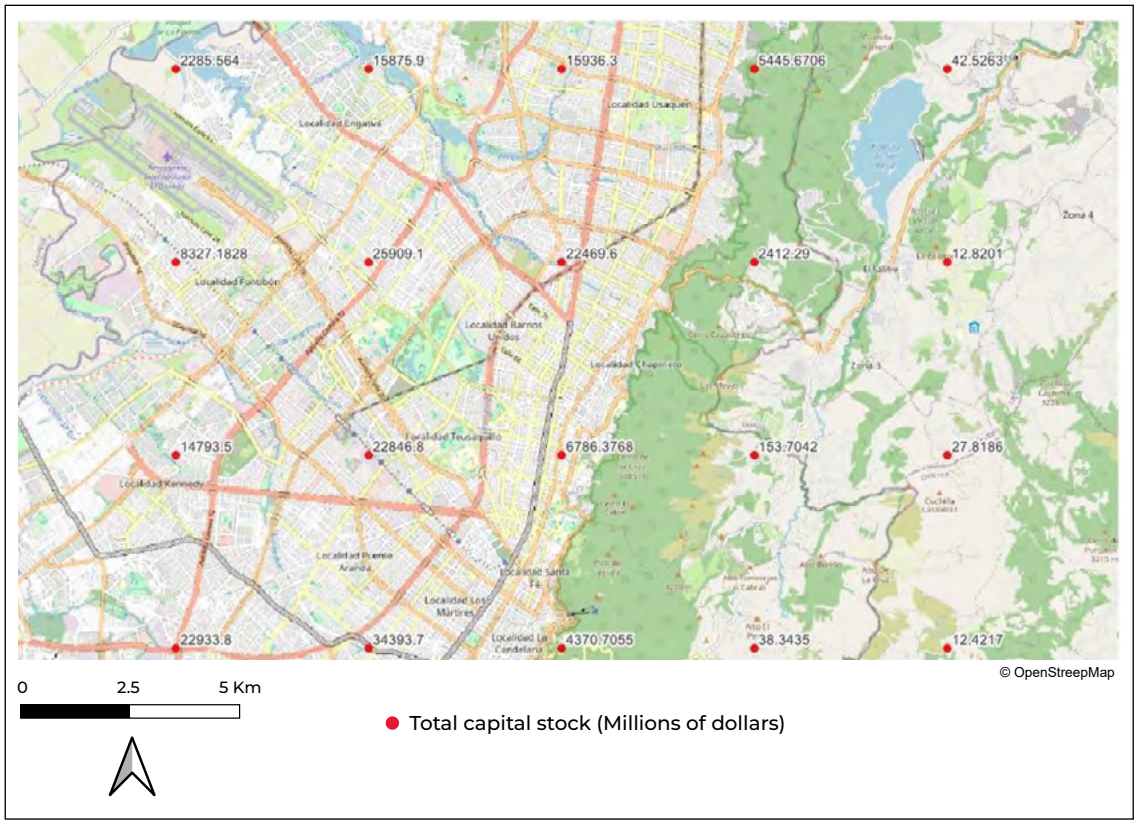

Source: GAR15.

[17] The Creative Commons Attribution NonCommercial Share-alike license (CC BY-NC-SA) allows others to distribute, remix, adapt, and create derivative works from a material, provided that proper credit is given to the original author, it is not used for commercial purposes, and new creations are licensed under the same terms (https://creativecommons.org/licenses/by-nc-sa/4.0/).

The GEM exposure model is available as a Global Exposure Map in shapefile format consisting of four layers representing the number of buildings, built-up area, total replacement value and total population. The maps of the number of buildings and total replacement value are available for direct download as high-definition PNG files under the CC BY-NC-SA 4.0[18] license , which requires attribution, non-commercial use and sharing of derivatives under the same license. In cases of commercial use or to obtain the complete set of layers as a shapefile, it is necessary to submit a specific request, where a customized license will be granted according to the use case. For non-commercial purposes, the license requires giving appropriate credit, including a link to the license and mentioning any changes made (GEM 2024b).

LitPop is a methodology designed to estimate the spatial distribution of physical asset values at a global level with high resolution. This approach uses nighttime light intensity and population data as proxies to model economic activity, assigning macroeconomic indicators, such as gross domestic product (GDP), to specific geographic cells. LitPop provides a homogeneous and consistent basis for modeling direct economic impacts in different regions of the world. The methodology is based on multiplying the nighttime light intensity by the population density in each geographic cell, thus creating an indicator that reflects the economic activity in that space. This value is then used to distribute nationally produced capital or other macroeconomic indicators, such as GDP or gross regional product (GRP), on a proportional basis. This process enables a spatial representation of physical asset values, adapted to different levels of resolution depending on the quality of the available data, to be obtained (Eberenz et al. 2019). **Figure 18** and **Figure 19** show an example of LitPop with data generated at a resolution of approximately 930 m.

Image: Flickr - IDB Sustainable Cities / Natal, Brasil

[18] The Creative Commons Attribution NonCommercial Share-alike 4.0 license (CC BY-NC-SA 4.0) allows others to share, copy, and adapt the material as long as proper credit is given to the original author, it is not used for commercial purposes, and derivative works are distributed under the same license (https://creativecommons.org/licenses/by-nc-sa/4.0/deed.es).

Figure 18. Asset value in millions of dollars LitPop generated with CLIMADA for the reference year 2025

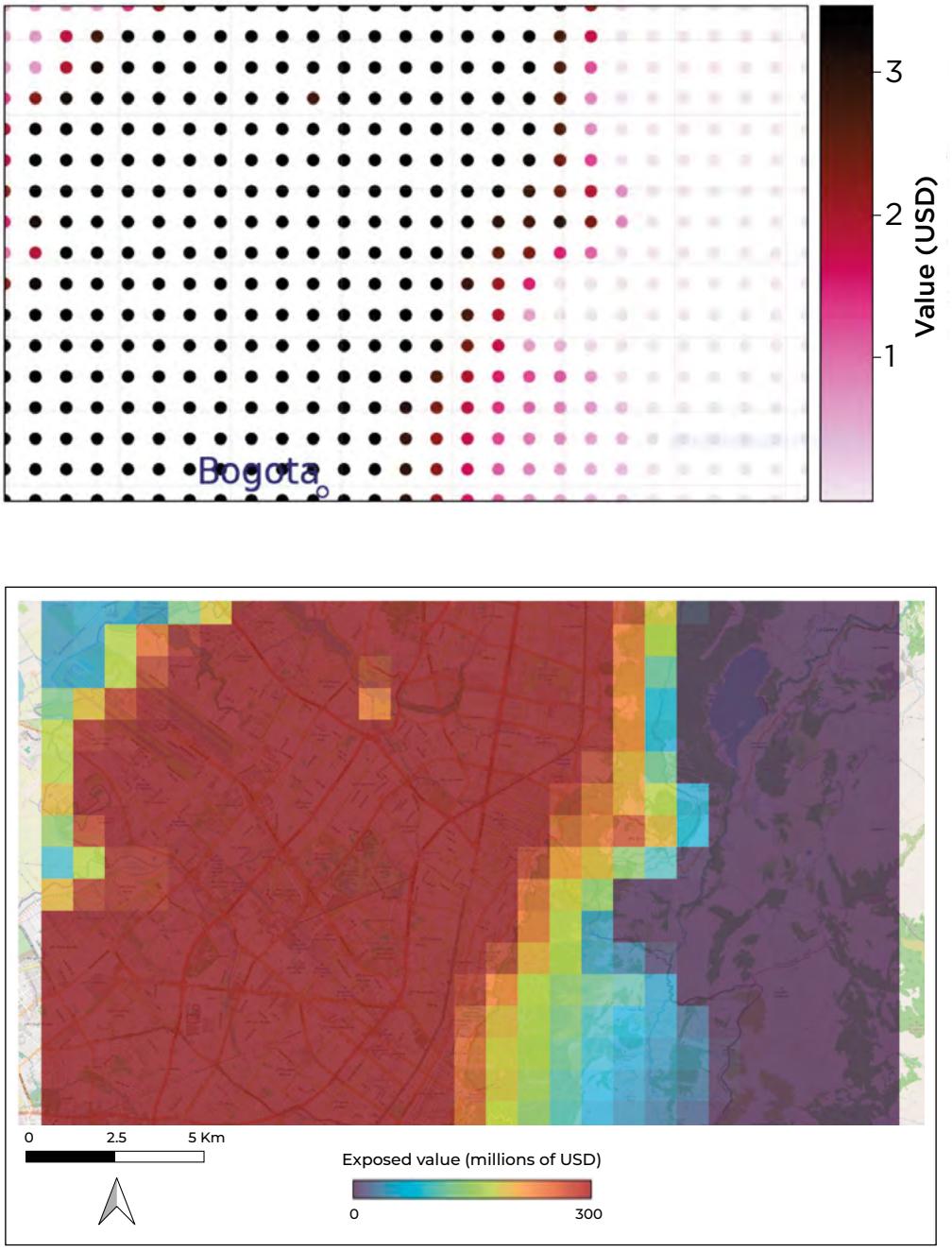

Note: layer generated for the same area shown in Figure 17. The upper image shows the CLIMADA output with values assigned to centroids, and the lower image shows the raster exported from CLIMADA.

Figure 19. LitPop population generated with CLIMADA for the reference year 2025

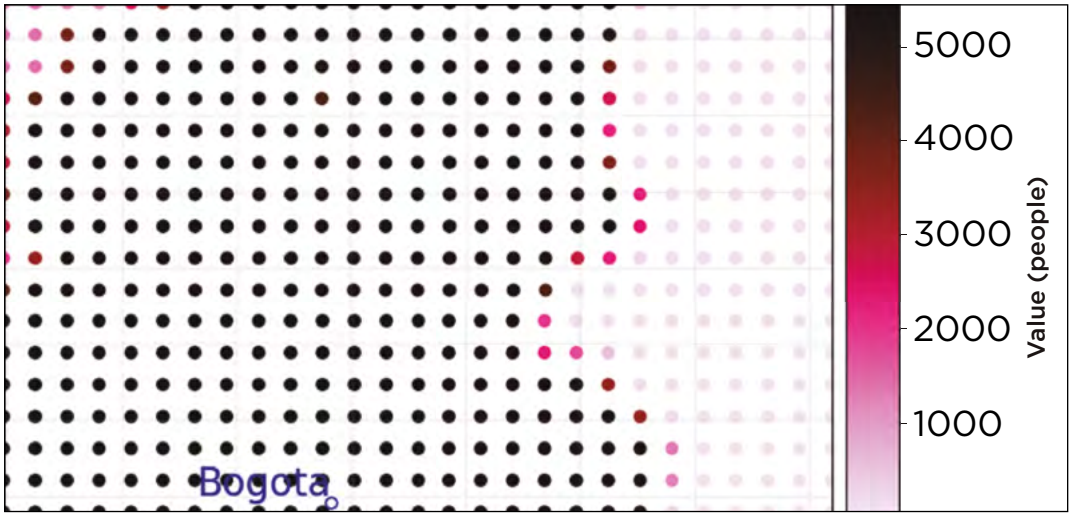

Note: layer generated for the same area shown in **Figure 17**.

Although the information generated through LitPop is extremely useful for coarse-scale risk analysis, one of its main limitations is the quality and resolution of population and nighttime light data, which vary significantly between countries, affecting the accuracy of the model. In addition, its top-down approach, while effective for large-scale analyses, does not consider local variations in infrastructure types and vulnerabilities, limiting its applicability for detailed assessments at the local level. Nighttime light data also present problems such as saturation in dense urban areas and blooming, where reflected light does not necessarily correspond to real economic activity. Finally, the lack of detailed subnational data makes it difficult to directly validate the model in certain contexts, and its reliance on national indicators such as GDP may not fully capture regional inequalities or specificities (Eberenz et al. 2019).

BlackMarble is one of the exposure classes generated by CLIMADA and is used to approximate economic exposure at the country and province level. This model interpolates GDP values and income groups based on nighttime light intensity in a specific year, thus enabling a spatially distributed estimate of economic exposure. For this purpose, BlackMarble uses satellite images of nighttime light from different sources. Between 2012 and 2016, NASA imagery with a resolution of 15 arcseconds (~500 m) is used, while for the years between 1992 and 2013, NOAA imagery with a resolution of 30 arcseconds (~1 km) is used. By default, NASA data is used for years after 2013, and NOAA data for years before that, although there is an option to select the closest source. In addition, the default resolution is that of the input image, but can be adjusted by interpolation. GDP and income group data are obtained from the World Bank database through the pandas-datareader API, and when values are not available, the closest in time are considered or data from the Natural Earth repository are used. **Figure 20** shows an example of Blackmarble with a resolution of approximately 460 meters.

Figure 20. Asset value in millions of dollars Blackmarble generated with CLIMADA

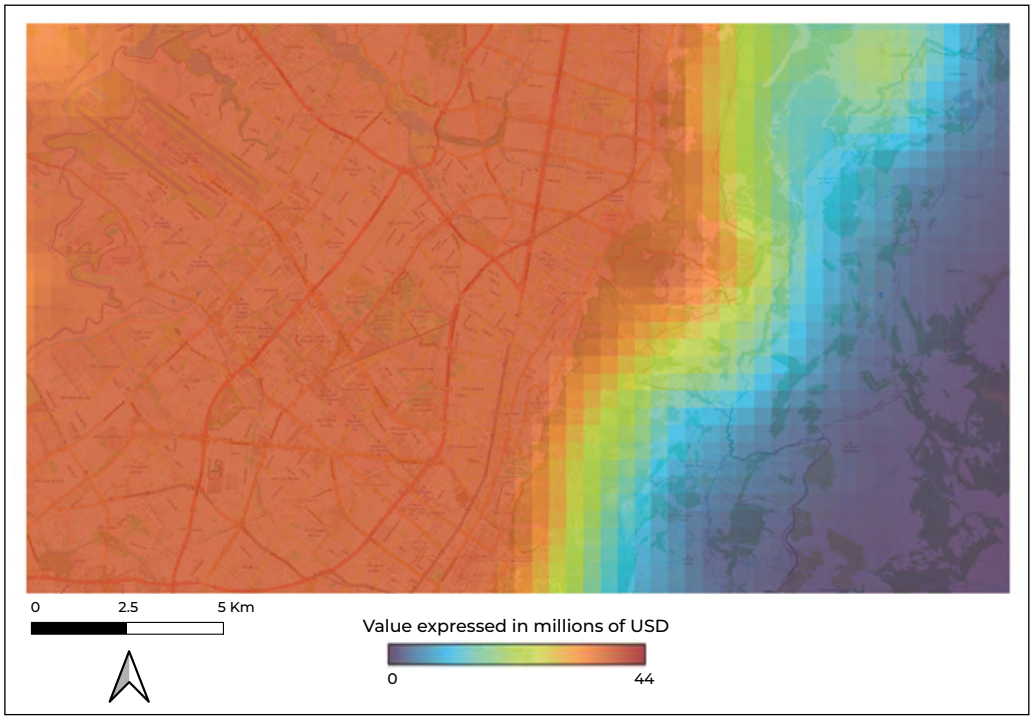

Most of the available exposure models provide sufficient information for risk assessment on a national and global scale. However, they tend to lack the resolution needed to perform urban-scale risk assessments with a high level of confidence. The main challenge in developing a high-resolution exposure model lies in the limited information available at the asset level (Mistry and Lombardi 2023). However, there is a very significant advance in the generation of detailed scale information that can be used for the construction of exposure layers as shown in section 7.1.2.

7.1.2. Available information that can be used to generate exposure layers

For large urban areas, exposure data can be obtained from open-source and proprietary databases, such as OpenStreetMap (OSM), Google Earth and locally generated cadastres. However, in small urban areas and rural regions, these data are often incomplete or non-existent, making it necessary to collect information through remote sensors and field work. Recent research has explored the use of stochastic exposure models, such as the one proposed by (Mistry and Lombardi 2023) which uses the Monte Carlo sampling method to consider the uncertainty related to the location of assets and their attributes in the exposure model. This approach recognizes the complexity and accuracy that exposure analyses require,

especially at more detailed scales. The following is a description of the main data sources with global coverage that can provide baseline information for building databases of locally exposed elements.

OpenStreetMap (OSM)[19,20z] is a free, collaborative mapping platform that provides geospatial data from around the world, created and maintained by a global community of volunteers. This data is collected in an open manner, allowing its use and modification under an open content license. In terms of exposure analysis, OSM data provides detailed information on infrastructure, such as roads, bridges, buildings, transportation networks, and other built assets (see **Figure 21**, **Figure 22** and **Figure 23**). These data can be used to map the location and characteristics of the exposed assets. In addition, OSM also provides information on elements relevant to disaster response and recovery, such as hospitals, fire stations, schools and shelter areas.

Image: Adobe Stock

[19] https://wiki.openstreetmap.org/wiki/About_OpenStreetMap

[20] https://www.hotosm.org/what-we-do

Figure 21. Extraction of different types of infrastructure available in OpenStreetMap in point format

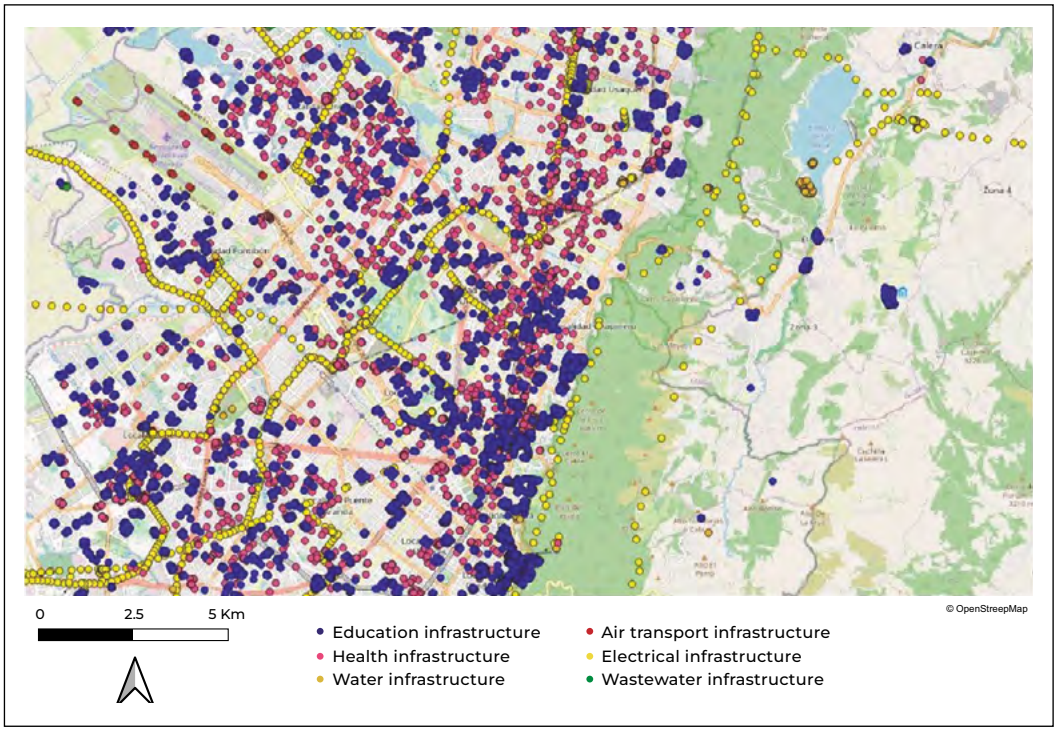

Source of infrastructure data: OpenStreetMap contributors (2017).

Humanitarian OpenStreetMap Team (HOT) is an organization that uses OpenStreetMap (OSM) data to support disaster response and preparedness efforts in vulnerable areas, particularly in regions where geospatial data is scarce or non-existent. HOT works in collaboration with local communities and humanitarian organizations to collect, enhance and update geospatial data to create detailed maps that facilitate exposure analysis and risk management. HOT's work focuses on real-time mapping during emergency situations, as well as improving OSM coverage in high-risk areas. In these cases, the team focuses on identifying the most vulnerable areas and updating infrastructure data, such as buildings, roads, bridges and other critical facilities that may be affected by a disaster. In addition, HOT organizes mapping campaigns in which volunteers, using satellite imagery and other data sources, contribute to the creation of maps that reflect the current situation on the ground. This information is crucial for conducting exposure analyses, as it enables humanitarian authorities and organizations to plan and execute more effective responses, identify risks accurately and coordinate interventions efficiently.

Figure 22. Extraction of different types of infrastructure available in OpenStreetMap in line format

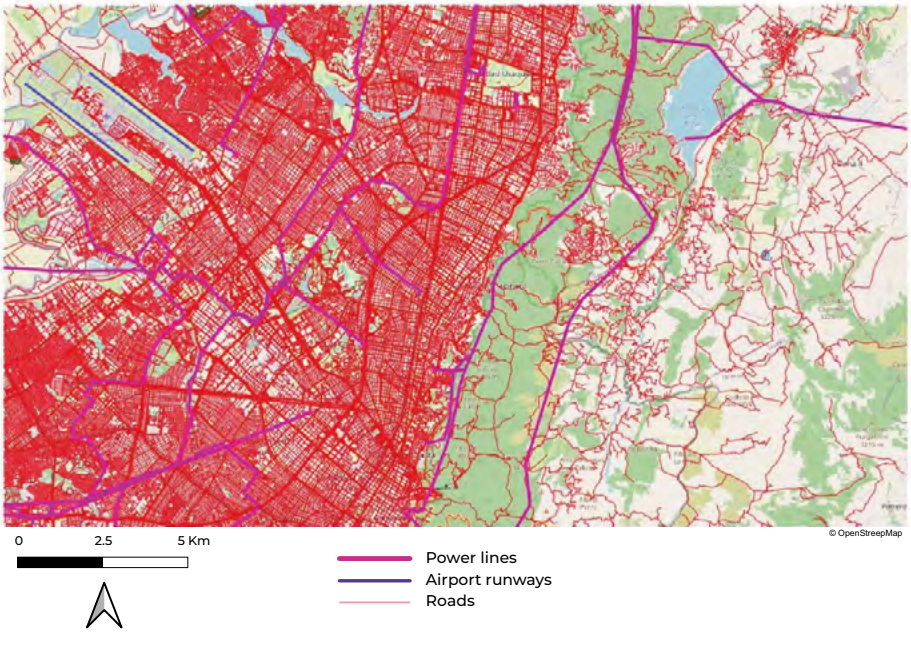

Source of infrastructure data: OpenStreetMap contributors (2017).

Figure 23. Extraction of buildings available in OpenStreetMap in polygon format

Source of building data: OpenStreetMap contributors (2017).

The Global Human Settlement Layer (GHSL)[21] is a project developed by the European Commission that uses remote sensing techniques to generate geospatial data layers related to human occupation and urban development on a global scale. These data are based on satellite imagery and other sources of geospatial information, and are designed to provide a detailed view of urban and human settlement areas, making them useful for exposure analysis in the context of disaster risk management. One of the main features of GHSL is its ability to identify built-up areas, providing data on the proportion of built-up area within each grid cell, which allows estimating the density and extent of urban settlements. The data most commonly used in risk analysis comes from layers such as GHS_BUILT_S2, which has a resolution of 10 meters and was derived from Sentinel-2 satellite images (2018). These data make it possible to map urban areas within areas affected by disasters, such as floods or earthquakes, and to calculate the exposure of infrastructure and population to these events. Unlike OpenStreetMap data, which relies on voluntary contributions, GHSL uses a methodology based on satellite image processing, which provides more uniform coverage, especially in remote or hard-to-reach areas. However, the spatial resolution, although high, may still present limitations for detecting smaller structures or areas with high variability in urban development, such as rural or semi-urban areas (Copernicus 2024). **Figure 24** shows an example of the layers of population, non-residential area and built-up area for the year 2025. The available information covers multiple time periods between 1975 and 2030.

WorldPop[22] is a global initiative that provides high-resolution spatial data on population distribution around the world. Using a combination of satellite imagery, national census and other geospatial data, WorldPop generates population maps at the grid level, which is crucial for performing exposure analysis in the context of disaster risk. These population maps can estimate the density and distribution of people in specific areas. In terms of risk analysis, WorldPop offers a layer of high-resolution data with population estimates at different geographic points, typically at the 100-meter level or lower, allowing for significant spatial accuracy. In addition, the WorldPop database also allows for future population projections, which facilitates long-term planning in terms of disaster preparedness. **Figure 25** shows an example of the population for a pixel size of 100 meters.

[21] https://ghsl.jrc.ec.europa.eu/data.php

[22] http://worldpop.org.uk

Figure 24. GHSL layers of population, non-residential area and built-up area

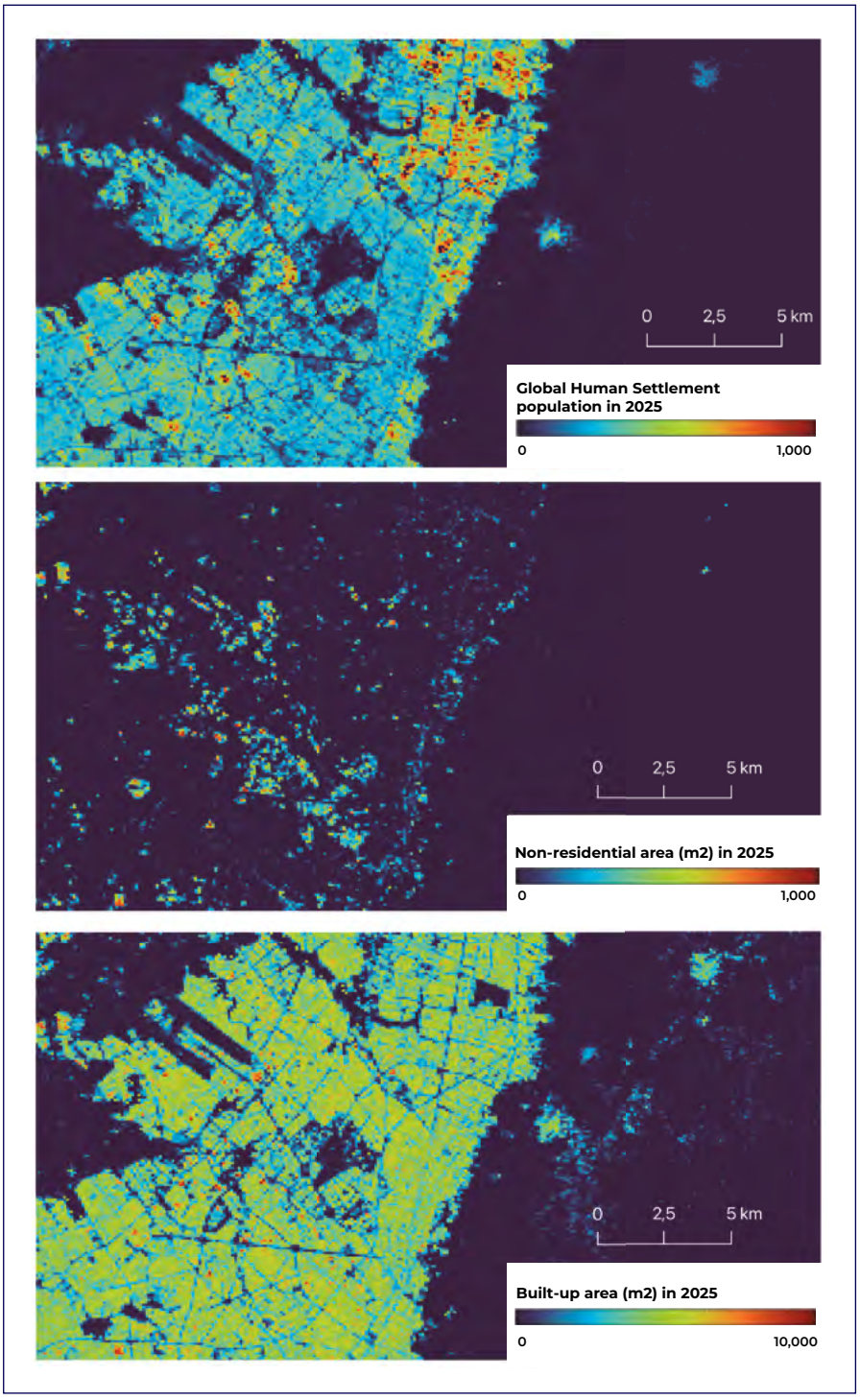

Source: Pesaresi and Politis (2023).

Figure 25. Population obtained from WorldPop

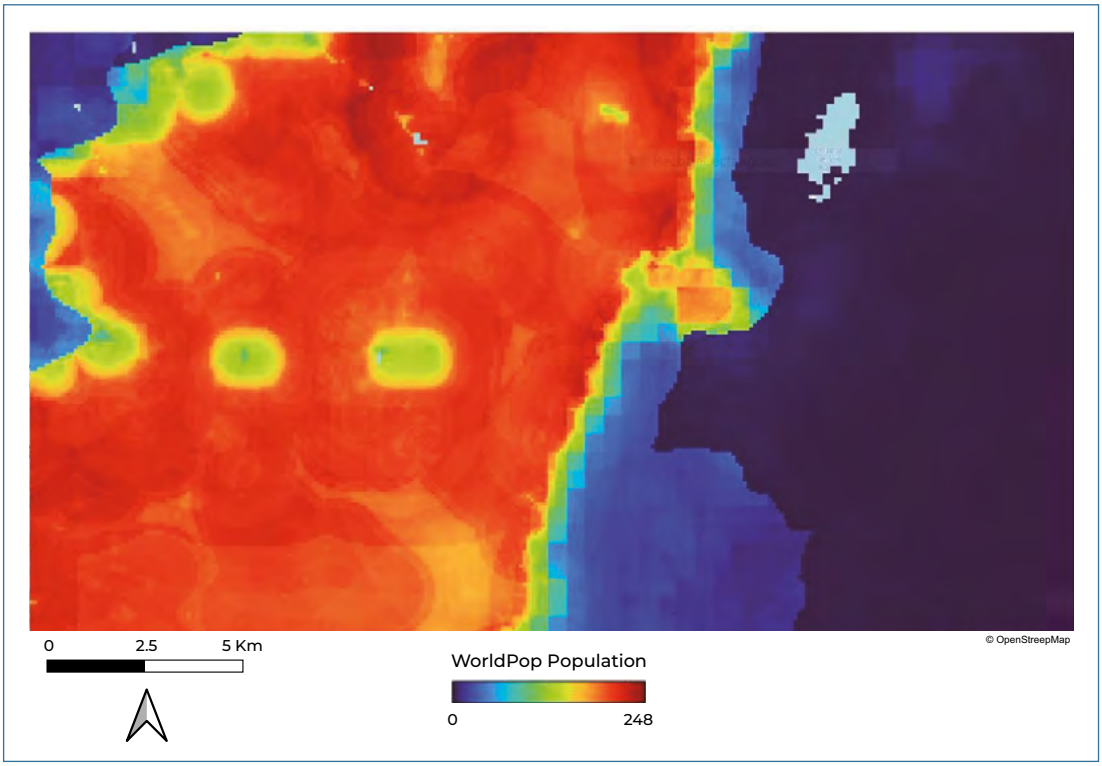

Source: University of Southampton (2018).

The **high-resolution population density maps developed by META** in collaboration with the Center for International Earth Science Information Network (CIESIN) represent an innovative tool for estimating population distribution. Through the use of artificial intelligence and the analysis of satellite images, these maps identify the location of buildings and distribute the population into 30-meter grids. The process includes census data collection, image analysis using machine learning algorithms, and population assignment based on building density in each mosaic. Thanks to this approach, demographic information is obtained, such as the number of children, women of childbearing age and older adults. Access to this data is public and available on Humanitarian Data Exchange (HDX) and Amazon Web Services (AWS) platforms (META 2025). **Figure 26** shows an example of the population information produced by META. Pixels with values correspond to grid cells where the presence of a structure has been detected. The population values are evenly distributed in each of these cells, representing an estimate of the population for the census area.

Figure 26. Population calculated by META

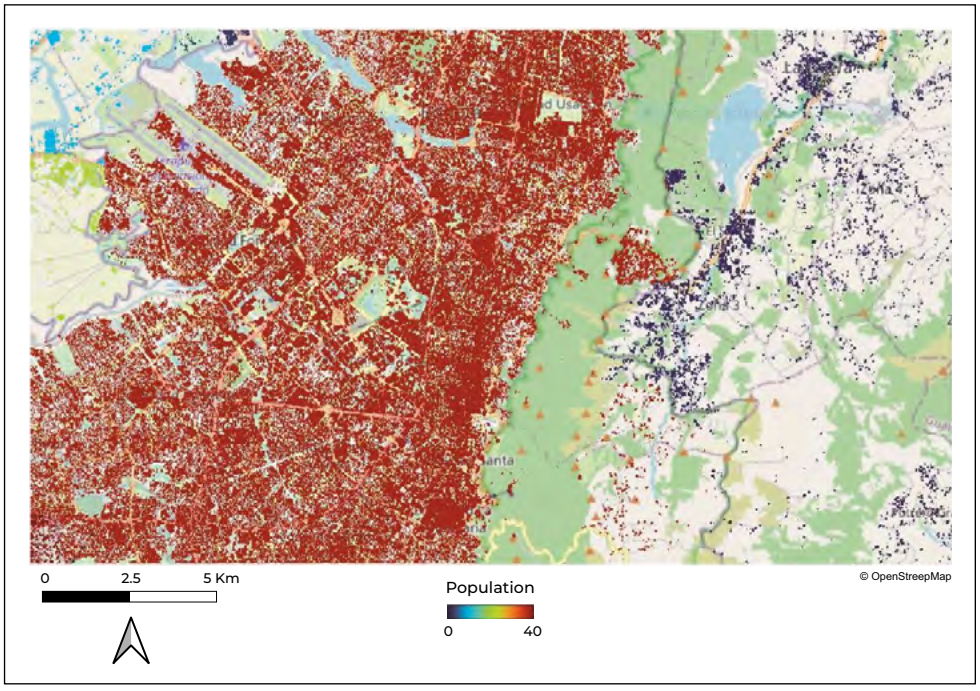

Source of population data: Humanitarian Data Exchange (HDX).

Microsoft AI Microsoft Bing Maps Building Footprints is a global initiative that provides open data on building margins around the world. Using high-resolution satellite imagery from sources such as Maxar, Airbus and IGN France, more than 1.4 billion buildings have been detected between 2014 and 2024. These data are accessible under the Open Database License (ODbL)[23], which allows them to be downloaded and used free of charge. The December 2024 update includes approximately 999 million building polygons in line-delimited GeoJSON format. In addition, the coordinates are referenced to the EPSG system: 4326, ensuring compatibility with geospatial analysis tools (Microsoft 2024).

The data extraction process consists of two stages: semantic segmentation using deep neural networks (DNNs), which identify the pixels corresponding to buildings in aerial images, and polygonization, where these pixels are converted into geometries. To improve data quality, confidence scores ranging from 0 to 1 have been implemented, indicating the certainty of detection. The data is evaluated using metrics such as Precision, Recall and Intersection over Union (IoU), and although the quality is high in most cases, it varies between dense urban

[23] The Open Database License (ODbL) allows users to freely share, modify and use a database, as long as they maintain proper attribution, share modifications under the same license, and keep derivative versions open (https://opendatacommons.org/licenses/odbl/).

and rural areas. This initiative supports the OpenStreetMap (OSM) ecosystem and is used in humanitarian applications, such as the HOT Tasking Manager platform, which facilitates mapping in vulnerable regions. The data is accessible through GitHub (Microsoft 2024). **Figure 27** shows an example of the buildings for a selected area.

Figure 27. Extraction of available buildings in Microsoft Bing Maps

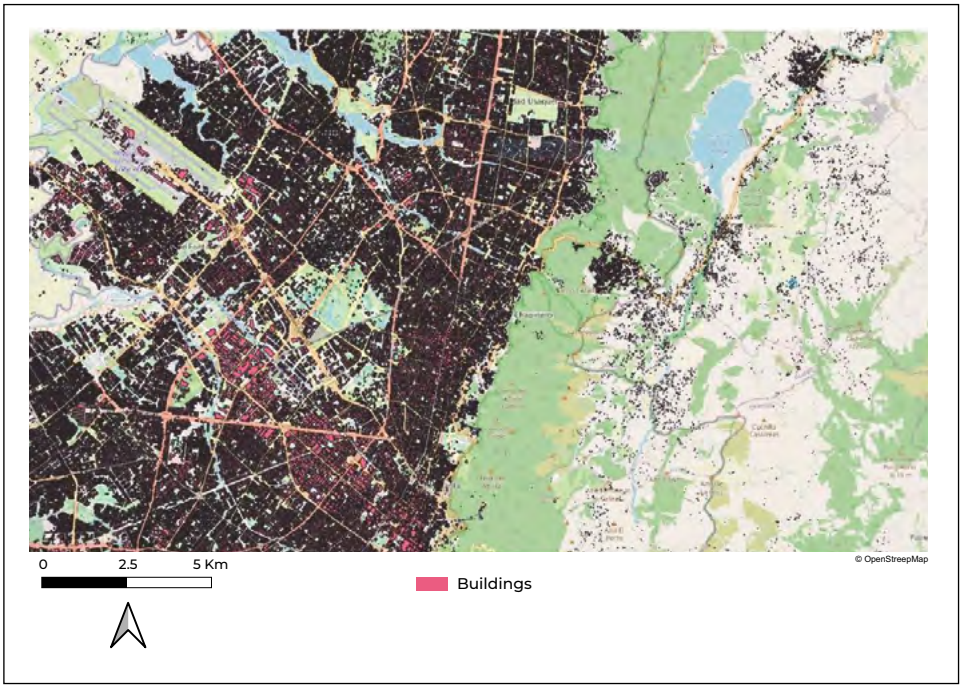

Source of building data: GlobalMLBuildingFootprints.

Google Building Footprints is a large-scale dataset that provides building outlines derived from high-resolution satellite imagery. The project, led from Google's Ghana office, focuses on the African continent and Global South regions, covering critical areas such as Africa, South Asia, Southeast Asia, Latin America and the Caribbean. The current version, v3, covers approximately 1.8 billion buildings distributed over an inference area of 58 million km^2. The dataset includes polygons describing the geometry of each building, confidence scores (range 0.65 to 1.0) indicating the probability that an identified object is a building, and a Plus Code representing the centroid of the building. The data are organized in CSV files, spatially segmented by level 4 S2 cells. Each record contains information such as latitude, longitude, area in square meters, geometry in WKT (well-known text) format (POLYGON or MULTIPOLYGON) and the Plus code of the centroid of the building. The deep learning model used in detection has undergone several enhancements since its initial release,

with significant updates in versions v2 and v3. In addition, confidence score thresholds are included to ensure specific accuracies of 80%, 85% and 90%, allowing for a more detailed control of data quality. This dataset is available under two open licenses: Creative Commons Attribution (CC BY-4.0) and Open Database License (ODbL) v1.0, allowing flexibility in its use as long as the established terms are respected (Google Research 2024). **Figure 28** shows an example of the buildings for a selected area.

Figure 28. Extraction of buildings available in Google Building Footprints

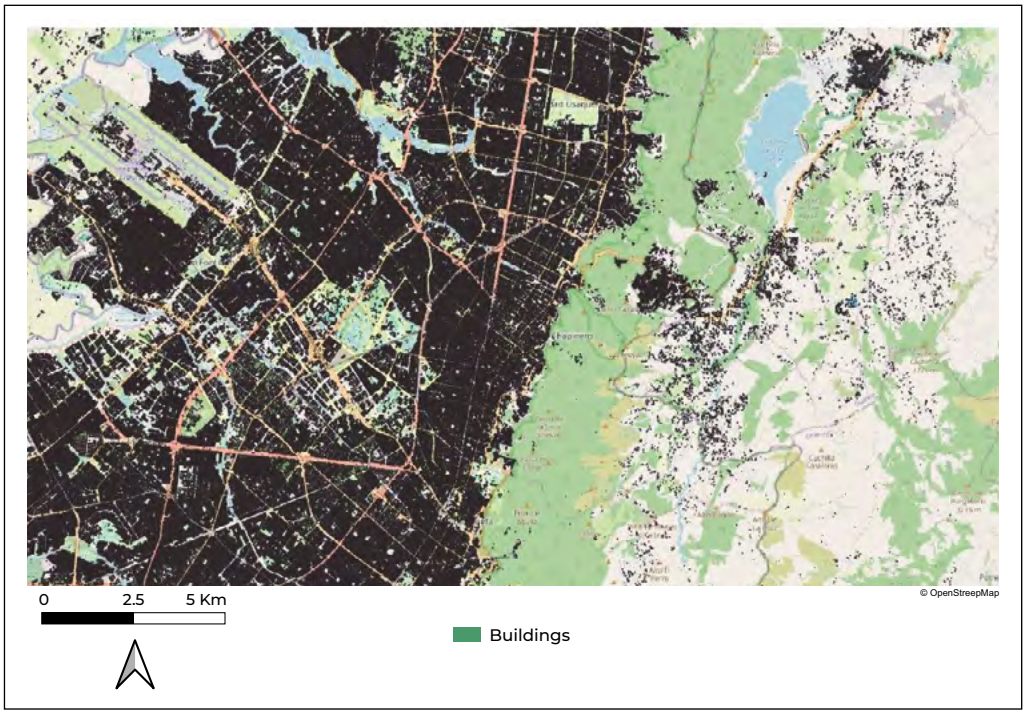

Source of building data: Google Research.

ML Road Detections Project. Microsoft, through Bing Maps, has released a global road dataset extracted from high-resolution satellite imagery, with a total of 48.9 million kilometers of roads detected and 1,165,000 kilometers of roads previously missing from OpenStreetMap (OSM). This project uses satellite imagery from Bing Maps, Maxar and Airbus, collected between 2020 and 2022, and makes the data available under the Open Database License (ODbL), which allows free download and use within the established terms.

The process of generating this data was carried out in four stages. First, semantic segmentation with convolutional neural networks (CNN) was applied to identify pixels corresponding to paths. These results were then transformed into road geometries through connectivity generation and improvement processes. Subsequently, redundant roads that already existed in OSM were excluded, and finally, the data were classified to discard low confidence items and define road types. The model used, based on UNet and ResNet architectures, was trained with 20,000 labeled images from various regions, including mountains, deserts and coastal areas, to ensure a varied geographic representation. Data quality was validated with specific metrics, such as a per pixel accuracy of 85.24% and an average path length similarity (APLS) of 87.53%, ensuring the connectivity of the generated road system. Prior to publication, an additional classifier confirmed that the missing paths in OSM were at least 95% accurate. The main objective of this effort is to strengthen the OpenStreetMap ecosystem, promoting community collaboration to improve the quality and coverage of road maps globally. Microsoft also encourages community contributions under licensing agreements that respect copyright and appropriate use of data (Microsof 2024). **Figure 29** shows an example of the pathways for a selected area.

Figure 29. ML Road Detections Project Roads

Source of road data: RoadDetections

7.2. VULNERABILITY

Image: Flickr - IDB Sustainable Cities / Nassau, Bahamas

Vulnerability curves make it possible to establish relationships between the level of damage or loss and the intensity of an event. There are efforts to generate information on **vulnerability curves at a global level** based on global data and modeling methodologies, such as the one carried out by Huizinga et al. (2017), who developed a series of vulnerability curves to assess the effects of flooding on buildings worldwide. Their research focused on the creation of a set of generic vulnerability curves that could be applied to different types of buildings, from residential to commercial and industrial infrastructures. The Huizinga curves use parameters such as flood height, type of construction and material of the structures to estimate the expected damage as a function of these factors. The work of Huizinga et al. (2017) relies on global data and a standardized methodology to create vulnerability curves that are as representative as possible for a variety of contexts. These curves are designed to be applied at a global level, which makes them useful in risk analyses conducted in regions with little specific information at the local or national level.

Currently, several risk modeling platforms integrate **vulnerability curves** to calculate economic losses and social impacts derived from natural phenomena. Vulnerability curves can be found in the CLIMADA functions, the CAPRA ERN-Vulnerability database, in HAZUS and **fragility functions** can be found within the IN-CORE database.

Global Earthquake Model Foundation (GEM) has an extensive database of vulnerability functions for use in seismic risk assessment with detailed documentation. GEM has developed more than 1,500 functions that consider a wide range of combinations of building materials, heights, lateral force resisting systems and seismic design levels. Fragility and vulnerability are derived through nonlinear time-history analysis applied to equivalent single-degree-of-freedom oscillators using an extensive set of ground motion records representative of various tectonic environments. The resulting functions are validated through tests that include calculating the average annual probabilities of collapse and the average annual loss rate for different locations, as well as comparing the results of simulations of historical events with observed damage and losses (GEM 2024c).

Image: Flickr - IDB Sustainable Cities / Santa Marta, Colombia

REFERENCES

Abid, S. K., N. Sulaiman, S. W. Chan, U. Nazir, M. Abid, H. Han, A. Ariza-Montes, and A. Vega-Muñoz, 2021: Toward an Integrated Disaster Management Approach: How Artificial Intelligence Can Boost Disaster Management. *Sustainability* 2021, Vol. 13, Page 12560, 13, 12560, https://doi.org/10.3390/SU132212560.

Akosah, S., I. Gratchev, D. H. Kim, and S. Y. Ohn, 2024: Application of Artificial Intelligence and Remote Sensing for Landslide Detection and Prediction: Systematic Review. *Remote Sensing* 2024, Vol. 16, Page 2947, 16, 2947, https://doi.org/10.3390/RS16162947.

Albano, R., I. Craciun, L. Mancusi, A. Sole, and A. Ozunu, 2017a: FLOOD DAMAGE ASSESSMENT AND UNCERTAINTY ANALYSIS: THE CASE STUDY OF 2006 FLOOD IN ILISUA BASIN IN ROMANIA -. *Carpathian Journal of Earth And Environmental Sciences*, 2.

——, L. Mancusi, and A. Abbate, 2017b: Improving flood risk analysis for effectively supporting the implementation of flood risk management plans: The case study of "Serio" Valley. *Environ Sci Policy*, 75, 158–172, https://doi.org/10.1016/J.ENVSCI.2017.05.017.

——, ——, A. Sole, and J. Adamowski, 2017c: FloodRisk: a collaborative, free and open-source software for flood risk analysis. *Geomatics, Natural Hazards and Risk*, 8, 1812-1832, https://doi.org/10.1080/19475705.2017.1388854/ASSET/A0A74E85-2E0F-4603-BD2C-08F8D37B77BD/ASSETS/IMAGES/TGNH_A_1388854_F0011_OC.JPG.

Albano, R., A. Sole, J. Adamowski, A. Perrone, and A. Inam, 2018: Using FloodRisk GIS freeware for uncertainty analysis of direct economic flood damages in Italy. *International Journal of Applied Earth Observation and Geoinformation*, 73, 220–229, https://doi.org/10.1016/J.JAG.2018.06.019.

Australian Water School, 2024: AI-assisted coding for water modellers - Live Training - Australian Water School. https://awschool.com.au/training/ai-python-for-modellers/?utm_medium=email&utm_campaign=509%20-%20New%20courses%20%20PyQGIS%20%20AI&utm_content=509%20-%20New%20courses%20%20PyQGIS%20%20AI+CID_c44a2139f0006be37d7c56ad00aefc09&utm_source=Email%20marketing%20software&utm_term=AI-assisted%20Python%20coding%20for%20water%20modelling (Accessed September 3, 2024).

Azizi, A., 2024: *A survey of seismic risk assessment using OpenQuake*.

Aznar-Siguan, G., and D. N. Bresch, 2019: CLIMADA v1: a global weather and climate risk assessment platform. *Geosci. Model Dev*, 12, 3085–3097, https://doi.org/10.5194/gmd-12-3085-2019.

World Bank, CEPREDENAC, ISDR, and ERN, 2009: User Manual - CAPRA-GIS.

Bentivoglio, R., E. Isufi, S. N. Jonkman, and R. Taormina, 2022: Deep learning methods for flood mapping: a review of existing applications and future research directions. *Hydrol Earth Syst Sci*, 26, 4345–4378, https://doi.org/10.5194/HESS-26-4345-2022.

BID, 2019: Methodology for Disaster Risk and Climate Change Assessment for IDB Projects: Technical reference document for teams responsible for IDB projects | Publications. https://publications.iadb.org/es/publications/spanish/viewer/Metodologia-de-evaluacion-del-riesgo-de-desastres-y-cambio-clim%C3%A1tico-para-proyectos-del-BID-Documento-tecnico-de-referencia-para-equipos-a-cargo-de-proyectos-del-BID.pdf (Accessed February 20, 2025).

Birkmann, J., 2006: *Measuring vulnerability to natural hazards: Towards disaster resilient societies*. U.N.U. Press, Ed. bepress,.

Bjånes, A., R. De La Fuente, and P. Mena, 2021: A deep learning ensemble model for wildfire susceptibility mapping. *Ecol Inform*, 65, 101397, https://doi.org/10.1016/J.ECOINF.2021.101397.

Blass, R., 2021: ETH Library Coupling Oasis LMF with CLIMADA. https://doi.org/10.3929/ethz-b-000480061.

De Bono, A., and M. G. Mora, 2014: A global exposure model for disaster risk assessment. *International Journal of Disaster Risk Reduction*, 10, 442–451, https://doi.org/10.1016/J.IJDRR.2014.05.008.

de Bono, A., and B. Chatenoux, 2015: A Global Exposure Model for GAR 2015. https://doi.org/10.13140/RG.2.1.3893.9041.

Bretherton, E., N. A. Horspool, Y. I. Syed, V. L. Miller, and R. Paulik, 2023: *RiskScape Case Studies: Informing Land-Use Planning Through Natural Hazard and Climate-Change Risk Modelling*. https://www.naturalhazards.govt.nz/assets/Publications-Resources/RiskScape-Case-Studies-Informing-Land-Use-Planning-Final-Report.pdf (Accessed January 12, 2025).

Cardona, O. D., M. G. Ordaz, E. Reinoso, L. E. Yamín, and A. H. Barbat, 2012: CAPRA-Comprehensive Approach to Probabilistic Risk Assessment: International Initiative for Risk Management Effectiveness.

Carr, A. B., M. A. Trigg, A. T. Haile, M. V. Bernhofen, A. N. Alemu, T. W. Bekele, and C. L. Walsh, 2024: Using global datasets to estimate flood exposure at the city scale: an evaluation in Addis Ababa. *Front Environ Sci,* 12, 1330295, https://doi.org/10.3389/FENVS.2024.1330295/BIBTEX.

CEPREDENAC, GFDRR, IDB, Spanish Fund for Latin America and the Caribbean, ISDR, and The World Bank, 2015: *CAPRA Initiative: Integrating Disaster Risk Information Into Development Policies and Programs in Latin America and the Caribbean Working Towards Safe and Sustainable Urban Environments*. https://ecapra.org/sites/default/files/documents/CAPRA%20Initiative%20Integrating%20disaster%20risk%20into%20development%20policies%20in%20LATAM.pdf (Accessed July 29, 2024).

Chantavilasvong, W., and L. Guerrero, 2019: Application of HAZUS-MH Flood Model in Developing Countries: The Case of Piura, Peru. NAKHARA (Journal of Environmental Design and Planning), 16.

Copernicus, 2024: Global Human Settlement - GHSL Homepage - European Commission. https://human-settlement.emergency.copernicus.eu/ (Accessed December 16, 2024).

Courty, L. G., R. L. Wilby, J. K. Hillier, and L. J. Slater, 2019: Intensity-duration-frequency curves at the global scale. *Environmental Research Letters*, 14, 084045, https://doi.org/10.1088/1748-9326/AB370A.

Datta, A., D. J. Wu, W. Zhu, M. Cai, and W. L. Ellsworth, 2022: DeepShake: Shaking Intensity Prediction Using Deep Spatiotemporal RNNs for Earthquake Early Warning. *Seismological Research Letters*, 93, 1636–1649, https://doi.org/10.1785/0220210141.

Deltares, 2024a: Delft-FIAT. https://storymaps.arcgis.com/stories/687a256881b94bf6ad20677543bb8cf2 (Accessed January 12, 2025).

——, 2024b: Delft-FIAT: A flood impact assessment tool | Deltares. https://www.deltares.nl/en/software-and-data/products/delft-fiat-flood-impact-assessment-tool (Accessed November 17, 2024).

Dewitte, S., J. P. Cornelis, R. Müller, and A. Munteanu, 2021: Artificial Intelligence Revolutionises Weather Forecast, Climate Monitoring and Decadal Prediction. *Remote Sensing 2021, Vol. 13*, Page 3209, 13, 3209, https://doi.org/10.3390/RS13163209.

Dis, M. O., E. Anagnostou, and Y. Mei, 2018: Using high-resolution satellite precipitation for flood frequency analysis: case study over the Connecticut River Basin. *J Flood Risk Manag*, 11, S514–S526, https://doi.org/10.1111/JFR3.12250.

Eberenz, S., D. Stocker, T. Röösli, and D. Bresch, 2019: Exposure data for global physical risk assessment. https://doi.org/10.5194/essd-2019-189

ETH Zurich, 2017a: CLIMADA overview — CLIMADA 5.0.0 documentation. https://climada-python.readthedocs.io/en/stable/tutorial/1_main_climada.html (Accessed February 5, 2025).

——, 2017b: Hazard: Tropical cyclones — CLIMADA 5.0.0 documentation. https://climada-python.readthedocs.io/en/stable/tutorial/climada_hazard_TropCyclone.html (Accessed February 6, 2025).

——, 2017c: Welcome to CLIMADA! — CLIMADA 5.0.0 documentation. https://climada-python.readthedocs.io/en/stable/index.html (Accessed August 27, 2024).

——, 2025a: ECA Case Studies – Weather and Climate Risks | ETH Zurich. https://wcr.ethz.ch/research/casestudies.html (Accessed February 6, 2025).

——, 2025b: CLIMADA Data Types. https://climada.ethz.ch/climada-api/data-types/ (Accessed February 9, 2025).

expert.ai, 2024: What Is Machine Learning? A Definition. https://www.expert.ai/blog/machine-learning-definition/ (Accessed September 30, 2024).

FEMA, 2020: GitHub - nhrap-hazus/hazpy. https://github.com/nhrap-hazus/hazpy?tab=readme-ov-file (Accessed January 1, 2025).

——, 2022a: Hazus Hurricane Model Technical Manual Hazus 5.1.

——, 2022b: *Multi-hazard Loss Estimation Methodology: Flood Model Hazus®-MH 5.1 Technical Manual*.

——, 2022c: Hazus Software.

——, 2022d: FEMA Factsheet: Hazus Flood Hazard Import Tool (FHIT)1.

——, 2022e: Hazus Tsunami Model Technical Manual.

——, 2022f: Multi-hazard Loss Estimation Methodology Earthquake Model Hazus ®-MH 5.1 Technical Manual. https://www.fema.gov/sites/default/files/documents/fema_hazus-earthquake-model-technical-manual-5-1.pdf (Accessed July 14, 2024).

——, 2023: What is Hazus? https://www.fema.gov/flood-maps/tools-resources/flood-map-products/hazus/about (Accessed July 7, 2024).

——, 2024a: FEMA Flood Map Service Center | Hazus. https://msc-fema-gov.translate.goog/portal/resources/hazus?_x_tr_sl=en&_x_tr_tl=es&_x_tr_hl=es&_x_tr_pto=tc (Accessed January 1, 2025).

——, 2024b: FEMA Flood Map Service Center: Hazus.

——, 2024c: Hazus User & Technical Manuals. https://www.fema.gov/flood-maps/tools-resources/flood-map-products/hazus/user-technical-manuals (Accessed July 7, 2024).

——, 2024d: Hazus 7.0 User Guide.

——, Hazus ®-MH 2.1 User Manual Hazus-MH User Manual ii.

FloodRise, 2024: FloodRISE - Tijuana River Valley Flood Hazards. https://ucirvine.maps.arcgis.com/apps/webappviewer/index.html?id=1d3fe4654858432aad4ca324b6e819ea (Accessed January 12, 2025).

FloodRiskGroup, 2021: GitHub - FloodRiskGroup/floodrisk2: FloodRisk2 is a QGIS 3.x plugin and is a new version of the previous FloodRisk for QGIS 2.x, having additional features. https://github.com/FloodRiskGroup/floodrisk2 (Accessed July 9, 2024).

Gegenleithner, S., M. Pirker, C. Dorfmann, R. Kern, and J. Schneider, 2024: Long Short-Term Memory Networks for Real-time Flood Forecast Correction: A Case Study for an Underperforming Hydrologic Model. *EGUsphere*, 2024, 1–24, https://doi.org/10.5194/egusphere-2024-1030.

GEM, 2024a: OpenQuake Integrated Risk Modelling Toolkit — Integrated Risk Modelling Toolkit 3.20.0 documentation. https://docs.openquake.org/oq-irmt-qgis/v3.20.0/ (Accessed July 29, 2024).

——, 2024b: Global Exposure Model | Global EarthQuake Model Foundation. https://www.globalquakemodel.org/product/global-exposure-model (Accessed December 16, 2024).

——, 2024c: GEM Vulnerability Model Documentation — GEM Vulnerability Functions 2022.1.1-dev documentation. https://docs.openquake.org/vulnerability/ (Accessed December 16, 2024).

——, 2024d: Overview of the OpenQuake engine — OpenQuake Engine 3.20.1 documentation. https://docs.openquake.org/oq-engine/manual/latest/underlying-science/overview.html (Accessed July 29, 2024).

——, 2024e: Release notes v3.23 — OpenQuake Engine 3.23 documentation. https://docs.openquake.org/oq-engine/master/manual/release-notes/whats-new-3.23.html (Accessed March 6th, 2025).

GFDRR, 2018: *MACHINE LEARNING for DISASTER RISK MANAGEMENT*. https://www.gfdrr.org/sites/default/files/publication/181222_WorldBank_DisasterRiskManagement_Ebook_D6.pdf (Accessed September 30, 2024).

Google, 2024a: Flood Forecasting: AI for Information & Alerts - Google Research. https://sites.research.google/floodforecasting/ (Accessed October 6, 2024).

——, 2024b: How Google uses AI to improve global flood forecasting. https://blog.google/technology/ai/google-ai-global-flood-forecasting/ (Accessed October 6, 2024).

Google Research, 2024: Open Buildings - Google Research - Open Buildings. https://sites.research.google/gr/open-buildings/ (Accessed December 16, 2024).

He, R., W. Zhang, J. Dou, N. Jiang, H. Xiao, and J. Zhou, 2024: Application of artificial intelligence in three aspects of landslide risk assessment: A comprehensive review. *Rock Mechanics Bulletin*, 3, 100144, https://doi.org/10.1016/J.ROCKMB.2024.100144.

Hochrainer-Stigler, S., 2014: *User Interface of the CatSim Model and Practical Guidelines*. https://pure.iiasa.ac.at/id/eprint/11212/1/XO-14-004.pdf (Accessed November 17, 2024).

——, R. Mechler, and G. Pflug, 2013: Modeling Macro Scale Disaster Risk: The CATSIM Model. 119–143, https://doi.org/10.1007/978-94-007-2226-2_8.

——, ——, and J. Mochizuki, 2015: A risk management tool for tackling country-wide contingent disasters: A case study on Madagascar. *Environmental Modelling & Software*, 72, 44–55, https://doi.org/10.1016/J.ENVSOFT.2015.06.004.

Huffman, G. J., and Coauthors, 2020: NASA Global Precipitation Measurement (GPM) Integrated Multi-satellite Retrievals for GPM (IMERG).

Huizinga, J., H. de Moel, and W. Szewczyk, 2017: *Global flood depth-damage functions. Methodology and the database with guidelines*. 1, pp. 108.

IIASA, 2024a: CATSIM - Inter-industry Impact Assessment - CATSIM - Inter-industry Impact Assessment - IIASA. https://previous.iiasa.ac.at/web/home/research/researchPrograms/RISK/catsimvariations.html (Accessed November 17, 2024).

——, 2024b: Catastrophe Simulation (CATSIM) | IIASA. https://iiasa.ac.at/models-tools-data/catsim (Accessed November 17, 2024).

——, 2024c: Financial preparation for natural disasters | IIASA. https://iiasa.ac.at/impacts/nov-2014/financial-preparation-for-natural-disasters (Accessed November 17, 2024).

InaSAFE, 2019a: InaSAFE concepts — InaSAFE Documentation Project 3.0.0 documentation. https://manual.inasafe.org/training/socialisation/inasafe_concepts.html (Accessed July 18, 2024).

——, 2019b: Introducing InaSAFE — InaSAFE Documentation Project 3.0.0 documentation. https://manual.inasafe.org/training/socialisation/introduction.html (Accessed July 18, 2024).

——, 2019c: InaSAFE 5.0 is released | InaSAFE. https://inasafe.org/news/inasafe-5-0-is-released/index.html (Accessed July 18, 2024).

——, 2019d: Roles & responsibilities | InaSAFE. https://inasafe.org/about-inasafe/governance/roles-responsibilities/index.html (Accessed July 18, 2024).

——, 2019e: *Case Study: InaSAFE during Jakarta's Flood in 2014*. https://inasafe.org/about-inasafe/cases/index.html (Accessed July 18, 2024).

——, 2023: Module 5: Calculating Damages and Losses — InaSAFE Documentation Project 3.0.0 documentation. https://manual.inasafe.org/training/old-training/intermediate/qgis-inasafe/405-calculating-damages-and-losses.html (Accessed January 20, 2025).

IN-CORE, 2024: IN-CORE. https://incore.ncsa.illinois.edu/ (Accessed July 31, 2024).

Ivić, M., 2019: ARTIFICIAL INTELLIGENCE AND GEOSPATIAL ANALYSIS IN DISASTER MANAGEMENT. https://doi.org/10.5194/isprs-archives-XLII-3-W8-161-2019.

Jain, H., R. Dhupper, A. Shrivastava, D. Kumar, and M. Kumari, 2023: AI-enabled strategies for climate change adaptation: protecting communities, infrastructure, and businesses from the impacts of climate change. *Computational Urban Science*, 3, 1–17, https://doi.org/10.1007/S43762-023-00100-2/FIGURES/3.

Jain, P., S. C. P. Coogan, S. G. Subramanian, M. Crowley, S. Taylor, and M. D. Flannigan, 2020: A review of machine learning applications in wildfire science and management. *Environmental Reviews*, 28, 478–505, https://doi.org/10.1139/ER-2020-0019/ASSET/IMAGES/ER-2020-0019TAB3.GIF.

Jiao, P., and A. H. Alavi, 2020: Artificial intelligence in seismology: Advent, performance and future trends. *Geoscience Frontiers*, 11, 739–744, https://doi.org/10.1016/J.GSF.2019.10.004.

Jones, A., and Coauthors, 2023: AI for climate impacts: applications in flood risk. *npj Climate and Atmospheric Science* 2023 6:1, 6, 1–8, https://doi.org/10.1038/s41612-023-00388-1.

Khan, C. B., and Coauthors, 2023: A Biologist's Guide to the Galaxy: Leveraging Artificial Intelligence and Very High-Resolution Satellite Imagery to Monitor Marine Mammals from Space. *J Mar Sci Eng*, 11, 595, https://doi.org/10.3390/JMSE11030595/S1.

König, N., 2017: Case Study of Hurricane Matthew - Loss Analysis with climada and Oasis LMF using ECMWF Forecast Data. .

Kou, G., D. Ergu, and Y. Shi, 2014: An integrated expert system for fast disaster assessment. Comput Oper Res, 42, 95–107, https://doi.org/10.1016/J.COR.2012.10.003.

Kropf, C. M., A. Ciullo, L. Otth, S. Meiler, A. Rana, E. Schmid, J. W. Mccaughey, and D. N. Bresch, 2022: Uncertainty and sensitivity analysis for probabilistic weather and climate-risk modelling: an implementation in CLIMADA v.3.1.0. *Geosci. Model Dev*, 15, 7177–7201, https://doi.org/10.5194/gmd-15-7177-2022.

Kulmesch, S., G. Paulus, and M. Leitner, 2010: Evaluation of the HAZUS-MH Loss Estimation Methodology for a Natural Risk Management Case Study in Carinthia, Austria.

Kulp, S. A., and B. H. Strauss, 2018: CoastalDEM: A global coastal digital elevation model improved from SRTM using a neural network. *Remote Sens Environ*, 206, 231–239, https://doi.org/10.1016/J.RSE.2017.12.026.

Lehigh University, and Florida Atlantic University, 2020: PRAISys. http://www.praisys.org/ (Accessed January 1, 2025).

van de Lindt, J. W., and Coauthors, 2023: The interdependent networked community resilience modeling environment (IN-CORE). *Resilient Cities and Structures*, 2, 57–66, https://doi.org/10.1016/J.RCNS.2023.07.004.

Llauca, H., W. Lavado-casimiro, K. León, J. Jimenez, K. Traverso, and P. Rau, 2021: Assessing Near Real-Time Satellite Precipitation Products for Flood Simulations at Sub-Daily Scales in a Sparsely Gauged Watershed in Peruvian Andes. *Remote Sensing 2021, Vol. 13, Page 826*, 13, 826, https://doi.org/10.3390/RS13040826.

Marulanda, M. C., M. L. Carreño, O. D. Cardona, M. G. Ordaz, and A. H. Barbat, 2013: Probabilistic earthquake risk assessment using CAPRA: Application to the city of Barcelona, Spain. *Natural Hazards*, 69, 59–84, https://doi.org/10.1007/S11069-013-0685-Z/METRICS.

Masood, M., M. Naveed, M. Iqbal, G. Nabi, H. M. Kashif, M. Jawad, and A. Mujtaba, 2023: Evaluation of Satellite Precipitation Products for Estimation of Floods in Data-Scarce Environment. *Advances in Meteorology*, 2023, 1685720, https://doi.org/10.1155/2023/1685720.

Mccarthy, J., 2007: WHAT IS ARTIFICIAL INTELLIGENCE?

McClean, F., R. Dawson, and C. Kilsby, 2023: Intercomparison of global reanalysis precipitation for flood risk modelling. *Hydrol Earth Syst Sci*, 27, 331–347, https://doi.org/10.5194/HESS-27-331-2023.

McSpadden, D., S. Goldenberg, B. Roy, M. Schram, J. Goodall, and H. Lipford, 2023: A comparison of machine learning surrogate models of street-scale flooding in Norfolk, Virginia. *Machine Learning with Applications*, https://doi.org/10.48550/ARXIV.2307.14185.

META, 2025: High-resolution population density maps from Data For Good at Meta. https://dataforgood.facebook.com/dfg/tools/high-resolution-population-density-maps#methodology (Accessed February 16, 2025).

Microsof, 2024: GitHub - microsoft/GlobalMLBuildingFootprints: Worldwide building footprints derived from satellite imagery. https://github.com/microsoft/GlobalMLBuildingFootprints?tab=readme-ov-file#will-there-be-more-data-coming-for-other-geographies (Accessed December 16, 2024).

Microsoft, 2024: GitHub - microsoft/GlobalMLBuildingFootprints: Worldwide building footprints derived from satellite imagery. https://github.com/microsoft/GlobalMLBuildingFootprints?tab=readme-ov-file#will-there-be-more-data-coming-for-other-geographies (Accessed December 16, 2024).

Mistry, H. K., and D. Lombardi, 2023: A stochastic exposure model for seismic risk assessment and pricing of catastrophe bonds. *Natural Hazards*, 117, 803–829, https://doi.org/10.1007/S11069-023-05884-4/TABLES/4.

Mohammadi, S. A., M. Nazariha, and N. Mehrdadi, 2014: Flood Damage Estimate (Quantity), Using HEC-FDA Model. Case Study: The Neka River. *Procedia Eng*, 70, 1173–1182, https://doi.org/10.1016/J.PROENG.2014.02.130.

Munich Climate Insurance Initiative, 2020: CLIMADA | ECA. https://eca-network.org/climada/ (Accessed July 21, 2024).

NASA, 2020: The IMERG multi-satellite precipitation estimates reformatted as 2-byte GeoTIFF files for display in a Geographic Information System (GIS).

——, 2024: Together, we can build a clearer picture of landslides.

National Institute of Water and Atmospheric Research Ltd, and Institute of Geological and Nuclear Sciences Ltd, 2024a: Overview — RiskScape 1.6.0 documentation. https://riskscape.org.nz/docs/intro/overview.html#overview (Accessed August 14, 2024).

——, and ——, 2024b: Release Changelog — RiskScape 1.6.0 documentation. https://riskscape.org.nz/docs/general/CHANGELOG.html#v1-6-0 (Accessed August 14, 2024).

National Institute of Water and Atmospheric Research Ltd and Institute of Geological and Nuclear Sciences Ltd, 2024c: Probabilistic modelling — RiskScape 1.7.0 documentation. https://riskscape.org.nz/docs/advanced/probabilistic.html (Accessed September 25, 2024).

——, 2024d: Models — RiskScape 1.7.0 documentation. https://riskscape.org.nz/docs/reference/models.html#models (Accessed September 24, 2024).

——, 2024e: Creating a RiskScape project — RiskScape 1.7.0 documentation. https://riskscape.org.nz/docs/intro/project-tutorial.html (Accessed September 24, 2024).

Nearing, G., and Coauthors, 2024: Global prediction of extreme floods in ungauged watersheds. *Nature 2024 627:8004*, 627, 559–563, https://doi.org/10.1038/s41586-024-07145-1.

Nevo, S., and Coauthors, 2022: Flood forecasting with machine learning models in an operational framework. *Hydrol Earth Syst Sci*, 26, 4013–4032, https://doi.org/10.5194/HESS-26-4013-2022.

Nirandjan, S., E. E. Koks, M. Ye, R. Pant, K. C. H. Van Ginkel, J. C. J. H. Aerts, and P. J. Ward, 2024: Physical vulnerability database for critical infrastructure hazard risk assessments-a systematic review and data collection. *Hazards Earth Syst*. Sci, 24, 4341–4368, https://doi.org/10.5194/nhess-24-4341-2024.

Nkwunonwo, U., M. Whitworth, and B. Baily, 2015: Relevance of Social Vulnerability Assessment to Flood Risk Reduction in the Lagos Metropolis of Nigeria. *Br J Appl Sci Technol*, 8, 366–382, https://doi.org/10.9734/BJAST/2015/17518.

OASIS, 2024a: Oasis LMF Documentation. https://oasislmf.github.io/home/introduction.html (Accessed November 11, 2024).

——, 2024b: FAQs :: Oasis Loss Modelling Framework. https://oasislmf.org/faqs (Accessed August 1, 2024).

Oasis LMF, 2024: Modelling methodology - Oasis LMF Documentation. https://oasislmf.github.io/sections/modelling-methodology.html#simulation-methodology (Accessed February 4, 2025).

OECD, and JRC, 2008: *Handbook on Constructing Composite Indicators*. OECD publishing, 1–162 pp.

OpenStreetMap contributors., 2017: Planet dump retrieved from https://planet.osm.org .

Papathoma-Köhle, M., M. Schlögl, L. Dosser, F. Roesch, M. Borga, M. Erlicher, M. Keiler, and S. Fuchs, 2022: Physical vulnerability to dynamic flooding: Vulnerability curves and vulnerability indices. J *Hydrol (Amst)*, 607, 127501, https://doi.org/10.1016/J.JHYDROL.2022.127501.

Pesaresi, M., and P. Politis, 2023: GHS-BUILT-H R2023A - GHS building height, derived from AW3D30, SRTM30, and Sentinel2 composite. *European Commission, Joint Research Centre (JRC),*.

Plevris, V., 2024: AI-Driven Innovations in Earthquake Risk Mitigation: A Future-Focused Perspective. *Geosciences* 2024, Vol. 14, Page 244, 14, 244, https://doi.org/10.3390/GEOSCIENCES14090244.

Prakash, N., A. Manconi, and S. Loew, 2021: A new strategy to map landslides with a generalized convolutional neural network. Scientific Reports 2021 11:1, 11, 1–15, https://doi.org/10.1038/s41598-021-89015-8.

Pregnolato, M., C. Galasso, and F. Parisi, 2015: A compendium of existing vulnerability and fragility relationships for flood: preliminary results. https://doi.org/10.14288/1.0076226.

PreventionWeb, 2023: RiskChanges: Open-Source Tool for Multi-Hazard Risk Assessment and Management | UN-SPIDER Knowledge Portal. https://www.preventionweb.net/drr-community-voices/open-source-tool-assist-multi-hazard-risk-assessment (Accessed January 1, 2025).

Rao, A., and Coauthors, 2020: Probabilistic seismic risk assessment of India. https://doi.org/10.1177/8755293020957374, 36, 345–371, https://doi.org/10.1177/8755293020957374.

RiskChanages, 2021: RiskChangesDesktop · PyPI. https://pypi.org/project/RiskChangesDesktop/#files (Accessed January 1, 2025).

RiskChanges, 2021: Tutorials on GUI — RiskChanges 1.0.0 documentation. https://sdss-documentation.readthedocs.io/en/latest/tutorials_gui.html (Accessed January 12, 2025).

Rodríguez, J. T., B. Vitoriano, J. Montero, and V. Kecman, 2011: A disaster-severity assessment DSS comparative analysis. *OR Spectrum*, 33, 451–479, https://doi.org/10.1007/S00291-011-0252-5/METRICS.

Rozelle, J. R., 2007: INTERNATIONAL ADAPTATION OF THE HAZUS EARTHQUAKE MODEL USING GLOBAL EXPOSURE DATASETS.

Rygel, L., D. O'Sullivan, and B. Yarnal, 2006: A method for constructing a social vulnerability index: An application to hurricane storm surges in a developed country. *Mitig Adapt Strateg Glob Chang*, 11, 741–764, https://doi.org/10.1007/s11027-006-0265-6.

Sapountzis, M., A. Kastridis, A. P. Kazamias, A. Karagiannidis, P. Nikopoulos, and K. Lagouvardos, 2021: Utilization and uncertainties of satellite precipitation data in flash flood hydrological analysis in ungauged watersheds. *Global Nest Journal*, 23, 388–399, https://doi.org/10.30955/GNJ.003905.

Scofield, R. A., 1987: The NESDIS Operational Convective Precipitation- Estimation Technique. *Mon Weather Rev*, 115, 1773–1793, https://doi.org/10.1175/1520-0493(1987)115<1773:tnocpe>2.0.co;2.

——, and R. J. Kuligowski, 2003: Status and outlook of operational satellite precipitation algorithms for extreme-precipitation events. *Weather Forecast*, 18, 1037–1051, https://doi.org/10.1175/1520-0434(2003)018<1037:SAOOOS>2.0.CO;2.

Scussolini, P., J. C. J. H. Aerts, B. Jongman, L. M. Bouwer, H. C. Winsemius, H. de Moel, and P. J. Ward, 2016: FLOPROS: an evolving global database of flood protection standards. *Natural Hazards and Earth System Sciences*, 16, 1049–1061, https://doi.org/10.5194/nhess-16-1049-2016.

Shameem Ansar, A., S. Sudha, and S. Francis, 2022: Identification and classification of landslide susceptible zone using geospatial techniques and machine learning models. *Geocarto Int*, 37, 18328–18355, https://doi.org/10.1080/10106049.2022.2138986.

Sheehan, B., M. Mullins, D. Shannon, and O. McCullagh, 2023: On the benefits of insurance and disaster risk management integration for improved climate-related natural catastrophe resilience. *Environ Syst Decis*, 43, 639–648, https://doi.org/10.1007/S10669-023-09929-8/FIGURES/2.

Souvignet, M., D. Florian, W. Ieneke, L. Mueller, D. N. Bresch, and K. Development Bank, 2016: Economics of Climate Adaptation (ECA)-Guidebook for Practitioners A Climate Risk Assessment Approach Supporting Climate Adaptation Investments.

Stalhandske, Z., E. Schmid, C. B. Steinmann, C. Kropf, and D. N. Bresch, 2022: Many-hazard Risk Assessment with the CLIMADA Data API. EGU22, https://doi.org/10.5194/EGUSPHERE-EGU22-8673.

——, C. B. Steinmann, S. Meiler, I. J. Sauer, T. Vogt, D. N. Bresch, and C. M. Kropf, 2024: Global multi-hazard risk assessment in a changing climate. *Scientific Reports* 2024 14:1, 14, 1–14, https://doi.org/10.1038/s41598-024-55775-2.

Sterlacchini, S., S. O. Akbas, J. Blahut, O.-C. Mavrouli, C. Garcia, B. Q. Luna, and J. Corominas, 2014: Methods for the characterization of the vulnerability of elements at risk. *Mountain Risks: From Prediction to Management and Governance*, T. Van Asch, J. Corominas, S. Greiving, J.-P. Malet, and S. Sterlacchini, Eds., Vol. 34 of, Springer Netherlands, 233–273.

Strauch, W., 2009: Estimation of precipitation using satellite imagery – contribution to early warning for landslides. https://webserver2.ineter.gob.ni/desliza/nesdis/lluvia/gif/tecnico.html (Accessed January 21, 2020).

Subramaniam, S., and Coauthors, 2022: Artificial Intelligence Technologies for Forecasting Air Pollution and Human Health: A Narrative Review. *Sustainability 2022, Vol. 14, Page 9951, 14, 9951*, https://doi.org/10.3390/SU14169951.

Sufi, F. K., 2022: AI-SocialDisaster: An AI-based software for identifying and analyzing natural disasters from social media. *Software Impacts*, 13, 100319, https://doi.org/10.1016/j.simpa.2022.100319.

——, and I. Khalil, 2024: Automated Disaster Monitoring from Social Media Posts Using AI-Based Location Intelligence and Sentiment Analysis. *IEEE Trans Comput Soc Syst*, 11, 4614–4624, https://doi.org/10.1109/TCSS.2022.3157142.

Sun, W., P. Bocchini, and B. D. Davison, 2020: Applications of artificial intelligence for disaster management. *Natural Hazards 2020 103:3*, 103, 2631–2689, https://doi.org/10.1007/S11069-020-04124-3.

Sven Willner, Inga Sauer, Lisa Novak, and Christian Otto, 2024: Global simulations of fluvial floods based on the ISIMIP2 ensemble of global hydrological models (v1.0). ISIMIP Repository. https://doi.org/10.48364/ISIMIP.303619 (Accessed February 9, 2025).

Tan, L., J. Guo, S. Mohanarajah, and K. Zhou, 2020: Can we detect trends in natural disaster management with artificial intelligence? A review of modeling practices. *Natural Hazards 2020 107:3*, 107, 2389–2417, https://doi.org/10.1007/S11069-020-04429-3.

Tedla, M. G., M. Rasmy, T. Koike, and L. Zhou, 2024: Evaluation of satellite precipitation products for real-time extreme river flow modeling in data scarce regions. *Proceedings of the International Association of Hydrological Sciences*, 386, 223–228, https://doi.org/10.5194/PIAHS-386-223-2024.

The World Bank, 2019: Fragility and Vulnerability Assessment Guide GPSS Global Program for Safer Schools GLOSI THE GLOBAL LIBRARY OF SCHOOL INFRASTRUCTURE GPSS.

Trinh, M. X., and F. Molkenthin, 2021: Flood hazard mapping for data-scarce and ungauged coastal river basins using advanced hydrodynamic models, high temporal-spatial resolution remote sensing precipitation data, and satellite imageries. *Natural Hazards*, 109, 441–469, https://doi.org/10.1007/S11069-021-04843-1/FIGURES/10.

United Nations General Assembly, 2015: Resolution adopted by the General Assembly on 3 June 2015. Sendai Framework for Disaster Risk Reduction 2015–2030. 1–24, https://doi.org/10.1093/oxfordhb/9780199560103.003.0005.

Universidad de Los Andes, 2024a: CAPRA-GIS | CAPRA | Probabilistic Risk Assessment Platform. https://ecapra.org/topics/capra-gis (Accessed July 29, 2024).

——, 2024b: About Us | CAPRA | Probabilistic Risk Assessment Platform. https://ecapra.org/about-us (Accessed July 29, 2024).

University of Southampton, 2018: WorldPop (www.worldpop.org) 100m Population. Version 2.0 estimates for numbers of people per pixel (ppp) and people per hectare (pph) for 2020, with national totals adjusted to match UN population division estimates (http://esa.un.org/wpp/).

USACE, 2024a: Risk Assessment Methodology. https://www.hec.usace.army.mil/confluence/fdadocs/techref/risk-assessment-methodology-167248960.html (Accessed August 22, 2024).

——, 2024b: Risk Measurement. https://www.hec.usace.army.mil/confluence/fdadocs/techref/risk-measurement-139729880.html (Accessed August 22, 2024).

——, 2024c: Monte Carlo Simulation. https://www.hec.usace.army.mil/confluence/fdadocs/techref/monte-carlo-simulation-159155747.html (Accessed August 22, 2024).

——, 2024d: Expected Annual Damage. https://www.hec.usace.army.mil/confluence/fdadocs/techref/expected-annual-damage-167248971.html (Accessed August 22, 2024).

——, 2024e: Average Annual Equivalent Damage with Uncertainty. https://www.hec.usace.army.mil/confluence/fdadocs/techref/average-annual-equivalent-damage-with-uncertainty-167249007.html (Accessed August 22, 2024).

——, 2024f: Damage Reduced With Uncertainty. https://www.hec.usace.army.mil/confluence/fdadocs/techref/damage-reduced-with-uncertainty-167249022.html (Accessed August 22, 2024).

——, 2024g: Deterministic System Performance Metrics. https://www.hec.usace.army.mil/confluence/fdadocs/techref/deterministic-system-performance-metrics-167248986.html (Accessed August 22, 2024).

Vickery, P. J., D. Wadhera, M. D. Powell, and Y. Chen, 2009: A Hurricane Boundary Layer and Wind Field Model for Use in Engineering Applications. *J Appl Meteorol Climatol*, 48, 381–405, https://doi.org/10.1175/2008JAMC1841.1.

Wanzala, M. A., A. Ficchi, H. L. Cloke, E. M. Stephens, H. M. Badjana, and D. A. Lavers, 2022a: Assessment of global reanalysis precipitation for hydrological modelling in data-scarce regions: A case study of Kenya. *J Hydrol Reg Stud*, 41, 101105, https://doi.org/10.1016/J.EJRH.2022.101105.

Wanzala, M. A., A. Ficchi, H. L. Cloke, E. M. Stephens, H. M. Badjana, and D. A. Lavers, 2022b: Assessment of global reanalysis precipitation for hydrological modelling in data-scarce regions: A case study of Kenya. *J Hydrol Reg Stud*, 41, 101105, https://doi.org/https://doi.org/10.1016/j.ejrh.2022.101105.

Wasko, C., S. Westra, R. Nathan, H. G. Orr, G. Villarini, R. V. Herrera, and H. J. Fowler, 2021: Incorporating climate change in flood estimation guidance. *Philosophical Transactions of the Royal Society A*, https://doi.org/10.1098/RSTA.2019.0548.

Van Westen, C., and W. Bakker, 2015: Software Development Report.

Xu, C., and Z. Xue, 2024: Applications and challenges of artificial intelligence in the field of disaster prevention, reduction, and relief. *Natural Hazards Research*, 4, 169–172, https://doi.org/10.1016/J.NHRES.2023.11.011.

Yang, L., J. Driscol, S. Sarigai, Q. Wu, H. Chen, and C. D. Lippitt, 2022: Google Earth Engine and Artificial Intelligence (AI): A Comprehensive Review. *Remote Sensing 2022, Vol. 14*, Page 3253, 14, 3253, https://doi.org/10.3390/RS14143253.

Yepes-Estrada, C., and Coauthors, 2023: Global building exposure model for earthquake risk assessment. *https://doi.org/10.1177/87552930231194048*, 39, 2212–2235, https://doi.org/10.1177/87552930231194048.

Yigitcanlar, T., K. C. Desouza, L. Butler, and F. Roozkhosh, 2020: Contributions and Risks of Artificial Intelligence (AI) in Building Smarter Cities: Insights from a Systematic Review of the Literature. *Energies 2020, Vol. 13, Page 1473*, 13, 1473, https://doi.org/10.3390/EN13061473.

Zhang, X., J. Zhang, C. Yuan, S. Liu, Z. Chen, and W. Li, 2020: Locating induced earthquakes with a network of seismic stations in Oklahoma via a deep learning method. *Scientific Reports 2020 10:1*, 10, 1–12, https://doi.org/10.1038/s41598-020-58908-5.

Zhu, Q., D. Zhou, Y. Luo, Y. P. Xu, G. Wang, and X. Gao, 2021: Suitability of high-temporal satellite-based precipitation products in flood simulation over a humid region of China. *Hydrological Sciences Journal*, 66, 104–117, https://doi.org/10.1080/02626667.2020.1844206.

Zhu, W., T. Tao, H. Yan, J. Yan, J. Wang, S. Li, and K. Xin, 2023: An optimized long short-term memory (LSTM)-based approach applied to early warning and forecasting of ponding in the urban drainage system. *Hydrol Earth Syst Sci*, 27, 2035–2050, https://doi.org/10.5194/HESS-27-2035-2023.

Image: Adobe Stock

ANNEXES

ANNEX A. CHARACTERISTICS OF EXISTING TOOLS FOR RISK CALCULATION

A.1. CAPRA (PROBABILISTIC RISK ASSESSMENT PLATFORM)

A.1.1. General description

CAPRA is a platform designed for disaster risk assessment using a probabilistic approach. The platform allows users to quantify and analyze the risk associated with various hazards, supporting informed decision-making in disaster risk management.

The CAPRA platform offers specific modules for hazard calculation related to floods, landslides, hurricanes, and earthquakes (Universidad de Los Andes 2024a). The risk assessment module is called CAPRA-GIS and allows probabilistic risk calculations based on hazard, exposure, and physical vulnerability data.

A.1.2. Applied methods

CAPRA applies probabilistic models to assess exposure and vulnerability to different types of hazards. It uses a modular approach that includes hazard assessment, exposure, vulnerability and damage calculation. The methods include stochastic simulations and scenario analysis to provide risk estimates.

CAPRA-GIS can process hazard results obtained from CAPRA modules or from other sources, provided that the hazard files are in the software's native format (.AME file extension). The main screen of the tool includes the following areas: a menu and tools area, a geographic display area, an area for displaying georeferenced data information, a status bar area, and a processing messages area, as shown in **Figure 30** (World Bank et al. 2009).

Figure 30. CAPRA-GIS main screen

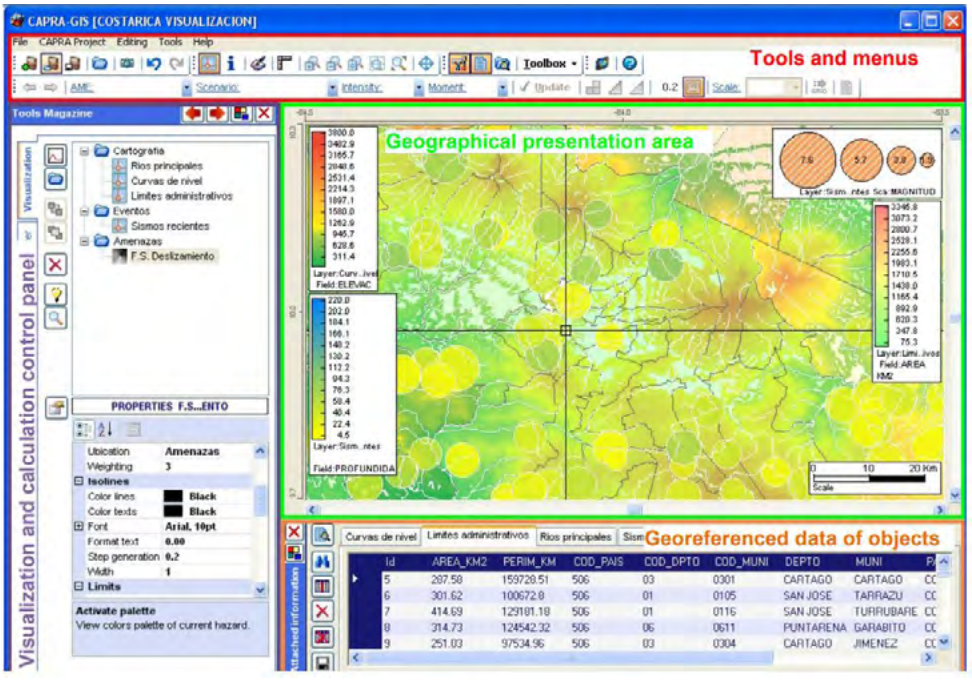

Source: World Bank et al. (2009).

The tool requires the following types of information (World Bank et al. 2009):

- **Hazard files (*.ame):** Hazard files can store any number of combinations of configurations, intensities, for a given frequency of occurrence.

- **ShapeFiles (*.shp):** These are vector layers that contain geographic information. The .shp files contain the exposed features, and their attributes must include the typology used to link them to a given vulnerability curve.

- **ERN vulnerability file (*.dat):** external text files containing references and additional parameters stored together with the project, used to configure the loss calculation.

  Once the three components are organized within a project, the calculations can be initiated to obtain the risk metrics, including the risk curve and the spatial distribution of damage. Calculations can be performed according to the scenario or probabilistically.

Figure 31. Risk calculation display window

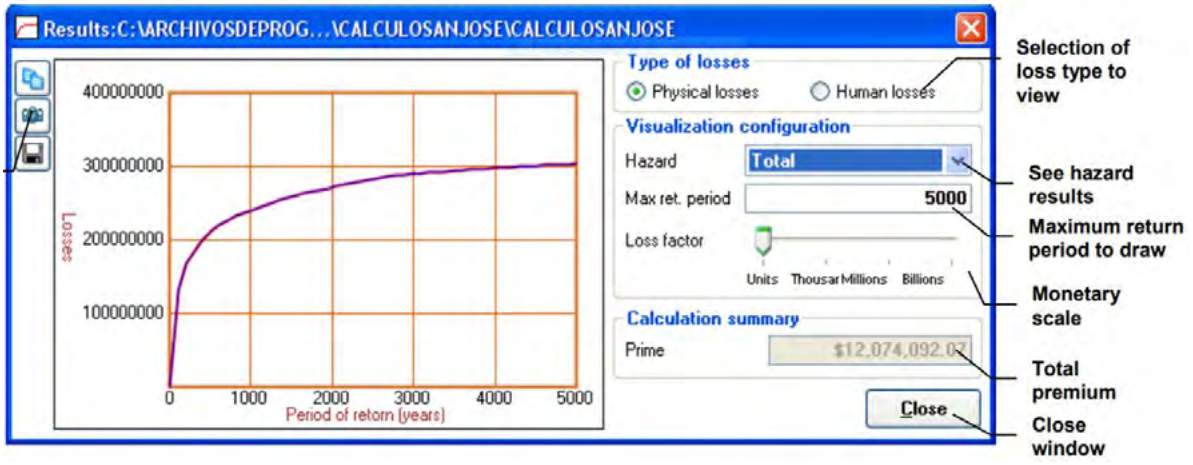

Source: World Bank et al. (2009).

A.1.3. Mathematical approach

The mathematical approach used by CAPRA is developed by Cardona et al. (2012) for the case of earthquakes, but the same approach is applied to all hazards. A summary is presented below.

Risk is calculated using the exceedance rate of loss values, $v\,(p)$. This quantity represents the expected number of events per unit of time that will generate losses equal to or greater than p. Its calculation is based on the Total Probability Theorem:

Equation 4

$$v(p) = \sum_{i=1}^{Events} \Pr\left(P > p \,\middle|\, \text{Event } i\right) \cdot F_A\left(\text{Event } i\right)$$

where $Pr\,(P > p \,|\, Event\ i)$ is the probability of loss exceedance given the occurrence of the event i, and F_A $(Event\ i)$ is the annual frequency of occurrence of the event i. The vulnerability functions are used to estimate $Pr\,(P > p \,|\, Event\ i)$. To calculate $Pr\,(P>p \,|\, Event\ i)$, it is assumed that, given an event with known magnitude and location, the intensity at the site where the structure is located follows a lognormal

distribution with a median and logarithmic standard deviation. Under this assumption, the required probability is obtained by combining two conditional distributions (Marulanda et al. 2013):

Equation 5

$$\Pr(P > p \mid \text{Event}) = \int_0^{\infty} (P > p \mid Sa) \cdot p_{SA}(Sa \mid M,R) dSa$$

where $p_{SA}(Sa \mid M,R)$ is the probability density function of the intensity Sa, given that an earthquake occurs with magnitude M at a distance R. Generally, $Sa \mid M,R$ is modeled by a lognormal distribution whose median and log standard deviation depend on M and R, and are determined from the ground motion prediction model selected by the analyst. The first term of the integral is obtained from the vulnerability relationship of the structure under analysis.

Economic losses are estimated by multiplying the damage ratio obtained in the vulnerability module by the value at risk of each asset class and location. Subsequently, losses are added as required in the analysis.

The main risk estimation metrics include the Average Annual Loss (AAL), the Loss Exceedance Curve (LEC), and the Probable Maximum Loss (PML). The AAL is the expected annual loss and is defined as the mathematical expectation of the annual loss:

Equation 6

$$\text{AAL} = \sum_{i=1}^{Events} \text{E}(P \mid \text{Event } i) \, F_A(\text{Event } i)$$

where $E(P \mid Event\ i)$ is the expected loss of the event i, and $F_A(Event\ i)$ is its annual frequency of occurrence. The LEC represents the annual frequency with which a specific monetary loss will be exceeded and is the most relevant metric in catastrophic risk management. Finally, the PML indicates the loss associated with a given exceedance frequency or return period. The PML curve is generally defined in terms of economic value or relative percentage with respect to the return period, and is used to determine the size of the reserves that insurance companies must maintain to avoid losses exceeding their financial capacity.

A.1.4. Recent advances in CAPRA

CAPRA-GIS version 2.4 introduces a 64-bit version that improves the management of large amounts of RAM, optimizing performance on 64-bit operating systems. In addition, this update includes enhanced security features such as buffer overflow protection, Data Execution Prevention (DEP), and PatchGuard, providing a more secure environment for probabilistic risk calculation. These improvements make

CAPRA-GIS more efficient for risk analysis. Unfortunately, version 2.4 dates from 2018, and the official website contains no information about updates to either the software or its manuals. In the case of the manuals, these were developed in 2009 (World Bank et al. 2009).

A.1.5. Development community

In July 2016, the World Bank launched an open call to manage and own the CAPRA website. After evaluation by a panel, the proposal submitted by Uniandes (Universidad de Los Andes – Colombia) was selected based on criteria such as its technical quality, international support, and knowledge and experience with CAPRA, achieving the highest evaluation score. Since January 2017, Uniandes has managed and owned the CAPRA platform (Universidad de Los Andes 2024b).

A.1.6. Limitations

One of the main limitations of CAPRA is the lack of documentation on the methods used to perform the calculations. This lack of documentation is also reflected in the creation of the .ame input file, which makes it difficult for users to generate the information required to perform risk calculations using only the documentation. On the other hand, the software code is not available in any repository, and although the initiative initially advocated for open-source code, it is currently not possible to access the code publicly.

A.1.7. Use cases

CAPRA has been used in several countries to assess disaster risk and develop mitigation strategies. For example, in Colombia, it has been applied for seismic and flood risk assessment, informing urban planning and risk management policies. It has also been used in infrastructure projects to ensure that constructions are resilient, such as the case of health, government, and educational infrastructure described in **Box 2**.

Box 2. Example of CAPRA application

CAPRA Case Study in the Metropolitan Area of San Salvador (AMSS)

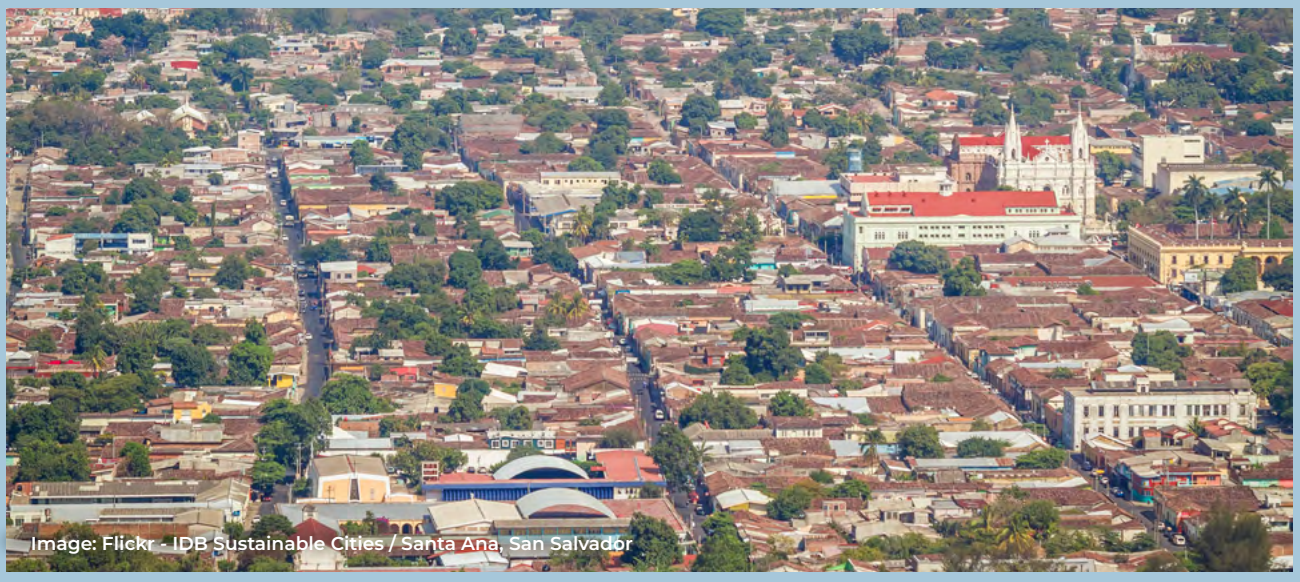

Image: Flickr - IDB Sustainable Cities / Santa Ana, San Salvador

Seismic hazard in the Metropolitan Area of San Salvador (AMSS) refers to the probability of an earthquake of a certain intensity occurring at a specific place and time. This hazard is determined by unmodifiable factors such as seismicity, which includes the frequency and magnitude of earthquakes, and the geology of the region. A key aspect of seismic hazard analysis is understanding regional seismic attenuation, which is the loss of energy experienced by a seismic wave as it travels through the ground.

To evaluate the seismic response in the AMSS, data were collected and validated on the area's geology, stratigraphic analyses, water well logs, and dynamic parameters, as well as accelerographic records. This information, managed by the monitoring office of the Ministry of Environment and Natural Resources (MARN), is essential for understanding how the soil and other site characteristics influence the magnitude and type of seismic motion. This includes the effects of soil type and the correspondence between the vibration periods of structures and the ground.

The seismic hazard and risk maps in the AMSS were developed using CAPRA and include multiple probable seismic scenarios, with a total of 24,996 possible seismic events. These maps provide estimates of peak ground acceleration and the associated structural movements for different building heights in each scenario. The maps are crucial tools for identifying areas with different levels of seismic response, helping to anticipate the impact of future earthquakes and facilitating risk planning and mitigation.

The vulnerability assessment in the AMSS included the development of vulnerability curves based on damage data from previous earthquakes and spectral acceleration records for each structure. A specific analysis was carried out on the buildings belonging to the Ministries of Health and Government, as well as on a 20% sample of the buildings of the Ministry of Education. This analysis considered factors such as year of construction, materials, previous damage, and structural characteristics, helping to identify the buildings most vulnerable to future seismic events.

Seismic hazard for a 500-year return period

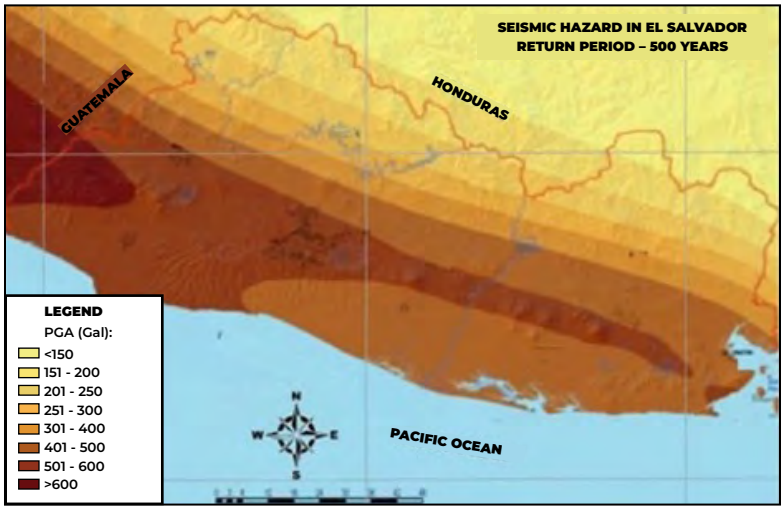

In response to the findings of the seismic vulnerability analysis, the Government of El Salvador designed a vulnerability reduction program with an initial focus on the education sector. This program seeks not only to address the urgent needs of buildings in critical condition but also to establish a long-term strategy to improve the structural and functional characteristics of both existing and new buildings. This effort complements other risk reduction policies implemented in recent years.

This initial analysis carried out with CAPRA provides an estimate of the probable damage based on the available information, highlighting the importance of assessing seismic vulnerability for decision-making. Although the results are open to revision, the analysis is crucial for identifying existing risk levels and developing strategies to reduce these risks to acceptable levels. In locations where earthquakes are frequent, such as urban areas like the AMSS, existing infrastructure and knowledge of potential hazards are key factors for risk mitigation planning.

Source: CEPREDENAC et al. (2015)

A.2. HAZUS

A.2.1. General description

Hazus provides a standardized national-level methodology developed by the United States Federal Emergency Management Agency (FEMA). It is distributed as free, GIS-based desktop software with a collection of inventory databases for each state and territory of the U.S. Hazus is used to assess hazard, vulnerability, and risk, and to estimate the physical, economic, and social impacts of earthquakes, hurricanes, floods, and tsunamis (FEMA 2023).

Hazus is a software designed to run on ArcGIS. The minimum supporting software requirements are: Esri ArcGIS 10.8.2, Microsoft Windows 10 or 11 64-bit (Pro & Enterprise), Esri's Spatial Analyst extension (required for flood and tsunami assessment), and Windows. NET Framework 4.8 (FEMA 2024b).

The Hazus program provides data, standalone analytical tools, and software that runs within Esri's ArcGIS Desktop platform. The separate tools include the Comprehensive Data Management System (CDMS) and several open-source modules that simplify risk analysis, data exports, and report generation. Hazus data includes baseline inventories for buildings, essential facilities, and infrastructure in the United States (FEMA 2022c).

Hazus includes other supplementary tools such as:

- **Flood Hazard Import Tool (FHIT):** an open-source tool that allows Hazus users to search for, download, and prepare publicly available flood hazard data for import into a Hazus flood study region. It currently supports storm depth models from ADCIRC (ADvanced CIRCulation Model) (FEMA 2022d).
- **Hazus Export Tool:** An open-source tool that facilitates the extraction and analysis of Hazus risk assessment results without requiring prior mapping or coding experience. The Export Tool allows multiple Hazus study regions to be processed quickly and efficiently (FEMA 2022d).

A.2.2. Applied methods

Hazus employs loss estimation models that use geographic tools to calculate physical, economic, and social losses.

The flood model shares a common modular software architecture with the earthquake and wind models. The user interface screens vary to some extent for each hazard type but have a common look and feel. A general description of the Hazus architecture and its various hazard components is provided in **Figure 32**.

The hazard models specific to Hazus are described below (FEMA 2023):

Earthquakes: estimates damage to structures, contents, inventories and economic losses. Evaluates the probability of damage to buildings and infrastructure based on USGS ShakeMap data. The model calculates damage and losses to buildings, essential facilities, transportation, utility lifelines, and population based on real-time earthquakes, scenarios, or probabilistic analyses. It also addresses the calculations required for debris management, fire following earthquakes, casualties, and shelter. Direct losses are estimated based on the physical damage to structures, contents, inventory, and building interiors. The earthquake model includes the Advanced Engineering Building Module for individual and group building analysis (FEMA 2024c).

Figure 32. Hazus software architecture with Hazus data tools

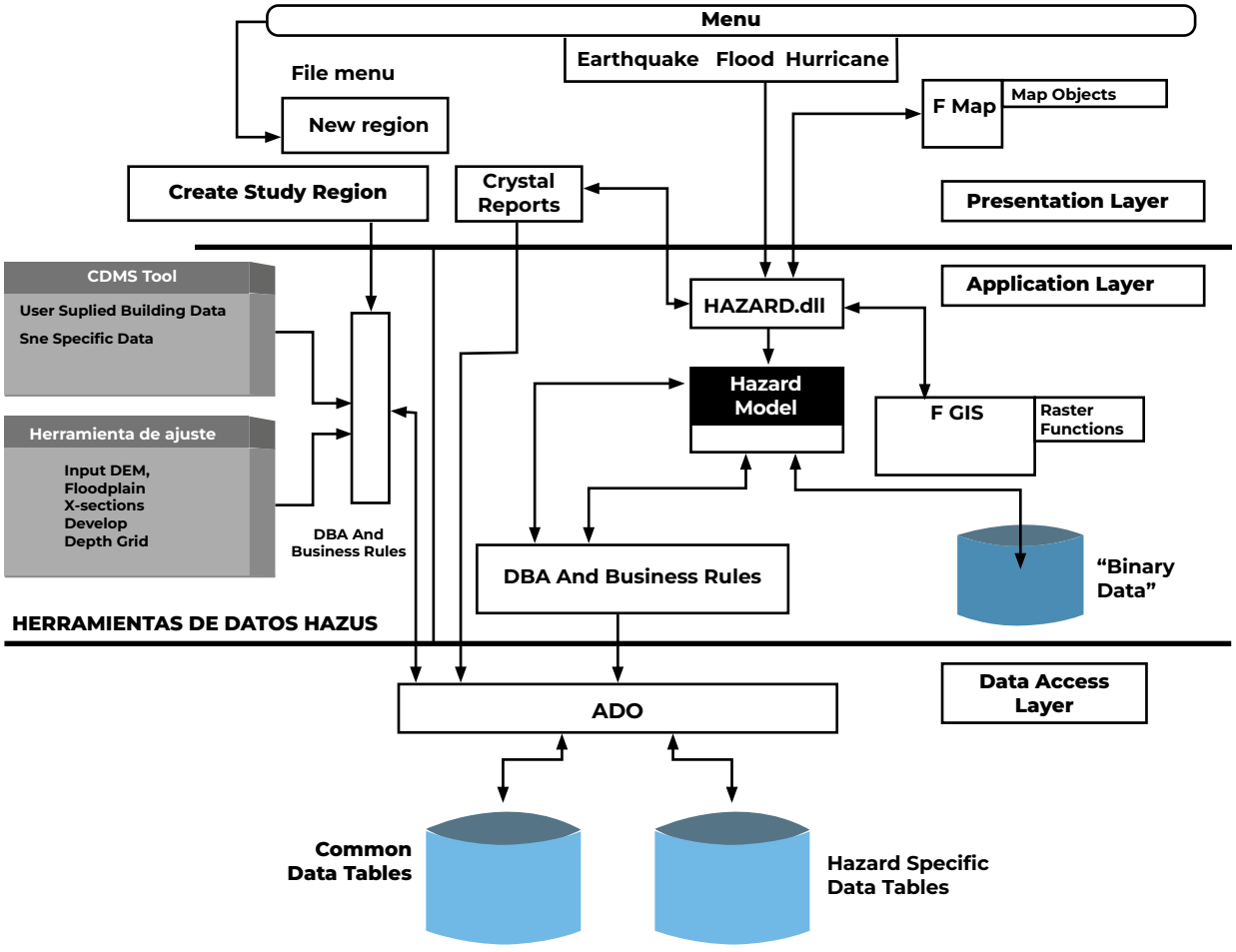

Source: FEMA (2022b).

Hurricanes: assesses damage from hurricane winds, debris generation, and economic losses. It calculates the physical and economic damage to buildings caused by wind and windborne debris. The wind hazard data are generated at the census unit level. The model considers maximum gusts, roughness of terrain, and tree cover data for historical storms or probabilistic events. The results can be combined with an internal storm surge model, or with surge data provided by the user, to estimate building damage caused by coastal flooding. The Hazus Hurricane Wind technical and user manuals provide information on model outputs, uncertainties, the execution of basic and advanced analyses, damage functions, debris generation, shelter requirements, storm surge, and impacts. The Technical Manual also includes validation studies of historical hurricanes (FEMA 2024c).

The Hazus methodology for hurricanes, shown in **Figure 33**, allows the consequences for a city or region to be estimated based on a hurricane scenario or a set of probabilistic events over 100,000 years. The information that can be generated includes quantitative estimates of losses in terms of direct costs for the repair and replacement of damaged buildings, loss of business income, relocation costs, household displacement, shelter requirements, debris quantities, and regional economic impacts, as well as functionality losses in terms of loss of function and restoration times for hospitals, police stations, fire stations, and emergency operations centers (FEMA 2022a).

Figure 33. Hazus Hurricane Model Methodology

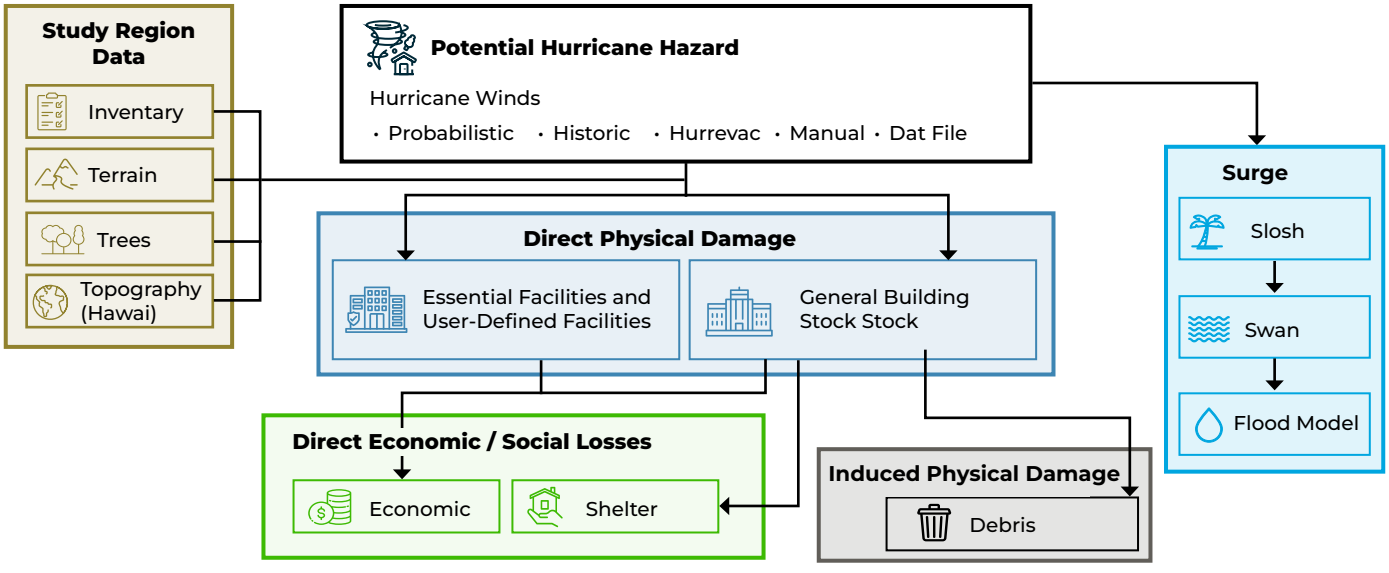

Source: FEMA (2022a).

The probabilistic model uses a life-cycle simulation approach in which the complete path of a hurricane or tropical storm is modelled, starting with its formation over the ocean and ending with its final dissipation. Using this approach, the central pressure is modelled as a function of sea surface temperature, storm track, and velocity, among other variables, and is updated at six-hour intervals throughout the storm history. Linear interpolation is used between the six-hour points. The approach is validated by comparing the statistics of the key parameters of the simulated hurricanes with those derived from historical data. This model includes a numerical wind field model (Vickery et al. 2009), which incorporates a complete nonlinear solution to the equations of motion (FEMA 2022a).

Floods: estimated damage to buildings, contents and economic losses. It calculates physical damage and economic losses caused by coastal or river flooding, using functions that relate flood depth and type to the degree of damage. The specific outputs include damage to building contents, lifelines, and economic losses. The flood loss estimation methodology consists of two modules that carry out basic analytical processes: 1) flood hazard analysis, and 2) flood loss estimation analysis. The model results can be visualized through a series of reports and maps (FEMA 2024c).

1. The flood hazard module uses discharge and terrain elevation, among other factors, to estimate flood depth and flow velocity. Users are also able to directly import user-defined flood hazard grids in multiple formats.

2. The flood loss estimation module calculates physical damage and economic loss from the hazard analysis results using vulnerability curves.

Figure 34 shows the flood model framework. At present, some features of the Flood Model are not yet available but are under development. In those cases, the models are shown in gray boxes, and the connections leading to those components are also in gray.

The methodology incorporates the most recent information available in the flood loss estimation methodology. For example, users can develop their own depth grids based on their hydrological and hydraulic models and use the most up-to-date damage functions. The modules include damage loss estimators that were not previously incorporated in most studies, such as indirect economic losses.

Depending on the user's experience, the flood model is designed to operate with a minimal user interface and data requirements, while also allowing users to preprocess higher quality data and perform more rigorous analyses. For example, the methodology allows simplified estimates of damage and losses, primarily using default data provided with the software. These damage/loss estimates do not require extensive inventory collection and can be performed on a modest budget. More accurate damage/loss estimates (analysis using data provided by the user) require more extensive inventory information at an additional cost to the user.

In all cases, a Digital Elevation Model (DEM) must be provided by users. The Flood Model has been designed to allow users to easily define the required DEM for their study area and obtain the National Elevation Dataset (NED) from the USGS website. The user can also provide their own DEM that meets the requirements of the model. Once a DEM is provided, the user can begin developing damage and loss estimates. They can be imported by users with higher quality terrain and improved flood hazard data (FEMA 2022b).

Figure 34. Flood model framework

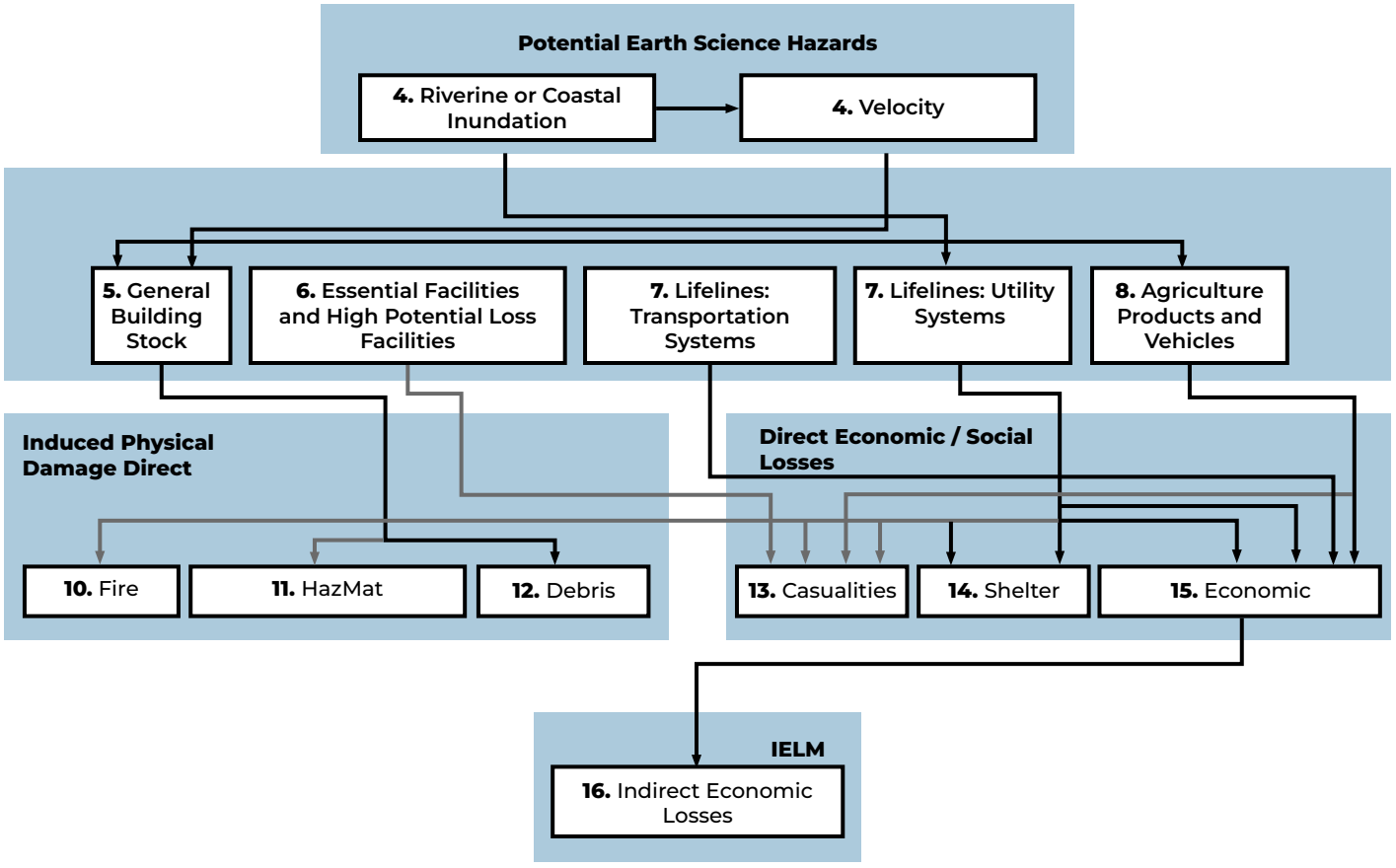

Source: FEMA (2022b).

The flood model includes a set of damage functions incorporating most of the curves available from the Federal Insurance Administration (now known as the Federal Insurance and Mitigation Administration within the Department of Homeland Security) and the U.S. Army Corps of Engineers U.S. The General Building Stock (GBS) includes residential, commercial, industrial, agricultural, religious, governmental, and educational buildings. Damage is estimated as a percentage and weighted by the flood area at a given depth for a specific census block. It is assumed that, within a given census block, the entire composition of the general building stock is uniformly distributed throughout the block. The inventory information required to determine the percentage of damage for the flooded area is derived from the relationships between specific occupancy classifications and building types. All three models (earthquake, wind, and flood) use common data to ensure that users do not encounter discrepancies in the inventory when switching from one hazard to another. In general, the flood model displays the GBS data at the census block level, while the hurricane and earthquake models display the GBS data at the census tract level (FEMA 2022b).

Tsunamis: evaluates infrastructure damage and economic losses. It estimates economic losses and physical damage to buildings due to tsunami wave depth and force in five high-risk states (California, Washington, Oregon, Hawaii, and Alaska), as well as in U.S. territories in the Pacific and Caribbean. The estimates can be combined with earthquake loss estimates to quantify additional impacts from near source tsunami events. The Hazus methodologies generate an estimate of the consequences of a tsunami scenario in a city, county, or coastal region. The resulting loss estimate will describe the magnitude of the damage and disruptions that may result from the modeled tsunami. The following information can be obtained (see **Figure 35**): quantitative estimates of losses in terms of direct costs for the repair and replacement of damaged buildings, direct costs associated with loss of function (for example, loss of business income, relocation costs) and casualties, and functionality losses in terms of loss of function and restoration times for user-defined facilities. The current version of the Hazus Tsunami model does not estimate the following: damage, loss, and functionality estimates for essential facilities and vital infrastructure; housing requirements; debris; and indirect economic losses (FEMA 2022e).

Figure 35. Hazus tsunami model methodology framework

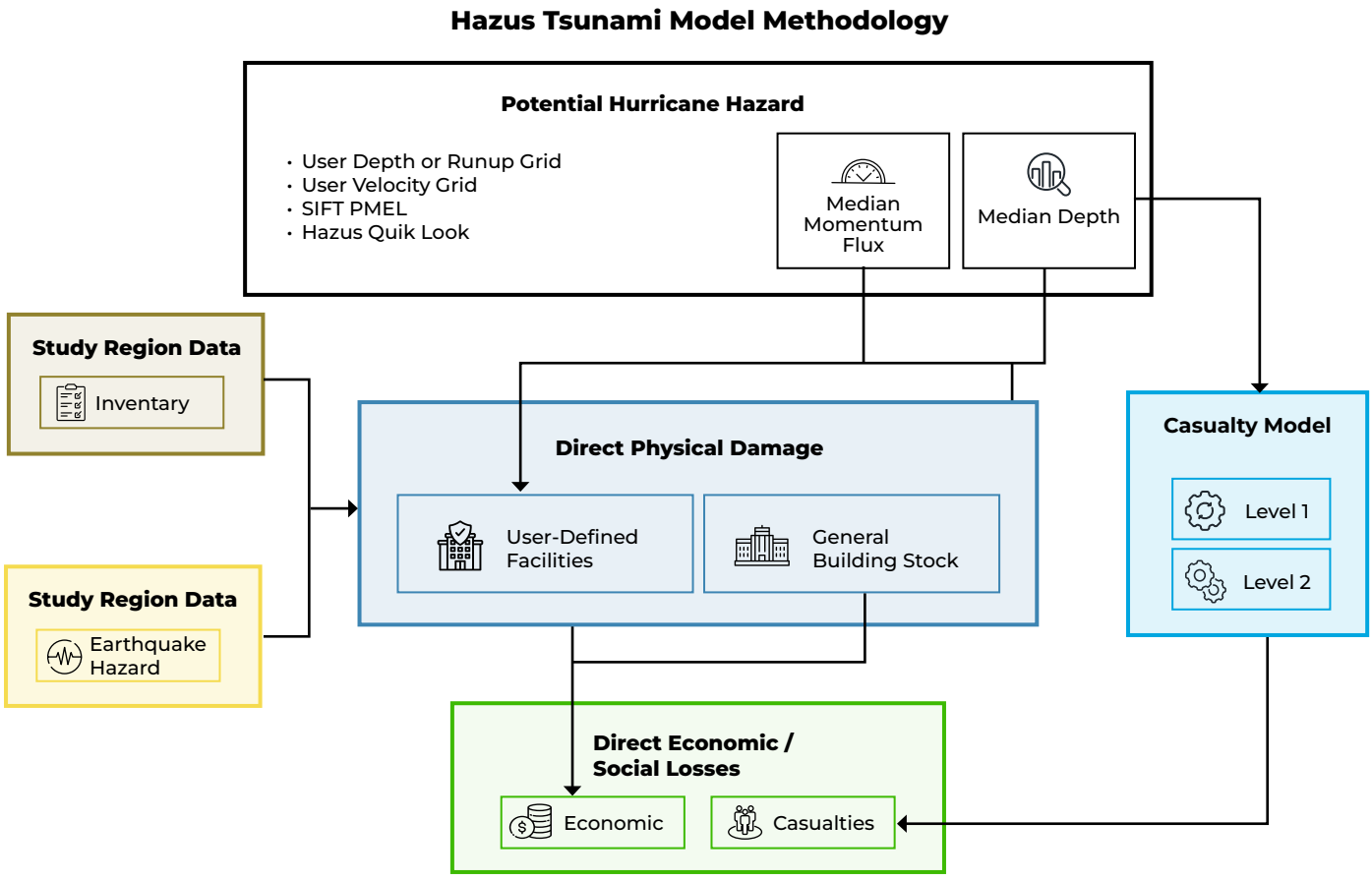

Source: FEMA (2022e).

These models are supported by user and technical manuals that provide detailed information on how the models work and how to generate loss estimates.

The development of each module involved the participation of an interdisciplinary group of experts. For example, the development of the flood methodology and software implementation was carried out by a team of flood loss experts consisting of engineers, hydraulic and hydrological modelers, emergency planners, economists, social scientists, geographic information system analysts, and software developers. The Flood Oversight Committee provided technical direction and review of the work.

Hazus risk analyses are divided into Basic or Advanced (see **Figure 36**), depending on the level of detail and effort required. Advanced analyses use more detailed local data for more accurate estimates.

Figure 36. HAZUS analysis levels

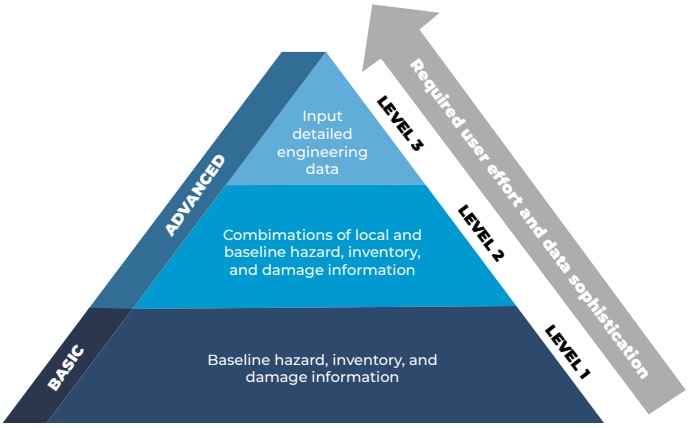

Source: FEMA (2023).

For example, in the case of floods, the Flood Model allows the following three levels of analysis:

Level 1

This is the simplest type of analysis, requiring minimal effort from the user, as it relies primarily on the information provided with the methodology (for example, census information, broad regional patterns of floodplain code adoption, etc.). The user is not expected to have extensive technical knowledge. While the methods require some user-provided input for execution, the type of input needed can be obtained by contacting government agencies or consulting published information. At this level, **the estimates will be coarse and are likely to be appropriate only as preliminary loss estimates to determine where more detailed analyses are warranted**. Some components of the methodology cannot be performed in a default data analysis, as they require a more detailed inventory than that provided with the methodology. The following are not included in the default data analysis: damage/losses due to ground failure or (riverbank) erosion, damage/losses due to earthquake induced flooding such as tsunamis, and damage/losses due to dam failures. At this level, the user has the option (not mandatory) to enter information on site-specific facilities, such as hazardous material sites or essential facilities, among others. It would take between one week and one month to collect relevant information, depending on the size of the region and the level of detail required by the user.

Level 2

analysis is intended to improve upon the results of Level 1 by taking into account additional data that are readily available, or can be easily converted or calculated to meet the methodological requirements. At Level 2, the user may need to determine the parameters of published reports or maps to be used as input for the model. It requires more extensive inventory data and greater effort on the part of the user than the default data analysis. The purpose of this type of analysis is to provide the user with the best possible flood damage/loss estimates that can be obtained using the standardized methods included in the methodology. Flood Model users must preprocess their flood hazard data for use in the Flood Model. It is likely that the user will need to hire consultants to assist in the implementation of certain methods. For example, users knowledgeable in hydrologic and hydraulic models are likely to be required to define flood depths. All components of the methodology can be performed at this level, and the loss estimates are based on locally developed (by the user) inventories. At this level, there are standardized analysis methods included in the software, but there is no standardized analysis for user-supplied data. The quality of the analysis and results improve as the user provides more complete data. Depending on the size of the region and the level of detail desired by the user, it would take between one and six months to obtain the information required for this type of analysis.

Level 3

analysis will require significant effort on the part of the user to develop information on flood hazard and exposure. This type of analysis incorporates the results of engineering and economic studies conducted using methods and software that are not included within the methodology. At this level, one or more technical experts would be needed to acquire data, perform detailed analyses, assess damages and losses, and assist the user in developing a more comprehensive inventory. At this level, there will be extensive involvement of local utility companies and owners of special facilities. The quality and detail of the results depend on the level of effort invested. It would take between six months and two years to complete an Advanced Analysis.

Each subsequent level builds on and adds to the data and analysis procedures available in the previous levels (FEMA 2022b). **Table 22** shows the level of information and analysis required for each component of the flood analysis.

Table 22. Example levels of analysis for flood cases

	Level 1	Level 2	Level 3
Hazard	Users provide the Digital Eleva-tion Model (DEM), typically the 30-meter DEM from the USGS. The Flood Model uses the default hazard data, including hydraulic unit codes and the accumulation methodology, to develop approximate stream centerlines. USGS regression equations and gauge records are used to determine dis-charge frequency curves.	Preprocessed user-supplied hazard data. The user will provide enhanced DEM, hydraulic, and hydrologic results for floods, including stream cross sections. Coastal analysis users provide polygons with elevations and the boundaries of the analysis area.	Similar to Level 2, although the user is likely to work with hydraulic models outside the Flood Model and the FIT.
Inventory	Introduce the default Hazus data methodology, enhanced for flood analysis. Assignment of census block data through statistical analyses and general assumptions for first floor elevation. General land use, lifelines, agriculture, vehicle inventory, essential facilities.	The user provides inventory data processed through CDMS. Users improve first floor elevation information and other attributes required for the flood loss estimation.	High-quality data on building value, flood vulnerabilities, contents, occupancies, and related factors, extended to industrial facilities and other high-value sites.
Damage curves	Regional curves consistent with the level of inventory detail, based on available depth damage curves from FIA or USACE. Library of available curves for user selection. The user can create their own damage curves using internal guidelines.	The user provides their own functions or specifically modifies the existing curve library to reflect local practices.	Curves supplied by the user, based on detailed building studies, specific crop conditions, etc.
Damage estimate	Damage estimates based on flood depth within a given census block. Losses developed for general construction materials, vehicles, agricultural products, selected transportation, and utility features.	As in Level 1, the estimation is improved through higher resolution and more accurate hazard data, greater inventory data detail, and modification of the damage curves.	As in Level 1, the estimation is improved through higher resolution and more accurate hazard data, greater inventory data detail, and modification of the damage curves.
Direct Losses/ Impacts	Repair or replacement cost, human casualties and shelter requirements, temporary housing, vehicles, crop and livestock losses.	As in Level 1, the estimation is improved through hazard data, greater inventory data detail, and modification of the damage curves.	As in Level 1, the estimation is improved through hazard data, greater inventory data detail, and modification of the damage curves.
Indirect Losses/ Impacts	Sectoral economic impacts.	Sectoral economic impacts.	Sectoral economic impacts.
Typical applications	Flood mitigation / regulatory policy formulation at the regional, state, and federal levels · Prefeasibility studies · Real-time emergency response without prior warning	Planning and zoning · Selection of mitigation alternatives · Engineering prefeasibility studies · Emergency planning and real-time re-sponse · Environmental impact analysis · Education	· Analysis of essential, cultural, and high potential loss facilities · Emergency planning and real-time response · Mitigation and engineering research · Scientific research

Source: FEMA (2022b).

A.2.3. Mathematical approach

The Hazus Flood Model up to version 6.1 required flood damages for the following range of return periods: 10-year, 25-year, 50-year, 100-year, and 500-year periods for the calculation of EAD. The Hazus Flood Model 6.1 calculates damages by census block (and by occupancy) for the range of return periods. In this version of the software, the EAD is estimated as described in **Equation 7** (FEMA 2022b).

Equation 7

$$AAL = (f_{10} - f_{25}) \frac{(L_{10} + L_{25})}{2} + (f_{25} - f_{50}) \frac{(L_{25} + L_{50})}{2} + (f_{50} - f_{100}) \frac{(L_{50} + L_{100})}{2} + (f_{100} - f_{500}) \frac{(L_{100} + L_{500})}{2} + (f_{500} - f_{500})$$

Where L_{xxx} corresponds to the damage or loss for return period xxx and f_{xxx} to the exceedance probability for the return period xxx. This equation can be simplified as shown in **Equation 8** (FEMA 2022b).

Equation 8

$$AAL = 0.030L_{10} + 0.04L_{25} + 0.015L_{50} + 0.009L_{100} + 0.006L_{500}$$

For Hazus version 7.0 any 3 or more return periods can be used for the calculations (FEMA 2024d).
In the Hazus tsunami and earthquake models, the output data developed by the building damage module are estimates of the cumulative probability of being in, or exceeding, each damage state for the relevant hazard parameter (or parameters, if combined). Discrete damage state probabilities are derived from the cumulative damage probabilities. These outputs are used directly as inputs for the direct economic and social loss modules (FEMA 2022e).

The tsunami building damage functions are presented as lognormal fragility curves that express the relationship between the probability of being in, or exceeding, a discrete damage state and the median estimate of the relevant hazard parameter (that is, the median maximum inundation height or the mean maximum momentum flux). **Figure 37** illustrates the fragility curves describing Moderate, Extensive, and Complete structural damage due to tsunami flow (i.e., peak mean momentum flow, F) (FEMA 2022e).

Figure 37. Example of a tsunami fragility curve

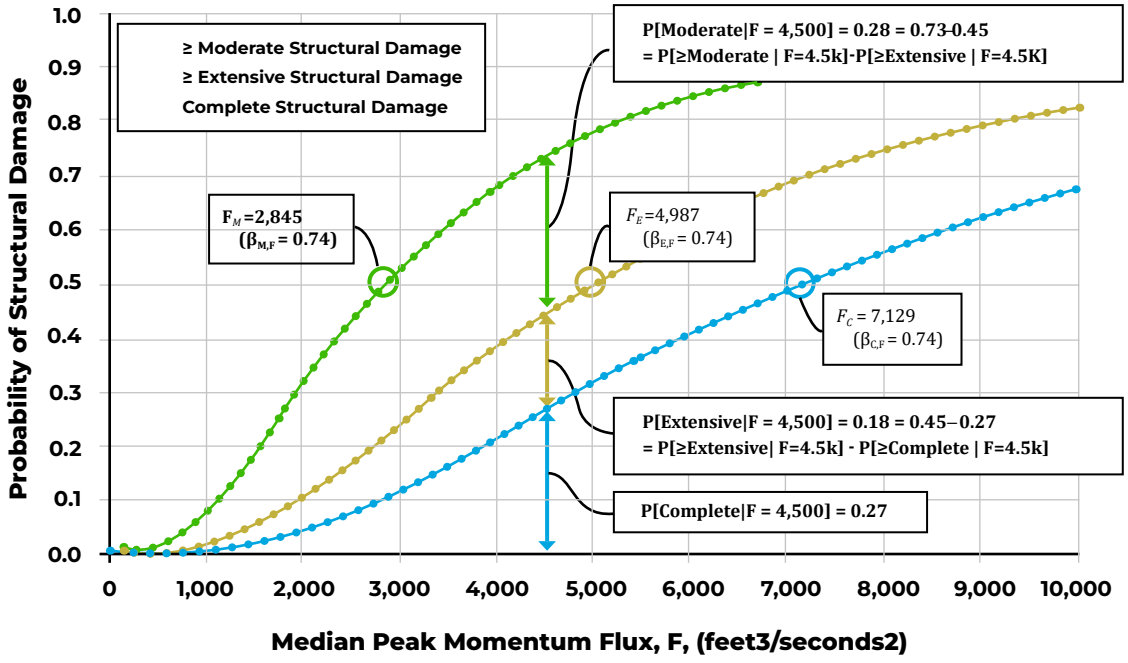

Source: FEMA (2022e).

Conceptually, the form of the tsunami building damage functions is the same as the lognormal fragility curve format used by the earthquake model. Each damage state curve is defined by the median value and the associated variability of the fragility parameter of interest. The variability of these fragility curves has two main components: the variability of the median estimate of the hazard parameter (that is, the uncertainty in the demand) and the variability of the median damage state value (that is, the uncertainty in the capacity) for the relevant hazard (FEMA 2022e).

Damage is classified into three main states: moderate, extensive, and complete. In both the tsunami and earthquake models, these terms are used to describe the extent and severity of the damage. In the case of earthquakes, an additional slight damage state is also considered, whereas for tsunamis this category is not included, as it is difficult to distinguish it from the absence of damage. Although the cause and manifestation of damage differ between tsunamis and earthquakes, the damage states are assumed to be equivalent when they represent a similar level of impact and severity (FEMA, 2022d).

Structural damage is calculated using **Equation 9** and **Equation 10**.

Equation 9

$$CS_{ds,i} = BRC_i \sum_{i=1}^{33} PSBTSTR_{ds,i} \times RCS_{ds,i}$$

Equation 10

$$CS_{i} = \sum_{ds=2}^{5} CS_{ds,i}$$

Where:
$CS_{ds,i}$ is the structural damage cost (repair and replacement costs) for damage state ds and occupancy i. Data on building replacement costs for each of the 33 occupancy classes can be found in the Hazus Inventory Technical Manual.

BRC_i is the replacement cost of the building for occupancy i.

$PSBTSTR_{ds,i}$ is the probability that the occupancy is in the structural damage state ds.

$RCS_{ds,i}$ is the structural repair and replacement ratio for occupancy i in damage state ds.

Hazus Tsunami also calculates content damage, restoration times, and building functionality for individual facilities defined by the user, as well as relocation expenses and loss of income and rent. The restoration functions, their associated methodology, and the derived functionality are available in the Hazus Earthquake Model Technical Manual (FEMA, 2022), according to the type of facility. In the tsunami model, a lookup table was implemented in the analysis parameters database so that users do not have to locate and use the restoration functions as must be done in the earthquake model (FEMA 2022e).

In the case of earthquakes, the Hazus methodology considers intensities for eight hazard levels, each with an associated probability, ranging from an earthquake with a 39% probability of being exceeded in 50 years (100-year return period) to one with a 2% probability of being exceeded in 50 years (2,500-year return period). Once the hazard data are processed, an internal analysis module in Hazus is used to convert the losses from the eight scenarios into an annualized earthquake loss (AEL). **Figure 38** illustrates an example of a risk curve using the Hazus method with eight damage values associated with exceedance probabilities. Hazus calculates the AEL by estimating the shaded area under the loss probability curve shown in **Figure 38**. This area represents an approximation of the EAD and is equivalent to taking the sum of the losses multiplied by their annual probability of occurrence. The criterion used by Hazus to select the number of points on the risk curve was computational efficiency versus marginal

improvement in accuracy. To determine the appropriate number of return periods, a sensitivity study was conducted comparing the stability of AEL results with the number of return periods for 10 regions of the United States, using 5, 8, 12, 15, and 20 return periods. The difference in AEL results obtained using 8, 12, 15, and 20 return periods was negligible (FEMA 2022f).

Figure 38. Damage curve and area under the curve as conceptualized by Hazus for seismic risk calculation.

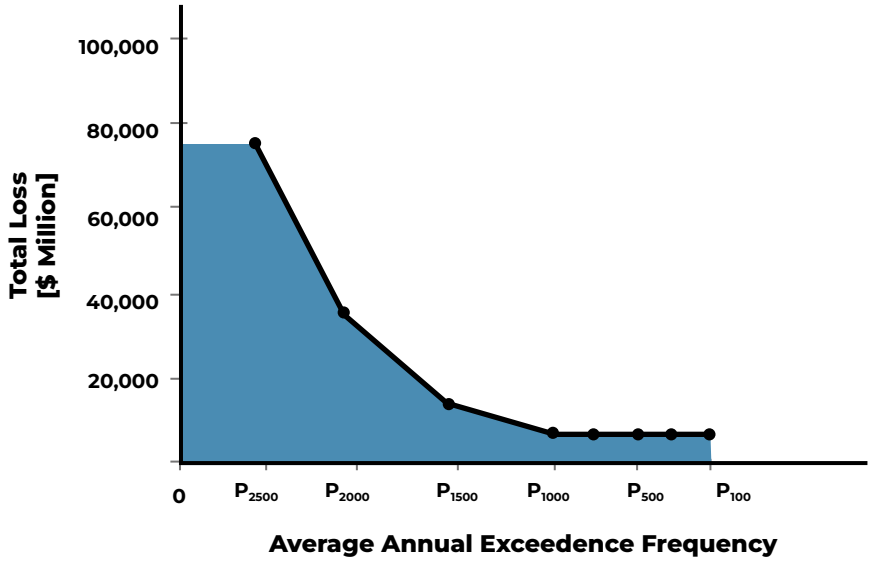

Source: FEMA (2022e).

The Hazus hurricane model uses a fully probabilistic approach to obtain the risk results. The Hazus methodology estimates the consequences of a hurricane in a city or region using a probabilistic event set whose extent varies depending on the geography. The storm track simulation model begins by randomly sampling an initial position, date, time, direction, and translational speed from one of the tropical storms listed in the HURDAT database. The number of storms to be simulated in any given year is obtained by sampling from a negative binomial distribution with a mean value of 8.4 storms per year and a standard deviation of 3.56 storms per year. The modeling approach allows the simulated storms to change direction, speed, and intensity, reproducing the continuously varying statistics associated with central pressure, direction, etc., along the U.S. coastline (FEMA 2022a).

The loss model is a physical model that calculates direct economic losses using a combination of explicit and implicit cost techniques (see **Figure 39**). The loss model subdivides buildings into subsets of costs. This approach provides significant flexibility in costs and the ability to process a wide range of building types. The loss model is designed to process detailed damage states of the building envelope and provides the additional capability to estimate economic losses to the building interior and contents, directly accounting for the volume of water that enters through damaged fenestrations (windows, doors, garage doors, etc.). The modeling approach is also suitable for estimating loss of use and repair time (FEMA 2022a).

Figure 39. Schematic representation of the loss model

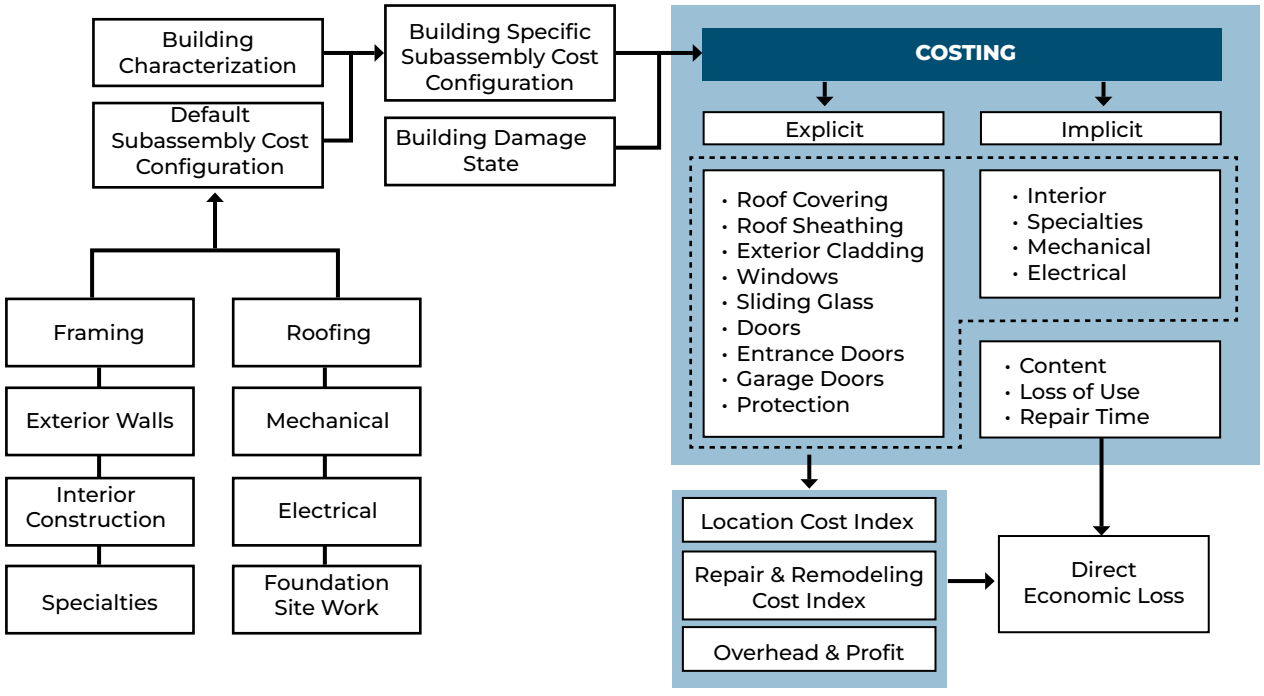

Source: FEMA (2022a).

The wind model follows a probabilistic approach based on the hazard–load–resistance–damage–loss methodology, developed within an individual risk framework. The performance of buildings under extreme winds is formulated probabilistically using structural reliability concepts. The probability of failure of individual elements (such as windows or doors) is estimated by comparing the wind load with the resistance of the element. Through simulations of different building types, damage probabilities are calculated and relationships between wind intensity and physical damage are established (FEMA).

The average annual loss from hurricanes accounts for all future losses caused by the hurricane hazard, resulting from possible hazard events of different magnitudes and return periods averaged per year. It can be used to help assess the benefits of mitigation and compare the economic risks of different hazards in the same location. Hazus can be used to generate the average annual loss by summing all losses produced during the 20,000-year hurricane simulation and dividing by 20,000 years (FEMA 2022a).

A.2.4. Recent advances and innovations

Hazus has incorporated continuous improvements in order to integrate the latest scientific and technological approaches. Recent updates include Hazus 7.0, which introduces important innovations by integrating advanced ArcGIS Pro capabilities, improving the interface and GIS analysis tools. Its main advances include streamlined workflows for floods and hurricanes, improved methodologies for coastal flood zones, and a more flexible average annual loss (AAL) calculation that allows the use of multiple depth grids for flood analysis. In addition, Hazus 7.0 simplifies data access by eliminating manual database configuration and consolidating information into a single file accessible for all territories of the U.S.

A.2.5. Development community

The Hazus program is managed by FEMA's Natural Hazards Risk Assessment Program and collaborates with other federal agencies, research institutions, and regional planning authorities. This collaboration ensures that Hazus resources incorporate the latest scientific and technological advances and meet the needs of the risk management community. (FEMA 2023).

A.2.6. Limitations

Although it is a powerful tool, its databases and models are primarily tailored to the U.S. context, but it can be used in other geographic areas with the necessary adaptations.

A.2.7. Use cases

Although Hazus is primarily used in the United States, there are adaptations and use cases in other countries. Kulmesch et al. (2010) used Hazus to analyze the flood risk in a region of Austria, Rozelle (2007 used and compared the results of the Hazus earthquake model in Nepal. There are also application cases in Latin America such as the one developed by Chantavilasvong and Guerrero (2019) which is presented in the **Box 3**.

Box 3. Example of Hazus application

Hazus Case Study in Piura (Peru)

Image: Adobe Stock

In northern Peru, in the Piura region, the rainy season runs from December to March and may continue until April during El Niño years. In 2017, a year marked by a strong El Niño event, rainfall was ten times higher than normal, causing estimated economic losses of $3.1 billion dollars nationwide. In Piura, the most affected region, four deaths were reported, hundreds of families were displaced, and approximately 15,000 hectares of crops were lost under water.

The study uses an adaptation of the U.S. Federal Emergency Management Agency's HAZUS-MH model. U.S. (FEMA). The proposed methodology addresses data and technical capacity limitations in Piura through an accessible and replicable approach, which includes: (i) a simple and user-friendly analysis using QGIS for spatial analysis, (ii) spatial distribution maps that identify areas at risk of flooding, (iii) monetary valuation of potential building damage costs, (iv) spatial flood risk analysis, and (v) delineation of flood areas.

The adapted model uses open-source tools such as QGIS to perform a spatial analysis of flood risk. The base data include NASA's SRTM3 Digital Elevation Model (DEM) and global flood depth–damage curves (Huizinga et al. 2017). The main methodological steps include:

- **Delimitation of flood areas:** Identification of flood-prone areas based on altitudes relative to estimated river levels.
- **Exposure assessment:** Overlay of flood maps with building data classified by construction materials (wood and concrete).

Structural damage calculation: Estimation of collapsed and damaged buildings using flood depth–damage curves.

Monetary valuation: Quantification of reconstruction and repair costs, providing economic estimates of potential impacts.

The maps produced show that many flood-prone areas have been developed as residential or commercial zones, exposing their inhabitants to river flooding. In the highest risk scenario, it is estimated that approximately 6,274,439 m² of buildings would be affected, with a potential cost of $4.2 billion dollars for the entire Piura region. This amount includes 5,821,163 m² of damaged buildings and 453,276 m² of collapsed buildings, affecting mainly low-income housing built with materials such as quincha or wood.

The HAZUS-MH model adapted to the Piura region proves to be a useful tool for estimating flood risks and quantifying economic impacts. However, the success of its implementation depends on: (i) improving the availability and quality of local data, (ii) training local authorities in risk analysis and mitigation planning, and (iii) promoting a participatory approach that empowers local stakeholders to manage their own climate risks. The methodology adapted from the HAZUS-MH model represents an important first step toward estimating flood risks in an accessible and effective way in Piura. Although data gaps and limitations exist, the simplicity and replicability of the approach make it a valuable tool for empowering local authorities and promoting more robust risk mitigation plans.

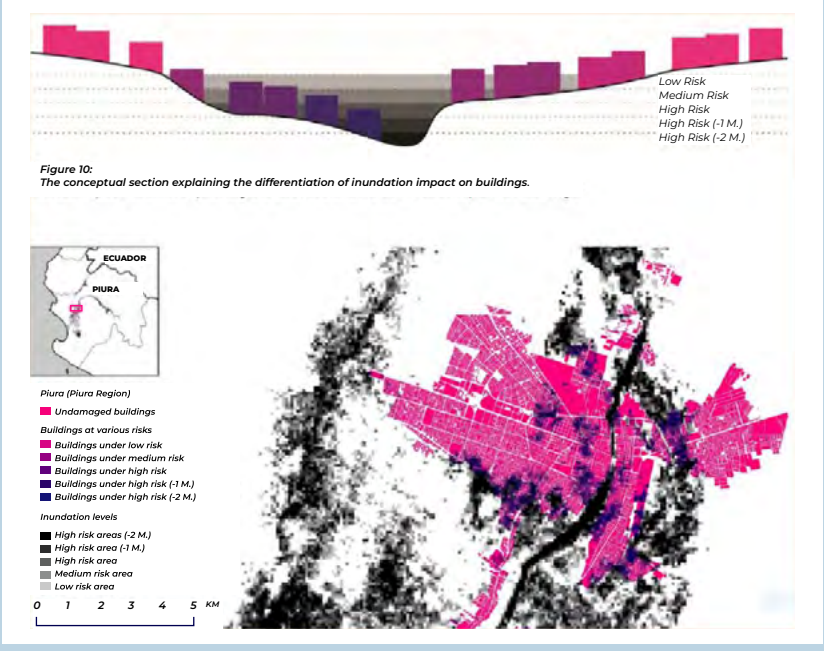

Figure 10:
The conceptual section explaining the differentiation of inundation impact on buildings.

Source: Chantavilasvong & Guerrero (2019)

A.3. RISKSCAPE: RISK ASSESSMENT TOOL

A.3.1. General description

RiskScape is an open-source spatial data processing application designed for multi-hazard risk analysis, developed jointly by GNS Science and the National Institute of Water and Atmospheric Research (NIWA) of New Zealand. Highly customizable, RiskScape enables modelers to adapt risk analysis to the specific needs of the domain and the input data being modeled. The tool can integrate data from various sources and formats, applying a range of geospatial, statistical, and data manipulation operations. This facilitates the modeling of a wide range of workflows in a consistent manner, simplifying the complexities inherent in managing geospatial data. In addition, RiskScape allows the execution of simple deterministic models on a laptop as well as computationally intensive probabilistic models on a high performance cloud computing instance (National Institute of Water and Atmospheric Research Ltd and Institute of Geological and Nuclear Sciences Ltd, 2024a).

A.3.2. Applied methods

RiskScape provides a wizard that guides users through the initial creation of a simple risk model by asking a series of questions related to their input data and the type of modeling they wish to perform. RiskScape uses its own scripting language to describe the model processing flow, known as the "pipeline". This pipeline defines a series of data processing steps, written as simple expressions similar to spreadsheet formulas or basic Python statements. RiskScape takes the answers from the wizard and converts them into pipeline code that it can run (see **Figure 40**).

Figure 40. Pipeline generation

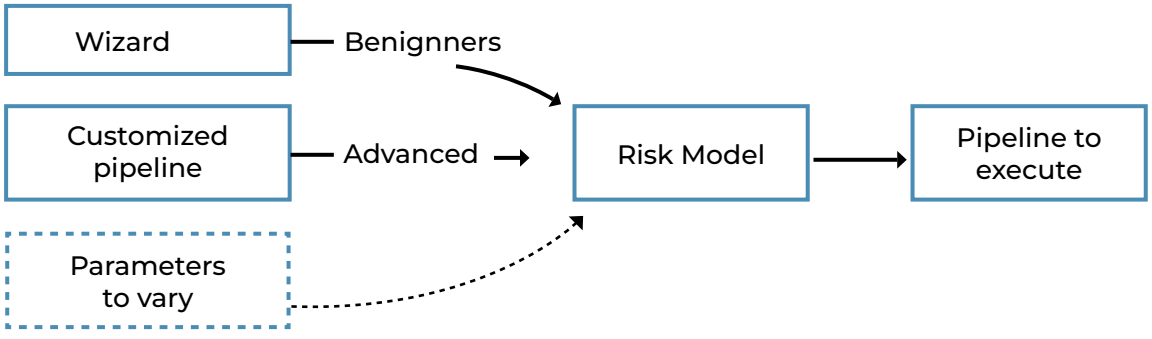

Source: National Institute of Water and Atmospheric Research Ltd and Institute of Geological and Nuclear Sciences Ltd (2024d).

As modelers become more advanced RiskScape users, they can fully customize their modeling workflow by defining it directly in the pipeline code, using the code generated by the wizard as a starting point. Currently, RiskScape is a command line interface (CLI) tool, so users run their models from the command line. Running a model means that RiskScape processes the input data according to the pipeline instructions and saves the results to a file.

A model can be run by varying the input data files or other assumptions. The details of the models and pipelines are stored in text files (for example, INI files) that tell RiskScape exactly what to do. This collection of files is called a project. A project defines the model workflows from start to finish, including which input data files and vulnerability functions to use. Projects organize RiskScape models so that related models, which involve similar hazards or affect the same features of interest, are grouped in a consistent manner.

A project contains the complete set of instructions needed to run one or more RiskScape models, including:

- **Sources of input data:** Data from various sources in GIS format, which can be used without the need for importing or preprocessing. The locations of the various input files and any additional instructions on how to load the data are specified in a RiskScape bookmark.

- **Functions:** Users can write their own Python functions to evaluate the impact of a hazard on an exposed element, such as estimating damage, calculating costs, or sampling a probabilistic curve. Advanced users can also use functions to manipulate or transform data at any point in the pipeline.

- **Types:** RiskScape uses a type system to represent the structure of the data as it flows through the model. Types define how input data can be manipulated, and the functions that can be used. Composite types can represent a set of attributes, such as a building asset or the consequence (loss, damage, etc.) of the hazard.

- **Models:** The model is the combination of input data, functions and other parameters that are applied to a data processing pipeline to produce results (see **Figure 41).** Models can be defined from saved answers from the wizard or directly in the pipeline code.

Figure 41. Project components

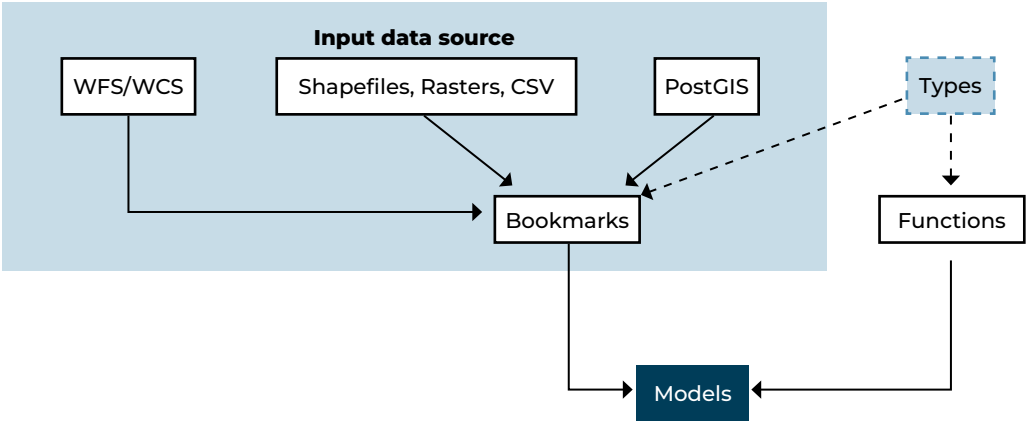

Source: National Institute of Water and Atmospheric Research Ltd and Institute of Geological and Nuclear Sciences Ltd (2024d).

RiskScape models are customized, predefined workflows (see **Figure 42**) that process geospatial data to perform risk analysis. When running a model, the risk of the data provided is analyzed. The workflow of a model includes several key phases: input data loading, geoprocessing, spatial sampling, consequence analysis, risk analysis, and report generation. The input data include exposure layers, which contain the elements at risk, and hazard layers. Optionally, additional layers can be added to improve the model results (National Institute of Water and Atmospheric Research Ltd and Institute of Geological and Nuclear Sciences Ltd 2024d).

Geoprocessing transforms geometric data prior to any risk analysis. Subsequently, spatial sampling combines the input data geospatially to determine the hazard intensity for each element at risk. The consequence analysis calculates the impact of the hazard on each element at risk, producing an event impact table that summarizes the results. Advanced users can perform additional risk calculations, such as the expected annual probability, during the risk analysis phase. Finally, the results are filtered and aggregated to generate customized reports, allowing a single model to produce multiple output files (National Institute of Water and Atmospheric Research Ltd and Institute of Geological and Nuclear Sciences Ltd 2024d).

Figure 42. Workflow

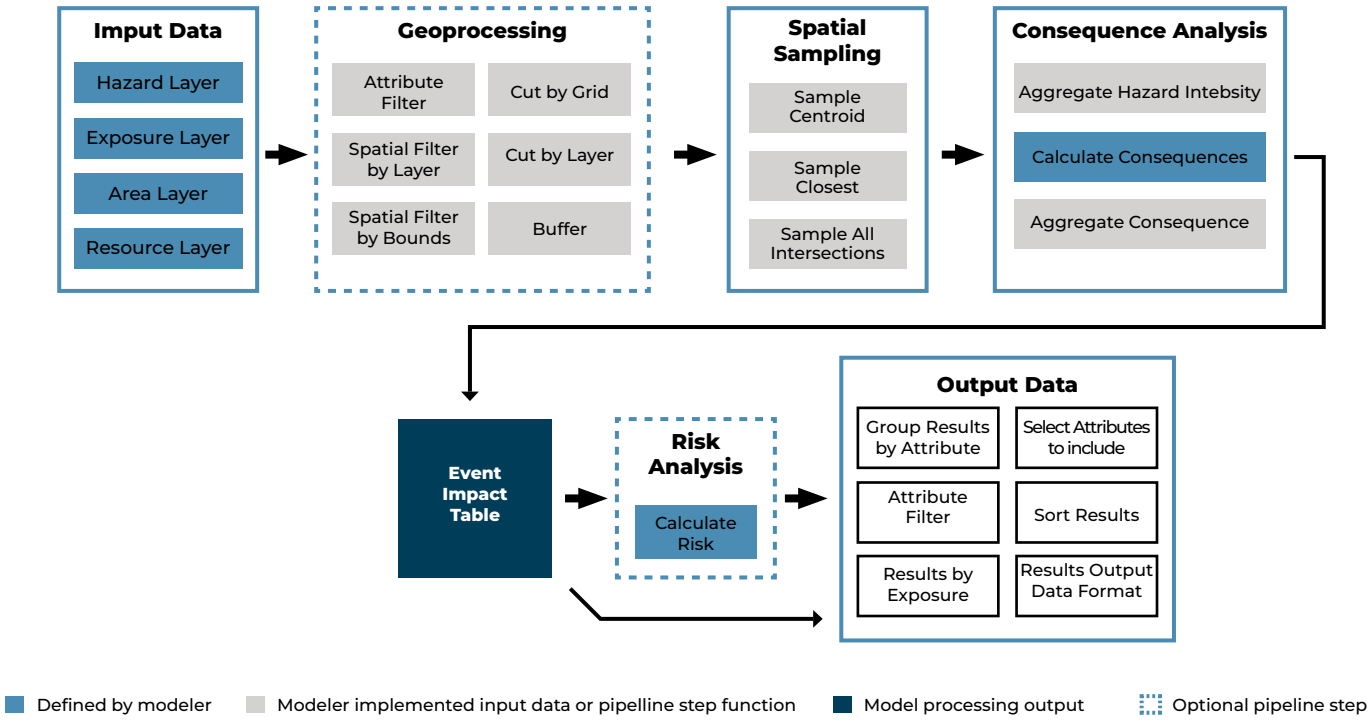

Source: National Institute of Water and Atmospheric Research Ltd and Institute of Geological and Nuclear Sciences Ltd (2024d).

Damage functions in RiskScape make it possible to analyze the impact of a hazard beyond simply determining whether a building is exposed or not. The user can define their own Python function to perform any type of risk analysis they wish. RiskScape uses a lognormal Cumulative Distribution Function (CDF) to calculate the conditional probability (between 0 and 1) that a building will be in a given damage state as a result of flooding. The five damage states used in the model are as follows (National Institute of Water and Atmospheric Research Ltd and Institute of Geological and Nuclear Sciences Ltd 2024e):

- **Slight:** Non-structural damage.
- **Minor:** Significant non-structural damage and minor structural damage.
- **Moderate:** Significant structural and non-structural damage.
- **Severe:** Irreparable structural damage requiring demolition.
- **Collapse:** Complete structural collapse.

The building fragility function (i.e., the shape of the lognormal CDF curve) varies according to the building's construction material. The damage model assigns an overall damage state to each building based on calculated probabilities, using a weighted random selection to determine the final damage level (National Institute of Water and Atmospheric Research Ltd and Institute of Geological and Nuclear Sciences Ltd 2024e).

RiskScape offers a variety of input and output formats as shown in **Table 23** (National Institute of Water and Atmospheric Research Ltd and Institute of Geological and Nuclear Sciences Ltd 2024d).

Table 23. Data Formats Accepted by RiskScape

Format	File extension	Support
arcgrid	asc	input data
csv	csv	input and output data
geojson	geojson, json	input and output data
geopackage	gpkg	input and output data
geotiff	tif, tiff	input data
kml	kml	input and output data
postgis		input data
shapefile	shp	input and output data
wfs		input data
NetCDF		input data
hdf5		input data

Source: National Institute of Water and Atmospheric Research Ltd and Institute of Geological and Nuclear Sciences Ltd (2024d).

A.3.3. Mathematical approach

In the RiskScape conceptual framework, the terms probabilistic model and scenario model are used to describe two different types of probabilistic modeling[24] (National Institute of Water and Atmospheric Research Ltd and Institute of Geological and Nuclear Sciences Ltd 2024c):

- **Probabilistic model:** It is a model in which the loss is calculated for many independent events in order to obtain probabilistic results, such as annualized losses or exceedance curves.
- **Scenario model:** This type of model calculates the loss for a single theoretical event, where there is uncertainty as to how the event will unfold. For example, how ground motion will propagate from the epicenter of an earthquake, or how ground conditions on the day of the event will affect the propagation of a flood following a levee breach.

[24] RiskScape define modelización probabilística como aquella que se refiere a un modelo de pérdidas que aborda ciertas incertidumbres presentes en el análisis.

There are two key components to building a probabilistic model in RiskScape: the generation of an event loss table and the calculation of probabilistic results (for example, the Annual Exceedance Probability, AEP). The structure of the model will depend largely on the hazard event dataset. The loss per event table calculates the total loss for each event, and its construction varies according to the input data (National Institute of Water and Atmospheric Research Ltd and Institute of Geological and Nuclear Sciences Ltd 2024c).

RiskScape considers the following approaches for probabilistic analyses:

- **Event-based:** each event in the input dataset is treated as having the same probability within the model itself (Monte Carlo simulation). The model depends on having enough events in the dataset to model uncertainty and generate a loss curve. A key aspect of event-based probabilistic models is the number of hypothetical event sets to which the events belong. Typically, this corresponds to the number of time periods, such as years, that are modeled, and it is necessary to calculate annualized losses. This set is called the Stochastic Event Set (SES).

  Once the total loss for each event is obtained, each event is assigned to a Stochastic Event Set (SES). This assigns each event to the calendar year in which it occurred.

  The SES is important for calculating the Average Annualized Loss, since some calendar years may have multiple events while others may have none. It is important to note that if no events occurred in a given SES (year), a loss of zero is assigned.

  To produce the risk curve, the losses are ranked from highest to lowest, and a probability is assigned by dividing the range by the number of event sets.

  To illustrate this method and the other methods presented in this section, the examples provided in the online RiskScape[25] documentation will be presented.

  The **Table 24** shows a dataset of 5 events for which the loss has been calculated.

Table 24. Example of 5 events for which loss has been calculated

Event	Event set	Loss
1	1	$1100
2	3	$500
3	4	$600
4	4	$200

[25] https://riskscape.org.nz/docs/advanced/probabilistic.html

Losses that exceed a given loss level are counted, as shown in **Table 25**.

Table 25. Count of loss events that exceed a given loss level.

Loss level	Count
100	4
250	3
500	2
750	1
1000	1

The exceedance rate (λ) is calculated for a unit time period (1).

Table 26. Exceedance rate

Loss level	Count	Calculation	λ
100	4	4 / (5 *1)	0.8
250	3	3 / (5 *1)	0.6
500	2	2 / (5 *1)	0.4
750	1	1 / (5 *1)	0.2
1000	1	1 / (5 *1)	0.2

Assuming that the events are independent, it is possible to use a Poisson distribution to calculate the Annual Exceedance Probability (AEP) by substituting the rate (λ) and the time period (T) into the formula 1 – exp(–λ * T).

Table 27. AEP calculation

Loss level	Count	λ	Calculation	AEP
100	4	0.8	1 - exp(-0.8 * 1)	0.55
250	3	0.6	1 - exp(-0.6 * 1)	0.45
500	2	0.4	1 - exp(-0.4 * 1)	0.33
750	1	0.2	1 - exp(-0.2 * 1)	0.18
1000	1	0.2	1 - exp(-0.2 * 1)	0.18

The return period or Average Recurrence Interval (ARI) can be calculated from the rate, as shown in **Table 28**.

Table 28. Calculation of the return period

Loss level	Count	λ	Calculation	ARI
100	4	0.8	1 / 0.8	1.25
250	3	0.6	1 / 0.6	1.66
500	2	0.4	1 / 0.4	2.5
750	1	0.2	1 / 0.2	5
1000	1	0.2	1 / 0.2	5

Based on weighted events: each event in the input dataset already has an associated probability or occurrence rate. This is the rate at which this event occurs during the defined period of time (usually annually). For example, a rate of 0.1 for a one-year period would mean that, on average, an event is likely to occur every ten years. A model based on weighted events provides good coverage of the range of possible events without requiring the large number of events needed for a Monte Carlo simulation.

For example, **Table 29** shows the losses for 5 events.

Table 29. Loss table for 5 events

Event	Ocurrence date	Loss
1	0.01	$1100
2	0.035	$500
3	0.04	$600
4	0.1	$200
5	0.05	$800

To calculate the Average Annual Loss (AAL), the sum of the rate × loss values is computed, resulting in an AAL of $112.50.

Table 30. Calculation of the Average Annual Loss

Event	Ocurrence rate	Loss	Rate x loss
1	0.01	$1100	$11.0
2	0.035	$500	$17.5
3	0.04	$600	$24.0
4	0.1	$200	$20.0
5	0.05	$800	$40.0
Total	**0.235**	**$3200**	**$112.50**

The formula rate x loss^2 is used to calculate the standard deviation. Adding the values results in $71,250. The square root of this value gives a standard deviation of $266.93.

Table 31. Calculation of the standard deviation

Event	Ocurrence rate	Loss	Rate x loss^2
1	0.01	$1100	12100
2	0.035	$500	8750
3	0.04	$600	14400
4	0.1	$200	4000
5	0.05	$800	32000
Total			**71250**

To calculate the annual exceedance probability, the occurrence rate of each event that exceeds a given loss level is added, which provides the total exceedance rate.

Table 32. Total exceedance rate

Loss level	Rate of exceedance
100	0.235
250	0.135
500	0.1
750	0.06
1000	0.01

The annual exceedance probability (AEP) can be calculated from the exceedance rate by applying 1 - exp(-λ × T).

Table 33. Calculation of the Annual Exceedance Probability (AEP)

Loss level	Rate of exceedance	Calculation	AEP
100	0.235	1 - exp(-0.235 * 1)	0.209
250	0.135	1 - exp(-0.135 * 1)	0.126
500	0.1	1 - exp(-0.1 * 1)	0.095
750	0.06	1 - exp(-0.06 * 1)	0.058
1000	0.01	1 - exp(-0.1 * 1)	0.01

The return period, or average recurrence interval (ARI), can be calculated from the rate as shown in **Table 34**.

Table 34. Calculation of the average recurrence interval (ARI)

Loss level	Rate of exceedance	Calculation	ARI
100	0.235	1 / 0.235	4.26
250	0.135	1 / 0.135	7.41
500	0.1	1 / 0.1	10.0
750	0.06	1 / 0.06	16.67
1000	0.01	1 / 0.01	100.0

Hazard-based: the input dataset contains a small number of events, each event has an occurrence rate (or return period). For example, the hazard input files could represent a flood with return periods of 10 years, 50 years, 100 years, etc. This differs from other probabilistic models, such as event-based models, where the exceedance probability is derived from the execution of the model itself.

The main advantage of the hazard-based approach is that only a small number of events is required to produce a probabilistic result. This is useful when it is not feasible to produce the thousands of hazard layers required for an event-based model.

A hazard-based probabilistic model requires each event in the model to have a known recurrence interval (or return period), which must be included in the hazard layers (or in the metadata). In addition, the loss function of the model must produce losses that increase

monotonically as the frequency of the hazard decreases. In other words, less frequent events must produce more severe losses for each exposed element at risk.

The probability of exceedance is given as a decimal number between 0 and 1. This is interpreted as the probability of an event of this intensity or greater occurring in a given period (usually years). An exceedance probability can be related to a return period using a probability mass function. In the examples provided by RiskScape, it is assumed that the Poisson distribution function is appropriate. When using the Poisson distribution, the return period is used as the rate, also known as lambda (λ). A return period can be converted to an exceedance probability (EP) using the **Equation 11**.

Equation 11

$$EP = 1 - e^{-\lambda x T}$$

Exceedance probabilities are often calculated from a return period (RP) using a simple approximation, as shown in **Equation 12**.

Equation 12

$$\frac{1}{RP}$$

But this is a poorer approximation than using the Poisson-based calculation. **Table 35** shows how the approximation method becomes less accurate as the probability increases.

Table 35. Comparison of the exceedance probability calculated using the Poisson method and the reciprocal method

Probability	Reciprocal ARI	Poisson ARI
0.001%	1000000	99999.49
0.1%	1000	999
25%	4	3.48
50%	2	1.44

With a hazard-based probabilistic model, there are not enough data points to use the same numerical method to calculate an AAL as in the case of event-based or weighted-event models. Instead, this method relies on the trapezoidal rule to estimate the area under the “curve” of the exceedance probability for each event and the corresponding calculated loss for that event.

Table 36. Example of probability of exceedance and associated losses

Event	Exceedance probability	Poisson ARI
1	0.1	$1000
2	0.01	$10000
3	0.001	$100000

Based on the data in **Table 36,** it is possible to plot the curve, and by using the trapezoidal method, the area under the curve can be estimated, which represents the AAL.

Figure 43. Excess and loss probability curve

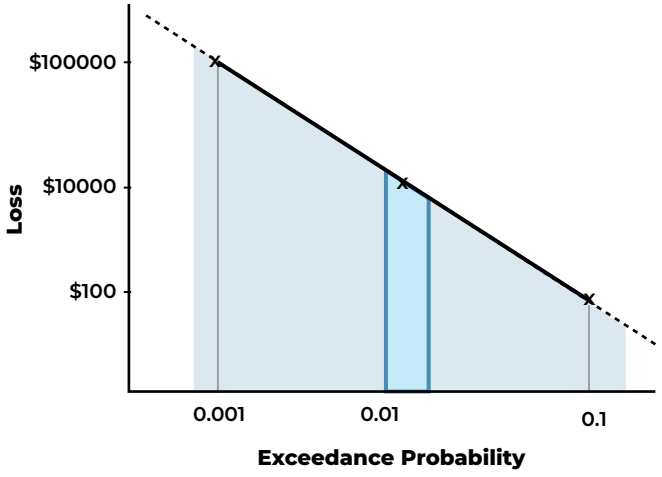

The **Figure 43** shows the shaded area (in log-log scale) below the curve plotted from the data points of the **Table 36**. Taking a "slice" between two points on the curve results in a trapezoidal shape (see the blue area in **Figure 43**). The trapezoidal method simply takes multiple segments between the minimum EP (i.e., 0.001) and the maximum EP (i.e., 0.1) and sums them. This results in the area under the curve between the data points of the first and last events. However, two parts of the curve are still missing: the left side between EP 0.0 and 0.001, and the right side between EP 0.1 and 1.0 (or when the loss becomes $0). Nothing can be done about the missing right-hand side of the curve; this depends on having hazard data that approach a zero-loss event as closely as possible. For the missing left-hand side, we know that the losses increase monotonically; therefore, the losses between 0.0 and 0.001 must be greater than or equal to the maximum known loss ($100,000). So, essentially, we can add an extra data point (EP=0.0, loss=$100,000) to the curve.

The trapezoidal method simply consists of taking the difference in value (exceedance probability) between two data points and multiplying it by the mean value (loss). The trapezoidal integration applied to the three example events, plus the additional data point EP=0.0, is shown in **Table 37**.

Table 37. Calculation of the area under the curve

Difference in EP	Average losses	Trapezoidal slice
0.1 - 0.01	($10,000 + $1,000) / 2	0,09 * 5500 = 495,0
0.01 - 0.001	($100,000 + $10,000) / 2	0,009 * 55000 = 495,0
0.001 - 0.0	($100,000 + $100,000) / 2	0,001 * 100000 = 100,0

The sum of the trapezoidal slices is $495 + $495 + $100 = $1,090.

Because the “trapezoidal” slice at EP = 0.0 is actually a rectangle, it can be simplified to just the maximum loss multiplied by the minimum EP. With this additional term at EP = 0.0, the AAL calculation for the loss curve area is equal to:

Equation 13

$$AAL = \int_a L_a + \sum_{RP_n=a}^{N} \Delta \int \frac{L_{RP_n} + L_{RP_{n+1}}}{2}$$

A.3.4. Recent advances and innovations

The latest improvements in the RiskScape software include significant changes and enhancements that affect both advanced users and the overall software experience. A notable change is the update of the GeoTools library, used for geometry processing, which improves stability and performance. New functionalities have been implemented, making advanced customization easier for users. In addition, a feature for working with two-dimensional functions has been added, and the error-handling functions have been improved (National Institute of Water and Atmospheric Research Ltd and Institute of Geological and Nuclear Sciences Ltd 2024b).

A.3.5. Development community

RiskScape is maintained and developed by GNS Science and NIWA, with financial support from the New Zealand Earthquake Commission (EQC). The user community includes scientists, urban planners, insurance companies, and government agencies that use the platform to model losses and risks associated with disasters.

A.3.6. Limitations

The main limitation of RiskScape is the need for advanced configuration and modeling, which may require specialized knowledge, particularly Python programming skills.

A.3.7. Use cases

RiskScape has been used throughout New Zealand and the South Pacific to help planners, government agencies, and insurance companies model disaster losses and risks. This is crucial for decision-making in land-use planning, insurance, and emergency response. For example, it has been used to analyze the exposure of residential buildings to earthquakes and for urban planning related to floods and landslides. **Box 4** shows an example of the use of RiskScape in land-use planning.

Image: Adobe Stock

Box 4. Example of RiskScape application

Case Study: Flood Risk Management at Te Auaunga / Oakley Creek, Auckland

Te Auaunga (Oakley Creek) is a river that flows from Mt Roskill through several western Auckland suburbs, discharging into the inner Waitematā Harbour near Point Chevalier. The area has been designated for urban densification through the Auckland Unitary Plan (AUP). Currently, the areas immediately adjacent to the waterbody are a mix of residential zones: houses and apartment buildings, mixed urban housing, and mixed suburban housing. There is potential for greater urban density through a land-use plan change that could allow a minimum of three three-storey dwellings.

The Auckland Council's Stormwater Operations Department developed the "Making Space for Water" program, which was presented to the Council in June 2023 and includes nine key initiatives:

- **Blue-green networks in critical flood-risk areas:** Stormwater solutions, park or open space enhancements, and property acquisition.
- **High-risk properties:** Work with property owners on engineering solutions, resettlement, and property acquisition.

- **Improvements to culverts and bridges:** Evaluation, replacement and improvement of vulnerable assets.
- **Management of overland flow paths:** Repair and maintenance of overland flow paths, as well as education for homeowners in their areas of influence.
- **Rural settlements:** Response to water needs in flood-affected communities, including marae and papakāinga, and support for community resilience planning.
- **Flood intelligence:** Investment in planning and modeling tools to improve Council decision-making.
- **Rehabilitation of waterbodies:** Vegetation management, slope stabilization, modification of waterbodies, and advisory support for homeowners.
- **Community-led flood resilience:** Advisory services for property owners in high-risk areas, targeted guidance for industries, public events, and awareness campaigns.
- **Increased maintenance:** Maximization of stormwater network efficiency, including street sweeping, sump cleaning, and weed removal in waterbodies.

This case study uses elements of those initiatives to consider four risk management approaches through land-use planning: Protect, Accept, Reduce, Avoid (PARA):

- **Protect:** Hard protective structures. This approach is not included in the case study, as it requires hazard modeling with structures, which is beyond the scope.
- **Accept (Accommodate):** Raise the floor elevations. The current requirements are 500 mm above a flood event with a 1% AEP (annual exceedance probability).
- **Reduce:** Blue-green networks that include stormwater solutions, green or open space enhancements, and resettlement.
- **Avoid:** Do not allow further development or intensification.

The objective is to use RiskScape™ to quantify the benefit of various PARA model intervention options for future risk on the floodplain. The process followed to create the RiskScape™ pipeline was as follows:

- Model the baseline future risk (with no changes to the existing land-use policy), then model the future risk with the policy intervention options to show the difference. The difference in future risk is used to show the potential risk reduction achieved by implementing the policies and to support the cost–benefit analysis.

- Model a series of scenarios with different AEPs (annual exceedance probabilities) to understand flood risk across a spectrum of possible scenarios. Scenarios with AEPs ranging from 5%, 2%, 1%, 0.5%, 0.2%, and 0.1% to 0.01% were used to account for a wide range of possible flood events.

- Select a planning time horizon. In this case, the year 2120 was chosen as the future risk date, which involves modifying the exposure data from the present to a potential exposure 97 years ahead.

- Examine future intensification levels. The land-use plan zones have varying levels of residential densification that may occur as a permitted activity but must comply with the standards.

- Define the maximum possible densification within the planning horizon.

- Generate future exposure datasets. Once the development rate is established, RiskScape™ generates future exposure datasets for each year between the current year (2023) and the future planning horizon (2120).

- Calculate risk over time. RiskScape™ calculates risk for each year using the hazard layers. If there were climate change or any other time-dependent factor in the hazard data, it could also be incorporated.

The results obtained with RiskScape™ are defined by two metrics (see the following figure): risk curves and the AAL (Average Annual Loss). Risk curves show the probability of exceeding a given loss level as a function of the AEP, with different mitigation options.

The option of raising floor elevations to a fixed value of 1000 mm reduces loss, but it is not as beneficial as linking it to an AEP-based model with an additional safety margin (freeboard). A reduction in losses is also observed when applying 5%, 2%, or 1% AEP models with freeboard. The AAL metric shows the reduction in losses over time, which is useful for cost–benefit analysis. By implementing various mitigation options, such as increasing floor elevations or including freeboard, a significant reduction in annual losses is achieved.

This case study demonstrates how RiskScape™ can be used to quantify the benefits of various policy interventions in flood risk management. By modeling different risk scenarios and applying various mitigation options, decision-making on land-use planning and flood resilience can be optimized, promoting more informed and efficient risk management for the community.

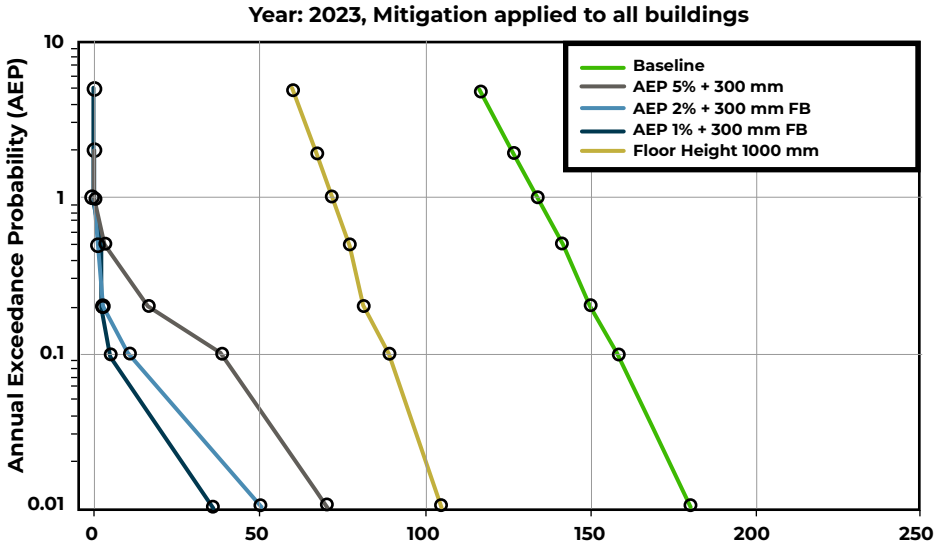

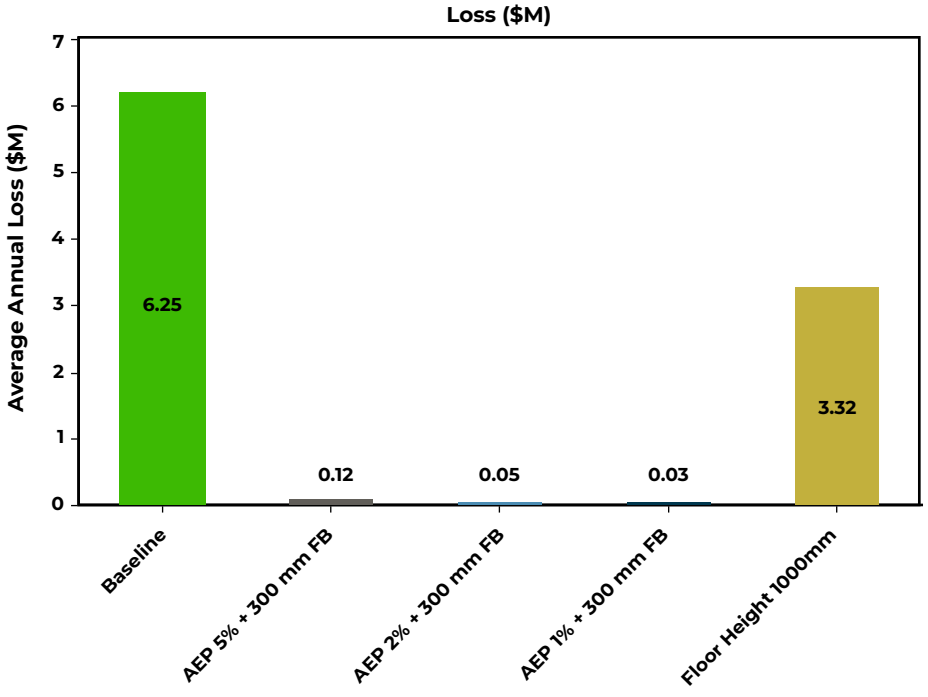

Source: Bretherton et al. (2023).

A.4. INASAFE

A.4.1. General description

InaSAFE (Indonesia Scenario Assessment for Emergencies) is an open-source software tool developed for assessing the impact of disasters such as earthquakes, tsunamis, and floods. It was developed through a collaboration between Indonesia's National Disaster Management Agency, the Australian Government, and the World Bank's GFDRR.

InaSAFE is open-source software that generates natural hazard impact scenarios to improve planning, preparedness, and response activities. It provides a simple yet rigorous way to combine technical information with input from local governments and communities to generate insights into the likely impacts of future disasters.

The InaSAFE project was initiated to provide a tool for disaster managers who want to understand the potential impacts of a disaster. Initially, the activity focused on Indonesia, a country highly vulnerable to various disasters such as floods, tsunamis, volcanoes, and earthquakes, as well as other localized hazards like landslides and wildfires. Since then, InaSAFE has been adopted for use in many other countries and is not specific to Indonesia (InaSAFE 2019b).

A.4.2. Applied methods

InaSAFE combines an exposure data layer (for example, the location of buildings) with a hazard scenario (for example, a flood footprint) and produces a spatial impact layer along with a statistical summary and action questions. The structure of the tool is shown in **Figure 44** indicating as input data the hazard and exposure layers to which an impact function is applied to produce maps, reports, and action lists. InaSAFE is designed to answer questions such as: "In the event of a flood similar to the 2013 Jakarta flood, how many people might need to be evacuated?" (InaSAFE 2019a).

Figure 44. InaSAFE Structure

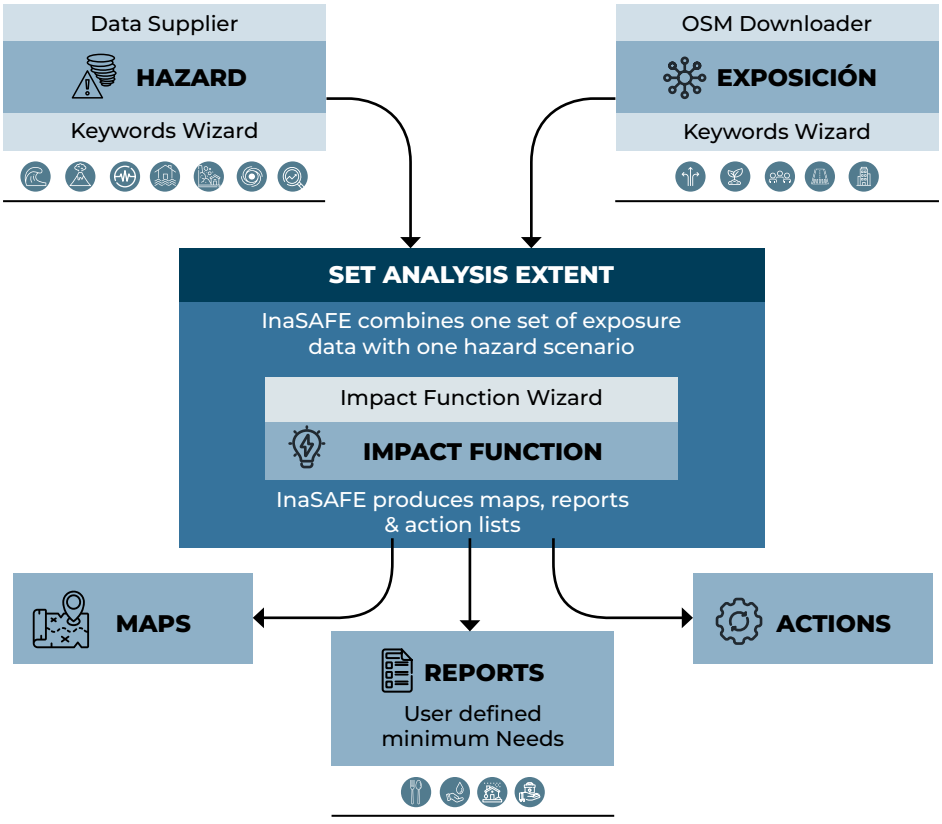

Source: InaSAFE (2019a).

InaSAFE can also disaggregate impact results by administrative boundaries and provide a breakdown of information on the gender and age of affected individuals depending on the input data used (InaSAFE 2019a).

The hazard data used in InaSAFE can represent a single event or multiple events. Single-event information is useful when estimating, for example, "how many people would be affected if another flood like the 2013 event were to occur." Multiple-event data are useful when planning for disasters that repeatedly affect the same area.

The type of hazard information used by InaSAFE is either vector or raster. In the case of vector information, a field is required to indicate whether the polygon is flood-prone or not. In the case of raster information, a simple grid is required with cell values representing water depth (InaSAFE 2019a).

Currently, InaSAFE supports four types of exposure data: roads, buildings, population, and land cover. With InaSAFE's flood impact functions for roads, it is possible to calculate which roads and of what type could be affected by a flood. Road data from OpenStreetMap can be downloaded directly using the OSM download tool provided by InaSAFE. In the case of the building inventory, InaSAFE requires a vector polygon layer with a field that includes the building type. Currently, InaSAFE only supports census data in raster format, but future versions are planned to assign population estimates to buildings using census data. Land cover information must be provided in vector polygon format with a field that contains the cover type. Location data can generally be obtained from national mapping agencies or through various online data sources. Location data are useful if you want to assess the impact of an event at a specific location. For location assessment, a vector point layer is used, which must include a field containing the location name (InaSAFE 2019a).

An Impact Function is a piece of software code in InaSAFE that implements a specific algorithm to determine the impact of a hazard on the selected exposure. An Impact Function is run once all input data have been prepared, the analysis extent has been defined, and the impact outputs are ready to be viewed. Each Impact Function generates results that may include an impact map layer, an impact summary, minimum needs, and action checklists (InaSAFE 2019a).

An impact layer is a new GIS dataset that is produced as a result of running an Impact Function. It will usually represent the exposure layer. For example, if a flood analysis is performed on buildings, the resulting impact layer will be a building layer, but each building will be classified according to whether it is dry or flooded (the output produced by InaSAFE is binary, indicating whether the building has been affected or not). InaSAFE applies its own symbology to the output impact layer to make it clear which buildings are affected. It should also be noted that the impact layer will include only the features or cells that fall within the analysis extent (InaSAFE 2019a).

While the impact layer represents spatial data, the impact summary consists of tabular and textual data. The impact summary provides a table (or series of tables) and other textual information showing the number of buildings, roads, or people affected, as well as additional useful information such as minimum needs breakdowns, action checklists, and summaries. The impact summary presents the results of the impact function in an easy-to-use format (InaSAFE 2019c). The results are limited to showing exposure, that is, the count of elements that fall within a given hazard category, although it includes impact functions capable of generating information on displaced population and fatalities (InaSAFE 2019a).

A.4.3. Recent advances and innovations

InaSAFE has released several versions, with significant improvements to the user interface and compatibility with QGIS. The latest version released is version 5.0.0, published in November 2018. This version includes support for QGIS 3.x. This version is a direct adaptation of the 4.4.0 code base, with some additional features added, such as a QGIS3 port using Python 3 and Qt 5 (InaSAFE 2019c).

A.4.4. Development community

InaSAFE was initially developed by the Indonesian National Disaster Management Agency (BNPB), the Australian Government, and the World Bank through the Global Facility for Disaster Reduction and Recovery (GFDRR). The Australian Government, in coordination with BNPB, promotes the development of InaSAFE through its use in six Indonesian provinces. Following its launch in October 2012, the Australia-Indonesia Facility for Disaster Reduction (AIFDR) organized contingency planning training in these provinces with support from the Humanitarian OpenStreetMap Team (HOT) and Gadjah Mada University (UGM) (InaSAFE 2019d).

The use of InaSAFE has generated many requests for new features, which have been prioritized by BNPB and the Australian Government and developed by Kartoza. Through GFDRR, the World Bank has developed an online version of InaSAFE to facilitate analysis without the need to download the software, and has also assisted other countries in implementing InaSAFE. The InaSAFE Technical Working Group, composed of representatives from BNPB, the Australian Government, and GFDRR, is responsible for the development and maintenance of the software (InaSAFE 2019d).

A.4.5. Limitations

One of the most significant limitations is that InaSAFE does not perform a quantitative economic risk analysis; the software is limited to exposure assessment.

A.4.6. Use cases

InaSAFE has been used in several risk assessment projects in Indonesia and other countries. It has been used for emergency planning, community preparedness and disaster response, helping local authorities to understand and mitigate disaster risks.

Box 5. Example of InaSAFE application

Case Study: Use of InaSAFE during the 2014 Jakarta Flood.

Background

Jakarta experiences seasonal flooding almost every year between December and February due to high rainfall. Geographically, it is a low plain where several rivers of West Java converge. The city's poor drainage conditions, along with its location, contribute to flooding during the rainy season. Under these circumstances, both the public and government officials need accessible and understandable information about the areas affected by flooding.

Recognizing the critical role of hazard maps in disaster management, the Australia–Indonesia Facility for Disaster Reduction (AIFDR) funded the Humanitarian OpenStreetMap Team (HOT) to assist the Jakarta Disaster Management Agency (BPBD DKI Jakarta) in mapping floods in 2014. Two GIS specialists from HOT worked every day for two months at Pusdalops BPBD DKI Jakarta to produce flood maps based on reports from the affected villages.

Implementation

The maps were developed using free software including InaSAFE and open-source software such as QGIS 2.0. The workflow involved several phases shown in the figure below:

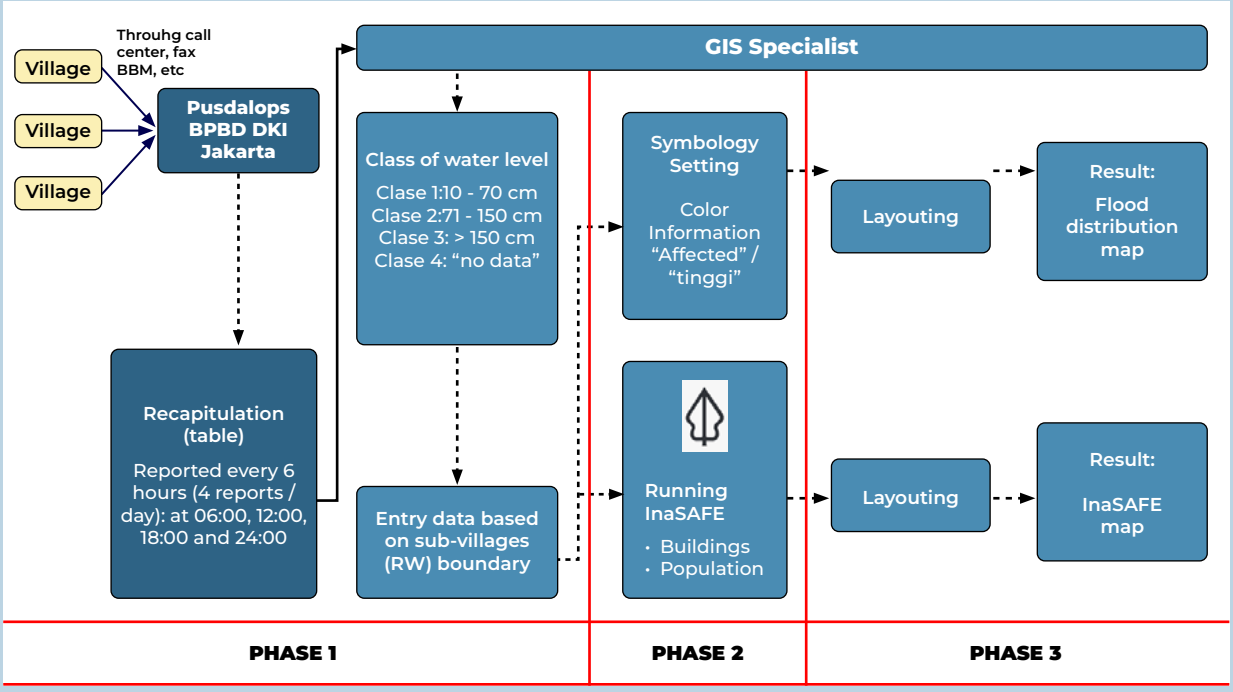

- **Data Collection:** Representatives from the affected villages reported to Pusdalops BPBD DKI Jakarta either through a call center, fax, or BlackBerry Messenger to provide information on the height and extent of the flood. These reports were summarized in a table that was sent to the head of Pusdalops and the Governor of Jakarta every six hours.

- **Map development:** The GIS specialists processed these tables into maps. The information on flood levels was classified into four categories and entered into QGIS 2.0, overlaid with the village boundary data from OpenStreetMap (OSM).

- **Distribution and Analysis:** The resulting maps included symbols to show the distribution and level of the flood. InaSAFE maps were also generated, integrating hazard and exposure data to calculate impact estimates.

Results

The collaboration between HOT and BPBD DKI Jakarta resulted in the generation of flood maps for the event that occurred between January 12 and February 10, 2014. These maps showed the flood level in the affected areas and provided an additional view of the number of affected buildings, as well as the estimated number of internally displaced people, using data obtained with InaSAFE. The maps were published on a daily basis and proved to be useful for official decision-making and aid distribution. The maps were also accessible to the public, benefiting both volunteers and journalists, and helping the population of Jakarta cope with the floods.


Image: Adobe Stock

Lessons Learned

For optimal functionality, two areas for improvement were identified:

- **Infrastructure Data:** Improvement to the completeness of infrastructure data, especially regarding public buildings, since current OSM data are limited.

- **Geographic Detail:** Increase the geographic detail of the analysis, moving from the sub-village level to more detailed levels, to provide more accurate information on the affected areas.

Source: InaSAFE (2019a).

A.5. OASIS LOSS MODELLING FRAMEWORK (OASIS LMF)

A.5.1. General description

The European Commission's H2020_Insurance project created the "Oasis Loss Modelling Framework (LMF)" for the modeling of risks associated with disasters and extreme climate events. The main outcome was the development of an open-source, collaborative, multi-hazard climate risk assessment platform designed to improve the information available to the (re)insurance sector and reduce the gap between insured and uninsured climate-related losses (Sheehan et al. 2023).

OasisLMF is a catastrophe modeling system that includes a set of data standards, an API, and tools and components for building and running models (OASIS 2024a). Although Oasis is open-source and anyone can install and run it free of charge, several companies offer commercial services and support related to Oasis. Some of these companies offer a hosted platform for running Oasis models, some have integrated Oasis into their own platforms, and others provide traditional support options for internal Oasis deployments (OASIS 2024b).

The main users of Oasis are (OASIS 2024a):

1. **Model developers,** who create, test and publish risk models. They are generally scientists or software developers who work in risk modeling companies or academic institutions.
2. **Risk analysts,** who operate the models in order to provide support in decision-making processes. The main group of users consists of analysts who work in insurance or reinsurance organizations and run the models to support pricing and portfolio management. This also includes users from government agencies.
3. **Enterprise risk systems in insurance or reinsurance organizations,** where Oasis risk models are integrated through APIs into pricing and portfolio management workflows.

The software components are described below and shown in **Figure 45** (OASIS 2024b).

1. **Oasis Platform:** a catastrophe modeling system that includes a set of data standards, an API, and tools and components for building and running models. It is the core foundation of Oasis, where most of the domain-specific code is implemented and performance is optimized.

2. **Oasis User Interface (UI):** a web application for uploading exposure data, running models implemented in Oasis, and retrieving output data. It is designed for operating models in (re)insurance companies in conjunction with existing exposure management and reporting tools; it is also useful for model evaluation and for use in public sector contexts. The UI was designed primarily for model evaluation and testing, rather than for the core aggregation of portfolios of insurers and reinsurers.

3. **Oasis Model Development Kit (MDK):** a set of tools for building, calibrating, and creating a model ready to be implemented in the Oasis Platform. It is designed for model developers or academic users, who are often familiar with working directly with data from the command line or programmatically.

4. **Oasis Model Library:** is a catalog of Oasis models hosted on AWS. It allows regression testing of the models after updates to the Oasis Platform code, as well as validation of the operation and scalability of the models.

Figure 45. Oasis Ecosystem

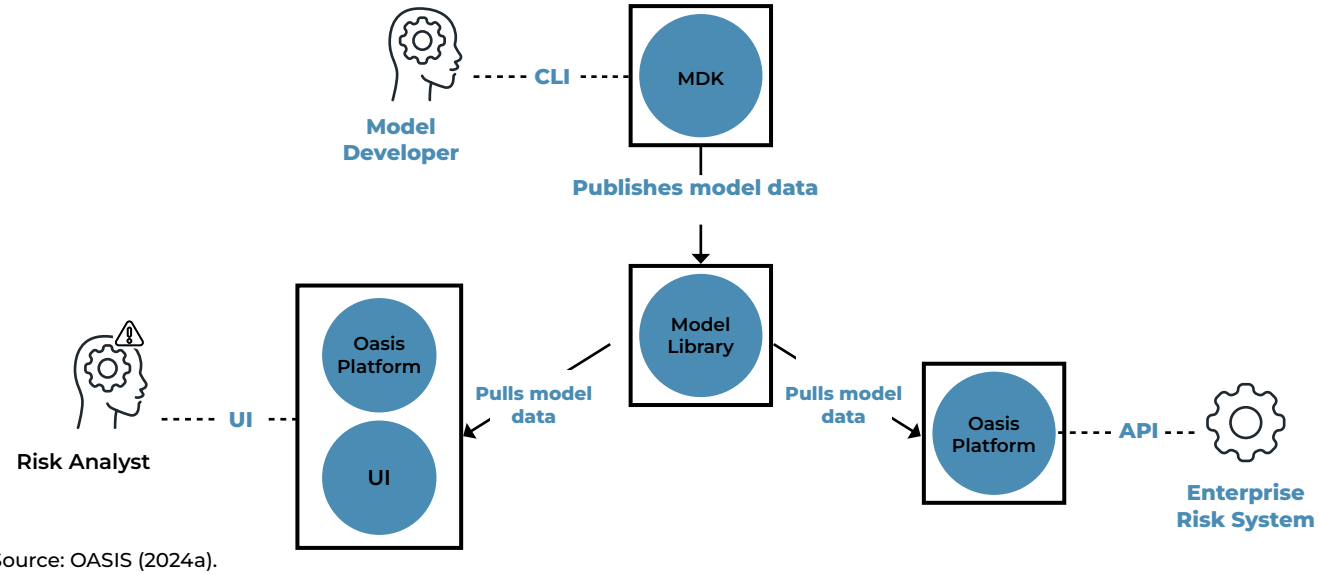

Source: OASIS (2024a).

The Oasis platform can be deployed on a server using Docker containers, or on cloud servers, such as AWS and Azure (OASIS 2024b).

Although there are numerous models available on the Oasis platform, **access to them depends on the agreements established between the user and the model provider**. More models can be added to the user's account once the agreements with the model providers have been established. However, most models are available for a limited time for evaluation purposes through a hosted environment (OASIS 2024a).

The cost of using Oasis varies depending on the models, the data used, the size of the organization and the number of users. An approximate guide to the licensing costs of the most relevant models (earthquakes and hurricanes in the U.S., earthquakes and typhoons in Japan, windstorms in Europe, and floods in the United Kingdom) for a 3-year agreement is shown below, as published in (OASIS 2024a). The prices indicated are in USD, do not include accommodation costs or taxes, and should only be taken as an approximate reference, as they may vary.

Small business: about **$479,000**

Medium-sized company about **$663,000**

Large company about **$930,000**

The models can be used free of charge as Open Access Models when hosted internally on the Oasis AWS server. The range of available models is constantly expanding according to demand and requirements. The initial models available include the country-level seismic risk models for Colombia, South Africa, and China developed by the GEM Foundation (Global Earthquake Model), as well as the CHAZ (Climate Hazard Model) developed by Columbia University.

A.5.2. Applied methods

An Oasis model is composed of the hazard and vulnerability modules. These modules are linked through a common intensity metric and are connected to the exposure data through a set of abstract identifiers: areaperil_id and vulnerability_id. **Figure 46** shows how the hazard and vulnerability modules are connected in an Oasis model (OASIS 2024b).

Figure 46. Connection of the hazard and vulnerability modules

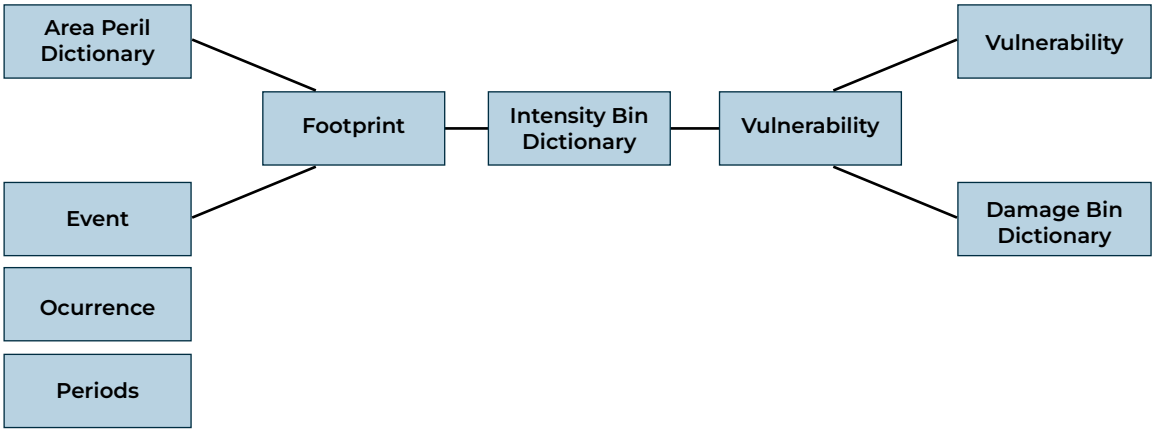

Source: OASIS (2024a).

The Oasis **Hazard Module** is based on the Footprint file, which describes the interaction between events and hazard areas, providing a probability distribution of intensity for each combination.

The **hazard area** abstractly represents a specific zone for a given hazard. It may be any type of area (grid cells, polygons, administrative regions, etc.). The areaperil_id is the identifier of the area and must be an integer value, although what it represents does not affect the calculation in Oasis.

The **event** is an abstract representation of a real or synthetic event that affects multiple hazard areas. It could be a flood, storm, earthquake, etc. The event_id is the event identifier and is an integer value.

The **Intensity** represents a discretized and abstract set of intensity measures specific to the hazard represented.

The **Vulnerability** Module in Oasis focuses on the "Vulnerability" file, which describes the interaction of intensities with vulnerability types, providing a probability distribution of the Damage Ratio for each combination.

The **Vulnerability Dictionary** abstractly represents various vulnerability functions. The vulnerability_id is the identifier and is simply an integer value representing that vulnerability function.

Damage represents a discretized and abstract set of damage ratios.

The final part of the model data definition in Oasis is the Occurrence file. This file details the occurrences of events over time and is used in time-based results. An optional extension of the Occurrence file is the Periods file, which allows a weight to be assigned to the occurrences.

The hazard module, the vulnerability module, and the occurrence definitions are combined using a common definition of intensity intervals to create a complete representation of an Oasis model.

The Oasis UI allows the user to generate multiple output reports. The Oasis core uses a Monte Carlo simulation that draws random samples from the loss distribution. The number of samples is defined by the user, and the level of convergence achieved within that sample set will vary depending on the model, the portfolio, and the results required.

The loss calculation consists of two steps: 1) calculation of probability distributions and 2) sampling method.

The term effective damageability refers to the method used to construct probability distributions.

The model input files for this stage of the calculation are:

- *footprint*
- *vulnerability*

The uncertainty of hazard intensity is represented in the footprint data, and the uncertainty of damage given the hazard intensity is represented in the vulnerability data. Both types of uncertainty are expressed as discrete probability distributions.

The effective damage is calculated during an analysis by convolving the hazard intensity distribution with the conditional damage distribution.

In the general case, the calculated effective damage distribution represents both the uncertainty in hazard intensity and the level of damage given that intensity.

However, it is common in some models for the hazard uncertainty distribution not to be present in the footprint. In these cases, each areaperil (which represents a geographic area or cell) in the footprint is assigned to a single hazard intensity band with a probability set to 1. In this case, the effective damage distribution is still generated, but it is identical to the conditional damage probability distribution in the vulnerability file for a single intensity range.

With the effective damageability method, a sample is always taken from the effective damage distribution; however, the represented sources of uncertainty may be only from damage or a combination of uncertainty in hazard intensity and damage, depending on the model files.

Monte Carlo methods are a broad class of computational algorithms that rely on repeated random sampling to obtain numerical results. The Oasis kernel (ktools) performs Monte Carlo sampling of gross losses from effective damage probability distributions by generating random numbers.

The probability distribution is provided by the effective damageability calculation described above, and the damage intervals are supplied by the damage bin dictionary, which is a third model input file.

A.5.3. Mathematical approach

In the OASIS LMF risk calculation process, the first step is to generate an event set that is representative of all possible events that may occur, together with their intensity and probability over a period of time long enough to capture a complete distribution, including the most extreme events. A 10,000-year simulation is usually used. Each event has a probability of occurring within the simulated period (Oasis LMF 2024).

For each event, a hazard footprint is generated, which contains an appropriate hazard indicator (intensity, for example wind speed, flood depth, etc.) that is related to damage through a vulnerability curve (Oasis LMF 2024).

Vulnerability curves link the hazard indicator to an average damage ratio (MDR), which is the proportion of the total value (for example, in terms of replacement cost) that would be lost for the asset being analyzed. In practice, exposed elements exhibit high variability in the damage caused by the same hazard due to many unknown factors that cannot be modeled, even when they are located very close to one another. This is accounted for through an uncertainty distribution around the average damage ratio at each hazard point, also known as secondary uncertainty (Oasis LMF 2024).

The loss calculation is the most important part of the OASIS LMF ktools core. For this calculation, the probabilities defined in the hazard footprint and vulnerability files are used together. These probabilities are represented by subscripts i and d to indicate that the uncertainty lies in intensity and damage, respectively (Blass 2021):

Equation 14

$$P_{id} = p^{f}_{i} * p^{v}_{d}$$

Where:

P_{id} is the probability that an intensity i will occur and cause damage d.
p^{f}_{i} is the probability mass for the intensity interval.
p^{v}_{d} is the probability mass for the damage interval.

This calculation of P_{id} is performed for each combination of event, hazard area (peril), and vulnerability function. Then, P_{id} is summed across intensity intervals:

Equation 15

$$P_d = \sum_i P_{id}$$

This results in $\boldsymbol{P_d}$, which is the probability of a damage interval d for each event, hazard area, and vulnerability function.

Since the probability distribution is discrete, the values can be summed to construct a cumulative distribution function (CDF), which is done in the *getmodel* executable file. This summation over the intensity and damage intervals produces a CDF for each combination of event, hazard area, and vulnerability.

There are two possible approaches for calculating losses (Blass 2021):

1. Deterministic Integration

In this method, the calculated damage probability distribution is integrated to obtain what is known as the damage factor. This factor, multiplied by the total insured value, results in the loss:

Equation 16

$$\chi_{E\Upsilon} = tiv_{\Upsilon} * d_{E\Upsilon}$$

Where:
$\boldsymbol{\chi_{E\Upsilon}}$ is the loss for event $\boldsymbol{\varepsilon}$ and coverage $\boldsymbol{\Upsilon}$.
$\boldsymbol{tiv_{\Upsilon}}$ is the total insured value.
$\boldsymbol{d_{E\Upsilon}}$ is the damage factor.

This method does not provide a standard deviation, since integration does not allow uncertainty calculations.

2. Random Sampling (Monte Carlo)

In this method, the same process is followed up to the calculation of the CDF. Then, instead of integrating, a random number generator is used to select a value between 0 and 1. As illustrated in **Figure 47**, if the generated random number is 0.82, it falls within a specific damage interval (for example, interval 2). Subsequently, within that interval, a specific proportion is calculated (for example, 31%), which results in a damage factor (0.584615 in the example). Through this process, a

damage value is selected from a range of possible values in the sample. Finally, as in the previous equation, by multiplying this factor by the total insured value, the loss corresponding to this sample is obtained.

Figure 47. Graphical Illustration of the Sampling Approach in Loss Calculation

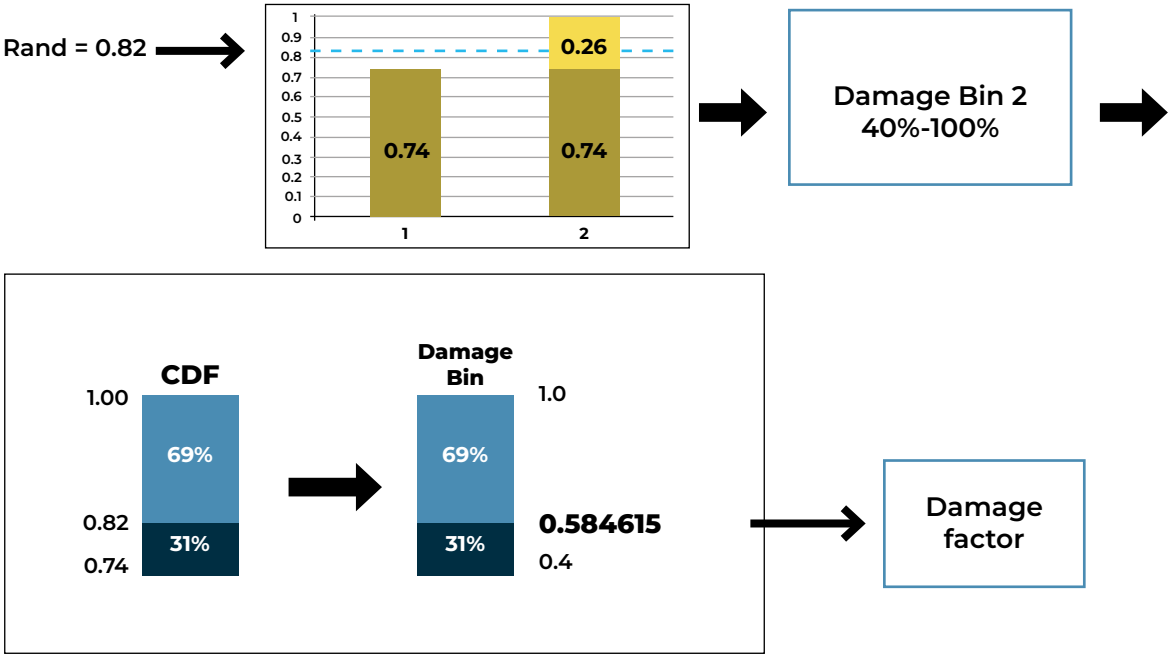

Source: Blass (2021) A random number is selected, which is used to sample the cumulative distribution function (CDF). This makes it possible to determine the corresponding damage interval. Then, the sample damage factor is obtained by applying the same proportion within that damage interval.

The financial module calculates losses after accounting for the impact of insurance policy conditions in order to provide the net loss for which the (re)insurance entity will be responsible. The (re)insurance company provides a list of all the policies it has underwritten, including information on the location and characteristics of the risk, such as occupancy type, age, construction material, building height, and replacement cost, as well as the policy terms and conditions. The catastrophe model then runs the entire event set through the portfolio and calculates the loss for each event in the model for each policy. This generates an event loss table. These event losses are then ordered by magnitude from largest to smallest to generate the Loss Exceedance Curve for the years simulated by the model (Oasis LMF 2024).

A.5.4. Recent advances and innovations

In recent years, Oasis has worked on the standardization of open data to improve interoperability and efficiency in the insurance industry. They have also launched Oasis Risk Explorer, a risk modeling tool for parametric insurance products that is specifically designed for low-income, vulnerable countries. Additionally, the Enterprise Oasis software is in its final stages of testing. This tool will enable the distribution of work across multiple cloud machines, significantly reducing the runtimes of complex models..

A.5.5. Development community

Oasis is supported by a diverse community that includes independent model developers, insurers, reinsurers, brokers, and governments. The platform is funded through member subscription fees and commissions on licensed models. They also collaborate with various organizations such as the Insurance Development Forum (IDF) and UNISDR on interoperability initiatives and global exposure projects. (OASIS 2024b). The GitHub repository is: https://github.com/OasisLMF.

A.5.6. Limitations

Although Oasis provides significant flexibility and access to catastrophe models, it has associated costs that arise from the use of models provided by different companies.

A.5.7. Use cases

Oasis is widely used in the insurance and reinsurance industry to assess catastrophe risk and develop parametric insurance products. A notable case is the use of climate-conditioned models, such as the Danube model developed by the Potsdam Institute, along with similar models created by JBA and Fathom. These models help insurers better understand the impact of climate change on catastrophic risk. **Box 6** shows a case study in which both CLIMADA and Oasis were used.

Box 6. Example of an Oasis application

Case Study: Hurricane Matthew

This case study examines the impacts of the different parameters used in loss models applied to Hurricane Matthew, using forecast data from ECMWF and the open-source tools CLIMADA and Oasis LMF. The analysis evaluates the influence of variables such as the radius of maximum winds (RMW), asset values, and the vulnerability curve on the loss estimates.

The evaluation used forecasts of Hurricane Matthew for three different dates (29 September, 4 October, and 7 October 2016), analyzing the track and intensity in relation to the estimated damage. Tests were carried out by varying the RMW, redistributing asset values, and altering the shape of the vulnerability curve. The implementation of a beta distribution for modeling secondary uncertainties was also considered.

The modification of the RMW produced results similar to those of the original function, but with a slight increase in the values. For the 4 October forecast, the impact of increasing the radius to 370 km was smaller than that observed in earlier forecasts. For the 7 October forecast, the influence of a fixed RMW of 3 km was substantially greater, with losses reduced by three orders of magnitude, while an RMW of 370 km increased losses by two orders of magnitude. The analysis showed that the proximity of the tracks to the U.S. coast where assets are concentrated amplifies the losses.

The results confirm that the RMW is directly related to the intensity of tropical cyclones. Previous studies (Emanuel 1989; Carrasco et al. 2014) corroborate the negative correlation between the size of the eye of the cyclone and its intensification. For example, compact cyclones, such as Hurricane Matthew in its early stages, exhibit greater intensification due to the reduced RMW.

The asset values in CLIMADA are based on nighttime lights satellite imagery adjusted by GDP and redistributed according to population density (see the following figure). When tested with redistributed average values, the losses decreased slightly because of the reduction in values in high-density regions and the increase in less-dense areas. This effect was particularly evident when implementing an RMW of 3 km, further decreasing the losses because of the lower probability of impacting densely populated areas.

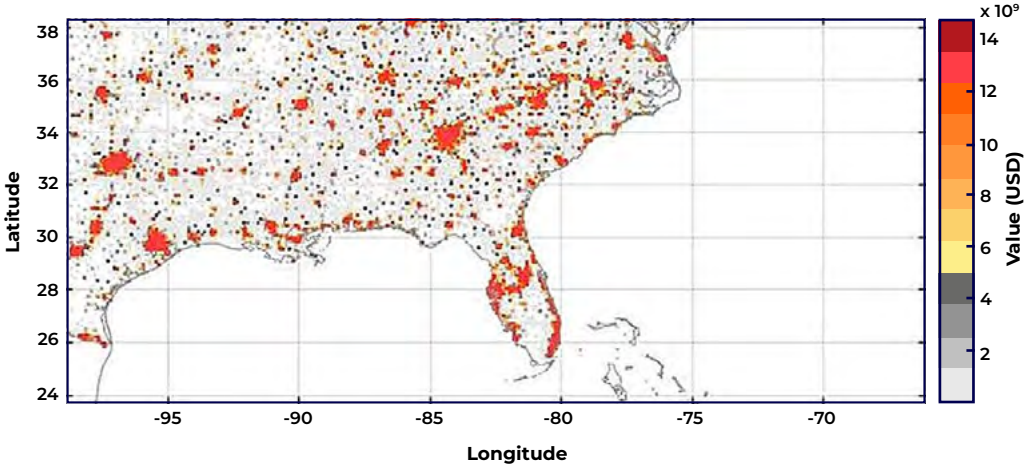

The standard CLIMADA curve is a logistic function with a maximum of 40%. Tests with linear and step functions showed results with high variability. The linear function increased losses because it included damage at lower wind speeds, whereas the step function reduced losses by restricting damage to wind speeds above 80 m/s. For the 29 September and 4 October forecasts, the step function did not result in any losses because of the hurricane's low intensity.

Among the parameters tested, the RMW showed the greatest impact on the losses. The tracks have a significant influence on the results, especially in forecasts such as the one from 29 September, where most of the cyclones affect the Caribbean, resulting in lower losses. Increasing the RMW raises the probability of impacting higher-value areas, amplifying the losses. On the other hand, redistributing the assets reduces the total losses by spreading values more evenly.

This study confirms that the RMW is the most critical variable in forecasting losses, directly correlated with the intensity of the cyclone. The integration of the CLIMADA and Oasis LMF models proved effective, with a strong correlation between the results. Improvements in the forecasts of cyclone intensity and size could refine the loss estimates, especially with greater inclusion of environmental factors that influence the RMW, such as inertial stability and surface entropy fluxes. In addition, incorporating factors such as the size of the outer core of cyclones would broaden the understanding of the associated impacts, providing more comprehensive and useful forecasts for risk mitigation and planning.

Source: König (2017).

A.6. INTERDEPENDENT NETWORKED COMMUNITY RESILIENCE MODELING ENVIRONMENT IN-CORE

A.6.1. General description

The Interdependent Networked Community Resilience Modeling Environment (IN-CORE) is software developed by Colorado State University to assess and improve the resilience of infrastructure and communities to disasters. Any hazard can be analyzed as long as it can be represented as a hazard object and fragility curves can be associated with the exposed elements. The Hazard viewer web tool allows users to view examples of hazard objects for earthquakes, tornadoes, hurricanes, and floods. IN-CORE integrates simulation models and data analysis to provide a comprehensive understanding of how different types of infrastructure respond to hazards. The IN-CORE platform is built on a Kubernetes cluster using Docker container technology (IN-CORE 2024).

In the IN-CORE platform, users can perform analyses that model the impact of disasters and evaluate the resilience and recovery of communities. The platform is comprised of IN-CORE Lab, pyIncore, web tools and web services (see **Figure 48**). The resources provided by the research community, such as exposure datasets, fragility curves, hazard files, among others, are stored on the IN-CORE servers at the National Center for Supercomputing Applications (NCSA) and can be seamlessly integrated to allow users to optimize disaster-resilience planning in communities and recovery strategies following a disaster (IN-CORE 2024).

The user must have an IN-CORE account recognized by the IN-CORE service. This account allows the user to access all public data in the system and to create data that will be accessible only to them.

Figure 48. Components of IN-CORE

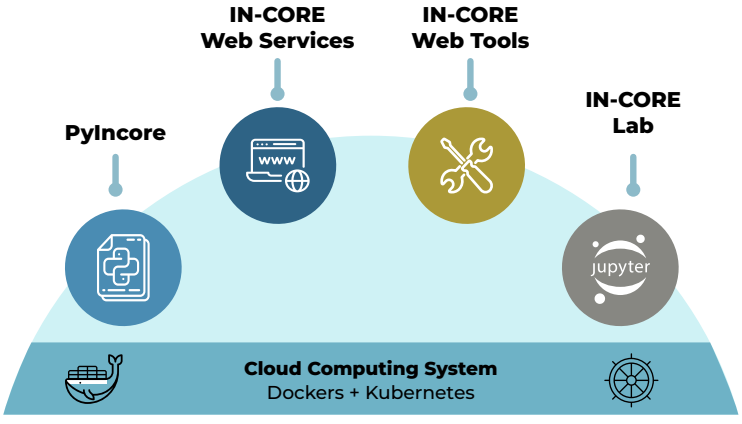

Source: IN-CORE (2024).

PyIncore is a Python package that consists of three main components: 1) a set of service classes for interacting with the IN-CORE web services described below, 2) IN-CORE analyses, and 3) visualization. PyIncore allows users to analyze infrastructure risk in selected areas, propagating the effect of physical infrastructure damage and loss of functionality to social and economic impacts.

The **IN-CORE web services** are written in Java using the JAX-RS specification and consist of a hazard service, a DFR3 service (damage, functionality, repair, recovery, and restoration), a data service, a geospatial visualization service, a semantic service, and a spatial service. These services allow users to create and access hazards, fragility functions, and data. Users can access and use these services through pyIncore and the IN-CORE web tools.

IN-CORE Web Tools is a set of web-based viewers for interacting with the different IN-CORE web services. The viewers allow users to browse and search datasets, hazards, fragility curves, repair curves, etc., as well as view the metadata and visualizations and download permitted items.

IN-CORE Lab is a custom Jupyter lab with pyIncore installed and hosted on an NCSA cloud system. It allows users to develop, run, and test their scientific model with pyIncore in their own workspace.

The IN-CORE platform can incorporate community-generated data, allowing users to intelligently optimize community disaster-resilience planning and post-disaster recovery strategies using interdependent physical systems models integrated with socioeconomic systems.

The resources provided by the research community, such as inventory datasets, fragility functions, hazard files, etc., are stored on the IN-CORE servers at NCSA and can be seamlessly integrated to allow users to optimize community disaster-resilience planning and post-disaster recovery strategies.

To use IN-CORE and pyIncore, Miniconda must be installed, followed by the installation of Jupyter Notebook and the pyIncore library.

The visualization package associated with pyIncore is called pyIncore-viz. It contains advanced Python packages and the methods required to visualize and disseminate IN-CORE results, primarily through Jupyter Notebooks. The Matplotlib library, used to create static visualizations in Python, is already part of pyIncore as a dependency.

A.6.2. Applied methods

IN-CORE uses the following steps in resilience analyses: (1) characterizing the current state of a community, including its vulnerabilities; (2) simulating hazard scenarios and the resulting impacts on community systems (damage, population displacement, loss of functions, and recovery of functions) to explore policy options that enhance resilience; and (3) calculating Community Stability Assessment

(CSA) based on Community Resilience Metrics (CRM) for the physical, social, and economic functions of a community, which provide resilience indicators at a given time relative to resilience objectives (van de Lindt et al. 2023).

The scientific algorithms implemented in IN-CORE are shown in the conceptual flow diagram **Figure 49**, much of which was completed during the first five years of development (van de Lindt et al. 2023).

Image: Flickr - BID Ciudades sostenibles / Santa Marta, Colombia

Figure 49. Conceptual flow diagram of the IN-CORE algorithms

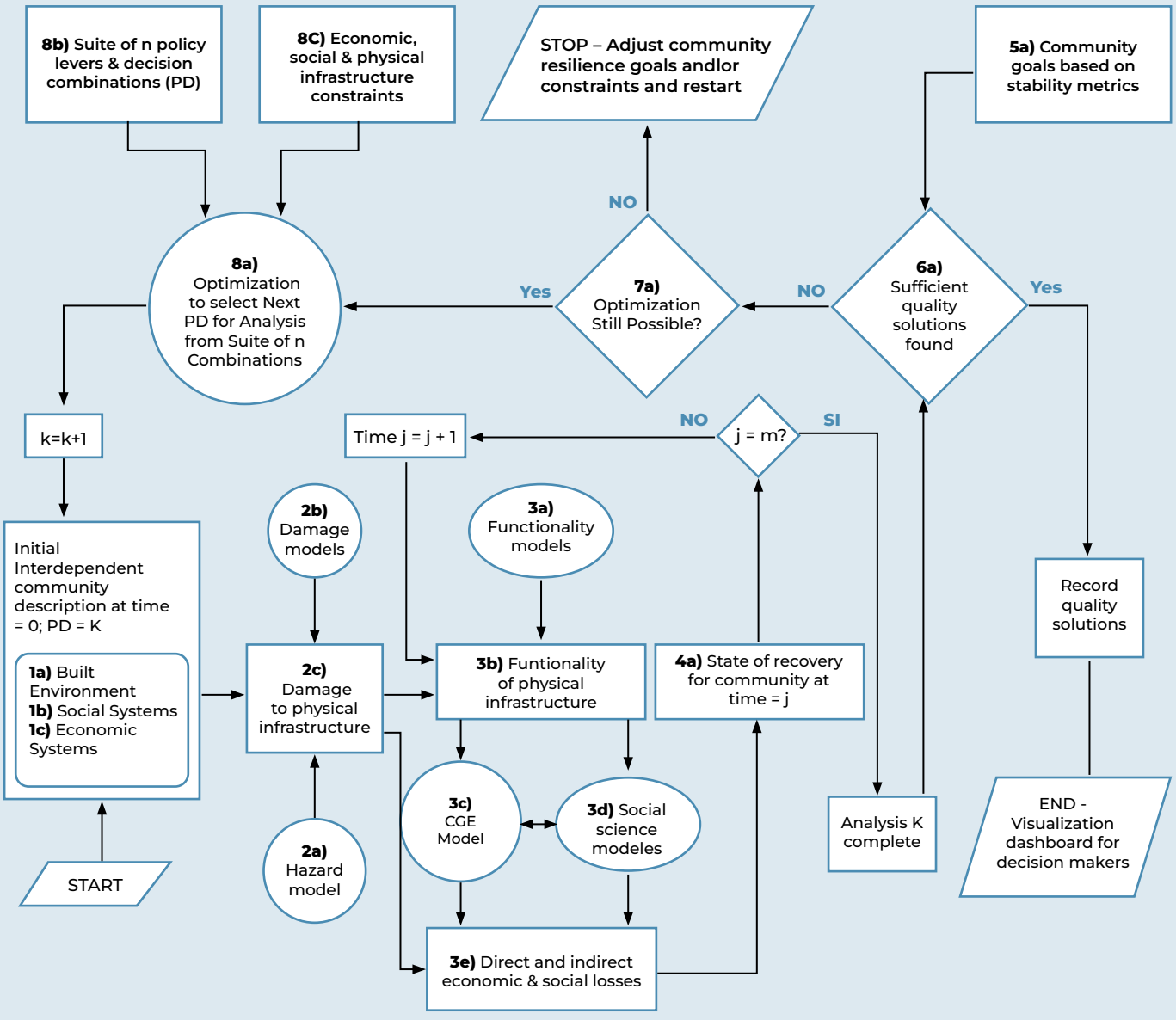

Source: van de Lindt et al. (2023).

The IN-CORE system is organized into several interdependent modules that enable the description, analysis, and planning of community resilience, integrating information from infrastructure and social and economic systems. The Interdependent Community Description module, located in the lower-left of **Figure 49**, It is composed of three key components: the built environment, social systems, and economic systems. The built environment component brings together spatial data, generally in geographic information system (GIS) format, including building footprints, infrastructure such as electricity, water, and gas networks, as well as the transportation network. This module describes how these infrastructures interrelate with buildings, facilitating the connection between the different systems of the community. The social systems, in turn, include data on population and households, which are assigned to specific buildings, providing detailed information on demographic characteristics such as age, sex, education, and occupation, and linking people to social institutions and workplaces. These data come from various public sources, such as the United States Census and the American Community Survey. The Economic Systems component describes the spatial distribution of jobs and industries and uses computable general equilibrium (CGE) models to simulate how households, businesses, and local government interact to generate economic activity. This model incorporates data on income, labor distribution, and workforce indicators indicators, providing a comprehensive picture of the local economy.

Regarding damage to physical infrastructure, the Physical Infrastructure Damage module combines built environment data with hazard models and damage models to assess how disasters affect infrastructure. There are two types of hazard models: Tier 1, which simulate hazards such as earthquakes, hurricanes, floods, and tornadoes using datasets contained in IN-CORE, and Tier 2, which allow more advanced simulations in which the hazards are supplied by the user. These models use fragility functions to estimate the expected damage as a function of hazard intensity. The process can also take into account the damage caused by cascading phenomena, such as the interaction between wind and storm surge in hurricanes or earthquake and tsunami damage.

The Physical Infrastructure Functionality module evaluates the ability of buildings and other infrastructure components to continue to function after a disaster, based on the level of damage sustained. This assessment is carried out using functionality models that determine whether a building or infrastructure can continue to perform its intended function. These models can be defined by the user and take into account the availability of essential services such as water and electricity. The results of this analysis are used in the CGE model to estimate the economic impacts of the damage, taking into account the condition of buildings and functional infrastructure, as well as social and economic data.

The Community Recovery module analyzes how the community recovers over time, evaluating both the physical recovery of buildings and the restoration of social and economic stability. A model-based approach is used for the recovery of housing and other infrastructure, taking into account financing policies and recovery statistics. This analysis makes it possible to track the evolution of recovery in different areas of the community and adjust intervention strategies based on progress.

Finally, the Solutions and Optimization module allows the effectiveness of different resilience policies to be evaluated. This module compares various disaster-mitigation and response strategies, taking into account the financial and social constraints of the community. Through this analysis, IN-CORE helps decision-makers identify the best options for improving community resilience, whether by mitigating risks or enhancing response capacity in the event of a disaster. The system outputs provide valuable information for optimizing the use of available resources and developing effective resilience strategies. In addition, IN-CORE has the capability to propagate uncertainty in predictions of household characteristics at the building level, as well as in predictions of population stability. Uncertainty is propagated through Monte Carlo simulation (MCS), which allows the analyst to obtain realizations of the hazard, the assignment of synthetic population to a household, or any other analysis, provided that the underlying statistics are known (van de Lindt et al. 2023).

The analyses incorporated into the platform are summarized in **Table 38**.

Table 38. Analyses incorporated into the IN-CORE platform

Type of Analysis	Description
Bridge damage	This analysis calculates bridge damage based on a specific type of hazard. Currently, earthquakes, tsunamis, tornadoes, and hurricanes are supported. The process for calculating structural damage is similar to that used for other infrastructure. First, a fragility curve is obtained based on the type of hazard and the characteristics of the bridge. The hazard intensity at the bridge location is calculated using the selected fragility curve. Using this information, the probability of exceeding each limit state and the probability of damage are determined. In the case of earthquakes, if the bridge dataset includes soil information, the median value of the fragility curve can be adjusted to account for liquefaction effects on damage. The results of this analysis are a CSV file containing the damage probabilities and a JSON file with information on the hazard and the associated fragility curves.
Recovery of sets of buildings	The code generates two output files: building-recovery.csv y cluster-recovery.csv.
Building damage	This analysis calculates building damage based on a specific type of hazard. Currently, earthquakes, tsunamis, tornadoes, hurricanes, and floods are supported. The process for calculating structural damage is similar to that used for other infrastructure. First, a fragility curve is obtained based on the type of hazard and the characteristics of the building. This fragility curve is used to calculate the hazard intensity at the building location. Using this information, it is possible to determine the probability of exceeding each limit state and the probability of damage. In the case of an earthquake, soil information can be used to adjust the damage probabilities and account for the effects of liquefaction. The results of this analysis are a CSV file containing the damage probabilities and a JSON file with information on the hazard and the associated fragility curves.
Economic Loss in Buildings	This analysis calculates economic loss in buildings based on the building's appraised value, the mean damage, and an inflation multiplier. The user must provide the inflation rate (as a percentage) between the appraisal year and the year of interest (current year, event date, etc.), as well as an optional occupancy multiplier. The analysis can be applied to mean building damage results for structural components, displacement-sensitive nonstructural components, acceleration-sensitive nonstructural components, or contents damage. The result of this analysis is a CSV file containing the structural losses based on the damage.
Building Functionality	The building functionality analysis calculates the probabilities of functionality under two situations: when buildings are in at least damage state 2 or higher, or when buildings are undamaged but lack access to electrical power. It is assumed that the availability of electrical power depends on the interdependence between buildings and substations, and between buildings and nearby poles. If both the utility pole closest to the building and the substation on which it depends are functional, the building is considered to have access to electrical power. The results of this analysis are: 1) a CSV file containing samples of functionality probabilities for direct comparison with Monte Carlo limit-state probability outputs and 2) a CSV file containing functionality probabilities.

Type of Analysis	Description
Nonstructural Damage in Buildings	This analysis calculates nonstructural damage in buildings based on a specific type of hazard. Currently, earthquakes, floods, and hurricanes are supported. The process is similar to the evaluation of other structural damage. The damage probabilities are obtained using fragility curves and a hazard definition. Each building site will have a PGA (peak ground acceleration), a measure of earthquake hazard for each scenario. It is also possible to account for the effect of liquefaction, defined as a change in stress conditions in which a material that is normally solid behaves like a liquid. Liquefaction Modification Factor (LMF) values are implemented as multiplication factors for the median values of the fragility function and must be present in the dataset. This analysis can include several types of fragility curves assigned to the building: acceleration-sensitive (AS) and displacement-sensitive (DS). The code covers normal and lognormal fragility functions with 3 limit states and generates an output CSV file with the corresponding damage states. The second output file is a JSON containing information about the hazard and the fragility functions.
Structural Damage in Buildings	This analysis calculates structural damage in buildings based on a specific type of hazard. Currently, earthquakes, tsunamis, tornadoes, hurricanes, and floods are supported. The process for calculating structural damage is similar to that used for other infrastructure. First, a fragility curve is obtained according to the hazard type and the characteristics of the building. From this fragility curve, the hazard intensity at the building location is calculated. Using this information, the probability of exceeding each limit state and the probability of damage are determined. In the case of an earthquake, soil information can be used to adjust the damage probabilities and account for liquefaction effects. The results of this analysis are a CSV file with the damage probabilities and a JSON file containing information on the hazard and the fragility curves.
Property Purchase Decision	This analysis helps identify candidate properties for purchase and allows practitioners and researchers to evaluate the potential equity outcomes of their selection under different scenarios. The result of this analysis is a CSV file containing the buildings that should be considered for purchase according to the established criteria. This can help local practitioners identify candidate properties for purchase selection and allows practitioners and researchers to evaluate the potential equity outcomes of their selection.
Capital Shocks	This analysis aggregates the building functionality states and calculates the total capital losses by sector. The capital stock shock for an individual building is equal to the functionality probability multiplied by the building value. This produces the capital stock loss in the immediate aftermath of a disaster. The analysis groups each of these individual losses according to their associated economic sector and calculates the total capital stock loss for that particular sector. The result of this analysis is a CSV file containing the building losses aggregated by sector and the calculated total capital stock loss.
Combined Building Damage from Wind, Waves, and Storm Surge	This analysis determines the maximum overall damage state of buildings caused by wind, flood, and wave damage. The results of this analysis are a CSV file with the maximum damage state for each hazard and the overall maximum damage, as well as a CSV file with the combined damage probabilities for the three hazards.

Type of Analysis	Description
Combined Building Loss from Wind, Waves, and Storm Surge	This analysis determines the total building loss caused by wind, flood, and wave damage. The result of this analysis is a CSV file with the individual components of struc-tural and contents loss, as well as the total loss.
Commercial Building Recovery	This analysis calculates the recovery time required for each commercial building from any damage state to full restoration. Currently, tornadoes are supported as a hazard. The methodology incorporates a multilayer Monte Carlo simulation approach and determines the recovery time in two stages, consisting of delay and repair. The delay model was modified according to the REDi framework and calculates the final outcomes derived from factors that impede recovery, such as post-disaster inspection, insurance claims, financing, and governmental permitting. The repair model follows the FEMA P-58 approach and is governed by fragility functions. The result of this analysis is a CSV file with stage-level recovery probabilities for each building.
Cumulative Building Damage	This analysis calculates building damage based on a specific type of hazard. The process for calculating structural damage is performed externally, and the results for earthquakes and tsunamis are imported into the analysis. Then, the damage intervals are calculated from the combined limit states. The result of this analysis is a CSV file with the damage probabilities.
Damage to Electrical Power Facilities	This analysis calculates damage to electrical power facilities based on a specific type of hazard. Currently, the supported hazards are: earthquake, tsunami, tornado, and hurricane. The process for calculating structural damage is similar to that for other infrastructure. First, a fragility function is obtained according to the hazard type and the characteristics of the electrical power facility. The hazard intensity at the facility location is calculated based on this fragility function. Using this information, the probability of exceeding each limit state and the probability of damage are determined. In the case of an earthquake, soil information can be used to modify the damage probabilities and incorporate liquefaction effects. The results of this analysis are a CSV file containing the damage probabilities and a JSON file with information on the hazard and the associated fragility curves.
Repair Cost of Electrical Power Facilities	This analysis estimates the repair costs of electrical power facilities for different simulation scenarios, based on their damage states, replacement costs, and damage ratios.
Restoration of Electrical Power Facilities	This analysis calculates the repair time and the percentage change in the functionality of an electrical power facility over time, based on input restoration curves. The restoration curves are obtained according to the hazard type and the class of the electrical facility, for example, low-voltage substations, large power plants, etc. Based on the applicable restoration curve, the percentage change in functionality can be obtained as a function of time, and the repair time at different levels of percentage change in functionality can also be calculated by inverting the restoration function.

Type of Analysis	Description
Analysis of Electrical Power Network (EPN) Functionality	This analysis calculates the functionality of electrical power networks. The calculation uses input from a Monte Carlo failure analysis, using information on damage to electrical power facilities as well as the topology of the electrical line network, to determine the functionality probability and the failure states of the corresponding electrical facility network through an accessibility analysis. The result of the analysis consists of a CSV file with the functionality probabilities for the electrical facilities and a CSV file with the functionality failure states.
Equity Metric	The algorithm calculates equity metrics to characterize inequality in the provision of infrastructure services between two groups of interest (for example, low-income versus non–low-income, minorities versus non-minorities, etc.). The metrics are based on the Theil T index, a common indicator for measuring inequality in the distribution of a scarce resource (for example, income). The metrics can also be applied to evaluate inequity in different scenarios involving other resources of interest. To calculate the metrics, a scarce resource is defined and computed within an infrastructure application. This resource can be any relevant value defined by the user, such as a resilience score (that is, the probability of service provision) or the recovery time. We have included a helper class where the recovery time is defined and prepared as the scarce resource. Other resources can also be explored if they are provided by the user. The equity metric makes it possible to evaluate equity in the current provision of infrastructure services, as well as to assess the equity benefits of a specific renewal plan, and it can be integrated into a broader decision-making process. The output metrics provide the following information: 1) Theil T Index - the total quantification of inequality in the distribution of the scarce resource within a community (distributive inequality); 2) Between-Zone Inequality (BZI) - the amount of inequality attributable to differences in resources between groups (restorative inequity); and 3) Within-Zone Inequality (WZI) - the amount of inequality due to differences in resources within individual groups.
Galveston Computable General Equilibrium (CGE) Model	A computable general equilibrium (CGE) model is based on fundamental economic principles. This model uses multiple data sources to reflect the interactions among households, businesses, and the relevant governmental entities that contribute to economic activity. The model is structured as follows: (1) households that maximize utility, supplying labor and capital and using their income to pay for goods and services (both locally produced and imported) and for taxes; (2) the production sector, with perfectly competitive firms that maximize profits using intermediate inputs, capital, land, and labor to produce goods and services for domestic consumption and export; (3) the governmental sector, which collects taxes and uses this revenue to fund public services; and (4) the rest of the world. The result of this analysis consists of CSV files containing information on domestic supply, gross income, factor demand before and after a disaster, and household counts.
Damage to Gas Facilities	This analysis calculates damage to gas facilities based on a specific hazard. Currently, the supported hazard is earthquakes. The process for calculating structural damage is similar to that for other components of the built environment. First, a fragility function is obtained based on the hazard type and the attributes of the gas facility. Then, the hazard intensity at the facility location is calculated. With this information, the probability of exceeding each limit state is determined, along with the damage probability. In the case of an earthquake, soil information can be used to modify the damage probabilities and incorporate damage due to liquefaction. The results of this analysis include a CSV file with the damage probabilities and a JSON file containing information on the hazard and the fragility functions.

Type of Analysis	Description
Sequential Housing Recovery at the Household Level	This analysis calculates the sequence of housing recovery states for each household using a population displacement dataset, a transition probability matrix (TPM), and an initial state vector. The computation classifies households into five zones to assign them a social vulnerability. Using this vulnerability together with the TPM and the initial state vector, a Markov chain computation simulates the most likely states, generating a history of changes in housing recovery for each household. The result of the computation is a history of changes in housing recovery for each household in CSV format.
Housing Recovery	The analysis predicts building values and changes in value over time following a disaster event. The model is calibrated using demographic data, parcel data, and building value trajectories after Hurricane Ike (2008) in Galveston, Texas. The model predicts building values at the parcel level over an 8-year observation period. The models rely on census data (Decennial Census or American Community Survey, ACS) and pre-disaster parcel data (year -1) as inputs for the prediction. The Galveston, TX example uses 2010 Decennial Census data, Galveston County Appraisal District (GCAD) data, and results from other analyses (that is, Building Damage, Housing Unit Allocation, Population Displacement). The CSV results contain the building values for the 6 years after the disaster event (with year 0 being the year of impact).
Housing Unit Allocation	This analysis compiles a detailed inventory of critical infrastructure with characteristics at the housing-unit level. The process aligns the housing-unit inventory with physical systems, such as the building inventory and the demand nodes of a potable-water network. The assignment of housing units to address points (buildings) provides a framework for accounting for uncertainty in community structure, which enables statistical analysis of hazard impacts. The result of this analysis is a CSV file containing detailed characteristics of households and housing units (number of people, race, tenure type, vacancy) assigned to individual dwelling units linked to specific buildings.
Interdependent Network Design Problem (INDP)	This analysis uses a decentralized approach to solve the Interdependent Network Design Problem (INDP), a family of centralized Mixed-Integer Programming (MIP) models that seek the optimal strategy for restoring disrupted interdependent network systems while satisfying budgetary and operational constraints.
Computable General Equilibrium (CGE) model for Joplin	A Computable General Equilibrium (CGE) model is based on fundamental economic principles and uses multiple data sources to reflect interactions among households, firms, and relevant government entities as they contribute to economic activity. The model considers: (1) households that maximize utility, supplying labor and capital to pay for goods and services (produced locally or imported) as well as taxes; (2) the productive sector, with competitive, profit-maximizing firms that use intermediate inputs, capital, land, and labor to produce goods and services for domestic consumption and export; (3) the government sector, which collects taxes and finances public services; and (4) the rest of the world. The result of this analysis is a set of CSV files containing domestic supply, gross income, factor demand before and after the disaster, and household counts.

Type of Analysis	Description
Empirical Building Restoration Model for Joplin	This model generates a random realisation of the restoration time for a building damaged by a tornado, estimating the time required to reach a specific level of functionality. The functionality levels in this model are defined according to Koliou and van de Lindt (2020) and range from Functionality Level 4 (FL4, the lowest functionality level) to Functionality Level 0 (FL0, full functionality). The distributions used in this code were generated from an empirical dataset collected in a longitudinal field study conducted after the 2011 tornado in Joplin, MO. These distributions represent the time required for a building to recover from an initial functionality level to a higher level (for example, from FL3 to FL0). The model applies exclusively to archetypes T1 through T5, which include only residential buildings according to Memari et al. (2018). The output of the model is a set of CSV values indicating the building's expected restoration time.
Machine-Learning-Enabled Computable General Equilibrium (CGE) Model – Joplin	The "Machine-Learning-Enabled Computable General Equilibrium (CGE) Model for Joplin" analysis combines advanced machine learning with traditional CGE models to provide unique insights into the economic impacts of disaster scenarios in Joplin. Trained on a comprehensive dataset of numerous simulated disasters and their economic effects, this hybrid approach excels at predicting the city's complex economic dynamics during various crises. A Computable General Equilibrium (CGE) model is based on fundamental economic principles and uses multiple data sources to reflect interactions among households, firms, and relevant government entities that contribute to economic activity. This model is structured around: (1) households that maximize their utility, supplying labor and capital and allocating their income to pay for goods and services (both local and imported) as well as taxes; (2) the productive sector, with competitive, profit-maximizing firms that use intermediate inputs, capital, land, and labor to produce goods and services for domestic consumption and export; (3) the government sector, which collects taxes and funds public services; and (4) the rest of the world. The results of this analysis are CSV files that include domestic supply, gross income, factor demand before and after the disaster, and household counts.
Machine Learning Enabled Computable General Equilibrium (CGE) Model for Salt Lake City	The "Machine Learning Enabled Computable General Equilibrium (CGE) Model for Salt Lake City" analysis combines advanced machine learning with traditional Computable General Equilibrium (CGE) models to provide unprecedented insights into the economic impacts of disaster scenarios in Salt Lake City. Trained on an extensive dataset of simulated disasters and their economic effects, this hybrid approach excels at predicting the city's complex economic dynamics during various crises. A computable general equilibrium (CGE) model is based on fundamental economic principles. It uses multiple data sources to reflect interactions among households, firms, and relevant government entities that contribute to economic activity. The model is based on the following components: • Households that maximize their utility and supply labor and capital, using their income to pay for goods and services (both local and imported) as well as taxes. • The production sector, with perfectly competitive, profit-maximizing firms that use intermediate inputs, capital, land, and labor to produce goods and services for both domestic consumption and export. • The government sector, which collects taxes and uses that revenue to fund the provision of public services. • The rest of the world, which interacts with the local economy. • The result of this analysis is a set of CSV files that include domestic supply, gross income, factor demand before and after the disaster, as well as household counts.

Type of Analysis	Description
Mean Damage	The process for calculating structural damage uses mean damage values and standard deviations derived from damage-ratio tables. The four probabilities of the damage states are multiplied by the mean damage and summed to obtain the mean damage for each individual structure (building, bridge, water facility, etc.). The result of this analysis is a CSV file with the damage probabilities.
Monte Carlo limit-state probability	This analysis calculates a limit-state probability using a stochastic process. The limit-state probability and damage state are derived using the damage-state dictionary in the input infrastructure dataset. The limit-state probability is calculated from all stochastic runs, and the limit state shows all infrastructure positions as a sequence of failed (0) and non-failed (1) states from each individual run. The result of this analysis is two CSV files: one containing the limit-state probability, named base_name_failure_probability.csv with the assigned housing units, and another containing the failure state, named base_name_failure_state.csv. The limit-state probability and damage state are derived using the damage-state dictionary in the input infrastructure dataset. The limit-state probability is calculated from all stochastic runs, and the limit state shows all infrastructure positions as a sequence of failed (0) and non-failed (1) states from each individual run. The result of this analysis is two CSV files: one containing the limit-state probability, named base_name_failure_probability.csv with the assigned housing units, and another containing the failure state, named base_name_failure_state.csv.
Multi-objective retrofit optimization model	This analysis computes a series of linear programming models for single- and multi-objective optimization related to the impact of extreme climate events on a community, using three objective functions: minimizing economic loss, minimizing population displacement, and maximizing building functionality. The analysis uses a set of mitigation strategies determined by the hazard type, such as the seismic retrofit of existing buildings or relocation in the case of tsunamis or floods. The parameters include the initial and final feedback levels of a building, the retrofit cost, and an objective coefficient that measures community resilience. The optimization model implemented in pyIncore has three objectives: economic loss, population dislocation, and building functionality. The calculation process is performed by iteratively solving constrained linear models using epsilon steps. The CSV results contain collections of optimal resource allocations.
Cascading network interdependence functionality	This analysis calculates cascading functionality based on the interdependencies between electric power facilities (EPF) and water distribution systems (WDS). The analysis uses the Leontief equation to calculate the functional dependencies between two interdependent networks, taking into account the functionality of each node. These dependencies capture the cascading effects on infrastructure functionality, expressed in terms of discretized time steps. The result of the calculation is a dataset containing the cascading EPN functionality along with the original discretized values.

Type of Analysis	Description
Pipeline damage	This analysis calculates pipeline damage based on a specific hazard. Currently, the supported hazards are earthquake and tsunami. The process for calculating structural damage is similar to that used for other parts of the built environment. First, a fragility function is obtained based on the type of hazard and the attributes of the pipeline. Next, the hazard intensity is calculated at the pipeline location. Using this information, the probabilities of exceeding each limit state and of damage are determined. If the pipeline dataset contains soil information, the mean value of the associated fragility function can be adjusted to account for liquefaction in the damage. The results of this analysis are a CSV file containing damage probabilities and a JSON file containing information on the hazard and the fragility functions.
Pipeline damage with repair rate	This analysis calculates pipeline damage in water pipelines based on a specific hazard. Currently, the supported hazard is: earthquake. The process for calculating structural damage is similar to that used for other parts of the built environment. First, a fragility function is obtained based on the type of hazard and the attributes of the pipeline. Next, the hazard intensity is calculated at the pipeline location. Using this information, the probabilities of exceeding each limit state and of damage are determined. If the pipeline dataset contains soil information, the mean value of the associated fragility function can be adjusted to account for liquefaction in the damage. The results of this analysis are a CSV file containing damage probabilities and a JSON file containing information on the hazard and the fragility functions.
Analysis of pipeline functionality	This analysis computes pipeline functionality using the repair-rate calculations derived from the pipeline damage analysis. The calculation is performed by generating Monte Carlo samples from Poisson-sample deviations derived from the damage analysis, which are then used as input to Bernoulli experiments to determine the average functionality. The results of this analysis are two CSV files: one containing the failure probability, named base_name_failure_probability.csv, and another containing the failure states, named base_name_failure_state.csv.
Repair cost of water pipelines	This analysis estimates the repair costs of water pipelines for different simulation scenarios, based on their damage states, replacement costs, and damage ratios.
Pipeline restoration	This analysis computes the restoration time of water pipelines after a specific hazard. The analysis does not depend on the type of hazard, as it operates on the results of the pipeline damage analysis and the repair rate, together with the restoration curves. The restoration curves are obtained according to the type of hazard and the pipeline diameter class. Based on the applicable restoration curve, the time required to repair each pipeline is determined. In calculating the repair times, the leak rate, break rate, pipeline length, and number of available workers are considered. One of the inputs to this analysis is the result of the pipeline damage analysis with the repair rate. The result of this analysis is a CSV file containing the estimated time required to repair each pipeline.

Type of Analysis	Description
Population displacement	This analysis calculates population displacement based on a specific hazard. First, the housing units, with detailed characteristics (tenure, household size, occupied or vacant), are assigned to the address points (buildings). This is done through the housing-unit allocation analysis. After assigning the housing units, the hazard event, defined through the Fragility and Hazard services, determines the loss in value for each structure, which serves as input for the displacement calculation. Displacement is calculated from four probabilities, based on a random beta distribution of the four damage factors presented by Bai et al. 2009, which correspond to the loss in value. The sum of these probabilities, multiplied by the probabilities of the damage states, is used as the probability of displacement. Since the process used to determine which households are displaced is probabilistic, an integer value is imported to initialize the random number generator, which determines whether a household is displaced. In addition, the characteristics of the block group, such as the percentages of African American and Hispanic population, are taken into account. The result of this analysis is a CSV file containing the displaced households and the related variables.
Recovery of residential buildings	This analysis calculates the recovery time required for each residential building from any damage state to full restoration. Currently, the supported hazards are tornadoes. The methodology uses a multi-layer Monte Carlo simulation approach and determines the recovery time in two stages, which include both the delay period and the repair period. The delay model was modified according to the REDi framework and computes the final outcomes by accounting for factors that delay recovery, such as post-disaster inspection, insurance claims, and the issuance of building permits. The repair model follows the FEMA P-58 approach and uses the fragility functions of Koliou and van de Lindt (2020). The result of this analysis is a CSV file containing recovery probabilities at building-level time steps.
Road damage	This analysis calculates road damage based on a specific hazard. Currently, the supported hazards are earthquake and tsunami. The process for calculating structural damage is similar to that used for other parts of the built environment. First, a fragility function is obtained based on the type of hazard and the attributes of the roads. Next, the hazard intensity is calculated. Using this information, the probabilities of exceeding each limit state and of damage are determined. If the road dataset contains soil information, the mean value of the associated fragility function can be adjusted to account for liquefaction in the damage. The results of this analysis are a CSV file containing damage probabilities and a JSON file containing information on the hazard and the fragility functions.

Type of Analysis	Description
Computable General Equilibrium (CGE) model of Salt Lake City	A computable general equilibrium (CGE) model is based on fundamental economic principles. This model uses multiple data sources to reflect the interactions of households, businesses and relevant government entities in their contribution to economic activity. The model is based on (1) households that maximize utility, supplying labor and capital, using their income to pay for goods and services (both locally produced and imported) and to pay taxes; (2) the production sector, with perfectly competitive firms that maximize profits by using intermediate inputs, capital, land, and labor to produce goods and services for both domestic consumption and export; (3) the government sector, which collects taxes and uses fiscal revenue to fund the provision of public services; and (4) the rest of the world. The result of this analysis is a set of CSV files containing domestic supply, gross income, pre- and post-disaster factor demand, and the number of households.
Computable General Equilibrium (CGE) model of Seaside	A computable general equilibrium (CGE) model is based on fundamental econom-ic principles. This model uses multiple data sources to reflect the interactions of households, businesses and relevant government entities in their contribution to economic activity. The model is based on (1) households that maximize utility, supplying labor and capital, using their income to pay for goods and services (both locally produced and imported) and to pay taxes; (2) the production sector, with perfectly competitive firms that maximize profits by using intermediate inputs, capital, land, and labor to produce goods and services for both domestic consumption and export; (3) the government sector, which collects taxes and uses fiscal revenue to fund the provision of public services; and (4) the rest of the world. The result of this analysis is a set of CSV files containing CGE simulations, domes-tic supply, and employment.
Social vulnerability	This analysis calculates a social vulnerability score for each zone associated with the census data. The calculation extracts the zoning and a social vulnerability score obtained by comparing demographic characteristics of interest with national average values. The result of the calculation is a dataset in CSV format.
Social vulnerability score	The result of the calculation is a dataset in CSV format. This analysis calculates a social vulnerability score for each zone associated with the census data. The calculation extracts the zoning and a social vulnerability score obtained by comparing demographic characteristics of interest with national average values. The result of the calculation is a dataset in CSV format.
Power grid damage due to tornadoes (EPN)	This analysis calculates damage to the electric power network (EPN) based on a particular hazard. Currently, the supported hazard is tornado. The process for calculating structural damage is similar to that used for other parts of the built environment. First, the fragility functions are obtained based on the type of hazard and the attributes of the network towers and poles. Based on the fragility function, the intensity of the hazard at the location of the infrastructure is calculated. This information is used to calculate the probability of exceeding each limit state, as well as the probability of damage. The results of this analysis are a CSV file containing damage probabilities and a JSON file containing information on the hazard and the fragility functions. Depending on the input data, this analysis also provides information on the number of damaged poles for each node, the repair cost for each node, the total repair cost of the network, and the total repair time of the network.

Type of Analysis	Description
Traffic flow recovery	This analysis calculates bridge damage by first calling the bridge damage analysis. Then it uses the nodes and links in the traffic flow path and the Average Daily Traffic (ADT) data for the bridges to calculate post-disaster traffic flow network recovery. In addition, the analysis can be used in stochastic calculations with an imported integer value to initialize the random number generator. The result of this analysis is a CSV file with the recovery trajectory timelines and the corresponding data.
Transportation recovery	This analysis calculates bridge damage by first calling the bridge damage analysis. It then uses nodes and links in the transport path and Average Daily Traffic (ADT) data from bridges to calculate post-disaster transport network recovery. In addition, the analysis can be used in stochastic calculations with an imported integer value to initialize the random number generator. The result of this analysis is a CSV file with the recovery trajectory timelines and the corresponding data.
Damage to water facilities	This analysis calculates the damage to water facilities based on a particular hazard. The hazards currently supported are: earthquake and tsunami. The process for calculating structural damage is similar to that used for other parts of the built environment. First, a fragility function is obtained according to the type of hazard and the characteristics of the building. Based on this fragility function, the hazard intensity at the building location is calculated. Using this information, the probability of exceeding each limit state is calculated, along with the probability of damage. In the case of an earthquake hazard, soil information can be used to modify the damage probabilities to account for liquefaction damage. The results of this analysis are a CSV file with the damage probabilities and a JSON file with information on the hazard and the fragility functions.
Water network functionality	This analysis calculates the functionality of the water networks. The calculation uses input from the Monte Carlo failure analysis, using information on damage to water facilities as well as pipe functionality data to determine the probability of functionality and the failure states for the corresponding water-facility network through an accessibility analysis. The result of the analysis consists of a CSV file with the functionality probabilities of the water facilities and a CSV file with the functionality failure states.
Repair Cost Analysis for Water Facilities	This analysis estimates the repair costs of the water facilities for different simulation scenarios, based on their damage states, replacement costs, and damage ratios.
Restoration of Water Facilities	This analysis calculates the repair time and the percentage change in functionality over time for the restoration of the water facilities, based on the mapped restoration curves. The restoration curves are obtained according to the hazard type and the water-facility class, for example, treatment plant, pumping plant, water storage tank, etc. According to the applicable restoration curve, we can obtain the percentage change in functionality as a function of time; we can also calculate the repair time at different levels of change in functionality by inverting the restoration function.

A.6.3. Mathematical approach

IN-CORE uses fragility curves to perform damage calculations. First, a fragility curve is obtained based on the hazard type and the attributes of the building (or any other exposed element). Based on the fragility curve, the hazard intensity at the building location is calculated. With this information, the probability of exceeding each limit state is calculated, along with the probability of damage. In the case of seismic hazard, soil information can be used to modify damage probabilities to include damage due to liquefaction (IN-CORE 2024).

Figure 50 shows an example of a risk curve obtained by IN-CORE. The seismic–tsunami hazard in the Cascadia Subduction Zone (CSZ) is used in this example to demonstrate the multi-hazard capabilities of the software. The probabilistic seismic–tsunami hazard analysis (PSTHA; Park et al. 2017) produced hazard maps for both earthquakes and tsunamis for seven recurrence intervals (100, 250, 500, 1,000, 2,500, 5,000, and 10,000 years). Building damage is calculated in IN-CORE by overlaying the hazard maps on the buildings and determining the site-specific intensity measures. Spectral displacement intensity measures and momentum flux intensity measures are used for earthquake and tsunami hazards, respectively. Next, the fragility curves are implemented to determine the probability that each building will experience the following damage states: (1) slight damage, (2) moderate damage, (3) severe damage, or (4) complete damage. These probabilities are then used to inform a Monte Carlo simulation in which the failure probability of the buildings is calculated. No reference to a specific function for calculating the EAD was found in the IN-CORE documentation, but because IN-CORE operates within the Python environment, the user can obtain the area under the curve by applying the functions available in Python.

Figure 50. Example of a risk curve generated by IN-CORE

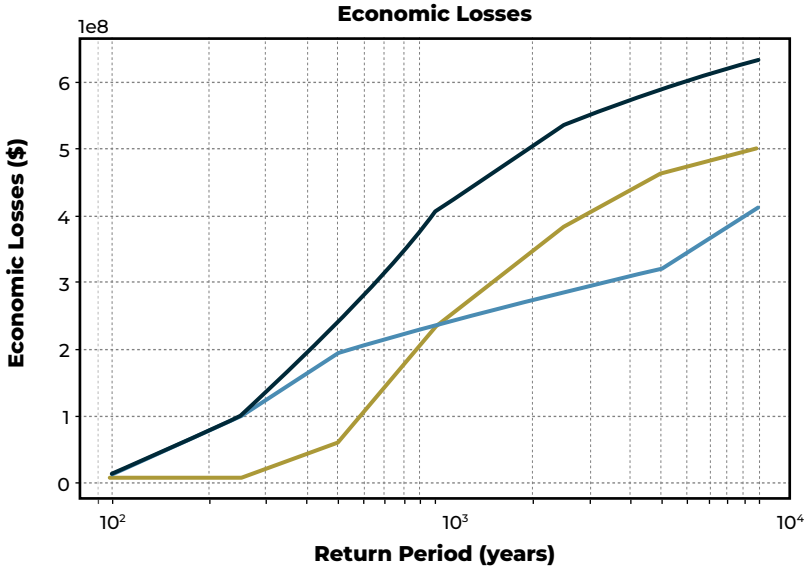

Source: IN-CORE (2024).

Notes: the blue line corresponds to earthquake economic losses, the red line to tsunami economic losses, and the black line to multi-hazard losses.

Figure 51. Tsunami and earthquake hazard maps

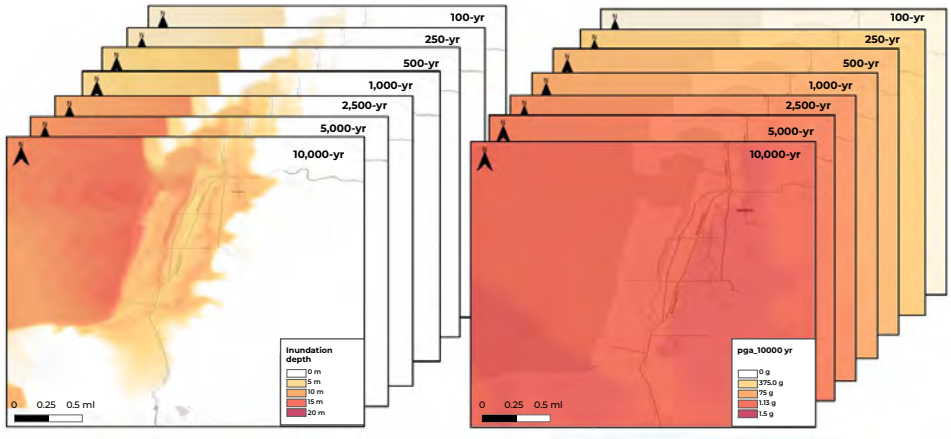

Tsunami Hazard **Earthquake Hazard**

Source: IN-CORE (2024).

A.6.4. Recent advances and innovations

The latest version is IN-CORE v5.3.0 released on April 12, 2024.

A.6.5. Development community

IN-CORE is developed by an interdisciplinary team of researchers at Colorado State University, in collaboration with other academic institutions, government agencies, and the private sector. This community works together to continually update and improve the software, ensuring that it remains at the forefront of infrastructure resilience research.

A.6.6. Limitations

One of the main limitations of IN-CORE is that it requires the user to be familiar with Python programming.

A.6.7. Use cases

IN-CORE has been used only in the United States. **Box 7** shows one of the examples that uses this software as a tutorial and is described in the documentation by van de Lindt et al. (2023).

Box 7. Example of an IN-CORE application

Case Study: Seaside, Oregon (Successive earthquake and tsunami events)

Image: Adobe Stock

Seaside, a small coastal city in the Pacific Northwest of the United States, was selected as a test case for applying the IN-CORE system, given its vulnerability to earthquake and tsunami hazards originating in the Cascadia Subduction Zone. The study generated the hazard layers associated with earthquake and tsunami hazards, focusing on five tsunami intensity measures: flow depth, velocity, momentum flux, arrival time, and inundation duration.

A multi-hazard damage analysis was then carried out to evaluate the combined impacts of the earthquake and the tsunami using a stochastic approach that accounts for the accumulated damage from the earthquake and the subsequent tsunami inundation. The probabilistic earthquake and tsunami damage analysis is incorporated as one step within a resilience-focused decision-support system that includes the evaluation of both direct and indirect economic losses.

The analysis also considers several components of the built environment, including the transportation, energy, and water sectors, as well as the demographic characteristics of the population. The damage, economic losses, and connectivity with critical facilities were analyzed to show the economic losses by hazard type and infrastructure.

Performance goals were established as part of the analysis: (1) robustness (for example, an acceptable level of damage) and (2) rapidity (for example, an acceptable time for recovery). A key aspect of this framework was that the goals were established as a function of the mean recurrence interval of the hazards. The results highlighted the impact of considering different performance goals, the introduction of ex ante and ex post measures, and the interdependencies among the various infrastructure systems on infrastructure resilience. Additionally, this study showed how the volume of debris increases with the mean recurrence interval (MRI) and how the location of the peak debris profile across the coast is related to the maximum limit of the tsunami runup.

The figure shown below presents the mean annualized economic risk for (a) buildings and (b) the transportation network (roads and bridges) as a function of the mean recurrence interval. The risk is disaggregated for seismic (blue), tsunami (red), and combined (black) hazards. In the left panel (A), the maximum risk for buildings occurs in the 250-year event and is due almost entirely to ground motion. On the other hand, in the right panel (B), the maximum risk for roads and bridges occurs in the 1000-year event, primarily due to the tsunami. This comparison highlights the need to evaluate risk in terms of both hazard type and infrastructure type for decision-making on community resilience.

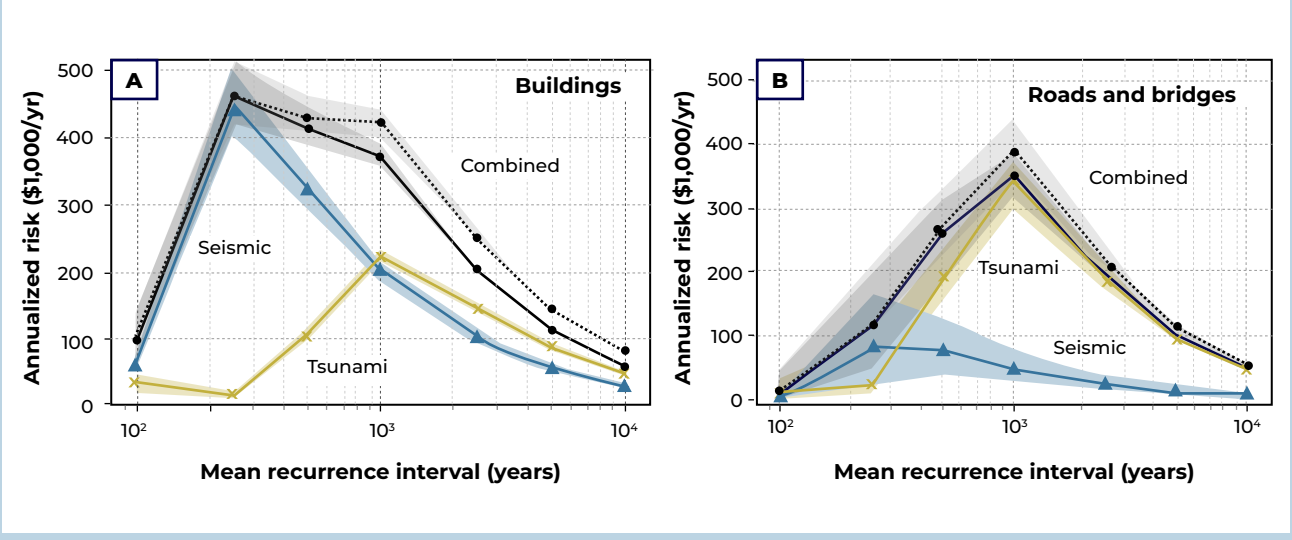

This case study demonstrates the importance of integrating multi-hazard risk analysis and evaluating local infrastructure in terms of its vulnerability to earthquake and tsunami hazards. The results obtained not only provide an understanding of the risks and potential economic losses but also inform strategies to improve community resilience to large-magnitude events.

Source: van de Lindt et al. (2023).

A.7. CLIMADA (CLIMATE ADAPTATION)

A.7.1. General description

CLIMADA (CLIMate ADAptation) is a quantitative climate risk modeling tool developed to evaluate the socioeconomic risk of extreme weather events. It is an open-source platform, available on GitHub[26], and was developed primarily in Python, MATLAB and Octave. The tool allows for risk analysis of different types of climate hazards (tropical cyclones, floods, droughts, etc.) at global, regional, and local scales, providing spatially explicit estimates of risk both at present and in future projections.. CLIMADA implements a fully probabilistic risk evaluation model (Aznar-Siguan and Bresch 2019).

CLIMADA provides a framework for users to combine exposure, hazard, and vulnerability data to calculate risk. Users can create probabilistic impact data from event sets, observe how climate change affects these impacts, and see how adaptation measures can change them effectively. CLIMADA also allows studies of individual events, historical event sets and forecasts(ETH Zurich 2017c).

In addition, efforts have been made to have interoperability and integration of CLIMADA with other tools such as OASIS LMF (Blass 2021) and OpenQuake[27].

A.7.2. Applied methods

CLIMADA implements a probabilistic risk evaluation model using state-of-the-art techniques such as Monte Carlo simulation. This approach allows the integration of different scenarios of economic development and climate impact, using historical and remote sensing data to produce hazard, vulnerability and risk maps. The model considers the combination of hazard, exposure (assets and people) and vulnerability to calculate risk. It also includes damage functions that relate the intensity of an event to its economic consequences for assets such as people, buildings, and public infrastructure. CLIMADA operates consistently worldwide at high resolution (10 km), as well as in local applications at the highest resolutions (100 m); however, the user can work with the information at whatever level of detail is available to them. The tool provides spatially explicit estimates of multi-hazard risk both for current conditions and for future projections (Munich Climate Insurance Initiative 2020). CLIMADA makes it possible to evaluate a full portfolio of adaptation measures, quantifying the potential for damage aversion and the cost–benefit relationship for each measure (Munich Climate Insurance Initiative, 2020). Adaptation measures include, for example, the construction of protective structures, spatial planning, ecosystem-based approaches, building regulations, and risk transfer (insurance) against some of the most extreme climate events. In this context, CLIMADA implements the Economics of Climate Adaptation methodology (Aznar-Siguan and Bresch 2019).

[26] The code is hosted on GitHub (https:// github.com/CLIMADA-project/climada_python) under the GNU GPL (GNU Operating System, 2007) license (Aznar-Siguan & Bresch, 2019)(Aznar-Siguan & Bresch, 2019).

[27] Verbal communication with the United Nations University.

The software design is modular and object-oriented, offering a simple collaborative framework and a parallelization strategy that allows for scalable computations on clusters (Aznar-Siguan and Bresch 2019).

The first step in the cost-benefit analysis is to determine the current risk (see **Figure 52**). Essentially, CLIMADA implements the concept of risk as defined by the IPCC (2014). CLIMADA combines hazard (for example, a wind footprint of a tropical cyclone), exposure (for example, an asset distribution), and vulnerability (the functional relationship between hazard intensity and impact) to calculate risk (Aznar-Siguan and Bresch 2019).

In addition, with CLIMADA it is possible to perform global uncertainty analyses, including uncertainty in hazard, exposure, and the impact function, through the methods implemented in the Unsequa module (Kropf et al. 2022).

Figure 52. Conceptualization of CLIMADA

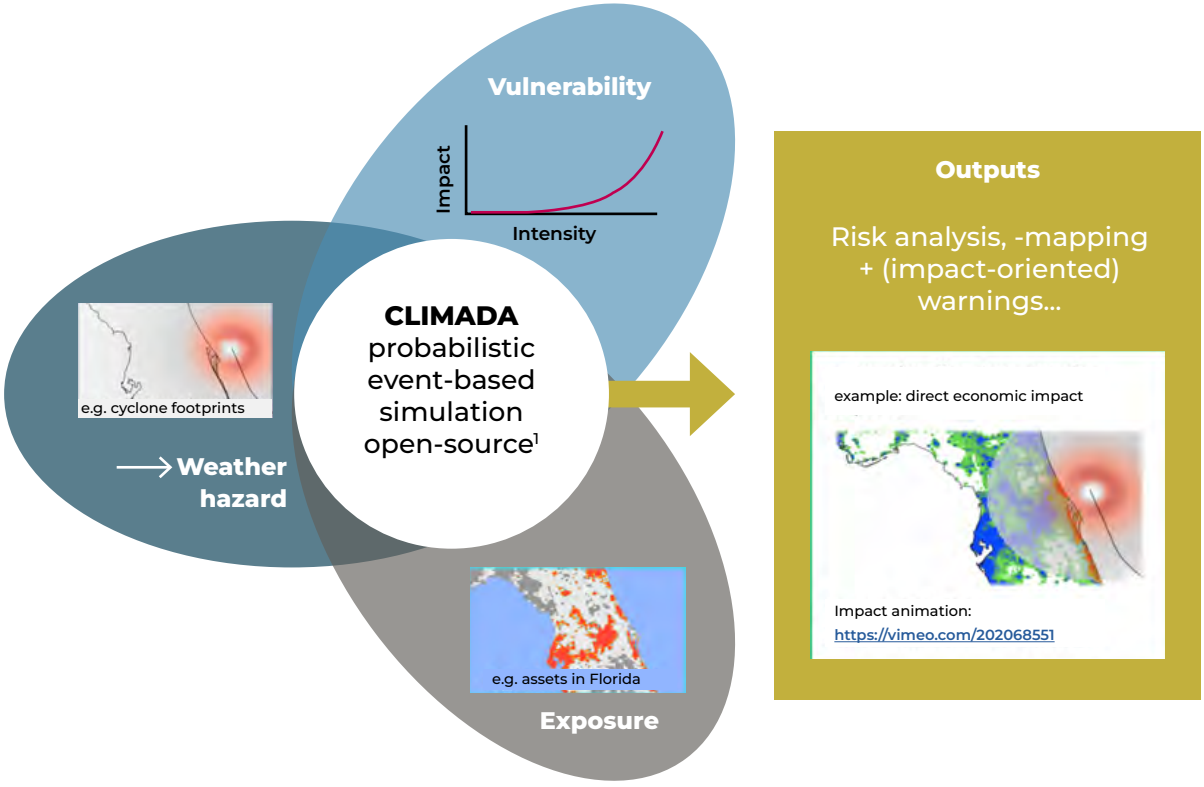

Source: Aznar-Siguan and Bresch (2019).

A.7.3. Mathematical approach

CLIMADA provides an event-based probabilistic approach that does not depend on any a priori probability distribution assumption. The CLIMADA damage model can be used for a wide variety of applications, for example, deterministically to evaluate the damage from a single event or to quantify risk based on a (large) set of probabilistic events (Aznar-Siguan and Bresch 2019). Exposure can be expressed in terms of a value that is not necessarily monetary, for example, in number of people.

The CLIMADA calculation engine uses damage or vulnerability functions to calculate the damage from a hazard to exposed elements and stores all resulting risk evaluation metrics. The architecture used by the risk calculation tool is shown in **Figure 53**. The hazard value is assigned to the exposed element's centroid coordinate, and the damage ratio derived from the damage functions is translated into direct damage by multiplying it by the exposed value, as shown in the **Equation 17** (Aznar-Siguan and Bresch 2019):

Equation 17

$$\chi_{ij} = val_j f_{imp}(h_{ij}|\gamma_j)$$

Where x_{ij} and h_{ij} are, respectively, the damage and intensity of the hazard due to event i at location j, val_j the exposure value at location j, γ_j are the exposure parameters j that characterize its vulnerability and f_{imp} the damage function. Damage is obtained for each exposed element and for each event that affects it (historical or stochastic). Based on this damage for the event and the frequency of each event, any risk metric can be obtained. The equations used by the tool, which have been derived from are shown below (Cardona et al. 2012).

- Expected annual impairment (EAI) at exposure j contained in attribute eai_exp:

Equation 18

$$EAI_j = \sum_{\bar{\imath}}^{N_{hist}} E\,[X|E_{\bar{\imath},j}]\,F(E_{\bar{\imath}})$$

Equation 19

$$EAI_j = \sum_{\bar{\imath}=1}^{N_{hist}} \sum_{\hat{\imath}} x_{\hat{\imath}} F(E_{\hat{\imath}}) = \sum_{i=1}^{Nev} x_{ij} F(E_i)$$

Where X is the damage random variable, E its expectation, E_i is an event and F its (annual) frequency; N_{hist} is the number of historical events; $\hat{\imath}$ represents a historical event; $\hat{\imath}$ represents all members of the event set $\hat{\imath}$; and Nev represents the total number of events. Event independence is assumed.

- The average annual impact (AAI) is contained in the attribute aai_agg and is the sum of the EAI across all exposures:

Equation 20

$$AAI = \sum_{j=1}^{Nexp} EAI_j$$

Where $Nexp$ is the number of exposed elements.

- Probable Maximum Impact (PMI): PMI represents the damage that is exceeded at a fixed low annual frequency (normally from 1/1500 to 1/250). It is obtained from the damage exceedance curve calculated with the calc_freq_curve method. Taking into account the total probability theorem, this curve is approximated by discretizing **Equation 21**.

Equation 21

$$v(x) = \frac{1}{T(x)} = P(X > x) = \sum_{i}^{Nhist} \int P(X > x|h) p(h|E_i) dh F(E_i)$$

Where $v(x)$ is the damage exceedance frequency x, $T(x)$ its equivalent return period, and h the hazard intensity; $p(h|E_i)$ is the probability density function of h given that the historical event E_i took place and it is calculated using the members of the event set. The probability of exceeding a damage value given the intensity h, $P(X>x|h)$, is calculated using the exposure values and their damage functions. CLIMADA assumes that the damage from an event across different exposures is independent.

CLIMADA also includes a module for uncertainty quantification and sensitivity analysis (Kropf et al. 2022). The unsequa module uses a Monte Carlo–based approach and applies standard uncertainty and sensitivity analysis methodologies. Its workflow begins with defining input variables and parameters, establishing probability distributions for the parameters that affect the model's key variables: hazard, exposure, vulnerability function, and adaptation measures. Using these distributions, samples of the parameter values are generated according to their respective probability distributions.

CLIMADA's engine then computes the model results for each sample, producing risk metrics or an evaluation of adaptation options. The results can be analyzed and visualized to understand the distribution of the model outputs. It is also possible to compute sensitivity indices to evaluate the influence of each input parameter on the model metrics (Kropf et al. 2022).

The parameter distributions may be of any type, including uniform, Gaussian, skewed, or discrete. CLIMADA allows the use of any distribution available in Python's SciPy.stats library.

To define the uncertainty of each variable, the user must specify a method that determines its value as a function of the uncertain parameters. The unsequa module provides auxiliary methods to support this parameterization, allowing two main approaches: the direct perturbation of a variable using statistical methods, or the incorporation of uncertain parameters into the underlying model that generates the variable. Since each variable is independent, it is possible to use both approaches simultaneously within the same study.

Uncertainty and sensitivity analysis is computationally expensive, as the computation time increases with the number of samples and the complexity of the model. Factors such as the spatial resolution of the exposure or the number of hazard events affect the time required. In external models such as hydrological models, the simulation time of the base model also has an influence. If the computations are prohibitively long, it is possible to precompute samples or use surrogate models.

In the final stage, the model output values are characterized and visualized, using graphical and statistical tools to understand uncertainties beyond mean values and standard deviations. Sensitivity indices quantify the influence of each uncertain parameter on the model results. Since CLIMADA is nonlinear, only global sensitivity indices are considered, computed using algorithms available in the SALib Python library, such as Sobol, Morris elemental effects and FAST (Kropf et al. 2022). Each method has specific sampling requirements and may provide different results, although they generally agree in identifying the most influential parameters.

Image: Adobe Stock

Figure 53. Simplified CLIMADA risk-evaluation architecture

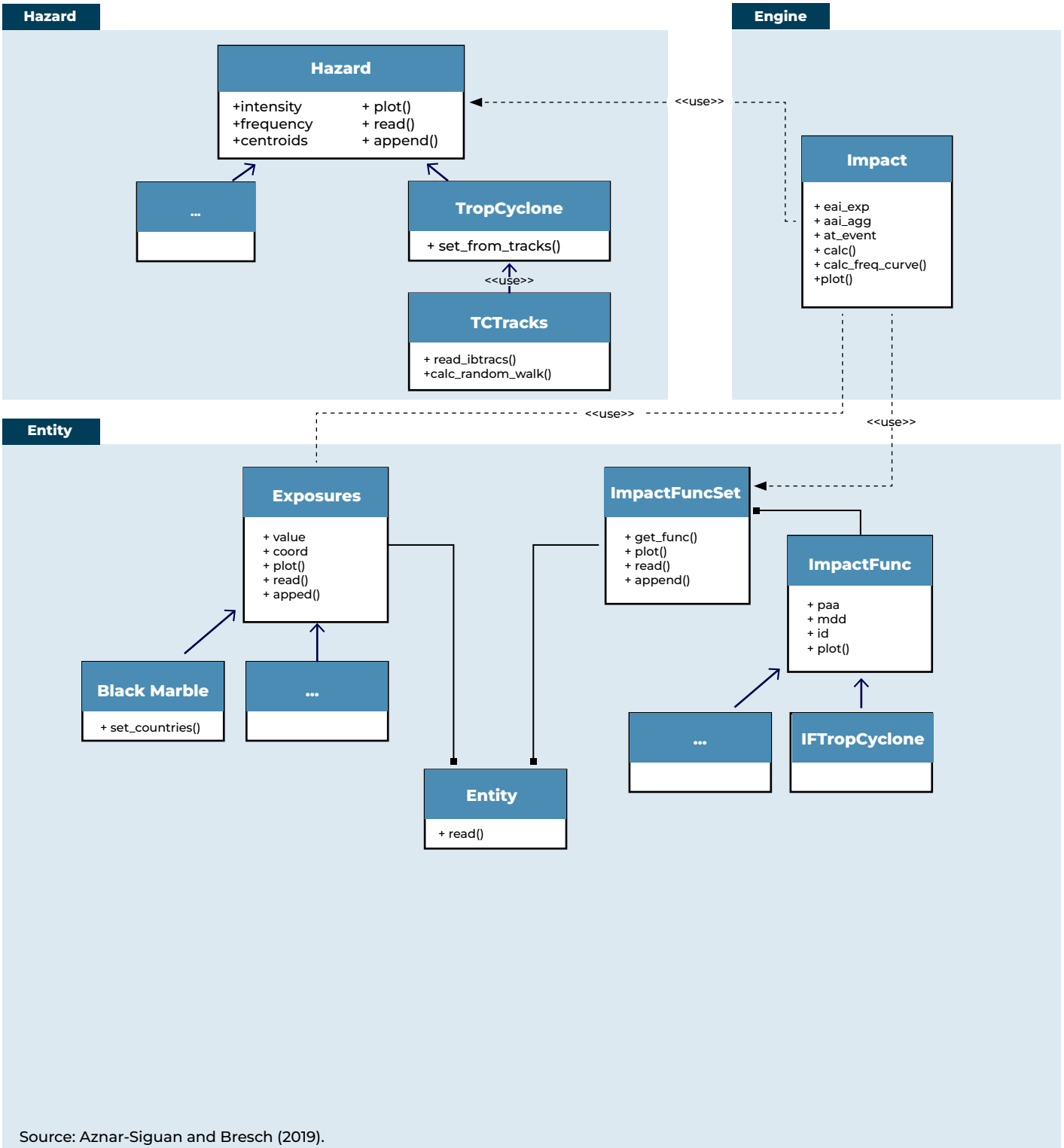

Source: Aznar-Siguan and Bresch (2019).

A.7.4. Recent advances and innovations

Recently, CLIMADA has improved its performance, scalability and maintainability. The tool includes global coverage of climate hazards such as tropical cyclones, fluvial flooding, agricultural droughts, and European winter storms, with historical and probabilistic event sets available under different climate-forcing scenarios.

A.7.5. Development community

CLIMADA is developed and maintained by the Weather and Climate Risks (WCR) research group at ETH Zurich. The developer community is active and promotes the interdisciplinary use of the platform, fostering international collaboration. The availability of CLIMADA as open-source software under the GNU GPL3 license has been essential for building confidence in the results.

A.7.6. Limitations

One of the main limitations of CLIMADA is that it requires the user to have coding knowledge in Python. On the other hand, it is worth noting that although CLIMADA was originally designed to analyze climate hazards, it can also compute risk for any type of hazard, provided it is represented as a Hazard-type object and a damage curve can be associated with the exposed elements.

A.7.7. Use cases

CLIMADA has been applied in more than twenty climate adaptation studies worldwide, where it served as a solid foundation for risk evaluation and for addressing and communicating uncertainties (Munich Climate Insurance Initiative 2020).

Image: Adobe Stock

Box 8. Example of a CLIMADA application

Case Study: Hurricane Irma and its Impact on the Non-Self-Governing Territories of the Caribbean

Image: Adobe Stock

The Caribbean region includes nineteen non-self-governing territories. The arrival of Hurricane Irma in September 2017, a Category 5 hurricane, provides a case study for comparing governmental responses and the impacts on these territories. The hurricane's track affected several islands, including sovereign nations such as Antigua and Barbuda and Saint Kitts and Nevis, as well as territories such as Saint Barthélemy, Sint Maarten, Anguilla, and the U.S. Virgin Islands.

Historically, these islands have relied on primary sectors such as agriculture, but have shifted toward tourism and offshore finance. This economic shift has implications for the financial impact of disasters, given the significant role that tourism and offshore finance play in their economies.

The Black Marble dataset, which uses NASA nighttime satellite data, was used to estimate the exposed economic value, allowing the spatial distribution of economic value across the affected islands to be estimated. This method involves disaggregating national GDP data to a 500-meter resolution, adjusted for distribution biases in urban and suburban areas using a quadratic transformation.

The tropical cyclone damage was modeled using CLIMADA's TropCyclone class, incorporating historical tropical cyclone tracks and wind speed after landfall. The damage function used is based on wind speeds, with adjustments for urban areas and varying income levels.

The study evaluated risk by combining the tropical cyclone hazard with economic exposure. The probabilistic models predicted damage levels for various return periods, revealing that all the islands face significant risk from intense cyclones. The analysis estimated that damage from a 100-year return period event could exceed USD 1 billion, with individual islands such as the U.S. Virgin Islands requiring substantial financial preparedness.

Economic damage computed by CLIMADA as a percentage of local exposure (per pixel). (a) Lesser Antilles; (b) Turks and Caicos Islands.

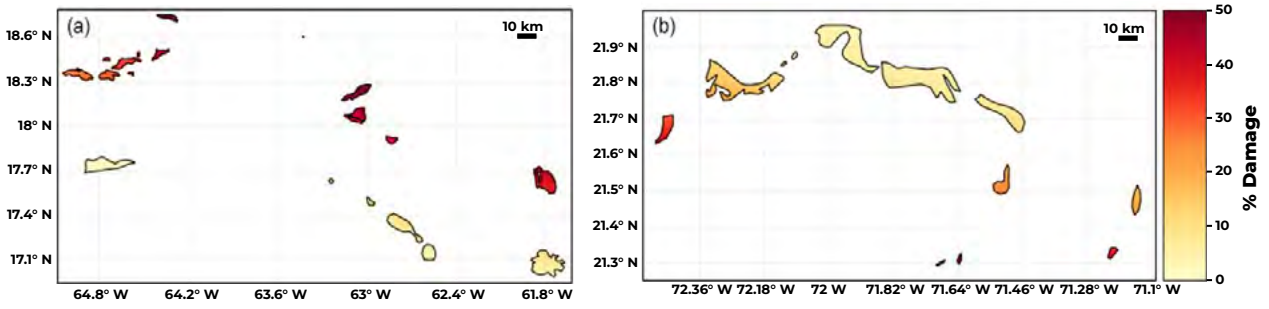

The damage estimates were compared with other sources such as EM-DAT, the National Hurricane Center, and ECLAC. The CLIMADA model results were consistent with these sources, demonstrating reliable estimates within the expected range. Variability in the damage estimates was observed due to differences in data sources and methodologies, but the model's predictions were generally robust.

The uncertainty analysis showed that socioeconomic factors are the largest contributors to variability in the damage estimates. Monte Carlo simulations indicated that extreme events could cause substantial damage, ranging from USD 12.5 to 21 billion under the most severe scenarios.

By applying advanced modeling techniques and leveraging satellite data, the study provides valuable insights into the financial impact of Hurricane Irma and offers a framework for improving disaster preparedness and response. The results can help metropolitan governments and territorial administrations develop effective strategies to mitigate future risks and improve resilience.

Source: Aznar-Siguan y Bresch (2019).

A.8. CATSIM (CATASTROPHE SIMULATION TOOL)

A.8.1. General description

CATSIM (Catastrophe Simulation Tool) is a model developed by IIASA (International Institute for Applied Systems Analysis) designed to help policymakers, especially in developing countries, devise public financing strategies for both the pre-disaster and post-disaster phases. The model allows the input of national data and poses "what-if" questions, showing the best combinations of financial strategies to suit current national circumstances. (IIASA 2024b) .

CATSIM provides a risk-based economic framework for evaluating the economic impacts of disasters and analyzing the costs and benefits of measures to reduce those impacts (Hochrainer-Stigler et al., 2013). It uses stochastic risk simulations for a specific region and examines the capacity of both the government and the private sector to finance response and recovery activities. The model also analyzes the government's contingent liabilities, the financial gaps that can arise after a disaster, and the options for reducing vulnerability, including financial-management strategies. It also incorporates a simple economic-growth framework to evaluate the macroeconomic impacts of disasters and the costs and benefits of measures intended to mitigate those effects (Hochrainer-Stigler et al. 2015).

The results it provides include (Hochrainer-Stigler et al. 2013):

- **Evaluation of contingent liabilities and financing gaps:** It identifies the potential financing gaps a country could face in the event of disasters.
- **Cost–benefit analysis of vulnerability- and risk-reduction options:** It makes it possible to assess the economic effectiveness of different risk-management strategies, such as prevention, national reserve funds, or sovereign insurance.
- **Support for policy planning:** It helps governments decide how to allocate resources between preventive measures (ex-ante spending) and post-disaster response measures (ex-post spending), taking into account their impact on economic resilience.

CATSIM is a standalone application with an easy-to-use graphical interface that allows the user to define parameters for hazard, vulnerability, and exposed elements. The graphical interface of the software is shown in **Figure 54**.

Since CATSIM focuses on national-level decision making, neither the input data nor the results are geospatial in nature. In general, the results are presented using interactive graphics that allow users to modify parameters and perform sensitivity analyses Hochrainer-Stigler et al. et al. 2015).

Figure 54. CatSim graphical interface

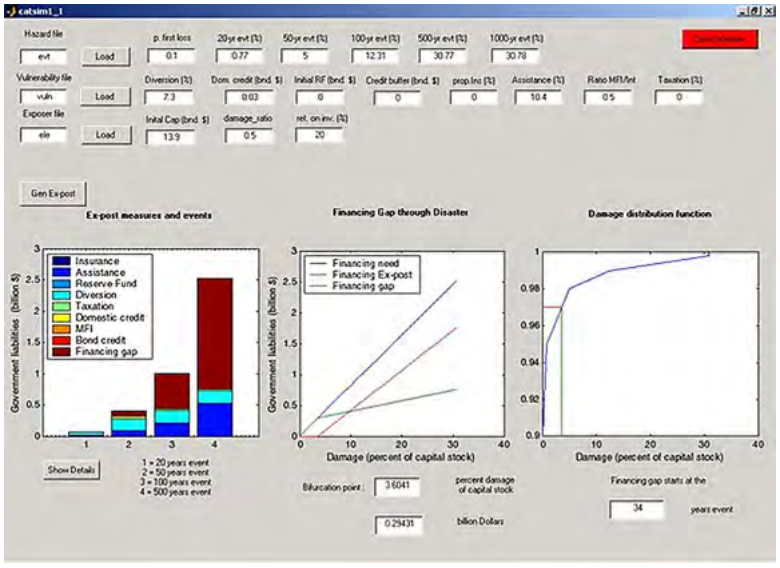

Source: IIASA (2024b).

A.8.2. Applied methods

CATSIM uses a modular approach that includes:

- **Risk assessment (Module 1):** It defines parameters for hazards, vulnerability, and exposed elements.
- **Analysis of financial strategies (Module 2):** It evaluates the costs and benefits of various financial strategies for managing risk, including their impact on key economic indicators such as economic growth and debt.

CATSIM uses stochastic simulations of disasters in a specific region to analyze the capacity of governments and the private sector to finance recovery and response after an event. Through Monte Carlo simulations, the model assesses disaster risks and allows the user to adjust parameters to test different assumptions related to hazards, exposure, vulnerability, general economic conditions and government response capacity. As an interactive capacity building tool, CATSIM illustrates the trade-offs and decisions faced by policymakers in building resilience to disaster risk (Hochrainer-Stigler 2014; Hochrainer-Stigler et al. 2013).

From a methodological perspective, CATSIM approaches the decision and modeling problem as a two-stage decision problem under uncertainty. The primary objective is to ensure sufficient and timely funding for post-disaster government obligations, including the provision of relief to the private sector and the reconstruction of public assets (Hochrainer-Stigler et al. 2013). The stages considered are:

- **First stage (ex-ante):** The government can allocate part of its budget to risk reduction (such as building a dam) or purchase insurance and other financial instruments to protect public assets (infrastructure, public buildings) and obligations to help the private sector. These measures, however, reduce the budget available for regular development activities, generating opportunity costs.

- **Second stage (ex-post):** After a disaster, budgetary decisions are made to fund recovery needs. However, financing losses solely with ex-post resources also affects the investment budget.

The shortfall of resources that cannot be covered by ex-ante or ex-post options is called the "resource gap". This gap negatively impacts key macroeconomic variables such as GDP, government revenues, and its budgetary position, increasing financial vulnerability and future risks (Hochrainer-Stigler et al. 2013).

CATSIM is implemented in five main steps (Hochrainer-Stigler et al. 2013):

1. **Modeling of direct asset loss risk:** Loss probabilities are calculated in monetary terms, based on the frequency and intensity of the hazards, the exposed elements and their physical vulnerability.
2. **Financial and economic resilience:** It measures the capacity of the government and the state to access savings to finance the reconstruction of public infrastructure and aid to the private sector. Resilience depends on the general economic conditions of the country.
3. **Financial vulnerability:** It is evaluated by simulating the risks to the public sector and the government's financial capacity to cover its post-disaster responsibilities under different magnitude scenarios.
4. **Impact of the resource gap:** The consequences of this gap are analyzed in macroeconomic variables such as economic growth and external debt, which reflect impacts on economic flows and complement the estimation of asset risks.
5. **Development of risk management strategies:** Strategies are designed to strengthen the resilience of the public sector and improve the risk management portfolio. These strategies are continually reviewed to assess their impact on reducing financial vulnerability within the modeling framework.

In the first step of CATSIM, the risk of direct losses is assessed in terms of the probability of losses on assets in a specific country or region. Following general practice, risk is modeled as a function of the hazard, the elements exposed to that hazard, and their physical vulnerability (Hochrainer-Stigler et al. 2013):

- **Natural hazards:** Events such as earthquakes, hurricanes or floods are described by their intensity (e.g., peak flows for floods) and recurrence (as 1 in 100-year events, i.e., with a 1% probability).
- **Exposure:** The exposure of the elements at risk is estimated as the total capital, both public and private.
- **Physical vulnerability:** Describes the degree of damage that the capital may suffer due to the hazard. The standard method consists of estimating vulnerability or fragility curves, which relate the degree of loss to the intensity of the hazard.

Based on this information, the potential losses caused by destructive events can be established in terms of the percentage of capital lost in a country, state or region. Return period and loss data serve as inputs to CATSIM, generating loss frequency distributions that relate probabilities to destroyed assets.

A.8.3. Recent advances and innovations

A web-based version is being developed to provide customized data to countries that have participated in workshops, allowing an interactive assessment of their risk to extreme events.

In addition, IIASA's Risk and Resilience team has developed a CATSIM module that quantifies the inter-industry impact of disasters. This model estimates the economic costs of disasters in various sectors, taking into account the existing productive structures in the economy and the estimated recovery time after the disaster. The model can be calibrated using commonly available datasets, such as input-output tables, and allows users to visualize the economic benefit of improved fiscal preparedness (faster disaster recovery). This software module has been developed as part of the CATSIM framework and can be used in policy assessments and capacity building activities. Additional software developments are being planned, which will include interface tools and other visualizations (IIASA 2024a).

Over the past eight years, the user interface and the underlying model framework of CATSIM have been tested, adjusted, and improved at various levels. These developments were based on more than 20 high-level workshops with key stakeholders held in countries such as Turkey, the Philippines, India, Nepal, Mexico, several Caribbean nations, and most recently in Madagascar in 2012 and 2015 (Hochrainer-Stigler et al. 2015).

A.8.4. Development community

IIASA has worked extensively with various international organizations such as the World Bank and the Inter-American Development Bank (IDB). In addition, it has collaborated with specific countries, such as Mexico and several Caribbean nations, to apply and optimize the use of CATSIM in disaster risk management.

A.8.5. Limitations

The model has been developed for national analyses to assess macroeconomic impacts and financial strategies for disaster risk management. It is not oriented toward risk evaluation at the local level. The current version of CATSIM is a stand-alone application, which may limit its integration with other tools and systems used in disaster risk management. In addition, CATSIM requires detailed national data, which may be a challenge for some countries with limitations in data availability and quality.

A.8.6. Use cases

CATSIM has been used in several World Bank projects and its World Development Report to estimate disaster risk in more than 80 countries. It also contributed to an Inter-American Development Bank initiative to establish the Regional Insurance Facility for Central America, which helps small countries pool risks and access external capital to cover them. In addition, CATSIM was instrumental in the design of the Caribbean Catastrophe Insurance Facility (CCRIF) in 2007, the first regional disaster risk management fund, supported by the World Bank and donors such as the United Kingdom's Department for International Development. In 2007, a workshop was held in Barbados with Caribbean countries to discuss risk management strategies, which helped identify efficient ways to address disaster risks (IIASA 2024c).

Between 2011 and 2012, IIASA used CATSIM to support a Madagascar government study on integrating disaster risk management and climate change into economic development following the impact of Cyclone Gafilo, which caused 363 deaths and damage equivalent to 5% of GDP (see **Box 8** for more details of this case study).

Finally, the CATSIM analysis is informing deliberations on the Loss and Damage Mechanism of the United Nations Framework Convention on Climate Change, including the creation of a global fund that absorbs different levels of risk and supports risk-reduction and financing activities in vulnerable countries (IIASA 2024c).

Image: Flickr - IDB Sustainable Cities / Panamá

Box 9. Implementation of the CATSIM Model in Madagascar

Image: Adobe Stock

In May 2012, Madagascar implemented the CATSIM model to integrate disaster risk management into fiscal and development planning, with support from the World Bank and GFDRR. The objective was to evaluate risk management strategies for events such as cyclones, which generate considerable economic losses.

2012 Workshop: Preliminary Risk Assessment

The CATSIM model was presented in a workshop with more than 30 representatives from various ministries (finance, education and infrastructure). Historical losses, preliminary risk estimates, and potential financial gaps in the face of disasters were analyzed.

Results of the probabilistic analysis:

- 100-year events: estimated losses of USD 1,047 million.
- Expected annual losses: 55 million USD on average.
- Available internal resources: up to USD 50 million, insufficient for events with return periods greater than 23 years.

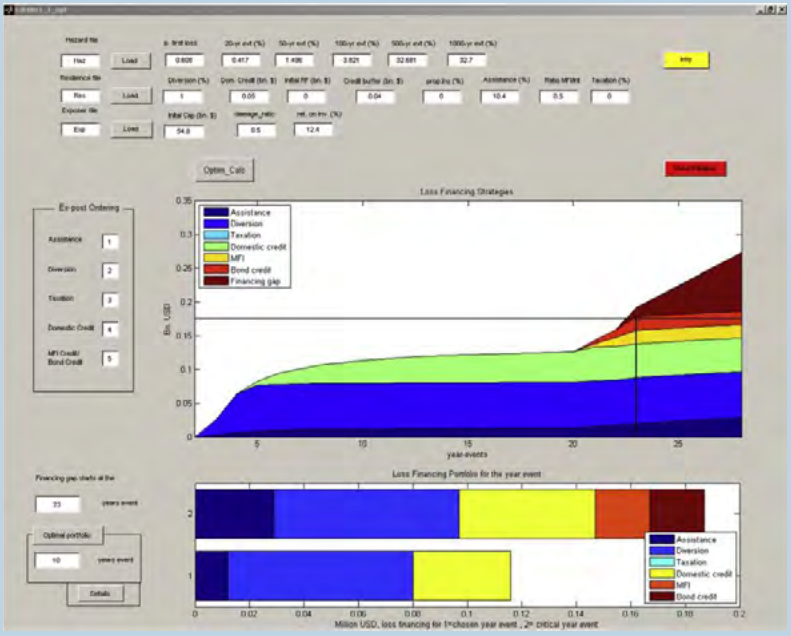

Financial vulnerability and resource gap for Madagascar using direct risk basis estimates. Note: The central figure shows the return periods on the x-axis and the required/available resources on the y-axis. The figure below is an interactive chart that allows users to explore the details of alternative fiscal resource allocation across different return periods.

Key findings: Significant gaps were identified in exposure and physical vulnerability data, prioritizing their improvement for future analyses.

2015 Workshop: Updated Evaluation

With more detailed data, the government reviewed financial strategies, highlighting options such as insurance and reserve funds. International models (FONDEN and CCRIF) were discussed to adapt financial protection mechanisms.

Challenges and Recommendations

Institutional strengthening and data: It is crucial to improve the collection and exchange of interministerial information.

Sustainable financing: Implement mixed financial instruments to cover frequent and extreme events.

Comprehensive planning: Integrate risk management with national priorities such as education and health.

The use of CATSIM in Madagascar highlights the need to balance economic development with disaster resilience, fostering inter-agency cooperation and preparedness for future events.

Source: Hochrainer-Stigler et al. (2015).

A.9. RISKCHANGES

A.9.1. General description

Developed collaboratively by the University of Twente and the GeoInformatics Center of the Asian Institute of Technology (UN-SPIDER Regional Support Office), RiskChanges operates as an open-source, cloud-based spatial decision-support system (RiskChanages 2021).

RiskChanges offers a set of functions designed to perform risk assessments. Its multi-user functionality facilitates collaboration between different stakeholders, enabling data sharing and collective knowledge generation. In addition, it supports multi-hazard evaluations that consider interactions and cumulative effects. Capabilities also include multi-asset analysis, vulnerability assessment, risk scenario modeling, risk comparison, and advanced spatial analysis with visualization (PreventionWeb 2023).

A.9.2. Applied methods

The platform allows users to analyze risks associated with multiple natural and anthropogenic hazards, taking their interactions into account; evaluate risks for different types of assets with varying spatial characteristics; access and share a database of physical vulnerability curves; compare current risks with future projections and different risk-reduction alternatives; and perform spatial risk analyses through a web-based mapping interface (RiskChanges 2021).

The exposure section in RiskChanges allows to calculate the interaction between exposed elements and hazards previously loaded in the platform. To perform this calculation, it is necessary to combine a layer of Elements at Risk (EAR) with a hazard layer by selecting them from the available options in the corresponding sections of the data management system. In addition, it is possible to aggregate the results to specific administrative levels using previously defined layers. If this aggregation is not desired, the calculation will be performed at the EAR layer level. Once these options have been configured, the system calculates the exposure and the results can be displayed or downloaded in tabular format.

From the calculated exposure, it is possible to estimate total losses based on the type of element at risk (EAR). Before proceeding, it is essential to have previously defined the connections between values and populations in the EAR section. Users can select the desired type of calculation and generate loss estimates from a list of precomputed exposures. The results are presented in a visual and tabular format, providing detailed information to assess the impacts of different events. (RiskChanges 2021).

Risk calculation in RiskChanges is based on previously estimated losses. Users may choose to perform a risk analysis for a single hazard or for multiple hazards. In the case of multi-hazard analysis, the process includes additional steps to integrate the combinations of losses associated with different return periods. Final results include metrics such as average annual loss (AAL) and are presented in visual and tabular formats.

The visualization interface in RiskChanges provides a layered window in the upper left corner, where users can navigate between previously calculated or aggregated data, including hazards, elements at risk, exposure, losses and risks. Interactive maps allow users to apply filters, edit styles (such as color palettes and opacity), and perform side-by-side comparisons between layers.

A.9.3. Recent Advances and Innovations

RiskChanges has the capacity to visualize and compare results in various ways, enabling a comprehensive and flexible analysis of risk scenarios. The platform integrates data directly from map servers and supports the loading of customized information in GIS formats. In addition, its cloud-based infrastructure facilitates access, data processing, and real-time collaboration among multiple users, optimizing management and decision-making in multi-hazard environments (RiskChanges 2021). The latest version is 2.1.0 as of June 2022.

A.9.4. Development community

RiskChanges was developed by the University of Twente and the GeoInformatics Center of the Asian Institute of Technology (UN-SPIDER Regional Support Office) however it is not clear that its development is continuing to date.

A.9.5. Limitations

The platform requires users to have basic knowledge of geographic information systems (GIS) and of risk-data interpretation. In addition, the documentation is very limited, so there is no clarity regarding the detail of the methods used.

A.9.6. Use Cases

RiskChanges has applications in a variety of areas, including risk assessment and mapping, risk reduction planning, disaster preparedness and response, and climate change adaptation. PreventionWeb (2023) mentions that applications exist in Nepal, India, the Caribbean and the Southern African Development Community (SADC) countries, however, little information on applications was found. The information available on the CMINE platform is shown in **Box 10**.

Box 10. Examples of RiskChanges Use

The CMINE platform website presents the following three application cases, although with limited information. The examples only show the hazard information that was used and that is not directly generated by the platform, without presenting an example of the type of results that RiskChanges produces. Unfortunately, no further information could be found.

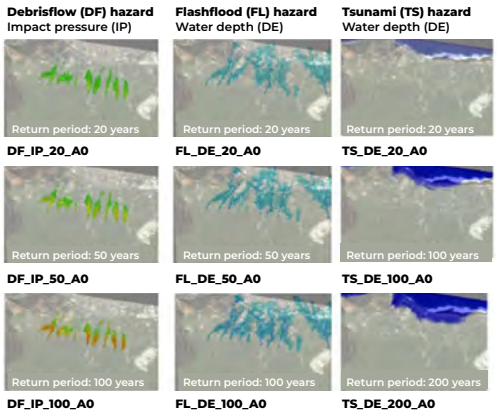

Current status

Simulation of a river flood on the Koshi River in northern Nepak. The elevation model is a 5mresolution WorldDEM Neo satellite estimate, which is commercially available worldwide. A discharge boundary condition is used to simulate an extreme flow event. The surface roughness coefficients are estimated using the integrated use of WorldCover 10 m.

Risk reduction alternative

Flash flood simulation in the Grande-Bay area in Dominica. This area was severely affected in 2017 by Hurricane Maria. A custom eleva-tion model with a 10-meter resolution was loaded here, although a similar result could be obtained using the 30-meter Copernicus elevation dataset. The land use and rainfall were loaded using FastFlood's integrated tools. Buildings and roads are displayed using the automatic download of OpenStreetMap data.

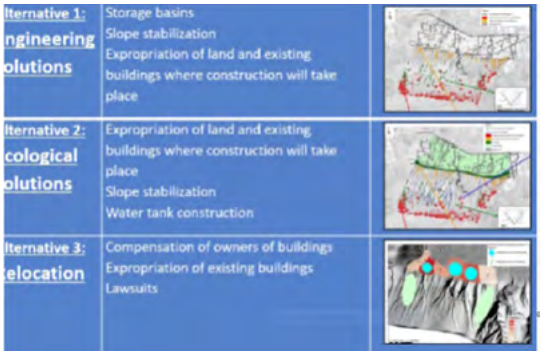

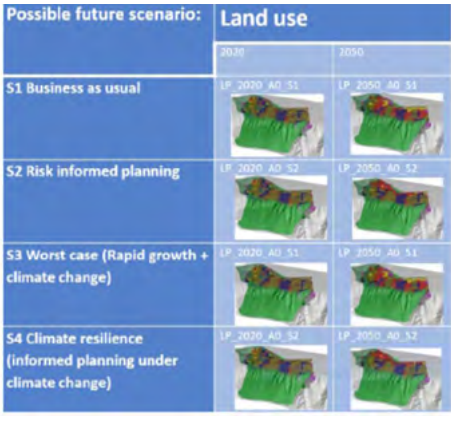

Future scenarios

The Geul River is a small fluvial system in the southern Netherlands with a minor extent in Belgium and Germany. In 2021, the extreme rainfall event that struck the northwestern part of the European continent caused flooding in this area and significant damage in cities such as Valkenburg.

This simulation uses automatic estimates of infiltration, channel characteristics, and elevation. A second model area is defined for Valkenburg using the upscaling algorithm. The observed flood extent, published by the National Ministry of Water and Infrastructure, is shown as an overlay.

Source: RiskChanges (2021).

A.10. FLOODRISK - QGIS PLUGIN

A.10.1. General description

FloodRisk is a free and open-source QGIS plugin that provides an assessment of flood consequences, including loss of life and direct economic damages. The plugin allows users to perform a simple risk assessment considering fixed events where the probability of each event is estimated separately and the consequences are calculated deterministically.

It includes types of direct tangible and intangible costs, accounts for structural and non-structural mitigation strategies, can be used for the analysis of future dynamics (considering risk dynamics), and promotes collaboration and communication through an open-source approach (Albano et al. 2017c).

The FloodRisk user interface consists of five main forms (**Figure 55**). These forms allow the user to be guided to populate the database with their own data to create or change FloodRisk project files and to perform risk analysis, i.e. economic flood damage assessment and loss of life estimation. The toolbar allows the activation of the main forms. In addition, FloodRisk contains several other forms (accessible from the main forms) to represent input and output data as graphs, tables and maps.

Figure 55. FloodRisk graphical user interface

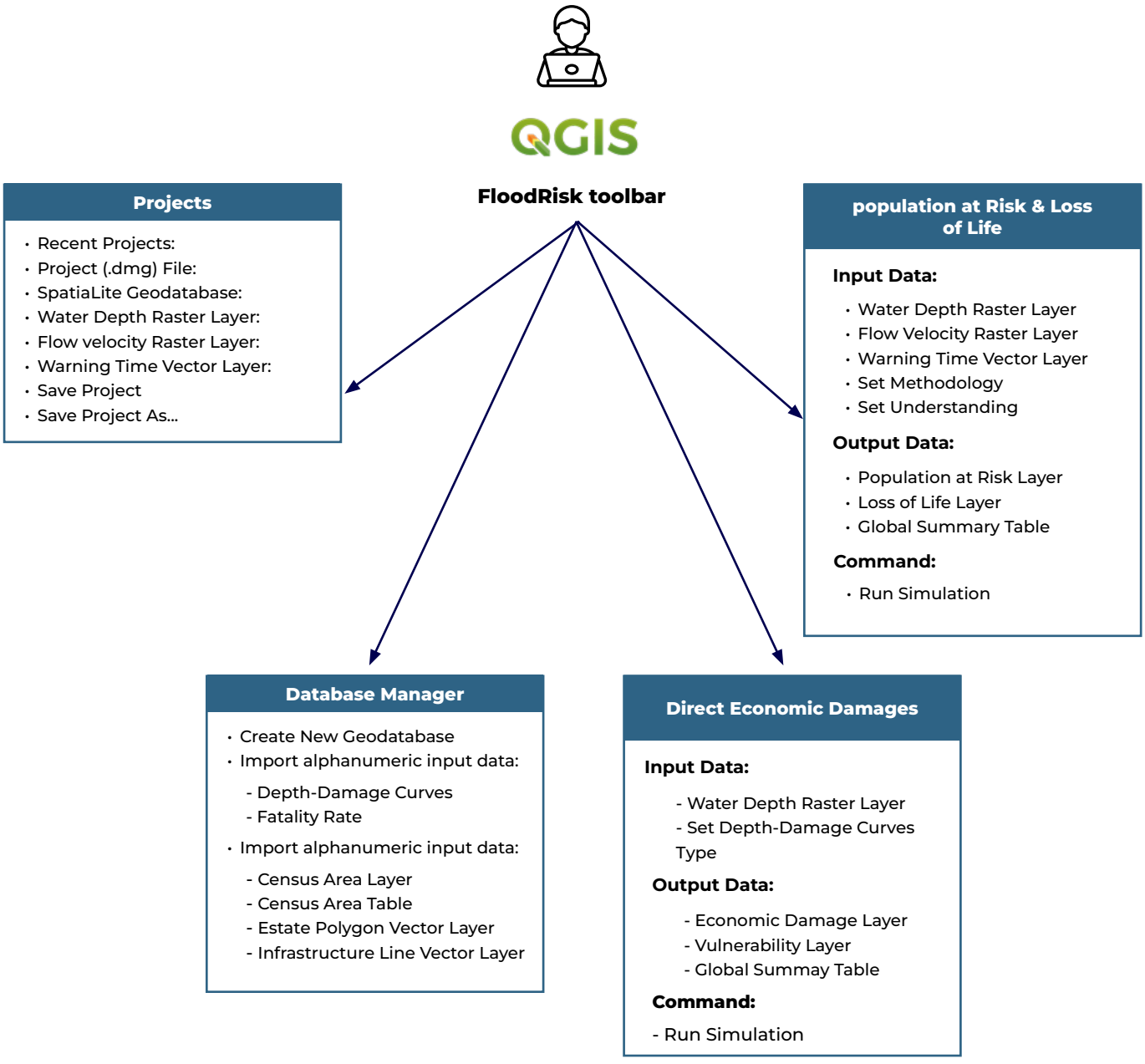

Source: Albano et al. (2017c).

A.10.2. Applied methods

FloodRisk uses depth-damage curves to assess direct economic damage to residential, commercial, and industrial properties. For the estimation of loss of life, the plugin first generates a map of the population at risk by overlaying the flood map with the population-density map. The loss of life is then obtained by multiplying the population at risk by the fatality rate selected by the user. These results are shown in the form of tables, graphs (histograms), and maps (Albano et al. 2017c).

The plugin allows the estimation of flood consequences, including loss of life and direct economic damages, in line with the approach of the European Floods Directive. The plugin integrates several flood-risk assessment techniques, including meteorological, hydrological, and socioeconomic approaches, within a GIS framework. This tool supports decision makers in evaluating flood mitigation strategies and promotes sustainable risk management practices.

The FloodRisk plugin framework is based on the unit-loss method, and therefore the parameters that define the exposed elements, the maximum damage values, and the damage functions strongly affect the results. In addition, FloodRisk allows the use of an object-based approach, which uses a large number of object types, such as a building map or a land-use approach (i.e., models based on aggregated surfaces, where the exposure data input takes the form of a land-use map) (Albano et al. 2017c).

The FloodRisk conceptual framework (see **Figure 56**) is based on the modeling of floods with different return periods, which combined with exposure and vulnerability information, allows the calculation of damages: with flood damages corresponding to different probabilities, a loss probability curve can be constructed, from which the expected annual damage (EAD) can be calculated. Finally, different flood risk reduction measures can be implemented in the damage model in order to calculate their effectiveness. With respect to vulnerability assessment, FloodRisk follows a standard approach, reflecting both the potential for a given receptor to experience damage in the event of flooding and the quantification of the number of properties or people that may be exposed to a given flood event should it occur. Therefore, flood risk is evaluated by combining the receptors exposed to the hazard with the susceptibility, value, and resilience of these receptors. Susceptibility describes the propensity of a particular receptor to experience damage during a given flood event. The standard approach, used in FloodRisk, to define the susceptibility of elements at risk and estimate direct flood damages is the use of damage functions. These functions define, for the respective elements at risk, the relationship between the characteristics of the hazard and exposure and the damage that can be expected under the given circumstances. Value is used to express the degree of damage to a receptor and may be expressed in monetary terms, such as the maximum value of the assets, or by intangible impacts (for example, the number of people who lose their lives) (Albano et al. 2017c).

Figure 56. Graphical representation of the FloodRisk

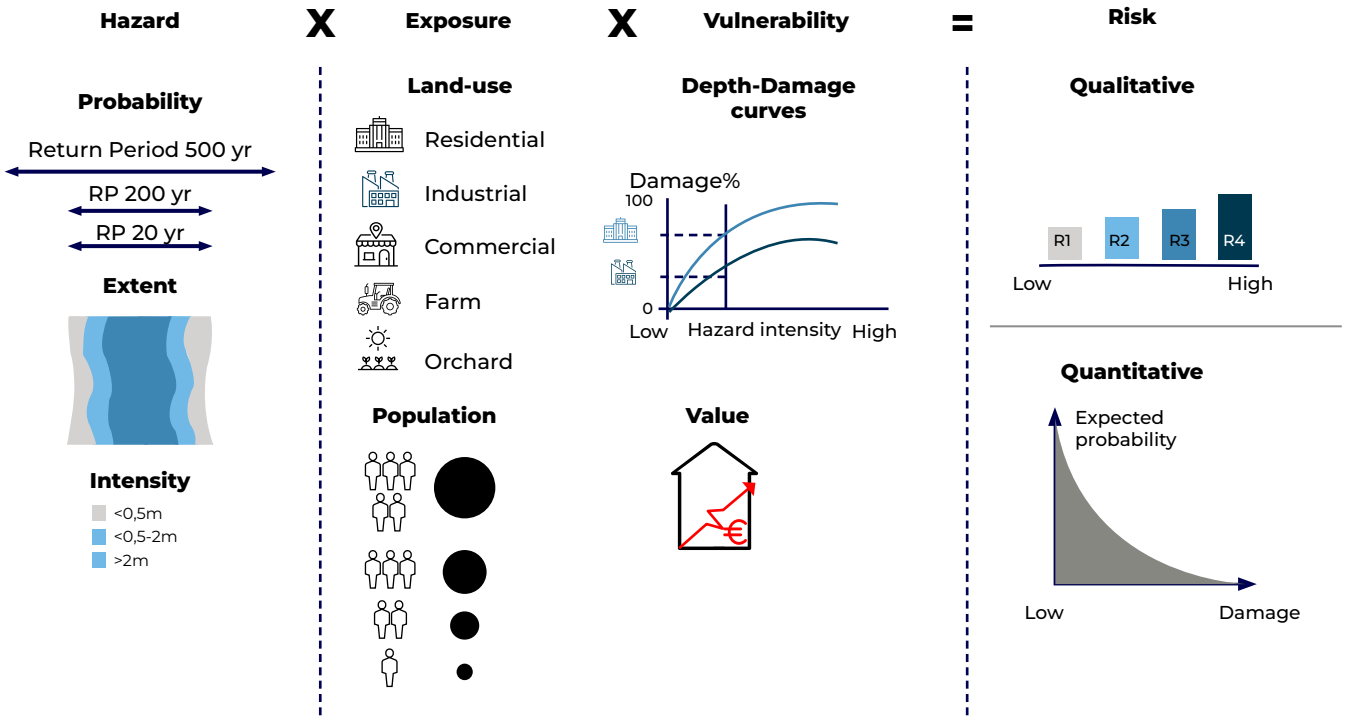

Fuente: Albano et al. (2017b).

A.10.3. Recent advances and innovations

FloodRisk had 5 versions, the last of which was generated in October 2020. It was later replaced by FloodRisk2 for QGIS 3.x, providing the evaluation of flood consequences in terms of loss of life and direct economic damage, as well as the quantitative evaluation of the benefits in terms of damage reduction resulting from mitigation measures (FloodRiskGroup 2021). The latest version of the plugin, FloodRisk2, developed for QGIS 3.x, includes additional features and enhancements over the previous version for QGIS 2.x. Among these enhancements are improved integration with QGIS and improvements to the user interface. Recent studies have explored the plugin's ability to analyze uncertainties in flood-damage evaluations, emphasizing the need for site-specific vulnerability curves and detailed building classification to reduce epistemic uncertainty (Albano et al. 2018).

A.10.4. Development community

FloodRisk is developed and maintained by the FloodRiskGroup community on GitHub linked to the University of Basilicata.

A.10.5. Limitations

One of the limitations of the FloodRisk plugin is that it performs risk estimations based on events with an associated probability, this approach generally involves the use of a few events, and is not originally designed to run hundreds of simulations. In addition, although the plugin allows for a choice of fatality rates, these may not adequately represent the specific conditions of each flood scenario.

A.10.6. Use cases

FloodRisk has been used in flood risk assessment projects in Europe. It was used in the case study of the 2006 flooding in the Ilisua basin in Romania (Albano et al. 2017a) and in the case study of the Serio River Valley (Albano et al. 2017b) described in the **Box 11**.

Image: Adobe Stock

Box 11. Example of FloodRisk Application

Implementation of FloodRisk in the Serio Valley: Case Study

Image: Adobe Stock

With an area of approximately 600 km², the Serio River Valley encompasses 52 municipalities with a total population of 200,000 inhabitants. The objective was to evaluate the feasibility of the FloodRisk approach in a real-world context, with data and resource constraints, focusing on the effectiveness of the results in meeting Flood Risk Management Plans.

Existing hazard maps of the Po River basin were adopted, showing flooded areas for different return periods. The spatial distribution of water depth was estimated based on water levels at various cross sections provided by the Po River basin authority. In addition, land use maps and census data were used to identify assets at risk.

The risk curves obtained with FloodRisk using 8 different damage curves are shown in the following figure:

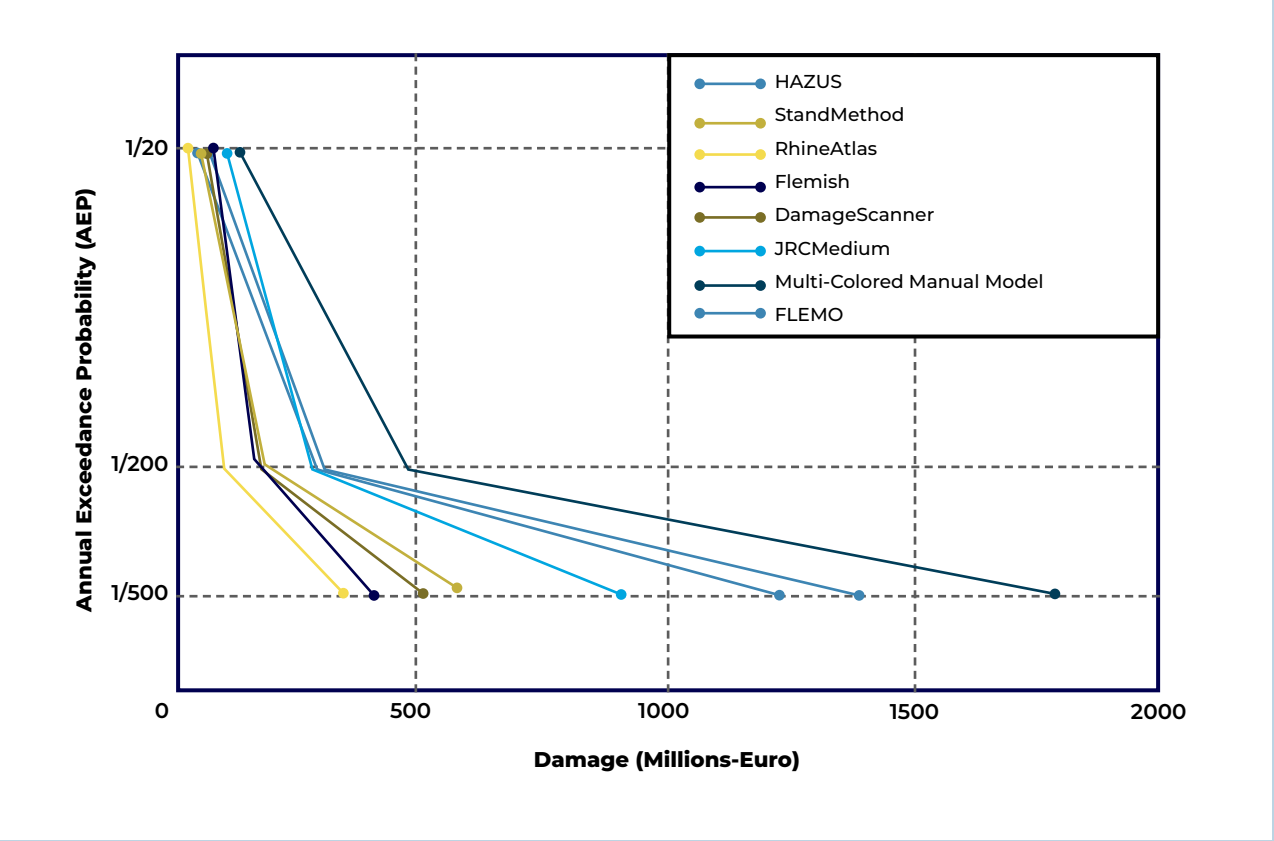

FloodRisk made it possible to evaluate the impact of structural and non-structural measures on socioeconomic risk reduction. A cost-effectiveness analysis was conducted of local measures for reconstruction and maintenance of river protection works, as well as of non-structural measures such as early warning systems.

FloodRisk results are conditioned by the availability and quality of the data, which generates significant uncertainties, especially in the depth-damage curves. A sensitivity analysis was carried out focusing on these curves, which are critical for the quantitative estimation of economic risks.

The FloodRisk approach proved to be effective for risk analysis and qualitative and quantitative flood risk mapping. Although it faces challenges such as data availability and uncertainty, it offers a robust tool to support decision making in flood-risk management and the planning of mitigation measures.

Source: Albano et al. (2017b).

A.11. FLOODRISE

A.11.1. General description

FloodRISE (Flood Resilience, Insurance, and Spatial Equity) is a project led by the University of California, Irvine, that focuses on improving flood resilience through the development of high-resolution flood hazard simulations. The project aims to provide flood risk visualizations that are useful for local decision making, involving communities in the process of co-developing flood hazard maps.

A.11.2. Applied methods

FloodRISE uses metric-scale flood hazard simulations to assess risks in different types of floods (coastal, fluvial, pluvial). The approach includes iterative stakeholder engagement through meetings, surveys, and training sessions to develop customized flood hazard maps for each community.

A.11.3. Recent advances and innovations

The project has addressed emerging challenges in coastal flooding, including nuisance and composite flooding. In addition, it has developed flood hazard visualizations that are accessible online through viewers, improving the understanding and management of flood risk in the communities involved.

A.11.4. Development community

FloodRISE is developed by an interdisciplinary team of researchers from the University of California, Irvine, in collaboration with various stakeholders, including local authorities, residents and other relevant stakeholders. This collaborative approach has been fundamental to the success of the project.

A.11.5. Limitations

The main limitation identified is that, although no specific information was found, the tool appears to be focused solely on hazard visualization despite stating on its website that it contributes to risk analysis and decision-making. Other limitations of the FloodRISE project include the need for high-resolution data and the reliance on the continued involvement of local stakeholders to maintain the relevance and accuracy of the visualizations.

A.11.6. Use cases

FloodRISE has been implemented in several communities, including the Tijuana River Valley and Newport Beach, where it has helped improve flood preparedness and response. The flood hazard maps developed have been used to plan and implement flood mitigation and adaptation measures.

Box 12. Example of FloodRise Application

Flood hazard Tijuana River

The project website displays the map visualization tool shown in the figure below. No additional information was found.

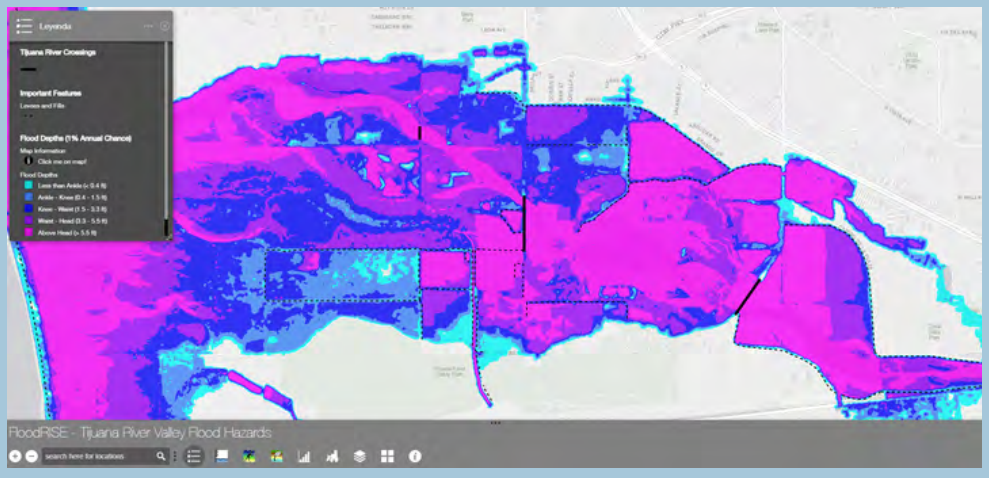

Source: FloodRise (2024).

A.12. Delft-FIAT

A.12.1. General Description

Delft-FIAT (Flood Impact Assessment Tool) is a tool developed by Deltares that is used to quickly assess the direct economic impacts of flooding on infrastructure, buildings, and roads. This open-source, Python-based tool is especially useful in climate-adaptation planning, as it allows rapid modeling of the impacts of different flood scenarios and the corresponding mitigation measures. Delft-FIAT stands out for its automation capacity and flexibility, which makes it an adaptable solution for different analysis needs.

Delft-FIAT is fast and can be automated. It allows multiple simulations through scripts or custom interfaces, making it possible to automatically calculate hundreds or even thousands of damage

estimates. This capability facilitates the evaluation of future risk associated with changing factors such as sea-level rise, storm frequency, increased precipitation, and population and economic growth. In addition, it allows the evaluation of the effectiveness of different interventions, such as improvements to drainage systems, construction of dikes, seawalls, drainage pumps, elevation of homes, or flood-protection measures, both under current conditions and under changing scenarios (Deltares 2024b).

Delft-FIAT simulations typically take approximately one minute per scenario and can be run in batch mode to analyze multiple user-defined scenarios. Its flexible architecture allows users to use the software in a variety of ways without modifying the code. For example, users can test different depth-damage functions or incorporate damage categories beyond the traditional ones, such as damage to infrastructure or disruptions to transport or businesses (Deltares 2024b).

Any type of damage that can be described using a depth-damage function can be analyzed with Delft-FIAT. In addition, the exposure data can be easily modified, and the hazard maps (flood maps) can come from any source. Delft-FIAT is also customizable, allowing its integration with custom-designed user interfaces to facilitate its use by people with less technical expertise. It can also interface with tools such as PowerBI, ArcGIS Online or flood modeling software, and even integrate with operational forecasting systems (Deltares 2024b).

The software also supports custom scripts to address specific questions. For example, the impacts of uncertainty in building floor heights or in the damage functions can be analyzed. This allows sensitivity analysis or integration of these uncertainties directly into damage estimates (Deltares 2024b). Another application of Delft-FIAT is the estimation of tipping points, that is, the moment when an adaptation intervention no longer meets the desired service levels. By running simulations under future conditions, it is possible to identify these inflection points. Users can also select specific metrics to assess levels of service, such as expected annual damages, the number of homes flooded in a 10-year return period event, or the number of affected households whose incomes are below the poverty level (Deltares 2024b).

A.12.2. Applied methods

Delft-FIAT uses a methodology based on depth-damage functions to assess the economic damages of floods. This approach allows any type of damage that can be described with a depth damage function to be modeled in the tool. In addition, its flexible architecture allows easy modification of the exposure data and adaptation of the hazard maps used as input. The software is designed to process large volumes of data quickly

A.12.3. Recent advances and innovations

The Delft-FIAT code is currently being restructured to improve its performance and flexibility, and will be released as open source software upon completion.

New features under development include (Deltares 2024b):

- Automatic generation of a customized summary report for each simulation, with metrics such as:
  - Number of homes damaged
  - Number of hospitals affected
  - Length of roads flooded above a user-defined threshold
- Calculation of equity-weighted damages to support more equitable cost-benefit analyses.
- Assessment of welfare impacts, with the objective of making more equitable assessments of adaptation options.
- Creation of a model builder for Delft-FIAT, designed to facilitate and accelerate the configuration and modification of models in Delft-FIAT.

A.12.4. Development community

Deltares, an applied research organization in the fields of water and subsoil, is leading the development of Delft-FIAT. The software is open source and available under the GNU GPL v3 license. The user community includes mainly flood risk experts and hydrological modeling specialists, who can contribute to the development and improve the capabilities of the software through platforms such as GitHub.

A.12.5. Limitations

Its accuracy depends on the quality of the input data, especially the flood maps and damage functions. In addition, although the tool is highly automatable, the initial setup and adaptation of the input data may require considerable technical knowledge.

A.12.6. Use cases

Delft-FIAT has been implemented in communities with abundant data as well as in those with limited resources. It is the basis for the national damage model in the Netherlands and has contributed to projects in the United States, Australia, Asia, Africa, Europe, the Caribbean, Central and South America, as well as in small island developing states (Deltares 2024b).

It is also part of FloodAdapt, a decision support tool to accelerate climate adaptation planning, currently in use in pilot projects in the United States, Europe, Asia and Africa (Deltares 2024b).

In addition, Delft-FIAT has been applied in projects such as interTwin, where it was integrated with other models to assess flood risks and develop mitigation strategies. It has served as a key resource for governments and organizations in planning climate change adaptation and evaluating the effectiveness of various flood mitigation measures.

Box 13. Example of Delft-FIAT Application

Resilient Caribbean: sea-level rise and adaptation potential in the Caribbean

Deltares and the World Bank, in collaboration with the Caribbean Disaster and Emergency Management Agency, assessed the impacts of sea level rise as a result of increased coastal flooding and erosion in the region using Delft-FIAT. The objective of the study is to derive indicators to estimate the resilience potential of each country in the region and its adaptation potential.

Source: Deltares (2024a).

A.13. HEC-FDA

A.13.1. General description

The HEC-FDA (Hydrologic Engineering Center - Flood Damage Reduction Analysis) software is a tool developed by the U.S. Army Corps of Engineers (USACE). Its main objective is to evaluate and quantify the economic damage associated with flood events, supporting decision making in flood-risk-reduction projects. HEC-FDA employs probabilistic methods to analyze the relationship between flood frequency and potential damage, allowing the estimation of benefits and costs associated with different risk-mitigation measures.

A.13.2. Applied methods

HEC-FDA (Flood Damage Reduction Analysis) integrates hydrological and hydraulic data, combined with economic information on structures and contents to calculate potential damage based on different flood scenarios. This is achieved through flood frequency analysis, damage curves, and vulnerability functions, allowing for a detailed and probabilistic assessment of the risks and economic benefits of mitigation projects.

The methodology applied in HEC-FDA focuses on flood risk assessment, which is defined as the combination of the probability of a flood event occurring and its consequences.

In this context, the hazard refers to the event that causes the damage, which in this case is a flood. HEC-FDA considers the hazard through hydrologic and hydraulic functions, which describe the frequency, discharge, water level, extent, and depth of the flood. Performance refers to the ability of a system, such as a dam or weir, to respond to the hazard. HEC-FDA evaluates performance using the levee elevation and a system response curve, which relates the hazard load to the probability that the system will fail (USACE 2024a).

The consequences are measured in terms of the economic damage resulting from a flood. For this purpose, HEC-FDA uses functions that relate the water level to the percentage of damage in the structures and their contents, integrating this information in a damage-frequency curve.
The exposure describes who and what are at risk of being damaged by the flood. Generally, in HEC-FDA, the exposure is represented by inventories of structures containing information on the population and properties potentially affected by the flood. HEC-FDA represents vulnerability using functions that correlate water depth with the percentage of damage, and also considers structural characteristics such as the elevation of the first floor.

As a result of the analysis, HEC-FDA calculates the Expected Annual Damage (EAD), a metric that combines the probability of a flood event occurring with its economic consequences. This calculation is made by integrating the information of the relationship between the water level frequency, the water level damage and the damage-frequency curve. (USACE 2024a).

In addition to EAD, HEC-FDA generates performance metrics that include the Annual Exceedance Probability (AEP), which measures the probability that a specific level will be exceeded in any given year, and the Conditional Non-Exceedance Probability (CNP), which indicates the probability that a specific target will not be exceeded, given that a hydrometeorological event occurs. HEC-FDA thus enables a detailed evaluation of flood risk, providing both an analysis of potential economic damage and an assessment of the capacity of defense systems to manage these risks (USACE 2024a).

Once the EAD is calculated, it is interpolated across the analysis years, discounted to the base year, and amortized to calculate the Average Annual Equivalent Damage. This process ensures that fluctuations in expected damage over time are considered, adjusting them to a present value that facilitates comparison between different flood risk mitigation alternatives (USACE 2024b).

A.13.3. Mathematical approach

The quantification of uncertainty in HEC-FDA applies Monte Carlo simulation to explicitly account for the uncertainty in the basic parameters used to determine flood damage. With this approach, each input parameter can be expressed as an empirical or analytical distribution, and the parameter values for each Monte Carlo simulation are selected using random numbers. This process can be applied to all input variables that are defined with uncertainty in the analysis. HEC-FDA relies on a random number generator and the empirical and analytical distributions in the statistical engine to run the Monte Carlo simulation (USACE 2024c).

Uncertainty can be explicitly included in the analysis by assuming a probability density distribution that best fits to describe the range of likely functions. The Monte Carlo simulation replaces a probability distribution with a very large sample of random values from that distribution and evaluates each member of the sample to form a new sample of the analysis result.

The approach implemented in HEC-FDA is called curve sampling and uses random sampling to perturb each function in the risk calculation within its uncertainty, producing a realization of each function. Each complete function (flow rate, water level, flood damage, etc.) is replaced by the randomly sampled function to generate a large sample of output curves.

To perform the traditional risk calculation, the peak discharge for a given frequency is obtained and related to a water level, and that water level is then related to a point on the vulnerability curve or the stage-damage curve for all frequencies, in order to develop a probability distribution for the damage (a damage-frequency curve). The Monte Carlo curve sampling process does the same thing, but instead of a point-to-point relationship, the process samples an entire curve within its uncertainty range. HEC-FDA uses Monte Carlo simulation to generate a new iteration of a curve by randomly selecting parameters within the uncertainty bands surrounding the curve. By randomly selecting the parameters that represent, for example, a discharge-frequency curve, the curve varies randomly, modelling the random nature of hydrological events. Each time, a new curve is obtained from which to extract data. This process is repeated many times to develop a sample of EAD that, when plotted, can be described using measures

of central tendency and dispersion (that is, mean and percentiles). The EAD sample represents all the uncertainty inherent in the inputs used in the estimation.

Figure 57 illustrates the process for one realization of the curve sampling, which produces an EAD estimate. The uncertainty and distribution bounds are represented by the bell-shaped curves and the dotted lines. With repeated random sampling (Monte Carlo analysis), uncertainty distributions are replicated to explicitly capture uncertainty in the risk calculation and risk metrics. Thousands of realizations are needed to fully reproduce the uncertainty around each function and thus around the EAD.

Figure 57. Risk calculation including uncertainty with curve sampling

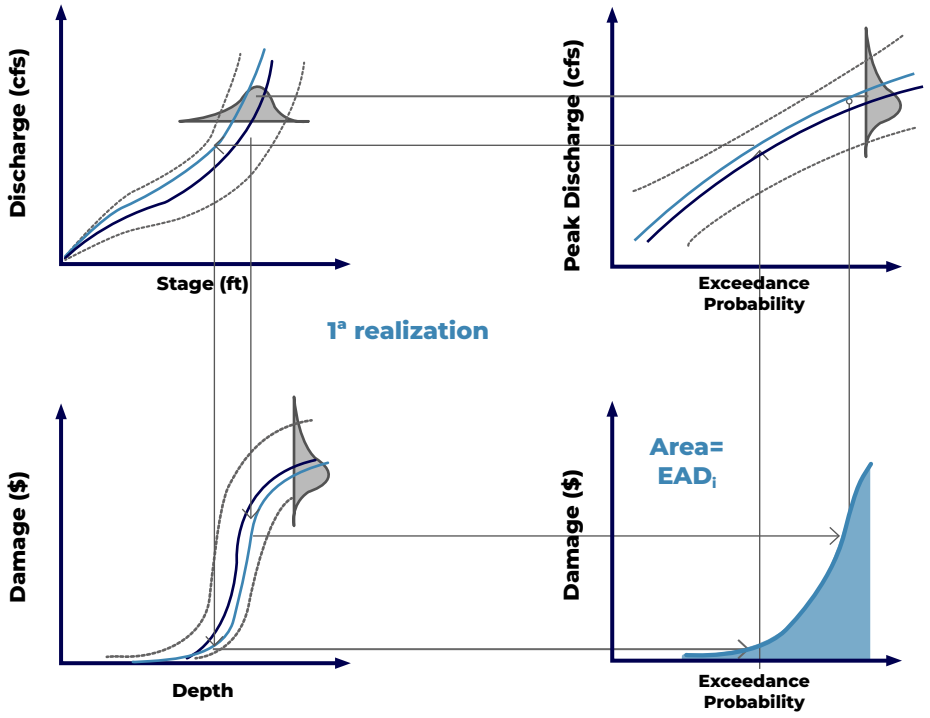

Source: USACE (2024c).

Mathematically, the EAD is defined by an equation that integrates the probability density function of the expected damage over the entire probability domain, thereby capturing the full range of possible damage in a single value, as shown in the following **Equation 22**.

Equation 22

$$E\,[\mathrm{X}] = \int_{-\infty}^{\infty} x\, f_x(x)\, dx = \int_{-\infty}^{\infty} (\,1 - F_x(x))\, dx =$$

$$F_x(X) = P(X \le x) \text{ y } 1 - F_x(X) = P\,(X \le x)$$

Where:
X = consequences, such as flood damage, loss of life, or emergency care costs.
$E\,[X]$ = expected value of the consequences
x = value of the consequences
$F_x(x)$ = probability density function of the probability of X
$F_x(x)$ = cumulative distribution function of X

This integration is performed graphically by HEC-FDA, using the trapezoidal rule to calculate the area under the damage-frequency curve. An example of the trapezoidal ruler is shown in panel (a) of **Figure 58**. For an exceedance probability interval, the area under the curve is calculated as a trapezoid in which the top of the trapezoid is a straight line between the two function values. This calculation is repeated over exceedance probability intervals between 0 and 1. As shown in panel (b) of the figure, the accuracy of EAD estimation can be improved by selecting smaller frequency intervals. HEC-FDA uses very small frequency intervals in the calculation (USACE 2024d).

Figure 58. Trapezoidal rule for curve integration

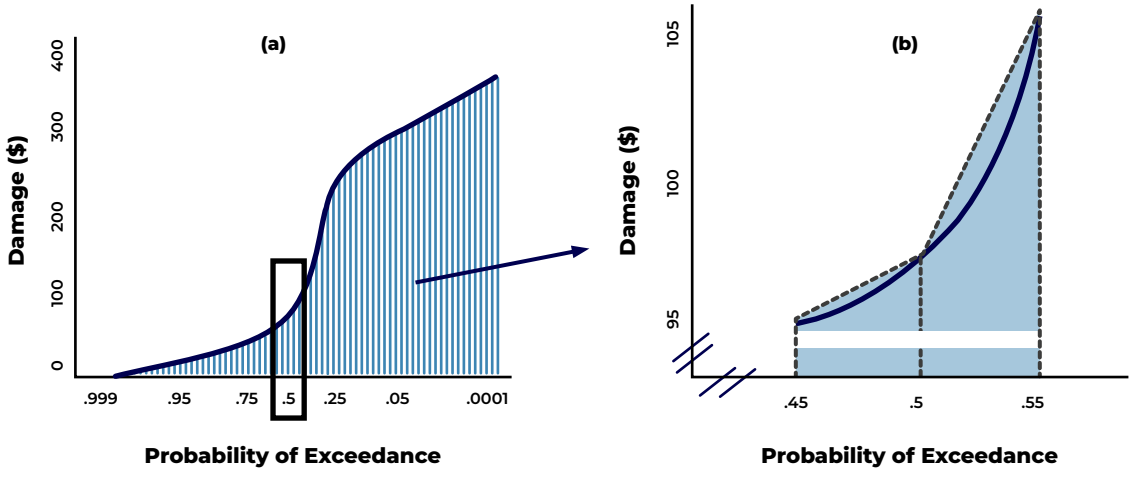

Source: USACE (2024d).

Figure 59 shows an example of EAD estimates resulting from the Monte Carlo analysis, describing the impact of epistemic uncertainties on the EAD.

Figure 59. Sample of EAD incorporating epistemic uncertainty using Monte Carlo simulation

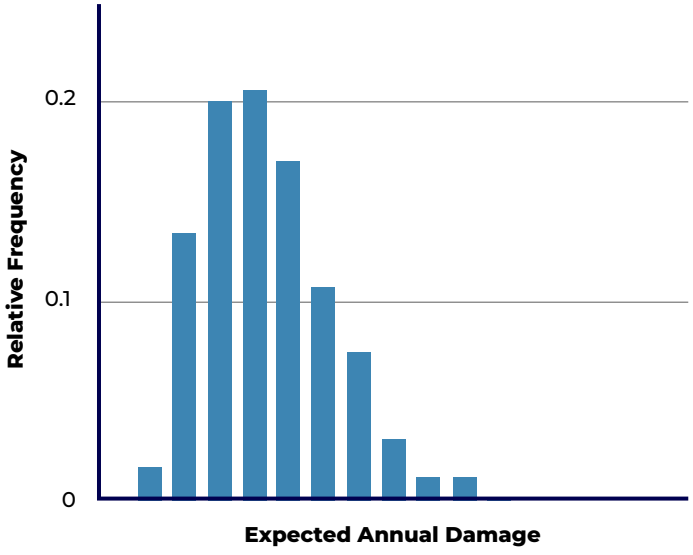

Source: USACE (2024c).

The Annual Average Equivalent Damage Distribution (AAED) is calculated assuming a perfect correlation between the expected annual damage distribution (EAD) of the base year and the EAD of future years. In other words, the first percentile of the base year EAD and the first percentile of the future EAD are used to calculate the first percentile of the AAED (USACE 2024e).

The damage reduction is calculated as the difference between the damage without the project and the damage with the project, and that damage can be expressed in terms of Expected Annual Damage or Average Annual Equivalent Damage. A perfect correlation between the two distributions is assumed, so the first percentile of the damage reduction is calculated by subtracting the first percentile of the damage with the project from the first percentile of the damage without the project (USACE 2024f).

In addition to the EAD, flood protection system performance metrics are also useful and very important. These metrics include the Annual Exceedance Probability (AEP), the Long-Term Exceedance Probability (LTEP), and assurance, or the Conditional Non-Exceedance Probability (CNP). The AEP and the LTEP can be calculated deterministically, whereas assurance is a statistic that requires the incorporation of uncertainty in the risk evaluation (USACE 2024g).

In addition to the EAD, flood protection system performance metrics are also useful and very important. These metrics include the Annual Exceedance Probability (AEP), the Long-Term Exceedance Probability (LTEP), and assurance, or the Conditional Non-Exceedance Probability (CNP). The AEP and the LTEP can be calculated deterministically, whereas assurance is a statistic that requires the incorporation of uncertainty in the risk evaluation (USACE 2024g).

A.13.4. Recent advances and innovations

Among the most recent improvements to HEC-FDA, the update to version 1.4.3 stands out, which includes adjustments to the way damage is calculated during infrequent flood events, such as those used in dam-safety evaluation. This version has been certified by the USACE Flood Risk Management Planning Center of Expertise, ensuring its applicability and accuracy in planning studies and hydraulic-infrastructure safety.

A.13.5. Development community

The development of HEC-FDA is carried out by the USACE Hydrologic Engineering Center, a center specialized in creating tools and software for water-resources management. The development community includes engineers, scientists and planners who collaborate in the continuous improvement of the software, ensuring that it meets the technical and regulatory needs in flood risk management studies. In addition, the platform is kept active with updates and certifications that reflect the latest developments in risk management.

A.13.6. Limitations

The software requires detailed and accurate data on local hydrology, existing structures, and their vulnerability to flooding. Without these data, the results may be inaccurate or unrepresentative. In addition, the complexity of its interface and the need for advanced technical knowledge may make it difficult for non-specialists to use.

A.13.7. Use cases

HEC-FDA is used primarily in the planning of flood-risk-mitigation projects. It has been implemented in dam safety studies, risk evaluations in urban areas, and in infrastructure planning to reduce vulnerability to flooding.

Image: Flickr - BID Ciudades sostenibles / Salina Cruz, México

Box 14. Example of HEC-FDA Application

Flood Damage Assessment in the Neka River Basin (Iran) using HEC-FDA

Image: Adobe Stock

The Neka River basin, located in the far east of Mazandaran Province, Iran, represents a critical region for flood risk management. Its strategic location and geographical characteristics, such as its origin in the heights of Shah Kooh, its mouth in the Caspian Sea and its extensive forest cover (80%), make this basin a relevant study area.

The Neka River runs for approximately 160 km and drains an area of 2004 km². Its longitudinal slope is 1.9%, with a channel that becomes more sinuous as it approaches the city of Neka.

Flood flows were calculated for return periods of 2, 5, 10, 20, 25, 50, 100 and 200 years with HEC-RAS, integrating Manning's roughness coefficients obtained from hydraulic studies and field visits.

The flood damage analysis was carried out considering:

- Six cover types based on land use were identified (residential, commercial, industrial, public, parks, and agricultural).
- The flow depths obtained from HEC-RAS for different return periods were stored in a format compatible with HEC-FDA.
- Damage curves were used for each land cover.

The following results were obtained from the analysis:

- The average annual loss was obtained for the urban region of Neka, which makes it possible to prioritize interventions.
- Risk maps and zoning: Using the outputs from the HEC-FDA model, flood risk zoning maps were generated, which are useful for urban planning and risk mitigation.
- Disaster management: The results provide key inputs for designing rescue maps and disaster management plans, including flood insurance strategies.

Source: Mohammadi et al. (2014).

A.14. OpenQuake

A.14.1. Introduction to OpenQuake

OpenQuake is an open-source tool developed in Python by the Global Earthquake Model (GEM) Foundation. It is designed for seismic risk evaluation through probabilistic models. OpenQuake allows users to simulate seismic events and assess their potential impacts in terms of damage and losses. The OpenQuake engine is installed as a stand-alone software that can be managed through a QGIS Plugin.

The plugin has been significantly expanded from its original purpose to work seamlessly with the OpenQuake Engine. This allows for a complete workflow in which hazard and risk calculations can be run directly in the QGIS environment, and the results are loaded as QGIS vector layers. The generated maps, such as hazard maps, are automatically styled according to the fields selected by the user. In addition, risk curves can be generated in a Data Visualization window, designed for this purpose (GEM 2024a).

A.14.2. Applied methods

OpenQuake uses a variety of methods for seismic risk calculation, including Probabilistic Seismic Hazard Analysis (PSHA) and event-based analysis. The platform also allows simulations of seismic scenarios and evaluation of the consequences of possible seismic events based on the definition of a fault rupture.

The risk component of the OpenQuake engine provides four main computational workflows shown in **Figure 60**.

Figure 60. Schematic of the main OpenQuake engine calculation workflows available in the risk component

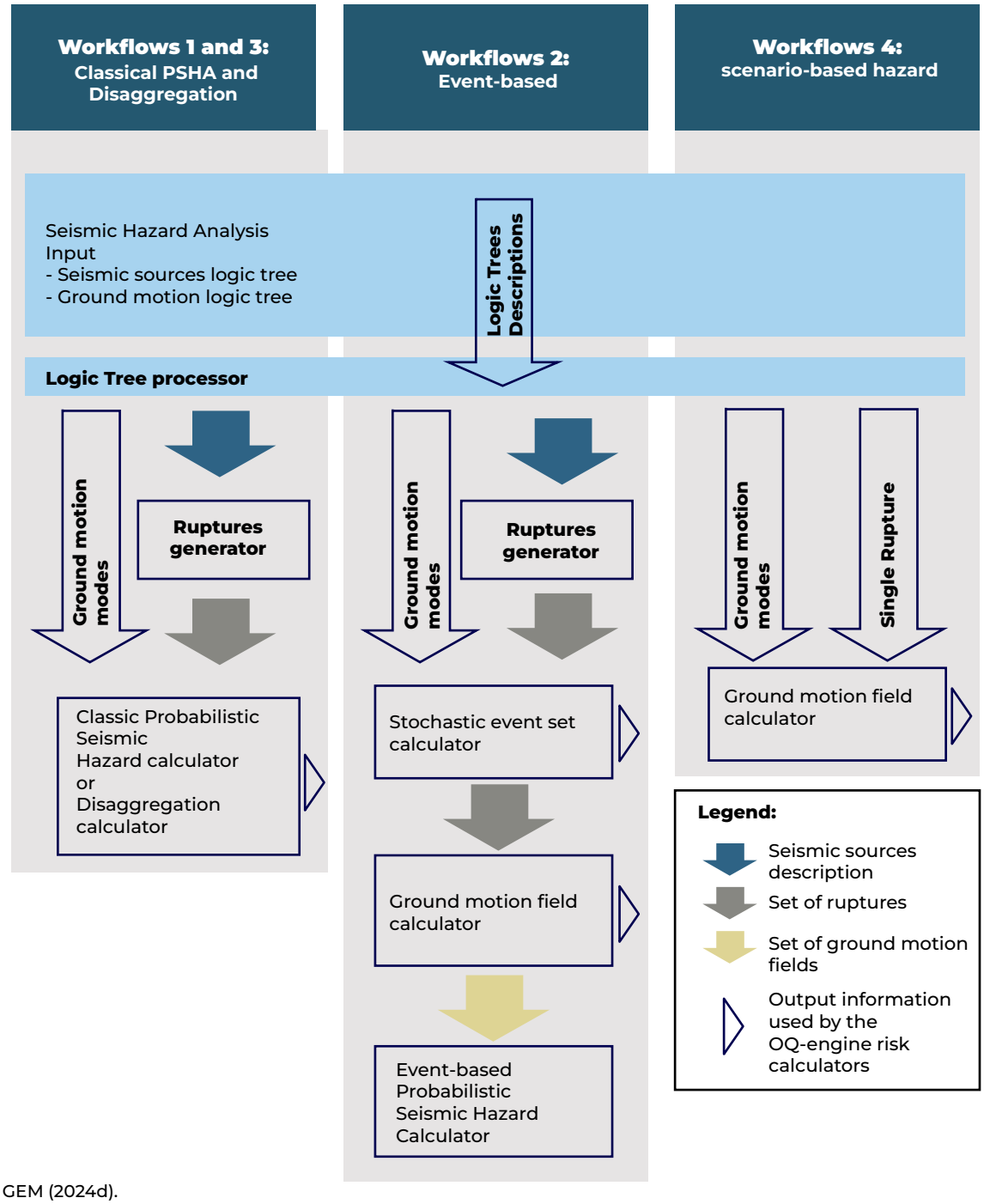

Source: GEM (2024d).

The methods used are described below (GEM 2024d):

- **Classical Probabilistic Seismic Hazard Analysis (PSHA):** It calculates hazard curves, hazard maps, and uniform hazard spectra, solving the PSHA integration proposed by Field et al. (2003). It is common in regional/national scale hazard assessments and specific studies. It uses hazard curves together with vulnerability and exposure models to derive loss exceedance curves and loss maps for different return periods.

- **Event-based PSHA:** It calculates stochastic event sets and ground motion fields for each rupture, including the spatial correlation of residuals within the event. It is a Monte Carlo-based method for PSHA. The generated synthetic catalogs are compared with real catalogs, and hazard curves and hazard maps are derived from the ground motion fields. These fields are essential for loss estimates, summing the losses per asset in each movement field to obtain a total loss exceedance curve representative of all assets.

- **Disaggregation:** Using a PSHA model, it is possible to identify the seismic scenarios that contribute the most to a specific hazard level at a given site. This is currently carried out following the classical PSHA methodology, but it will be added to the event-based calculator in future development phases.

- **Scenario-based Seismic Hazard Analysis (SHA):** Given a seismic rupture and a ground motion model, sets of ground motion fields can be calculated. This method is typical for loss analyses at the urban scale because it makes it possible to capture the correlation of losses among the assets in a portfolio. These fields are used with a fragility/vulnerability model to calculate the distribution of damage/loss in a collection of assets.

The main input information sources required, in addition to the hazard, for a risk calculation with the OpenQuake engine are an exposure model and a physical vulnerability model or fragility model (along with the calculation type and the region of interest).

A.14.3. Mathematical approach

OpenQuake offers three calculation types, which are described below (GEM 2024d).

Scenario-based calculation

The OpenQuake scenario-based risk calculator computes losses and loss statistics from a single event for a collection of assets, using a set of ground motion fields. These fields model the random variability in the ground motion prediction equations and may or may not include the spatial correlation of ground motion residuals.

The steps for the calculation are as follows:

1. The intensity levels at each site are combined with a vulnerability function for each asset, from which a loss rate is randomly extracted.

2. The engine takes the vulnerability function assigned to each asset and checks if the coefficient of variation is zero. If so, loss rates are derived on the basis of the mean loss ratio for each intensity measure level. If not, and if the uncertainty is defined, random sampling is performed following the probability distribution of the corresponding vulnerability function, $\log LR_n = \mu + \epsilon\sigma$. Where μ and σ represent the mean and standard deviation of the logarithm of the loss rates, respectively, and ϵ is a term that follows a standard normal distribution with a mean of zero and a standard deviation of one. The method used to sample epsilon depends on whether the correlation between the vulnerability uncertainty of the assets in a given taxonomy must be considered.

3. The mean loss rate for each asset across all possible simulations of the scenario event can be calculated using the formula:

Equation 23

$$LR = \frac{\sum_{n=1}^{m} LR_n | \mathrm{IML}}{m}$$

Where m represents the number of simulated ground motion fields and IML represents the intensity measure levels.

Calculation based on probabilistic events

The event-based probabilistic risk calculator uses stochastic event sets and ground motion fields to calculate loss exceedance curves for each asset in an exposure model. This process combines intensity measurement levels with vulnerability functions to determine loss rates, which can be independent or correlated. Losses are calculated for all ground motion fields and sorted by loss rate. Then, the exceedance rate and the exceedance probability of each loss rate are calculated. In addition, a disaggregation of losses by magnitude/distance or geographic coordinates can be performed.

In this method, losses are estimated for each asset for each event in the same way as in the scenario-based calculation, and then sorted from highest to lowest. The exceedance rate for each loss is calculated by dividing the number of exceedances of that loss by the number of stochastic event sets multiplied by the duration of each event set. Therefore, the highest loss will have zero exceedances, the next loss rate will have one exceedance, and so on.

The following formula is used to calculate the exceedance rate:

Equation 24

$$\lambda\ (L_n) = \frac{NE_L}{TSES}$$

Where λ represents the exceedance rate of the respective loss ratio, NE_L represents the number of exceedances of the given loss, and $TSES$ represents the time period of all stochastic event sets, that is, the number of stochastic event sets multiplied by the duration of each one.

Assuming a Poisson distribution of the occurrence model, the probability of exceedance of the loss set in a given time period can be derived using the following formula:

Equation 25

$$PE(L_n) = 1 - exp - \lambda_n \text{ x } t$$

Where t represents the time period used to produce the stochastic event set.

For the disaggregation of losses, it is necessary to provide the coordinates of the locations where this procedure must be applied. Then, for the selected locations, the OpenQuake engine calculates the sum of the losses (considering all assets present at each of the selected sites) for each seismic event. Additionally, the rupture distance (Joyner–Boore) is estimated, along with the coordinates of the point within the vertical projection of the rupture plane that is closest to each site.

The OpenQuake engine calculates the range (maximum and minimum values) of magnitudes, distances, latitudes, and longitudes across all events, and using the defined increment for each parameter, a set of linearly spaced intervals is calculated. Then, the losses from each seismic event are aggregated depending on which magnitude/distance or latitude/longitude combination they fall into.

The resulting losses for each parameter pair (magnitude/distance and latitude/longitude) are divided by the total loss for all events.

Classical PSHA-Based Risk Calculation

The classical PSHA-based risk calculator is used to compute loss exceedance curves for individual assets, calculated site by site using hazard curves. This calculator requires hazard curves as input, which can be calculated by the OpenQuake engine. At present, this calculator can only compute direct losses, although insured losses will be included in future versions.

To use this calculator, hazard curves must first be converted into probability mass functions (e.g., probability of occurrence of a discrete set of intensity measurement levels). To do this, the engine begins by reading the intensity measure levels of the discrete vulnerability functions and calculates the midpoint between consecutive levels. Two consecutive values define the interval bounds for each intensity measure level, and by relating these bounds to the hazard curve, the engine computes the corresponding exceedance probabilities.

The probability of occurrence (PO) of the intensity measure levels that fall within each interval can be derived by subtracting the exceedance probabilities of the lower and upper bounds, as described in the following formula:

Equation 26

$$PO = PE\,[lowerbound] - PE\,[upperbound]$$

The discrete vulnerability functions for each asset are converted into loss-ratio exceedance matrices (for example, matrices that describe the probability of exceedance of each loss rate for a discrete set of intensity measure levels). These matrices have a number of columns equal to the number of intensity measure levels defined in the vulnerability function, and a number of rows that can range from the number of loss ratios defined by the discrete function to any multiple of that number. To properly capture the probability distribution of loss rates by intensity measure level, the exceedance probabilities must be calculated not only for the loss rates defined in the vulnerability function, but also for many intermediate values between consecutive loss rates. After several sensitivity analyses, it appears that five intermediate values between consecutive loss rates is a reasonable choice; however, this is a parameter the user can adjust.

Finally, each column of the aforementioned matrix is multiplied by the probability of occurrence of the respective intensity measure level (taken from the hazard curves) to produce a matrix of conditional loss-rate exceedance. Then, for each loss rate, the exceedance probabilities are summed, yielding a loss-rate exceedance curve, whose set of loss rates can be multiplied by the asset value provided by the exposure model to obtain an absolute loss exceedance curve.

A.14.4. Recent advances and innovations

Version 3.23 of the OpenQuake Engine is a Long-Term Support (LTS) update that delivers significant performance improvements, especially for large models, with speeds 3 to 4 times higher compared with version 3.16. It introduces new functionalities in risk and hazard calculation, including improvements in site model management, scenario calculations, and the incorporation of new Ground Motion Prediction Equations (GMPEs). Additionally, the OQ-Impact project has been integrated, expanding impact assessment capabilities, and several bugs have been fixed to improve the software's stability and accuracy (GEM 2024e).

Additionally, in terms of functionality, beginning with version 3.19 all documentation associated with the use of the platform was unified and migrated to a web page (https://docs.openquake.org/oq-engine/master/manual/index.html), which improves its accessibility and makes the required information easier to find.

A.14.5. Development community

The OpenQuake engine is developed through close and ongoing collaboration between GEM's scientific and IT teams. The development process is carried out openly to encourage the participation of experts working in the fields of seismic hazard and risk analysis, as well as those specialized in software development (GEM 2024d).

The OpenQuake code is available on GitHub, which ensures thorough version control and makes it easier to track feature implementations and bug fixes. It also ensures that previous versions of the software can be easily retrieved. When a developer submits new code to the main repository, the record of the change is preserved. If the code is intended to resolve an error or bug identified in the bug tracking system, or to implement a new feature in response to a request, the code contribution record should indicate the specific error or feature that the code change is intended to address. In this way, a comprehensive and auditable record is maintained of each identified issue and of the code changes made to resolve it (GEM 2024d).

A.14.6. Limitations

Given its long track record and its development community, which continually improves the platform, the limitations of OpenQuake are more related to its functionality than to its capability. As a tool capable of handling very complex models, it can have a steep learning curve, especially for users with limited experience in risk modeling, which is reflected in the fact that the developers themselves recommend that users have a master's level background in seismology to use the platform correctly.

The tool currently has a website dedicated exclusively to training in the use of the platform (https://www.training.openquake.org/), which provides several modules and resources for learning aimed at beginning users. However, these resources were developed in 2020 for version 3.9 of the platform, so most of the content is now out of date.

Additionally, it is a tool developed solely for seismic risk, which means it requires a very high degree of specialization and commitment, even though it can be used for only a single hazard. This generates the requirement to have multiple platforms, models and professionals to assess risks in a multi-hazard context.

A.14.7. Use cases

OpenQuake has been used in numerous seismic risk assessment projects worldwide. There are examples of applications in Latin America, the United States, Europe, Asia and Africa (Azizi 2024).

Image: Adobe Stock

Box 15. Example of OpenQuake Application

Case Study: Implementation of OpenQuake for Seismic Risk Assessment in India

Image: Adobe Stock

The probabilistic seismic risk for India was estimated using the OpenQuake platform to improve understanding of seismic hazards and risks across the country. This model serves as a critical tool for assessing exposure, vulnerability, and risk, enabling the establishment of rational risk mitigation targets and the prioritization of disaster management investments.

The study highlights the challenges encountered in developing a national seismic risk model, particularly the lack of detailed information on the current building inventory and the scarcity of seismic fragility and vulnerability models for various building types in India. Previous assessments have focused mainly on scenario-based analyses for specific cities, which, although valuable, do not provide the resolution needed for risk analysis at the national level.

The OpenQuake engine was used to compute seismic hazard metrics, including peak ground acceleration (PGA) and spectral acceleration, using a probabilistic seismic hazard assessment (PSHA) approach. The model incorporates a wide range of building types and construction practices, which makes it possible to understand risk across different regions. The results include mean hazard maps and loss exceedance curves, which are essential for planning and preparedness activities.

Map of the annual average loss for India obtained with OpenQuake

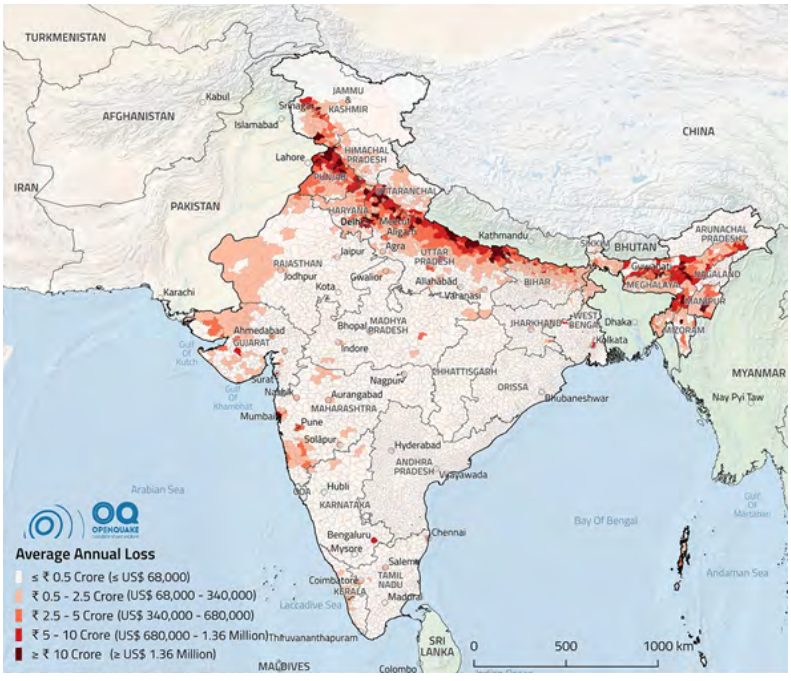

Additionally, the study emphasizes the importance of continuous improvement of the model through local assessments and the collection of empirical data. The open nature of the datasets and model components fosters collaboration among experts and stakeholders, promoting a community-driven approach to seismic risk management.

In conclusion, the implementation of the OpenQuake platform for seismic risk assessment in India represents a significant advancement in the field of disaster risk reduction. The model not only provides critical information for improving national seismic design codes, but also serves as a basis for future research and informed decision-making on risks in earthquake-prone areas.

Source: Rao et al. (2020).

ANNEX B. ANNEX TYPES OF DATA

The main types of data required for hazard, vulnerability and exposure assessment in disaster risk studies, as well as their common formats and the software tools used for their processing are:

- **Vector data:** represent geographic elements using geometries such as points, lines and polygons. Each geometry is associated with an attribute table containing descriptive information about that element (ESRI, Esri Products, s.f.)

  Points: represent unique locations, such as wells, sensors or weather stations.

  Lines: represent linear elements such as rivers, streets or electrical networks.

  Polygons: represent areas such as lakes, agricultural areas or administrative boundaries.

  Most common extensions: .shp, .geojson, .dwg, .dxf, .kml

- **Point clouds:** are massive sets of points in 3D space, each with X, Y, Z coordinates and sometimes with additional information such as intensity or classification (soil, vegetation, buildings). They are commonly generated by LiDAR (Light Detection and Ranging) sensors from drones or airplanes.

  These point clouds allow the creation of 3D models of terrain, buildings or vegetation, and can be used to generate products such as Digital Elevation Models (DEM) or Surface Models (SLM). (Neuvition, s.f.).

  Most common extensions: .las, .xyz

- **Raster and satellite images:** they are composed of a regular grid of pixels, where each pixel contains a value (such as color, temperature, elevation, etc.). These images are used to represent continuous phenomena on the earth's surface. Satellite imagery is a type of raster captured by remote sensors mounted on satellites. They can contain multiple spectral bands and allow analysis of variables such as vegetation (NDVI), temperature, soil moisture, and more (ESRI, Esri Products, s.f.).

  Most common extensions: .tiff, .geotiff, .img.

- **Spatio-temporal data:** contains georeferenced information that varies over time. That is, they not only have a spatial dimension (latitude, longitude, altitude), but also a temporal dimension (hour, day, year, etc.). This type of data allows the analysis of changes in climate, weather patterns, evolution of hazards, among others. (NOAA, s.f.)

  Most common extensions: .nc, grib

The following table summarizes the main extensions and data types used:

Table 1. Data types, formats and tools used.

Data	Data type	Common Formats	Analysis Tools / Software
Geospatial data	Elevation, slope, relief (DEM, DTM), contour lines	• .tif, • .asc, • .las, • .xyz	ArcGIS, QGIS, Global Mapper, CloudCompare, LAStools
	Land cover and land use	• .tif, • .mgi, • .shp, • .geojson	Google Earth Engine, ArcGIS, QGIS, SNAP
Climatic and meteorological	Precipitation, temperature, wind, extreme events	• .nc, • .csv, • .grib, • .json	R (climate4R), Python (xarray, pandas), GEE, Panoply
	Climate indices (NDVI, SPI, SPEI, FWI)	• .nc, • .tif, • .csv	R (raster, SPEI package), Python, ArcGIS Pro, GEE
Socioeconomic and demographic	Population density, poverty, critical services	• .csv, • .shp, • .xlsx	Tableau, Power BI, ArcGIS Insights, R (ggplot2, dplyr)
	Critical infrastructure and service networks	• .shp, • .dwg, • .dxf	AutoCAD, ArcGIS, QGIS
Specific threats	Geological faults, volcanoes, landslides, basins, etc.	• .shp, • .tif, • .kml, • .geojson	ArcGIS, QGIS, SAGA GIS, GRASS GIS
Climate models	Projections CMIP6, ERA5, CHIRPS, CRU	• .nc, • .zip, • .grib	Climate Data Store Toolbox, Python (xarray), Panoply, QGIS

Image: Flickr - BID Ciudades sostenibles / Natal Brasil


IDB
Improving lives